BioMed Research International

Molecular Biomarkers: Tools of Medicine

Guest Editors: Prabir K. Mandal, Shivani Soni, R. Renee Reams, Tiziano Verri, and Sudhish Mishra

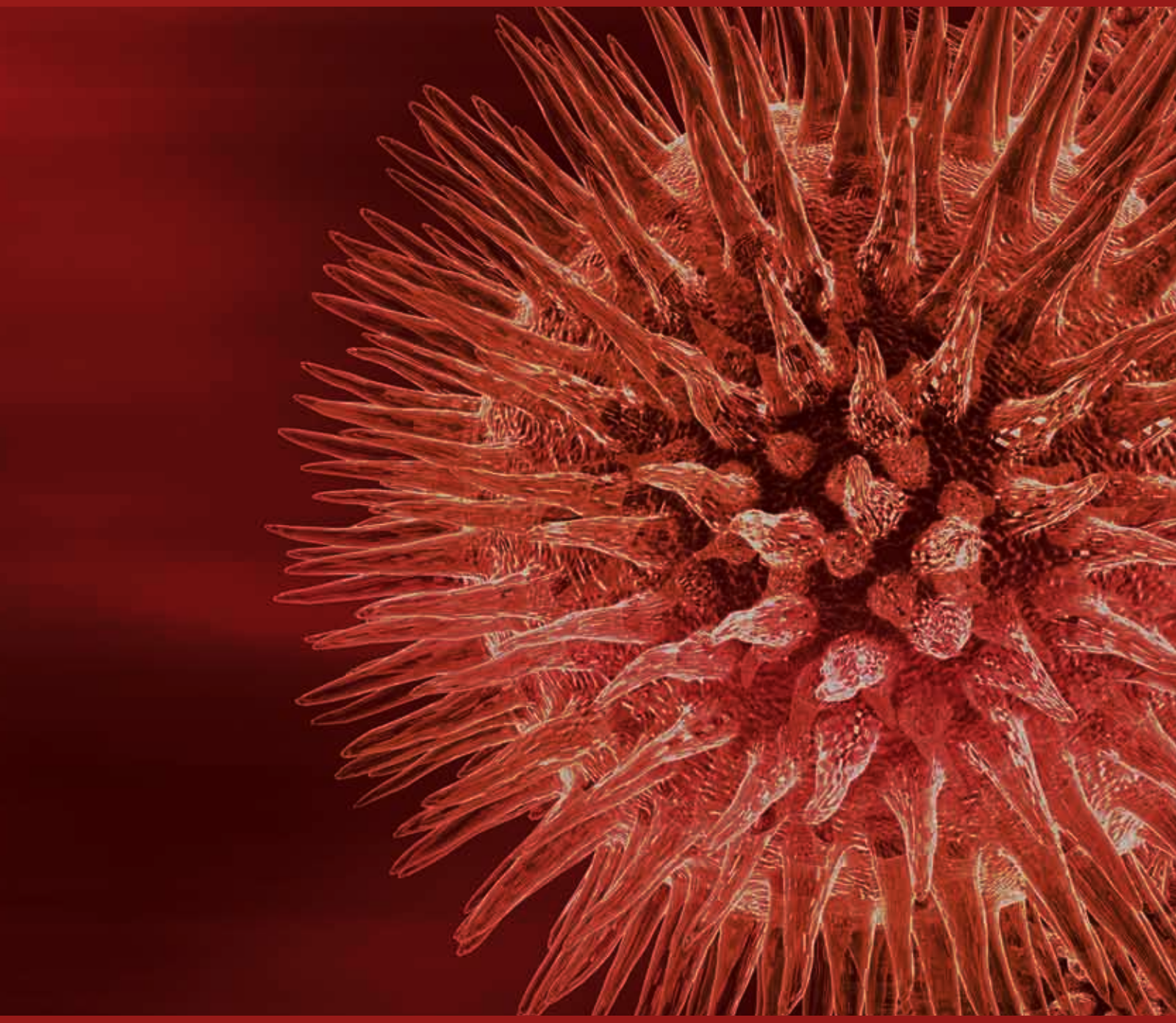

Molecular Biomarkers: Tools of Medicine

BioMed Research International

Molecular Biomarkers: Tools of Medicine

Guest Editors: Prabir K. Mandal, Shivani Soni, R. Renee Reams, Tiziano Verri, and Sudhish Mishra

Contents

Hindawi Publishing Corporation
BioMed Research International
Volume 2013, Article ID 595496, 2 pages
http://dx.doi.org/10.1155/2013/595496

Editorial

Molecular Biomarkers: Tools of Medicine

Prabir K. Mandal,[1] Shivani Soni,[2] R. Renee Reams,[3] Tiziano Verri,[4] Anita Mandal,[1] and Sudhish Mishra[5]

[1] *Department of Biology, Edward Waters College, 1658 Kings Road, Jacksonville, FL 32209, USA*
[2] *Department of Biological Sciences, Alabama State University, Room No. 325, Life Science Building 1627, Hall Street, Montgomery, AL 36104, USA*
[3] *College of Pharmacy & Pharmaceutical Sciences, Florida A&M University, 1520 M L King Boulevard, Tallahassee, FL 32307, USA*
[4] *Laboratory of General Physiology, Department of Biological and Environmental Sciences and Technologies, University of Salento, I-73100 Lecce, Italy*
[5] *Department of Translational Science and Molecular Medicine, MSU College of Human Medicine and Van Andel Institute, 333 Bostwick Avenue NE, Grand Rapids, MI 49503, USA*

Correspondence should be addressed to Prabir K. Mandal; prabir.mandal0807@ewc.edu

Received 11 October 2013; Accepted 11 October 2013

Molecular biomarkers are emerging as the key indices for the management of patients with significant diseases. Motivated by the systematic effort to define the human genome, the creation of rapid analytic technologies for evaluating nucleic acids and proteins has provided the technological "boom" for the development of molecular biomarkers. Collaboration and cooperation between stakeholders involved in biomarker development, application, and regulation may be the most expeditious route toward the translation of laboratory discovery into patient management. In summary, intensive research has originated multiple factors or biomarkers that are likely to be helpful in diagnosis, characterization, and therapy selection of different patients. A thorough understanding of the relevance of each biomarker will be the key to efficiently diagnose a disease and direct the patients towards the drugs more likely to be of benefit based on their particular profile.

The papers selected for this special issue represent an excellent panel for addressing the molecular biomarkers as the future tools of medicine. This special issue contains thirteen papers.

In the paper entitled "*Circulating microRNAs and kallikreins before and after radical prostatectomy: are they really prostate cancer markers?*," M. G. Egidi et al. presented 38 patients with prostate cancer. They suggested that two miRNAs (miR-21 and miR-141) could be involved in post surgical inflammatory processes. Postoperative serum kallikreins showed a significant decrease, highlighting the potential usefulness of kallikreins apart from PSA as potential prostate cancer markers.

In the paper entitled "*A novel differential predict model based on matrixx-assisted laser ionization time of flight mass spectrometry and serum ferritin for acute graft-versus-host disease*,". C.-Y. Zhang et al. investigated the possibility of pre warning the risk of an acute graft-versus-host disease (aGVHD) before and after allogeneic hematopoietic stem cell transplantation (allo-HSCT) by serum profiling combining with serum ferritinin. Their joint prewarning model could predict the risk of aGVHD, especially severe aGVHD before transplant which provide a reliable method to continuously monitor the condition of patients.

In the paper entitled "*The use of multidimensional data to identify the molecular biomarker for pancreatic ductal adenocarcinoma*," L. Zhuang et al. presented that they have adopted an integrative approach to simultaneously identify biomarker and generate testable hypothesis from multidimensional omics data. They have found that PER2 expression was highly associated with the survival data, thus representing a novel biomarker for earlier detection of pancreatic ductal adenocarcinoma (PDAC).

In the paper entitled "*Clinical evaluation and cost-effectiveness analysis of serum tumor markers in lung cancer*," R. Wang et al. showed that combinations of four tumor

markers (SCCA, NSE, CEA, and CYFRA21-1) improved the sensitivity for lung cancer and different combination panels had their own usefulness. NSE, CEA, and CYFRA21-1 were the optimal combination panel with highest Youden's index (0.64), higher sensitivity (75.76%), and specificity (88.57%), which can aid in clinical diagnosis of lung cancer.

In the paper entitled "*Immune parameters in the prognosis and therapy monitoring of cutaneous melanoma patients: experience, role, and limitations*," M. Neagu et al. reported the follow-up for 36 months of the immune parameters of patients diagnosed in stages I–IV, namely, pre- and post-surgery immune circulating peripheral cells and circulating intercommunicating cytokines.

In the paper entitled "*Comparative gene expression profiling in human cumulus cells according to ovarian gonadotropin treatments*," S. Assou et al. provided an exclusive study characterizing gene expression profiles in cumulus cells (CCs) of periovulatory follicles from patients undergoing HP-hMG and rFSH gonadotropin treatments during *in vitro* fertilization cycles. This project has characterized the expression of these genes as biomarkers of *in vitro* embryo quality.

In the paper entitled "*Aptamers: novel molecules as diagnostic markers in bacterial and viral infections?*," F. M. Zimbres et al. urged an urgent need to discover novel diagnostic as well as therapeutic tools against infectious agents. They viewed that the systematic evolution of ligands by exponential enrichment (SELEX) represents a powerful technology to target selective pathogenic factors as well as entire bacteria or viruses. SELEX uses a large combinatorial oligonucleic acid library (DNA or RNA) which is processed by a high-flux *in vitro* screen of iterative cycles.

In the paper entitled "*Distribution of ABO blood group and major cardiovascular risk factors with coronary heart disease*," S. Biswas et al. viewed that the AB blood group decreases the risk of CHD in healthy controls; it might be due to the higher concentration of high density lipoprotein cholesterol (HDL-c), while the O blood group increases the risk of CHD due to lower HDL-c levels in Bengali population of eastern part of India.

In the paper entitled "*Immunomodulatory effect of continuous veno-venous hemofiltration during sepsis: preliminary data*," G. Servillo et al. reported that severe sepsis and septic shock are the primary causes of multiple organ dysfunction syndrome (MODS), which is the most frequent cause of death in intensive care unit patients. Many pro- and anti-inflammatory mediators, such as interleukin-6 (IL-6), play a key role in septic syndrome. Continuous renal replacement therapy (CRRT) removes in a nonselective way pro- and anti-inflammatory mediators. The authors investigate the effects of continuous venovenous hemofiltration (CVVH) as immunomodulatory treatment of sepsis in a prospective clinical study.

In the paper entitled "*Acetylcholinesterase as biomarker in environmental and occupational medicine: new insights and future perspectives*," M. G. Lionetto et al. viewed that Acetylcholinesterase (AChE) is a key enzyme in the nervous system (NS), since it terminates nerve impulses by catalyzing the hydrolysis of acetylcholine. As a specific molecular target of organophosphate and carbamate pesticides, AChE activity and inhibition are a human biological marker of pesticide poisoning. Thus, it is used to study the effects of the exposure to organophosphate and carbamate pesticides on NS in occupational and environmental medicine. This paper reviews and discusses the recent findings about AChE, including its sensitivity to other pollutants and expression of different splice variants. These insights open new perspectives for the use of this biomarker in environmental and occupational human health monitoring.

In the paper entitled "*Polyisoprenylated methylated protein methyl esterase is both sensitive to curcumin and overexpressed in colorectal cancer: implications for chemoprevention and treatment*," F. Amissah et al. discussed polyisoprenylated methylated protein methyl esterase (PMPMEase) which cocatalyzes the polyisoprenylation pathway required to process various monomeric G proteins. Mutation of these G proteins is considered to be responsible for 50% of colorectal cancers. This interesting finding suggests that elevated PMPMEase activity and its overexpression can be one of the candidate markers for early diagnosis of colorectal cancer. Susceptibility of this enzyme to curcumin also suggests that PMPMEase can be a potential candidate for targeted anticancer therapy.

In the paper, entitled "*Emerging therapeutic biomarkers in endometrial cancer*," P. Dong et al. reviewed the current status of molecular therapies tested in clinical trials and mainly discussed the potential therapeutic candidates that are possibly used to develop more effective and specific therapies against endometrial cancer progression and metastasis.

In the paper entitled "*Mouse prostate epithelial luminal cells lineages originate in the basal layer where the primitive stem/early progenitor cells reside: implications for identifying prostate cancer stem cells*" J. Zhou et al. have developed an *in vivo* cell fate tracing mouse model and an *in vivo* slow-cycling cell label mouse model to provide further insight into this question. Through genetic manipulation in the animals, their findings indicate that the basal cell lineage can produce more differentiated luminal cells; the putative mouse prostate stem cells (which are slow-cycling and responsible for tissue maintenance) likely reside in the basal layer.

Though the selected topics and papers are not an exhaustive representation of the entire area of molecular biomarkers and tools of medicine, yet they represent the rich and many-faceted knowledge that we have the privilege of sharing with the readers.

Acknowledgments

We would like to thank the authors for their excellent contributions and patience. Last but not the least, the fundamental work of all reviewers on these papers is also greatly acknowledged.

Prabir K. Mandal
Shivani Soni
R. Renee Reams
Tiziano Verri
Anita Mandal
Sudhish Mishra

Hindawi Publishing Corporation
BioMed Research International
Volume 2013, Article ID 295635, 9 pages
http://dx.doi.org/10.1155/2013/295635

Research Article

Defects in Base Excision Repair Sensitize Cells to Manganese in *S. cerevisiae*

Adrienne P. Stephenson, Tryphon K. Mazu, Jana S. Miles, Miles D. Freeman, R. Renee Reams, and Hernan Flores-Rozas

Florida A&M University, College of Pharmacy & Pharmaceutical Sciences, 1520 Martin Luther King Boulevard, Dyson Building Room 221, Tallahassee, FL 32307, USA

Correspondence should be addressed to Hernan Flores-Rozas; hernan.floresrozas@famu.edu

Received 1 July 2013; Accepted 10 September 2013

Academic Editor: Shivani Soni

Manganese (Mn) is essential for normal physiologic functioning; therefore, deficiencies and excess intake of manganese can result in disease. In humans, prolonged exposure to manganese causes neurotoxicity characterized by Parkinson-like symptoms. Mn^{2+} has been shown to mediate DNA damage possibly through the generation of reactive oxygen species. In a recent publication, we showed that Mn induced oxidative DNA damage and caused lesions in thymines. This study further investigates the mechanisms by which cells process Mn^{2+}-mediated DNA damage using the yeast *S. cerevisiae*. The strains most sensitive to Mn^{2+} were those defective in base excision repair, glutathione synthesis, and superoxide dismutase mutants. Mn^{2+} caused a dose-dependent increase in the accumulation of mutations using the *CAN1* and *lys2-10A* mutator assays. The spectrum of *CAN1* mutants indicates that exposure to Mn results in accumulation of base substitutions and frameshift mutations. The sensitivity of cells to Mn^{2+} as well as its mutagenic effect was reduced by N-acetylcysteine, glutathione, and Mg^{2+}. These data suggest that Mn^{2+} causes oxidative DNA damage that requires base excision repair for processing and that Mn interferes with polymerase fidelity. The status of base excision repair may provide a biomarker for the sensitivity of individuals to manganese.

1. Introduction

Manganese (Mn) is a trace element that has been extensively documented for its varied role in the body's homeostasis. As an essential nutrient, Mn is required for the normal function and development of the brain [1], metabolism of proteins, lipids, and carbohydrates [2–4], and also as a functional unit for many enzymes [3–5]. Therefore, deficiencies that affect fetal development [6] and excess Mn (environmental exposure and/or elevated dietary Mn [7]), can result in disorders and disease.

There is increasing concern for the use of organic compounds containing manganese in industrial settings. In recent years, methylcyclopentadienyl manganese tricarbonyl (MMT) gained approval for use in the United States as an octane enhancing fuel additive used in unleaded automotive gasoline. Exposure to Mn has also increased through occupation and environmental settings. This includes agrochemicals such as the fungicides, maneb and mancozeb, and pesticides in the agriculture and forest industries [8] as well as in the case of miners, smelters, welders, and workers in battery factories [9]. The increase in atmospheric levels could result in potential health risks.

At elevated levels of exposure, Mn has been shown to cause manganism, which is an excess of manganese in the basal ganglia [10]. Manganism is characterized by neurological symptoms resembling the dystonic movement associated with Parkinson's disease (PD) [11–13] and therefore is a risk factor for idiopathic Parkinson's disease (IPD). Although Mn has been studied for years, the mechanism by which it causes neuronal damage is not well understood. Studies suggest that neurotoxicity is not caused by a single factor but that it appears to be regulated by a number of factors including apoptosis, oxidative injury, DNA damage, mitochondrial dysfunction, and neuroinflammation [14–18].

The mutagenicity of Mn has been extensively documented [19]. Mn has been shown to cause damage to DNA in multiple cell-based assays [18, 20], to interfere with the

fidelity of DNA replication [21], to activate the DNA damage response [22], to induce mutations in T4 phage replication [23] and yeast mitochondria replication [24, 25], and, inhibit repair factor PARP in human cells [26], albeit not scoring as a direct mutagen in the Ames test [27]. Despite its mutagenicity, Mn is not classified as a carcinogen in humans. The reasons for this discrepancy are still not clear.

Research on manganese toxicity has increased in recent years. However, the mechanisms underlying its multiple toxicities (neurotoxicity, genotoxicity, mutagenicity, etc.) [19] remain a mystery. It is possible that redundant mechanisms of DNA repair exist which are effective to handle the levels of Mn to which cells are exposed.

The goal of the current study is to gain insight into the pathways that are involved in DNA damage/repair that contribute to protecting cells from the toxicity of manganese (Mn). The yeast *S. cerevisiae* was utilized as a model system to study the genotoxic effects of Mn. Yeast has proven to be an excellent eukaryotic model for studying metal, and players identified through genetic studies virtually all have homologues in humans. In our study, we use two well-established mutator assays. The *CAN1* assay was used to measure the induction of forward mutations, and the *lys2-10A* reversion assay was used to assess replication fidelity. Furthermore, this study examines the protective effects of the antioxidants N-acetylcysteine and glutathione, as well as Mg^{2+} on Mn-induced toxicity and mutagenesis.

2. Materials and Methods

2.1. General Genetic Methods and Strains. Yeast extract/peptone/dextrose (YPD, 1% yeast extract, 2% peptone, 2% dextrose, 2% agar) and synthetic complete (SC, 0.67% yeast nitrogen base without amino acid, 0.087% amino acid mixture, 2% dextrose, 2% agar) media or the corresponding drop-out media were as described in [28, 29]. Homozygous haploid deletion strains library (Parental strain BY4741: MATa his3Δ1 leu2Δ0 met15Δ0 ura3Δ0) was obtained from Thermo Scientific (Pittsburgh, PA, USA).

2.2. Chemicals. Manganese chloride tetrahydrate ($MnCl_2$-$4H_2O$), N-acetylcysteine (NAC), glutathione (GSH), canavanine, and yeast media were purchased from Sigma-Aldrich (St. Louis, MO, USA).

2.3. Sensitivity of Strains to Mn^{2+} and Effect of NAC and GSH. The concentration of Mn^{2+} for strain exposure was determined experimentally using the wild type parental strain, BY4741. Briefly, single colonies were grown for 16 h on YPD with or without Mn^{2+} at 30°C with shaking. Cells were then washed with and resuspended in sterile water. Serial dilutions were spotted onto YPD and plates were incubated at 30°C. Cell growth was monitored daily and sensitivity was scored after 3 days. Colonies were counted and survival (in percentage) was calculated relative to the untreated control. Each strain was tested using at least five independent colonies for each Mn^{2+} concentration tested. To determine the effect of thiol-based antioxidants, cells were cotreated with Mn^{2+} and N-acetylcysteine (NAC) or glutathione (GSH) at the concentrations indicated in each figure. Survival was calculated as described above.

Table 1: Strains used in this study.

Gene	ORF	Function
HSP104	YLL026W	Protein disaggregase
RAD2	YGR258C	Nucleotide excision repair endonuclease
RAD52	YML032C	Homologous recombination
SOD2	YHR008C	Mitochondrial superoxide dismutase
RAD18	YCR066W	Postreplication repair
CTA1	YDR256C	Catalase activity
SOD1	YJR104C	Superoxide dismutase activity
MLH1	YMR167W	Mismatch repair
GSH2	YOL049W	Glutathione synthetase activity
GSH1	YJL101C	Glutamate-cysteine ligase activity
APN1	YKL114C	Base excision repair
UBC13	YDR092W	DNA postreplication repair
RAD27	YKL113C	Base excision repair, DNA replication
RAD30	YDR419W	Bypass synthesis DNA polymerase
NTG1	YAL015C	Base excision repair

Wild type: strain BY4741 (MATa his3Δ1 leu2Δ0 met15Δ0 ura3Δ0).
RDKY3590 (MATa, ura3-52, leu2D1, trp1D63, hom3-10; lys210A).

2.4. Mutation Analysis. The effect of Mn^{2+} on the accumulation of mutations was assessed by the *CAN1* forward mutation assay and the *lys2-10A* mutation reversion as previously described [30, 31]. Mutation rates were determined by fluctuation analysis using at least five independent colonies [29, 32]. Each fluctuation test was repeated at least three times. The *CAN1* forward mutation assay relies on the introduction of mutations on the *CAN1* gene which encodes the arginine permease allowing mutant cells to grow on plates containing the toxic arginine analog, canavanine. The *lys2-10A* reversion assay is based on the restoration of the open-reading frame in a mononucleotide run of 10 adenines within the *lys2* allele of strain RDKY3590 (Table 1), allowing mutant cells to grow on plates lacking lysine.

2.5. DNA Sequence Analysis. Spectrum analysis was carried out by selecting mutants (Can^r) on selective minimum media drop-out plates containing canavanine [29]. Chromosomal DNA was isolated from the mutants and the relevant region of *CAN1* was amplified by PCR and sequenced [30]. Sequence was carried out at MCLAB (San Francisco, CA, USA). Sequence analysis was carried out using Sequencher (Gene Codes, Ann Arbor, MI, USA).

2.6. Statistical Analysis. Data analysis and graphing were performed using the GraphPad Prism 4 software package. Specific analysis for each experiment is indicated in each figure legend. In most cases, the mean of at least three experiments is plotted together with the standard deviation. Differences between mean values and multiple groups were

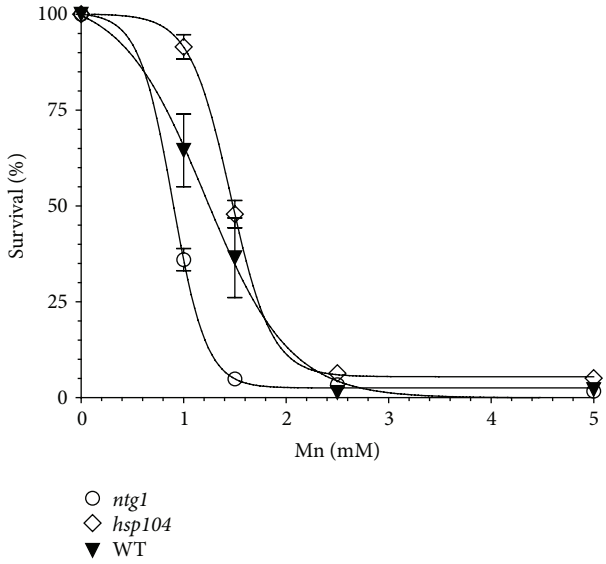

Figure 1: Dose-dependent response of selected yeast strains to Mn^{2+}. Wild-type parental strain (BY4741) was tested for growth on media after exposure to 0, 0.5, 1.5, 2.5, and 5 mM Mn^{2+} as indicated in Materials and Methods. Survival was determined by counting the number of colonies in the respective dilutions and calculated based on the growth of cells not exposed to Mn^{2+} (100% survival). Mutant strains *ntg1* and *hsp104* that display increased and reduced sensitivity to Mn^{2+}, respectively, are shown for comparison. The curve was fitted by nonlinear Sigmoidal dose response (variable slope).

analyzed by one-way analysis of variance (ANOVA). Statistical significance was set at $P < 0.05$.

3. Results

3.1. Sensitivity of S. cerevisiae Strains to Mn^{2+}. To perform a comparative analysis of the differential sensitivity of yeast strains, we first determined the dose of Mn^{2+} appropriate for the study. We initially used the wild type strain to determine the range of Mn^{2+} concentrations and found that there was a linear response in a narrow window between 1 and 2.5 mM (Figure 1), with the higher concentration resulting in viability below 5%, which did not significantly increase at higher concentrations of Mn^{2+}. All selected strains were then exposed to this range of Mn^{2+} concentrations. Figure 1 shows a comparison between the wild type strain, the disaggregase *hsp104* mutant, which displays higher tolerance to Mn^{2+}, and the base excision repair *ntg1* mutant, which is more sensitive. Mn^{2+} at 1.5 mM was determined to be the optimal concentration for the strain comparison (Figure 1). At this concentration, wild-type cells displayed approximately 40% survival and sensitive strains showed higher sensitivity relative to the wild-type strain (Figure 1).

Based on published evidence and a recent report by Stephenson et al. [18], we selected several mutant strains that play a role in the mutagenicity avoidance and may be involved in processing Mn^{2+}-induced DNA damage (Table 1). These mutants strains include those defective in nucleotide excision repair (*rad2*), postreplication repair (*rad18*, *rad27a*, and *ubc13*), base excision repair (*apn1*, *rad27*, and *ntg1*), homologous recombination (*rad52*), DNA mismatch repair (*mlh1*), and DNA damage bypass (*rad30*), glutathione synthesis (*gsh1* and *gsh2*), oxidative stress (*sod1*, *sod2*, and *cta1*), and protein disaggregation (*hsp104*). Quantitative analysis involved exposing the cells to Mn^{2+} as described under Materials and Methods and spotting serial dilutions onto nonselective media YPD for colony counting. As observed in Figure 2(a), no significant difference was observed on the growth rate of each strain in the absence of Mn^{2+} (control panel), except for slow growing strain *ntg1*. However, upon treatment with Mn^{2+}, the strains displayed differential sensitivity to the metal. All strains tested were sensitive to Mn^{2+} however, only the *hsp104* mutant displayed less sensitivity than the wild type (48% versus 37%; Figure 2(b), black bar). No significant difference between *rad2* (33.2% survival) and the wild type was observed, suggesting that Mn^{2+}-induced DNA damage does not result in bulky adducts that require NER for processing. Similarly, no significant difference between *rad52* (31% survival) and the wild type indicates that no significant DNA damage is processed to DNA double-strand breaks that require homologous recombination for repair. Interestingly, the oxidative stress mutants *sod1*, *sod2*, and *cta1*, (15%, 21%, and 17% survival, resp.) were approximately 2-fold more sensitive than wild type and the glutathione synthesis mutants *gsh1* and *gsh2* (10.6% and 13.6% survival, resp.) were 3-fold more sensitive. Mismatch repair mutants *mlh1* displayed 14.5% survival, suggesting that Mn^{2+} induces an increased load of mismatches that cannot be repaired. More striking was the sensitivity of the base excision repair mutants *apn1*, *rad27*, and *ntg1*, (9.5%, 9.2%, and 4.9% survival), which were over 4-fold more sensitive to Mn^{2+} than wild type (Figure 2(b)), with *ntg1* being the most sensitive (7.5-fold). In addition, *ubc13* and *rad30* mutants were also highly sensitive (~4-fold higher than wild type), further suggesting the generation of Mn^{2+}-induced DNA damage.

3.2. Attenuation of the Sensitivity to Mn^{2+} by Exogenous Antioxidants. Considering that oxidative stress mutants *sod1*, *sod2*, and *cta1* and glutathione synthesis mutants *gsh1* and *ghs2* displayed higher sensitivity to Mn^{2+} than wild-type, we tested if antioxidants would protect from Mn^{2+}-induced cytotoxicity. As shown in Figure 3, exogenously added NAC and GSH protected both the wild-type and the hypersensitive strain *ubc13*. The concentration of Mn^{2+} was increased to 2 mM to effectively determine the protective effects of the antioxidants on wild-type cells, resulting in 20% survival. Cotreatment of wild-type cells with 2 mM Mn^{2+} and 20 mM NAC increased the survival to 42%, a 2-fold increase (Figure 3). Similarly, cotreatment with 10 mM GSH increased survival to 44%, a 2-fold increase (Figure 3). To test the protective effect of NAC and GSH on a sensitive strain, we selected *ubc13*, which displayed 9% survival when treated with 1.5 mM Mn^{2+}. Cotreatment with 20 mM NAC and 1.5 mM Mn^{2+} increased its survival to 28.5%, a 3-fold increase. Cotreatment with 1.5 mM Mn^{2+} and 10 mM GSH resulted in 74% survival, an 8.4-fold increase (Figure 3). It should be noted that

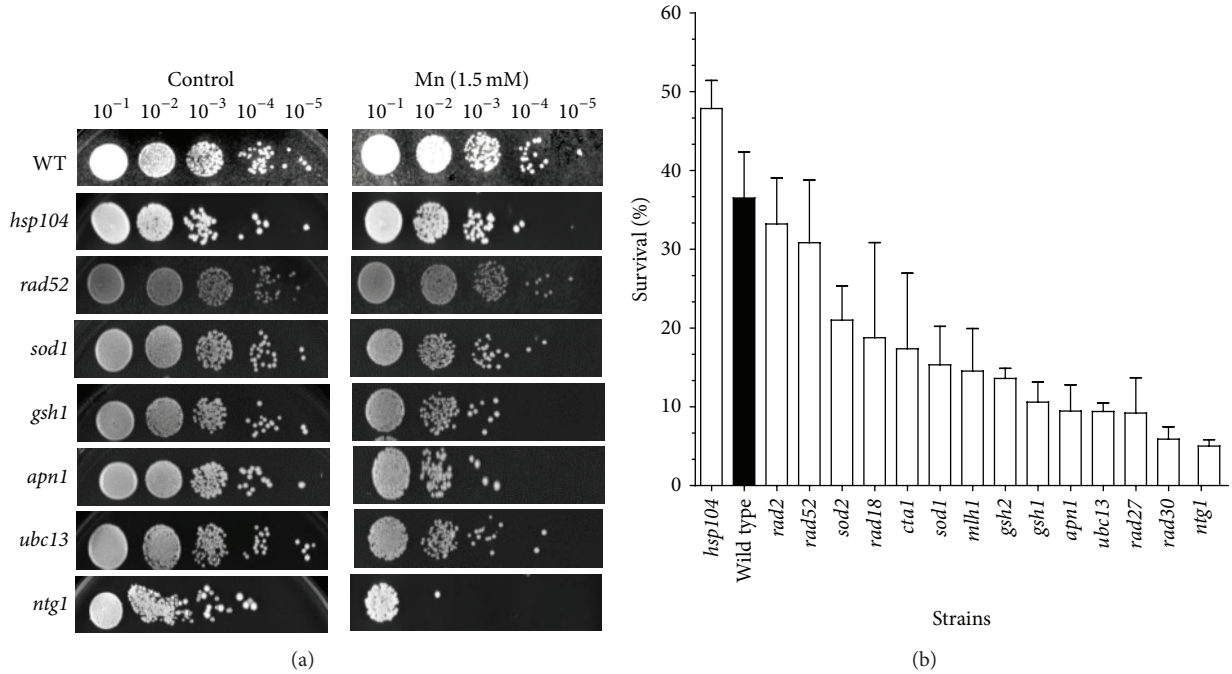

Figure 2: Sensitivity of yeast strains to Mn^{2+}. (a) The survival of the strains in 1.5 mM Mn^{2+} was determined as described in Section 2. Serial dilutions (1 : 10–1 : 10^5) of treated cultures were spotted on YPD plates. Growth was scored after 3 days of incubation at 30°C. The serial dilutions of the strains are shown. (b) Quantification of the survival of the tested strains. Survival was determined by counting the number of colonies in the respective dilutions and calculated based on the growth of strains not treated with Mn^{2+}. Strains are presented as being ordered from least to more sensitive. Wild-type strain is depicted by a black bar.

cotreatment with either NAC or GSH alone did not have an effect on the growth of *ubc13* or wild-type strains.

3.3. Analysis of the Mn^{2+}-Induced Mutator Phenotype of Yeast. The mutagenicity of Mn^{2+} has been extensively documented [19]. To determine the extent to which exposure to Mn^{2+} increases the accumulations of mutations and to quantify the increase in the mutation rate of wild-type yeast cells, we utilized the *CAN1* forward mutation assay [33], as described in Section 2. As shown in Figure 4, the mutation rate increased 12-fold (from 1.9×10^{-7} to 23.1×10^{-7}) when wild-type cells were treated with 1.5 mM Mn^{2+}. Based on the ability of antioxidants to reduce the toxicity of Mn^{2+} (Figure 3), we tested if cotreatment with NAC or GSH could also reduce the Mn^{2+}-induced increase of the mutation rate. In fact, 20 mM NAC reduced the mutation rate by 1.5-fold (from 23.1×10^{-7} to 15.5×10^{-7}), while 10 mM GSH reduced the mutation rate by 2-fold (from 23.1×10^{-7} to 11.8×10^{-7}), consistent with the ability of these antioxidants to reduce Mn-induced toxicity (Figure 3).

3.4. Mutation Spectrum of CAN-Resistant Mutants. The *CAN1* forward mutations assay provides a useful tool to identify the nature of the mutations that are generated from Mn^{2+} exposure. For this purpose, we amplified the *CAN1* gene from canavanine-resistant colonies treated with 1.5 mM Mn^{2+} and completely sequenced the ORF to identify the mutation. Table 2 shows the spectrum of mutations of 20 independent canavanine-resistant colonies. A single mutation was identified in each isolate. Mutations are indicated first by the original base, its numerical sequence position, followed by the mutant base. The majority (70%) of the mutations were base-substitution mutations with 40% (8/20) being transitions and 30% transversions (6/20). The rest (30%) were frameshift mutations, of which 10% (2/20) were insertions and 20% (4/20) were deletions of single nucleotides at the position indicated. No complex mutations such as large deletions, insertions, duplications, or gross chromosomal rearrangements were found. No hotspot was found, although some base-substitution mutations were observed twice (G1196A, G1555A and A1417T; Table 2).

3.5. Mn^{2+}-Induced Reversion Mutations in the lys2-10A Allele Which Can Be Reduced by Mg^{2+}. The Mn^{2+}-induced accumulation of frameshift mutations prompted us to investigate if Mn^{2+} may be promoting polymerase slippage. For this purpose, we treated a yeast strain carrying the *lys2-10A* allele, where the *LYS2* gene has a mononucleotide run of 10 adenines resulting in an out-of-frame gene, which can be restored by a frameshift mutation. We observed a dose-dependent increase in the mutation rate of this strain with increasing concentrations of Mn^{2+} (Figure 5(a)). Even at low concentrations of Mn^{2+} (0.25 mM), the mutation rate increased by 13-fold (from 2.1×10^{-6} to 27.8×10^{-6}) and was 30-fold (2.1×10^{-6} to 62.3×10^{-6}) and 76-fold (2.1×10^{-6} to 160×10^{-6}) higher at 1.5 mM and 3 mM concentrations of Mn^{2+}, respectively (Figure 5(a)). To determine if Mn^{2+} was

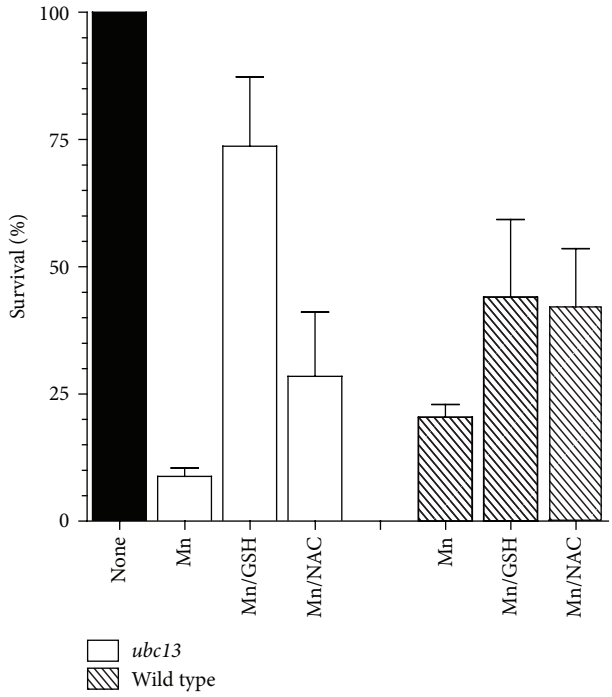

Figure 3: Attenuation of the cytotoxic effect of Mn^{2+} by exogenous antioxidants. Sensitive strain *ubc13* was treated with 1.5 mM Mn^{2+}, 1.5 mM Mn^{2+} plus 10 mM glutathione (GSH), and 1.5 mM Mn^{2+} plus 20 mM N-acetylcysteine (NAC), as described in Section 2. Survival was determined relative to untreated strain (100% survival). Wild-type strain was treated with 2 mM Mn^{2+}, with or without cotreatment with GSH and NAC, as described in Section 2. At least 5 independent colonies were tested. Average survival plus standard deviation is shown.

Table 2: *CAN1* mutation spectrum of wild-type yeast exposed to Mn^{2+}.

Base substitution mutations	
Transitions (8/20)	Transversions (6/20)
G522A	A312T
G550A	A375C
C623T	T380G
G670A	A1417T (×2)
G1196A(×2)	A1645T
G1555A (×2)	
Frameshift mutations	
Insertions (2/20)	Deletions (4/20)
	C417
T740	T1143
T628	G1259
	G1474

displacing Mg^{2+} in the DNA synthesis reaction, we tested if exogenously added Mg^{2+} could both increase the survival of the strain as well as reduce its mutator phenotype. As shown in Figure 5(b), cotreatment of the strain with 1.5 mM Mn^{2+} and 10 mM Mg^{2+} significantly increased the survival to 100% (figure) and reduced the mutation rate by 2-fold (Figure 5(c)).

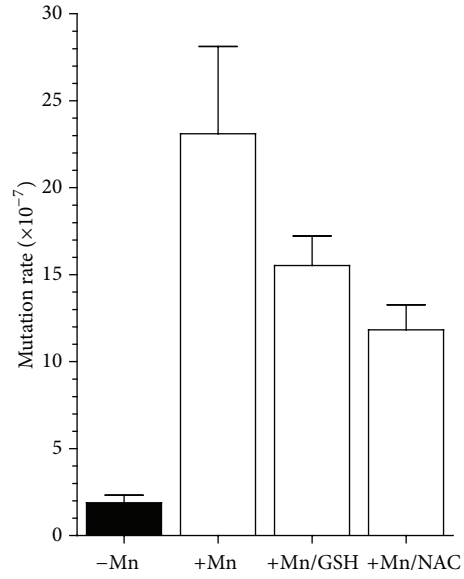

Figure 4: Effect of Mn^{2+} on the mutation rate of the *CAN1* forward mutation assay. The *CAN1* assay detects any mutation which inactivates the *CAN1* gene (arginine permease) and allows cells to grow on plates containing the toxic arginine analog, canavanine. The assay was performed using the wild-type strain in the presence of 1.5 mM Mn^{2+} or cotreated with 1.5 mM Mn^{2+} and 10 mM GSH or 1.5 mM Mn^{2+} and 10 mM NAC as indicated. Appearance of colonies on canavanine containing plates is scored and mutation rates are determined as described in Section 2. and standard deviation is included at the top of each bar.

4. Discussion

Manganese is an essential trace metal required for normal physiological function. However, excess Mn exposure is associated with several disease states. Significant research focuses on chronic exposure to Mn which has been shown to cause manganism [10], a neurological disease referred to as idiopathic Parkinson's disease (IPD) that presents symptoms resembling the dystonic movement associated with Parkinson's disease (PD) [11–13]. Numerous studies suggest that the neurotoxicity as a result of Mn exposure is a consequence of a variety of factors including apoptosis, oxidative injury, DNA damage, mitochondrial dysfunction, and neuroinflammation [14–18]. Of particular interest is the mutagenicity of Mn. Despite extensive knowledge of the DNA damaging properties of Mn, little is known about the pathways involved in the response and repair of Mn-induced DNA damage.

In the present work, we investigate the contribution of various DNA repair pathways to the survival of yeast cells exposed to Mn toxicity. We selected mutant strains in key components of the major DNA repair pathways, as described in Table 2. Initial observation indicates that yeast cells are relatively tolerant to Mn^{2+}, displaying reduced viability only when concentrations reach over 1 mM (Figure 2), which is several orders of magnitude higher than for other metals, such as Cd^{2+}, which is toxic at the μM level [31]. Interestingly, the sensitivity of yeast cells to Mn^{2+} is almost complete when

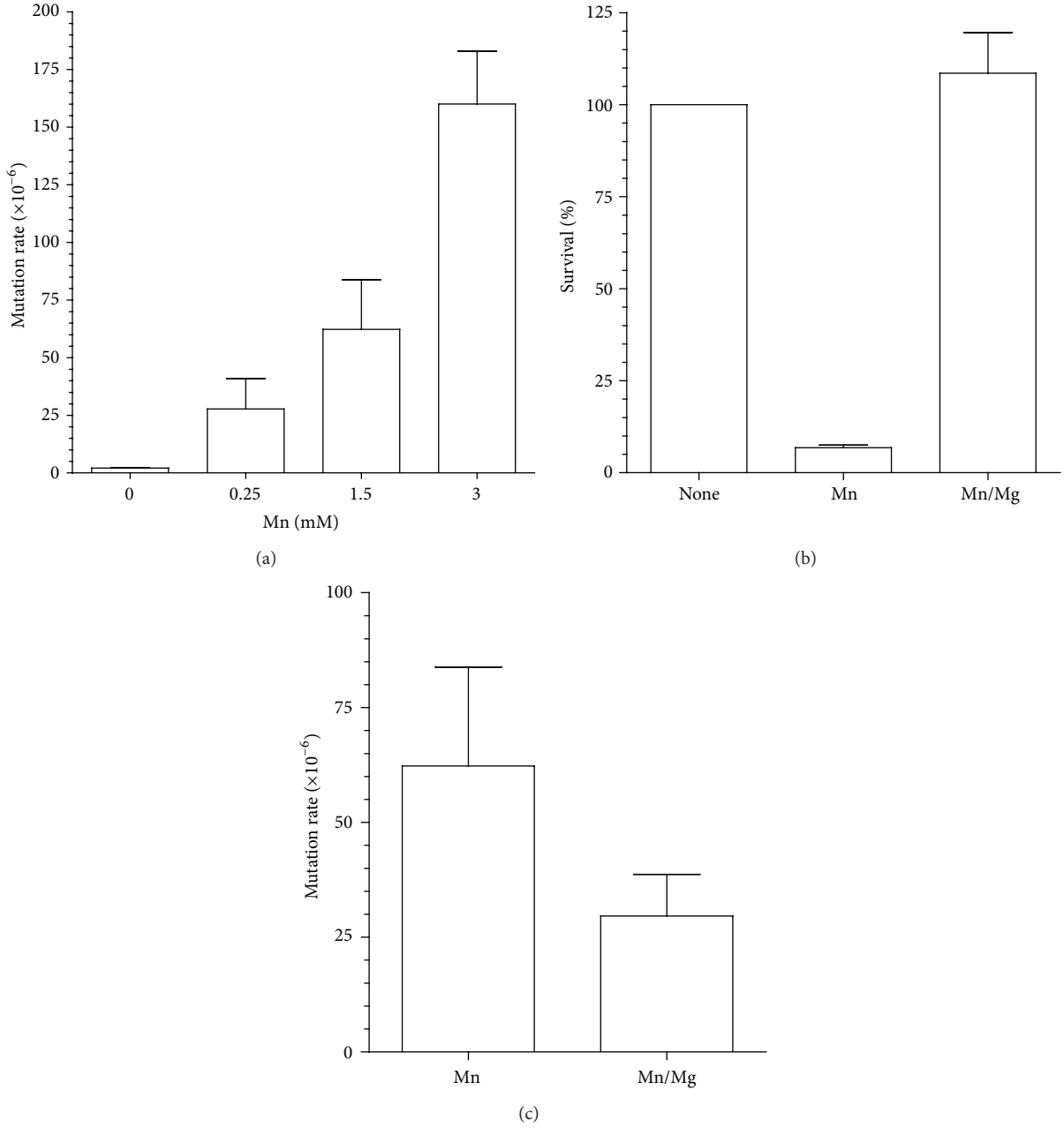

FIGURE 5: Effect of Mn^{2+} and Mg^{2+} on the mutation rate of the reversion of the *lys2-10A* allele. (a) Mutation rates determination by the yeast mutator assay using a strain carrying the *lys2-10A* allele was performed in the presence of increasing concentrations of Mn^{2+}. The appearance of Lys^+ revertant colonies indicates a mutator phenotype. Rates are calculated as described in Section 2 and standard deviation is included at the top of each bar. (b) Cotreatment with 10 mM Mg^{2+} protects cells from the toxicity of Mn^{2+}. Survival was determined as described in Section 2. (c) Cotreatment with 10 mM Mg^{2+} reduces the accumulation of mutations on the *lys2-10A* allele induced by 1.5 mM Mn^{2+}. Each bar corresponds to the average of three sets of experiments using five independent colonies per set.

the concentration of Mn^{2+} reaches 2.5 mM (Figure 2) displaying a linear response within this concentration window. For this reason, the strain comparison was performed at the 1.5 mM concentration. All strains displayed varying degrees of sensitivity, and all except the *hsp104* strain, were more sensitive than the wild type, suggesting that no significant toxic levels of protein aggregation are induced by Mn^{2+}.

Cells possess three major excision repair pathways: (i) base excision repair (BER) which is responsible for the repair of damaged bases resulting primarily from oxidative damage [34], (ii) nucleotide excision repair (NER) which plays a major role in the repair of large DNA adducts and UV damaged DNA [35, 36], and (iii) DNA mismatch repair (MMR), a postreplicative mechanism, improves the fidelity

of DNA replication by removing misincorporated bases by the DNA polymerase [37]. In addition, cells possess recombination repair, which in yeast is primarily performed by homologous recombination (HR) [38]. These pathways act in concert to respond to exogenous damage and guarantee genome stability. Some of these pathways have been shown to be defective in neurodegenerative diseases [39, 40] and participate in response to neurotoxic agents [41, 42]. Our data suggests that BER plays a major role in the cellular response to toxic levels of Mn^{2+} as mutants *apn1*, *rad27*, and *ntg1* were more than 4-fold sensitive to Mn^{2+} than wild type (Figure 2(b)) and *ntg1* was the most sensitive (7.5-fold). *NTG1* is a DNA N-glycosylase which removes the oxidized damaged base on both nuclear and mitochondrial DNA [43]. The DNA damage generated by Mn^{2+} appears to interfere with DNA replication, as indicated by the high sensitivity of strains *ubc13*, a DNA-damage-inducible gene, member of the error-free postreplication repair pathway [44], and *rad30* mutants, which are defective in translesion synthesis DNA polymerase eta, required for bypass synthesis at sites where replication forks are stalled due to damaged bases. Conversely, NER does not appear to play a major role in the repair of Mn^{2+}-induced DNA damage, as indicated by similar survival of *rad2* mutant to the wild type. Similarly, the lack of a strong Mn^{2+}-induced phenotype in the *rad52* strain suggests that no significant DNA damage is processed to DNA double-strand breaks, which requires homologous recombination for repair.

It appears that oxidative stress plays a major role in Mn^{2+} cytotoxicity as indicated by the increased sensitivity of the superoxide dismutase (*sod1* and *sod2*) and catalase mutants (*cta1*). This is further supported by the ability of NAC to improve the survival of the wild-type strain and the DNA repair strain *ubc13* (Figure 3). Exogenous addition of glutathione, which serves both as a reducing agent and a chelator to Mn, further protected the strains from Mn^{2+} exposure.

A significant increase in the accumulation of mutations was observed in cells exposed to Mn^{2+}, using two distinct mutator assays. The *CAN1* forward mutation assay indicated a 12-fold increase in the mutation rate when cells were exposed to 1.5 mM Mn^{2+}. Similar to the effect on survival, NAC and GSH reduced the increase in the mutation rate, suggesting that the mutations are at least the result of oxidative damage to DNA. Analysis of the mutations in the *CAN1* gene in these yeast cells indicates that most base substitutions are accumulated (70%), while 30% were frameshifts mutations. In combination with the increased mutation rate, cells exposed to Mn^{2+} have a significantly higher accumulation of frame shift mutations. This is distinct from spontaneous mutations (not exposed to Mn^{2+}), where 10% of the mutants analyzed had complex mutations [29, 45]. The increase in frameshift mutations was also observed when the mutation rate was measured using the *lys2-10A* allele. This increase was dose-dependent and ameliorated by Mg^{2+}, concomitant with an increase in cell survival. In fact, Mg^{2+} has been shown to protect cells from Mn^{2+} toxicity [46–48]. It is possible that the mutation rate increase is the result of Mn^{2+} intoxication of the DNA polymerase by displacing Mg^{2+} [21], which would require MMR for repair, explaining the increased sensitivity of the *mlh1* strain.

The adverse effect of Mn^{2+} in DNA polymerase fidelity has been previously reported [21] and proposed to be due to replacement of Mg^{2+}, which is essential in the reaction. However, recently, a series of studies have shown that some viral polymerases, such as those of coronavirus [49] and poliovirus [50], have exclusive requirement for Mn^{+2} in their synthetic activity. Similarly, the incorporation of nonnucleoside triphosphate analogs is accomplished by X family DNA polymerases in an Mn-dependent manner [51], while cellular error-prone DNA polymerase iota, isolated from tumor cells, was shown to utilize Mn^{2+} [52] in DNA synthesis. This is an interesting observation because DNA polymerase iota is inducible by Mn^{2+} and could in part contribute to the mutagenesis observed in Mn^{2+} exposed cells.

Most published work on the toxicity of manganese has focused on Mn^{2+}, while there was some claim that Mn^{3+} was the toxic species. However, recent work indicates that Mn^{3+} has a significantly reduced toxicity compared to Mn^{2+} [53, 54]. In addition, since manganese has a similar ionic radius to calcium, Mn^{2+} has been shown to interfere with Ca^{2+} metabolism [19, 55]. However, there are no reports of Ca^{2+} having an effect on BER.

The data presented in this study indicates that Mn^{2+}-induced DNA damage is in part due to oxidative stress and requires base excision repair. Considering the well-known relationship between DNA repair defects and neurodegenerative diseases, and the involvement of DNA repair in response to neurotoxic agents, the status of base excision repair, or some of its key components, may prove to be useful as biomarkers to determine the susceptibility to toxic damage from excess exposure to Mn^{2+}. There is currently a lack of well-validated biomarkers for manganese exposure. Manganese overexposure leads to cognitive, motor, behavioral effects in children [56] and manganese is associated with Parkinson's disease in adults [11–13]. Persons most likely to be exposed to excessive levels of manganese are manganese coal miners and welders. However, there is currently no way to determine who will suffer severe effects after Mn overexposure. Thus, preventive strategies and biomarker development for BER status are strongly supported by our findings. An assay that monitors the BER status of exposed individuals could be used in conjunction with other recently proposed biomarkers for Mn exposure which measure delta-amino levulinic acid levels [57] and the Mn/Fe ratio [58]. While these two biomarkers can detect exposure to Mn, an assay evaluating BER status would be of more value as a preventative strategy with its inherent potential to distinguish individuals who would be more severely affected by Mn exposure from those who would not.

Authors' Contribution

Adrienne P. Stephenson and Tryphon K. Mazu shared equally in this work.

Acknowledgments

The authors are grateful for the support provided by the Gene and Cell Manipulation Facility of Florida A&M University. This project was supported by the National Center for Research Resources and the National Institute of Minority Health and Health Disparities of the National Institutes of Health through Grant nos. 2 G12 RR003020 and 8 G12 MD007582-28. They appreciate the support from the following funding agencies: Association of Minority Health Professions Schools, Inc. (AMPHS) and the ATS/DR Cooperative Agreement no. 3U50TS473408-05W1/CFDA and no. 93.161 (RRR) NIEHS/ARCH 5S11ES01187-05 (RRR).

References

[1] J. R. Prohaska, "Functions of trace elements in brain metabolism," *Physiological Reviews*, vol. 67, no. 3, pp. 858–901, 1987.

[2] L. S. Hurley, "The roles of trace elements in foetal and neonatal development," *Philosophical Transactions of the Royal Society B*, vol. 294, pp. 145–152, 1981.

[3] L. S. Hurley, C. L. Keen, and D. L. Baly, "Manganese deficiency and toxicity: effects on carbohydrate metabolism in the rat," *NeuroToxicology*, vol. 5, no. 1, pp. 97–104, 1984.

[4] F. C. Wedler, "3 Biological significance of manganese in mammalian systems," *Progress in Medicinal Chemistry*, vol. 30, pp. 89–133, 1993.

[5] US Environmental Protection Agency, "National Center for Environmental Assessment," 1999.

[6] US Department of Health and Human Services, *Toxicological Profile for Manganese*, The Agency for Toxic Substances and Disease Registry, Ed., US Department of Health and Human Services, Atlanta, Ga, USA, 1992.

[7] L. E. Gray Jr. and J. W. Laskey, "Multivariate analysis of the effects of manganese on the reproductive physiology and behavior of the male house mouse," *Journal of Toxicology and Environmental Health*, vol. 6, no. 4, pp. 861–867, 1980.

[8] D. Mergler and M. Baldwin, "Early manifestations of manganese neurotoxicity in humans: an update," *Environmental Research*, vol. 73, no. 1-2, pp. 92–100, 1997.

[9] A. Wennberg, A. Iregren, G. Struwe, G. Cizinsky, M. Hagman, and L. Johansson, "Manganese exposure in steel smelters a health hazard to the nervous system," *Scandinavian Journal of Work, Environment and Health*, vol. 17, no. 4, pp. 255–262, 1991.

[10] M. Aschner and D. C. Dorman, "Manganese: pharmacokinetics and molecular mechanisms of brain uptake," *Toxicological Reviews*, vol. 25, no. 3, pp. 147–154, 2006.

[11] T. R. Guilarte, "Manganese and Parkinson's disease: a critical review and new findings," *Environmental Health Perspectives*, vol. 118, no. 8, pp. 1071–1080, 2010.

[12] D. B. Calne, N.-S. Chu, C.-C. Huang, C.-S. Lu, and W. Olanow, "Manganism and idiopathic parkinsonism: similarities and differences," *Neurology*, vol. 44, no. 9, pp. 1583–1586, 1994.

[13] L. Normandin and A. S. Hazell, "Manganese neurotoxicity: an update of pathophysiologic mechanisms," *Metabolic Brain Disease*, vol. 17, no. 4, pp. 375–387, 2002.

[14] D. L. Stredrick, A. H. Stokes, T. J. Worst et al., "Manganese-induced cytotoxicity in dopamine-producing cells," *NeuroToxicology*, vol. 25, no. 4, pp. 543–553, 2004.

[15] C.-J. Chen and S.-L. Liao, "Oxidative stress involves in astrocytic alterations induced by manganese," *Experimental Neurology*, vol. 175, no. 1, pp. 216–225, 2002.

[16] K. Seth, A. K. Agrawal, I. Date, and P. K. Seth, "The role of dopamine in manganese-induced oxidative injury in rat pheochromocytoma cells," *Human and Experimental Toxicology*, vol. 21, no. 3, pp. 165–170, 2002.

[17] C. G. Worley, D. Bombick, J. W. Allen, R. Lee Suber, and M. Aschner, "Effects of manganese on oxidative stress in CATH.a cells," *NeuroToxicology*, vol. 23, no. 2, pp. 159–164, 2002.

[18] A. P. Stephenson, J. A. Schneider, B. C. Nelson et al., "Manganese-induced oxidative DNA damage in neuronal SH-SY5Y cells: attenuation of thymine base lesions by glutathione and N-acetylcysteine," *Toxicology Letters*, vol. 218, pp. 299–307, 2013.

[19] G. B. Gerber, A. Léonard, and P. Hantson, "Carcinogenicity, mutagenicity and teratogenicity of manganese compounds," *Critical Reviews in Oncology/Hematology*, vol. 42, no. 1, pp. 25–34, 2002.

[20] M. de Meo, M. Laget, M. Castegnaro, and G. Dumenil, "Genotoxic activity of potassium permenganate in acidic solutions," *Mutation Research*, vol. 260, no. 3, pp. 295–306, 1991.

[21] R. A. Beckman, A. S. Mildvan, and L. A. Loeb, "On the fidelity of DNA replication: manganese mutagenesis in vitro," *Biochemistry*, vol. 24, no. 21, pp. 5810–5817, 1985.

[22] P. Olivier and D. Marzin, "Study of the genotoxic potential of 48 inorganic derivatives with the SOS chromotest," *Mutation Research/Genetic Toxicology*, vol. 189, no. 3, pp. 263–269, 1987.

[23] A. Orgel and L. E. Orgel, "Induction of mutations in bacteriophage T4 with divalent manganese," *Journal of Molecular Biology*, vol. 14, no. 2, pp. 453–457, 1965.

[24] A. Putrament, H. Baranowska, and W. Prazmo, "Induction by manganese of mitochondrial antibiotic resistance mutations in yeast," *Molecular and General Genetics*, vol. 126, no. 4, pp. 357–366, 1973.

[25] W. Prazmo, E. Balbin, and H. Baranowska, "Manganese mutagenesis in yeast. II. Conditions of induction and characteristics of mitochondrial respiratory deficient Saccharomyces cerevisiae mutants induced with manganese and cobalt," *Genetical Research*, vol. 26, no. 1, pp. 21–29, 1975.

[26] J. Bornhorst, F. Ebert, A. Hartwig, B. Michalke, and T. Schwerdtle, "Manganese inhibits poly(ADP-ribosyl)ation in human cells: a possible mechanism behind manganese-induced toxicity?" *Journal of Environmental Monitoring*, vol. 12, no. 11, pp. 2062–2069, 2010.

[27] D. R. Marzin and H. V. Phi, "Study of the mutagenicity of metal derivatives with Salmonella typhimurium TA102," *Mutation Research*, vol. 155, no. 1-2, pp. 49–51, 1985.

[28] E. Alani, R. A. G. Reenan, and R. D. Kolodner, "Interaction between mismatch repair and genetic recombination in Saccharomyces cerevisiae," *Genetics*, vol. 137, no. 1, pp. 19–39, 1994.

[29] D. X. Tishkoff, N. Filosi, G. M. Gaida, and R. D. Kolodner, "A novel mutation avoidance mechanism dependent on S. cerevisiae RAD27 is distinct from DNA mismatch repair," *Cell*, vol. 88, no. 2, pp. 253–263, 1997.

[30] H. Flores-Rozas and R. D. Kolodner, "The Saccharomyces cerevisiae MLH3 gene functions in MSH3-dependent suppression of frameshift mutations," *Proceedings of the National Academy of Sciences of the United States of America*, vol. 95, no. 21, pp. 12404–12409, 1998.

[31] S. Banerjee and H. Flores-Rozas, "Cadmium inhibits mismatch repair by blocking the ATPase activity of the MSH2-MSH6 complex," *Nucleic Acids Research*, vol. 33, no. 4, pp. 1410–1419, 2005.

[32] G. T. Marsischky, N. Filosi, M. F. Kane, and R. Kolodner, "Redundancy of Saccharomyces cerevisiae MSH3 and MSH6 in MSH2-dependent mismatch repair," *Genes and Development*, vol. 10, no. 4, pp. 407–420, 1996.

[33] K. Ekwall and T. Ruusala, "Budding yeast CAN1 gene as a selection marker in fission yeast," *Nucleic Acids Research*, vol. 19, no. 5, p. 1150, 1991.

[34] G. L. Dianov and U. Hubscher, "Mammalian base excision repair: the forgotten archangel," *Nucleic Acids Research*, vol. 41, pp. 3483–3490, 2013.

[35] K. Diderich, M. Alanazi, and J. H. J. Hoeijmakers, "Premature aging and cancer in nucleotide excision repair-disorders," *DNA Repair*, vol. 10, no. 7, pp. 772–780, 2011.

[36] K. Sugasawa, "Regulation of damage recognition in mammalian global genomic nucleotide excision repair," *Mutation Research*, vol. 685, no. 1-2, pp. 29–37, 2010.

[37] B. D. Preston, T. M. Albertson, and A. J. Herr, "DNA replication fidelity and cancer," *Seminars in Cancer Biology*, vol. 20, no. 5, pp. 281–293, 2010.

[38] R. Amunugama and R. Fishel, "Homologous recombination in eukaryotes," *Progress in Molecular Biology and Translational Science*, vol. 110, pp. 155–206, 2012.

[39] J. J. Reynolds and G. S. Stewart, "A single strand that links multiple neuropathologies in human disease," *Brain*, vol. 136, pp. 14–27, 2013.

[40] D. K. Jeppesen, V. A. Bohr, and T. Stevnsner, "DNA repair deficiency in neurodegeneration," *Progress in Neurobiology*, vol. 94, no. 2, pp. 166–200, 2011.

[41] I. I. Kruman, G. I. Henderson, and S. E. Bergeson, "DNA damage and neurotoxicity of chronic alcohol abuse," *Experimental Biology and Medicine*, vol. 237, pp. 740–747, 2012.

[42] K. Doi, "Mechanisms of neurotoxicity induced in the developing brain of mice and rats by DNA-damaging chemicals," *Journal of Toxicological Sciences*, vol. 36, no. 6, pp. 695–712, 2011.

[43] I. Alseth, L. Eide, M. Pirovano, T. Rognes, E. Seeberg, and M. Bjørås, "The Saccharomyces cerevisiae homologues of endonuclease III from Escherichia coli, Ntg1 and Ntg2, are both required for efficient repair of spontaneous and induced oxidative DNA damage in yeast," *Molecular and Cellular Biology*, vol. 19, no. 5, pp. 3779–3787, 1999.

[44] J. Brusky, Y. Zhu, and W. Xiao, "UBC13, a DNA-damage-inducible gene, is a member of the error-free postreplication repair pathway in Saccharomyces cerevisiae," *Current Genetics*, vol. 37, no. 3, pp. 168–174, 2000.

[45] P. J. Lau, H. Flores-Rozas, and R. D. Kolodner, "Isolation and characterization of new proliferating cell nuclear antigen (POL30) mutator mutants that are defective in DNA mismatch repair," *Molecular and Cellular Biology*, vol. 22, no. 19, pp. 6669–6680, 2002.

[46] K. J. Blackwell, J. M. Tobin, and S. V. Avery, "Manganese uptake and toxicity in magnesium supplemented and unsupplemented Saccharomyces cerevisiae," *Applied Microbiology and Biotechnology*, vol. 47, no. 2, pp. 180–184, 1997.

[47] R. Malcová, M. Gryndler, and M. Vosátka, "Magnesium ions alleviate the negative effect of manganese on Glomus claroideum BEG23," *Mycorrhiza*, vol. 12, no. 3, pp. 125–129, 2002.

[48] A. Peters, S. Lofts, G. Merrington, B. Brown, W. Stubblefield, and K. Harlow, "Development of biotic ligand models for chronic manganese toxicity to fish, invertebrates, and algae," *Environmental Toxicology and Chemistry*, vol. 30, no. 11, pp. 2407–2415, 2011.

[49] D. G. Ahn, J. K. Choi, D. R. Taylor, and J. W. Oh, "Biochemical characterization of a recombinant SARS coronavirus nsp12 RNA-dependent RNA polymerase capable of copying viral RNA templates," *Archives of Virology*, vol. 157, pp. 2095–2104, 2012.

[50] S. Crotty, D. Gohara, D. K. Gilligan, S. Karelsky, C. E. Cameron, and R. Andino, "Manganese-dependent polioviruses caused by mutations within the viral polymerase," *Journal of Virology*, vol. 77, no. 9, pp. 5378–5388, 2003.

[51] E. Crespan, S. Zanoli, A. Khandazhinskaya et al., "Incorporation of non-nucleoside triphosphate analogues opposite to an abasic site by human DNA polymerases β and λ," *Nucleic Acids Research*, vol. 33, no. 13, pp. 4117–4127, 2005.

[52] A. V. Lakhin, A. S. Efremova, I. V. Makarova et al., "Effect of Mn(II) on the error-prone DNA polymerase iota activity in extracts from human normal and tumor cells," *Molecular Genetics, Microbiology and Virology*, vol. 28, no. 1, pp. 1–7, 2013.

[53] P. Huang, G. Li, C. Chen et al., "Differential toxicity of Mn^{2+} and Mn^{3+} to rat liver tissues: oxidative damage, membrane fluidity and histopathological changes," *Experimental and Toxicologic Pathology*, vol. 64, no. 3, pp. 197–203, 2012.

[54] T. E. Gunter, C. E. Gavin, M. Aschner, and K. K. Gunter, "Speciation of manganese in cells and mitochondria: a search for the proximal cause of manganese neurotoxicity," *NeuroToxicology*, vol. 27, no. 5, pp. 765–776, 2006.

[55] A. Pinsino, M. C. Roccheri, C. Costa, and V. Matranga, "Manganese interferes with calcium, perturbs ERK signaling, and produces embryos with no skeleton," *Toxicological Sciences*, vol. 123, no. 1, pp. 217–230, 2011.

[56] S. Zoni and R. G. Lucchini, "Manganese exposure: cognitive, motor and behavioral effects on children: a review of recent findings," *Current Opinion in Pediatrics*, vol. 25, pp. 255–260, 2013.

[57] V. Andrade, M. L. Mateus, M. C. Batoreu, M. Aschner, and A. P. Dos Santos, "Urinary delta-ALA: a potential biomarker of exposure and neurotoxic effect in rats co-treated with a mixture of lead, arsenic and manganese," *Neurotoxicology*, vol. 38, pp. 33–41, 2013.

[58] W. Zheng, S. X. Fu, U. Dydak, and D. M. Cowan, "Biomarkers of manganese intoxication," *NeuroToxicology*, vol. 32, no. 1, pp. 1–8, 2011.

Hindawi Publishing Corporation
BioMed Research International
Volume 2013, Article ID 891391, 9 pages
http://dx.doi.org/10.1155/2013/891391

Research Article

Practical Guidance for Implementing Predictive Biomarkers into Early Phase Clinical Studies

Matthew J. Marton and Russell Weiner

Merck Research Laboratories, Clinical Biomarkers and Diagnostics Laboratory, 126 E. Lincoln Avenue, Rahway, NJ 07065, USA

Correspondence should be addressed to Matthew J. Marton; matthew_marton@merck.com

Received 28 June 2013; Accepted 11 September 2013

Academic Editor: Sudhish Mishra

The recent U.S. Food and Drug Administration (FDA) coapprovals of several therapeutic compounds and their companion diagnostic devices (FDA News Release, 2011, 2013) to identify patients who would benefit from treatment have led to considerable interest in incorporating predictive biomarkers in clinical studies. Yet, the translation of predictive biomarkers poses unique technical, logistic, and regulatory challenges that need to be addressed by a multidisciplinary team including discovery scientists, clinicians, biomarker experts, regulatory personnel, and assay developers. These issues can be placed into four broad categories: sample collection, assay validation, sample analysis, and regulatory requirements. In this paper, we provide a primer for drug development teams who are eager to implement a predictive patient segmentation marker into an early clinical trial in a way that facilitates subsequent development of a companion diagnostic. Using examples of nucleic acid-based assays, we briefly review common issues encountered when translating a biomarker to the clinic but focus primarily on key practical issues that should be considered by clinical teams when planning to use a biomarker to balance arms of a study or to determine eligibility for a clinical study.

1. Introduction

At many biopharmaceutical companies, predictive biomarker assays are developed and validated either internally or externally with partner companies with expertise in molecular analyses. In either case, a multidisciplinary internal biomarker team will be needed to define assay requirements, select a diagnostic company partner, develop a workplan, and oversee the assay development and validation processes (reviewed in [1]). The team typically includes representatives from various departments, such as preclinical development, the clinical therapeutic area, Program management, Regulatory Affairs, clinical statistics, and Companion Diagnostics. Regular team meetings are highly recommended and are intended in part to facilitate communication and to ensure the team is able to adapt to both major changes (such as a change in clinical development timeline or target indication) and minor changes (such as changes to the list of clinical sites or to the specimen collection method) that may affect assay development or validation.

2. Sample Collection Considerations

2.1. Sample Collection Method. After the identification of the biomarker and the source tissue from which the predictive biomarker will be assayed, the next most important consideration is how the sample will be collected and preserved in the clinical setting. Four key guiding principles are the following: (1) the collection method should utilize noninvasive or minimally invasive techniques (e.g., blood, plasma, and hair follicles) instead of more invasive techniques (e.g., tissue biopsies), if possible, (2) the amount of specimen requested should be minimized, yet be sufficient for analysis and possible retesting of the specimen, (3) the collection and preservation method should be demonstrated to be technically and logistically feasible in a clinical setting before planning its use in a clinical study, and (4) the collection method should preserve the sample quality quickly and not introduce a sample collection bias, especially when the analyte is labile or sensitive to subtle changes in temperature or handling conditions. The final procedure for collecting,

processing, storing, and shipping the clinical samples is typically documented in a Procedures Manual (also called Operations Manual), which is a set of detailed instructions for clinical sites and the central laboratory and which typically is a collaborative effort between the assay developer and the clinical research associate. Since the Procedures Manual is usually needed 1–3 months before the first patient is enrolled, it is important to establish the details of the collection method early in the process, typically during clinical protocol development. For common sample collection procedures, a standard method may already exist in the company's method repository, complete with a supply list and site training materials. However, for unusual methods or novel specimen types, or if multiple analytes need to be measured from the same specimen, the team should allow several months for the development and validation of a novel collection method that is appropriate for the clinic. For example, a recent protocol in our laboratory required from the same sample the analysis of multiple biomarkers (RNA, DNA, and protein) including one predictive biomarker to identify eligible patients. Because RNA is more labile than the other analytes, it was important to stabilize the RNA-based pharmacodynamic biomarker first, even though it was less crucial than the DNA-based patient selection biomarker and exploratory protein-based biomarker. This required the development of a complicated collection method in which the sample was split, one half immediately placed into preservative while the other was further processed. This also highlights the need for clinical biomarker teams to prioritize the desired biomarkers if the amount of specimen available becomes limiting. For complicated or unusual procedures done at the clinical site, it may be necessary to train personnel at the clinical site in person or to create visual aids for training (such as videos, slide presentations, and operations cards) and to perform a pilot experiment to qualify a site to do the procedure.

2.2. Importance of Retaining Samples for Potential Bridging Studies. In some programs, late phase studies may be supported using a clinical trial assay (CTA; see Table 1 for definitions), even though the drug will require an *in vitro* diagnostic (IVD) device at product launch. This might occur when a clinical team wants to quickly transition from a promising phase II study that used a CTA to a pivotal phase III study before the companion diagnostic is in its final form. In that case, it may be necessary to "bridge" results from the CTA or other prototype assays to the final assay by reanalyzing the samples using the assay in its final IVD configuration to support the diagnostic device Pre-Market Approval (PMA) filing. As discussed below in the Regulatory Considerations section, companion diagnostic teams should avoid relying on a bridging strategy if at all possible. But when this is necessary, it will be crucial to plan, even for early phase studies, to obtain enough samples so that some can be stored and then reanalyzed using the version of the assay that will be submitted for health authority approval. There are many challenges with a bridging approach. First, if the samples are stored prior to sample analysis, auditable chain-of-custody documentation and rigorous sample stability studies are likely to be required. This can be a significant amount of work, and it likely means that merely storing samples for bridging studies in a good laboratory practice (GLP) environment will be insufficient. Second, sample banking and retention can also be challenging since the FDA requires that 90–95% of samples be available for retesting if using the data to support a PMA filing. Third, and most significantly, discordant results between the CTA and the final assay are inevitable and introduce risk into the device approval, since unexplained discordant results could cause regulatory authorities to question the technical performance of the diagnostic device.

2.3. Special Considerations for Formalin-Fixed Slide-Based Assays. Use of formalin-fixed paraffin-embedded (FFPE) tissue in a predictive biomarker assay introduces additional challenges, one of which is ensuring the stability of the analyte after sectioning until the sample is analyzed. This is a significant concern for immunohistochemical (IHC) assays since protein stability can vary considerably depending on the analyte [2]. If the analyte is unstable, variability in the time in storage or shipment can confound analytical results. Ideally, clinical sites would submit an entire block for the analysis so that the central lab can complete the sectioning and then perform the sample analysis in a controlled timeframe. However, this may not be possible, either because the original block cannot be found or because the site will not agree to send the entire block. If this is the case, it is recommended that a cut slide stability study be performed to assess the stability of the analyte in sectioned slides. If degradation of signal is observed in a timeframe less than that which is necessary to perform the analysis, it may be necessary to use freshly sectioned slides.

Another critical parameter for a FFPE-based patient selection assay, but one issue that sometimes is overlooked or given insufficient attention, is the minimum percent of tumor required for the assay. This can be difficult to determine empirically, but for prospective enrollment assays it is important to specify if there is a chance the CTA will progress to a companion diagnostic. For example, the cobas BRAF test only requires 5% tumor [3], whereas other assays specify a minimum of 30% tumor [4] or specify that specimens with tumor content below 50% should be macrodissected [5]. How percent of tumor is calculated should also be carefully defined, whether it will be by percent nuclei or percent area. When selecting clinical sites, teams should consider a site's ability to have slides marked by a licensed pathologist and its ability to perform macrodissection, in case that is necessary. When requesting FFPE sections, the best practice is to collect two additional sections (immediately before and after the section(s) being tested) that can be used for H&E staining to assess the tumor content and pathology of the sample analyzed. This is especially true for assays that require multiple sections (e.g., some RNA- or DNA-based assays require three 10-micron sections per assay).

2.4. Postcollection Handling and Shipping of Clinical Samples. The details of the postcollection handling and sample shipping conditions should not be overlooked. For assays that require specialized processing after collection, such as

Table 1: Definitions.

Clinical Trial Assay (CTA): a predictive biomarker assay that is either: (1) a prototype form of a planned IVD kit, or (2) a laboratory-developed test that will not be commercialized and sold as a kit to other labs. If the CTA is essential for safe and effective use of the drug, then it must be bridged to a companion diagnostic.
Laboratory-Developed Test (LDT): an *in vitro* diagnostic test that is developed, validated and used exclusively for in-house diagnostic purposes.
In vitro diagnostic (IVD): any "device" intended for use in the diagnosis of disease or other condition, or in the cure, mitigation, treatment, or prevention of disease, in man or other animals. These devices must be cleared by the FDA through either the 510 (k) premarket notification process or must be approved through the PreMarket Approval (PMA) processes [17].
Companion Diagnostic: an *in vitro* diagnostic device that provides information that is essential for the safe and effective use of a corresponding therapeutic product [17] and that will be commercialized along with the therapeutic. In general, this test must be clinically validated along with the drug in the registrational trials.
Investigational Use Only (IUO): a regulatory term for a medical device undergoing validation in a clinical trial. A companion diagnostic is labeled as IUO while used in a registrational clinical trial [15].

ex vivo cytokine induction or purification of peripheral blood mononuclear cells (PBMCs), two key variables that need to be optimized and controlled are the time between collection and processing and the shipping temperature [6]. The team will have to weigh several factors to decide whether these pre-analytical steps are performed locally or centrally. A central lab may have more carefully controlled procedures, but if the time needed to ship to the central lab can directly impact the biomarker, it may be necessary to consider the use of local labs. The challenge is that local labs frequently do not have the required expertise or equipment, and this likely means extra effort for training, on-site monitoring, and establishing quality-control procedures at each clinical site. (See the Sample Analysis Considerations section below for additional concerns about using local laboratories.) For highly sensitive, single cell-based assays such as ELI-spot assays, it may be possible to use cryopreserved samples but there is no shortcut to doing controlled sample shipping studies to determine whether whole blood can be used or whether samples should be cryopreserved prior to shipping. Shipping conditions can also affect the shipment of FFPE slides and blocks. Although they are typically shipped at ambient temperatures, samples preserved in paraffin are at risk for melting, especially in the summer months, due to hot seasonal weather or from high temperatures encountered in transit. The Centers for Disease Control and Prevention recommend that blocks or slides be shipped with a frozen gel ice-pack. For frozen specimens, it is reasonable to consider a combination of dry ice and frozen gel ice-packs if the shipment is expected to take more than several days, as the ice-packs will remain frozen after the dry ice has sublimated. The actual temperature experienced can be tracked by radio frequency identification (RFID-) enabled temperature-tracking devices that are built into a shipping container. Alternatively, low technology solutions, such as temperature indicator labels that change color if the temperature exceeds a preset limit, are an inexpensive investment to monitor the integrity of the clinical sample-containing shipment.

3. Assay Considerations

3.1. General. Analytical validation always starts with intended use (Figure 1). It drives the development of the assay analytical validation plan. It is a good idea to document the intended use in some controlled document, such as an Assay Charter, which should describe the assay, the assay output, how "positive" and "negative" calls are made, and how the results will be used to determine patient eligibility. When a predictive marker will be used to direct patient enrollment or to balance arms of a study, the assay will need to be performed in a Clinical Laboratory Improvement Amendments (CLIA) laboratory. Since clinical labs are also regulated at the state level, it is possible that a "CLIA-certified" lab may not be certified to analyze samples from certain states. Therefore, it is important to confirm that the lab has the necessary certifications from each state where patients will be enrolled and to allow sufficient time for a newly certified CLIA lab to obtain all the needed state licenses. Most CLIA labs follow Clinical and Laboratory Standards Institute (CLSI) guidelines for determination of standard assay parameters such as precision, accuracy, limit of detection, specificity, and reference range. Although it is not unique to predictive biomarker assays, obtaining clinical specimens for assay validation and the determination of interpatient variability of the study population is critical to the success of the assay. When it is necessary to establish a threshold, that is, the clinical decision point, for a quantitative continuous biomarker, obtaining appropriate validation samples is frequently the rate limiting step in assay validation, so it is wise for the team to establish the strategy (purchase commercially or collaborate, e.g.) for obtaining the samples early in the assay validation phase. The rest of this section will highlight some concerns specific to predictive biomarkers.

3.2. Clinical Trial Assay Development Timeline. It is important for the team to build adequate time into the schedule for assay development. The lead time for assay development and validation depends greatly on the assay platform and the complexity of the assay. This time could be as little as one month for an already-developed assay (e.g., a single prevalidated SNP TaqMan assay) to more than six months for a complex assay (e.g., multianalyte flow cytometry or microarray-based RNA expression signature) or for an assay that has not been deployed previously as a patient enrollment criterion. Even assays that may appear to be already validated

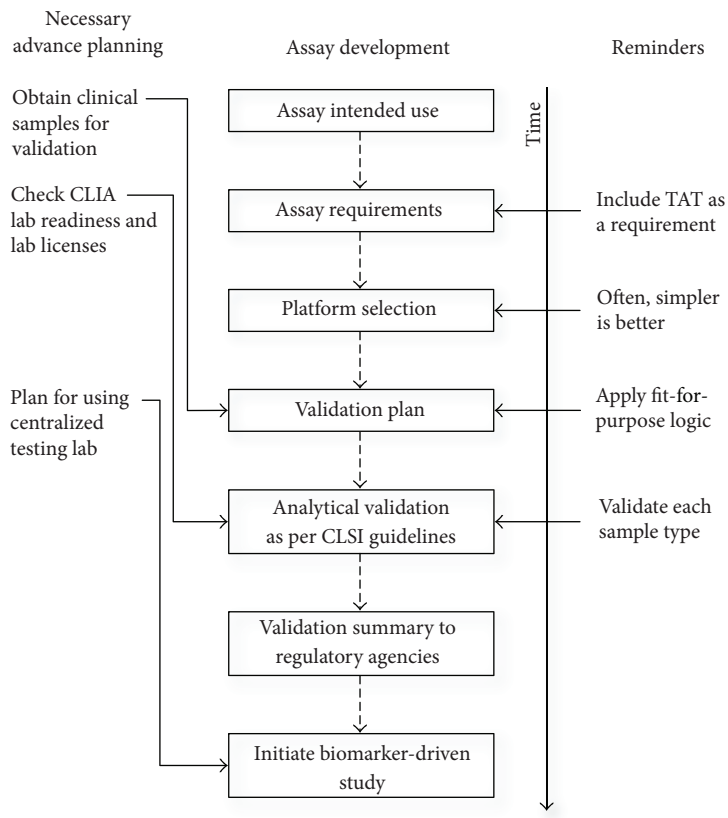

Figure 1: Schematic diagram of assay development activities. Development begins with defining the intended use, which is documented along with assay requirements. After platform selection, a validation plan is developed and executed according to CLSI guidelines. The validation summary is sent to the regulatory agencies prior to the initiation of the clinical study. Reminders discussed in the text are shown to the right. The relative timing of when steps that require advance planning should start is shown to the left.

can take a considerable amount of time to validate if the sample preservation method is changed. For example, when translating a microarray RNA expression signature from fresh frozen to FFPE specimens, different probes may need to be selected and validated, which essentially means that the assay has to be redeveloped before it can be validated [7]. Another factor that can impact assay timelines dramatically is the lead time for an agreement with a Testing Lab or diagnostic partner, which can easily add several additional months, especially if there are intellectual property issues to address. Finally, if the study plans to utilize a Testing Lab not previously used, the Testing Lab may need to undergo a more rigorous qualification or biosample handing audit for a predictive biomarker than may be necessary for other types of biomarkers.

3.3. Validation Strategy and Fit-for-Purpose Validation. The assay development team should propose a plan of how to validate the clinical trial assay in the CLIA lab to the rest of the team for its input and feedback and to ensure alignment on the project specifics (sample type, collection method and any unique aspects of the biomarker). It is important to note that even if a predictive biomarker assay is developed and validated internally, the analytical validation of the assay will most likely have to be repeated in the CLIA lab supporting the clinical study. If the clinical trial assay will be assayed from more than one tissue, each sample type (e.g., tumor tissue, plasma, and bone marrow) will need to be validated since the preservation method may influence analyte abundance. Even though the predictive biomarker assay will have to be performed in a regulated laboratory, the fit-for-purpose concept is still applicable. Thus, the nature of the clinical study (e.g., phase I, II) and the extent to which the biomarker proof-of-concept has been established is taken into account when devising the validation plan. For a phase I study, one must plan the appropriate level of validation while avoiding overinvesting in an assay for a compound with an uncertain future (most compounds in phase I fail). For example, a common principle in analytical validation is to validate each specific tissue type and the specific population expected in the clinical study. However, some early phase oncology studies enroll patients with any tumor type, that is, what is sometimes called an all-comers study. In such studies, it is impractical to validate every possible tumor type. Thus, the analytical validation strategy must not only consider what is practical and the scientific value of a rigorous validation of each tumor type but also the cost, since sample acquisition and assay development costs to validate each tumor type can easily exceed one million US dollars. Such flexibility, however, does

not apply to an *in vitro* diagnostic assay supporting a pivotal phase III study. In that case, every tumor type in the study must be analytically validated.

3.4. Assay Technology Selection and Assay Readout. There are significant tradeoffs between platforms when selecting the technology for a predictive biomarker assay, and some platforms are more technically difficult to validate than others. Take, for example, the choice of validating RNA expression levels by quantitative PCR (qPCR), microarrays, or next-generation sequencing. qPCR is more straightforward but becomes impractical when assaying many dozens of genes. One possible tradeoff is to reduce the number of genes in the RNA expression signature, even though this may introduce risk related to whether the smaller signature will be as predictive as the original, larger signature. Validation of a microarray or sequencing platform, on the other hand, is much more challenging but the breadth of data obtained offers the opportunity to refine the biomarker so that it is more predictive in a subsequent trial. The team will need to consider whether the benefit of one platform justifies the added complexity, especially if the platform is one that has not previously been used for predictive biomarkers. Even though several microarray-based RNA expression assays have been cleared by the FDA [8, 9], none have gone through the PMA process, and implementing them into a clinical protocol is still challenging currently. Thus, when there is a high confidence that the drug/assay combination will be successful and that a regulated device will be required, it may be wise to use the simplest technology. In this save vein, when developing one's own assay, it may be a good idea to avoid use of novel proprietary reagents or kits if there is concern about the supplier's ability to supply material consistently or to manufacture the material under GMP, which will be required if a companion diagnostic is required.

3.5. Using an FDA-Approved Diagnostic. Just because an assay is an FDA-cleared or FDA-approved *in vitro* diagnostic device does not mean that it is validated for use as a clinical trial assay. Just like any other predictive biomarker assay, it must be validated for the specific intended use, that is, specific tissue type, specific patient population, and specific collection method. For example, a *KRAS* mutation test was approved for testing FFPE specimens from colorectal cancer patients [10]. Although FDA-approved, this test cannot be used as a predictive marker for blood specimens or for other tissue types without validation of the specific tissue or collection method.

3.6. Next Generation Sequencing (NGS)-Based Predictive Biomarkers. The clinical application of massively parallel sequencing, usually called next generation sequencing, presents many technical, operational, and regulatory challenges that are specific to the technology. In the context of early phase drug studies, the type of NGS assay most commonly deployed is one designed to direct patient treatment by detecting tumor sample mutations in dozens to hundreds of cancer-related genes. Although several guidance documents addressing these cancer gene panel assays have been published recently [11], noticeably absent is an FDA Guidance Document that defines analytical validation requirements to ensure accuracy of mutation calls. Furthermore, since each laboratory or company may have its own mutation calling algorithm, this lack of clarity means there is no consensus on how to ensure the reliability of mutation calls. Thus, it is first imperative to fully define and understand the mutation detection pipeline and quality control steps being used, especially if working with an external partner. Furthermore, consistent with one guidance document [11], both analytical validation studies and clinically actionable mutation calls should be confirmed with an orthogonal mutation calling technology. Gene panels may be the most used assay now, but it will be only a short time until data from whole exon sequencing or RNA-sequencing (RNA-Seq) tests will be used as predictive biomarkers. These assays generate much more data and thus raise issues surrounding patient consent and independent review board (IRB) approvals. For example, RNA-Seq assays are likely to require the same patient consent and IRB approval as genetic profiling since RNA-Seq enables determination of single nucleotide polymorphisms (SNPs), some of which are clinically actionable because they are strongly associated with disease susceptibility or progression. Likewise, it will be necessary to put into place unambiguous policies that clearly explain that how patient data will be handled and reported, especially for unintended findings from NGS studies.

4. Sample Analysis Considerations

The primary considerations in the sample analysis arena are turnaround time (TAT), cost and whether to use a local laboratory.

4.1. Turnaround Time. When considering TAT, it is important to focus on the total TAT from the patient's perspective, not just the TAT to perform the assay or the logistics involved to get the sample to the Testing Lab. For example, if an assay requires a previously prepared diagnostic sample (such as a formalin-fixed, paraffin-embedded block), it may take several weeks to obtain the block for sample analysis from the local hospital if it was collected there. A TAT greater than two weeks may have an adverse effect on patient recruitment due to fierce competition for patients eligible for clinical studies and because some diseases (such as various leukemias) can progress very rapidly. Therefore, it is critical to understand how delays can impact the ultimate stakeholders, that is, patients and physicians. The clinical team should think through the logistic details of the end-to-end process, from sample acquisition, pathological analysis at the clinical site (H&E and/or macrodissection, if applicable), shipment to central laboratory (if applicable), shipment to CLIA laboratory, and workflow at the CLIA lab through the sending of the patient test report to the clinical site. It can be informative to ask the Testing Lab to provide a detailed hour-by-hour workflow of sample analysis as a way to spark discussions of how to reduce TAT. For mutation detection or

gene expression assays, depending on the assay, the Testing Lab may need up to 10 business days to perform the assay and report results. Assays that require macrodissection of FFPE slides may take even longer time. To expedite TAT, the team can consider (1) sending the specimen directly to the Testing Lab instead of first sending to a central lab for sample accounting, (2) asking the Testing Lab to accept Saturday shipments or work on weekends, or (3) asking the Testing Lab to arrange shifts to accommodate a longer workday. Although in some cases it may be worth establishing multiple Testing Labs in different geographic regions to reduce TAT, in general, this may not impact TAT unless overnight shipment from the clinical site to the Testing Lab is unavailable.

4.2. Use of Local Laboratories. When is it acceptable to use an assay performed at a local laboratory for patient eligibility decisions? In general, teams should use assays validated in a centralized Testing Lab instead of assays performed at local labs (e.g., hospital labs) for eligibility decisions. Performing the assay at the local lab may have the benefit of shorter TAT but can have the liability of having greater variability resulting from (1) different laboratory methods or instruments, (2) different validation standards and quality control processes, (3) different histopathological practices in the macrodissection of tumor from nontumor, and (4) lab-to-lab variability due to a subjective or difficult-to-standardize assay (e.g., IHC). These concerns even apply to common assays (such as *KRAS* and *EGFR* mutation detection and Ki-67 IHC) and may result in discordant results. For example, a 2006 study showed a high degree of discordance between HER2 IHC results from a centralized lab compared to data from local labs at clinical sites [12]. More recently, André et al. (2013) reported results of retrospective analyses of a phase II study in which local labs were used to detect *KRAS* mutations to determine colorectal cancer patient eligibility for treatment with an anti-EGFR antibody. The authors found that 6 of the 60 enrolled patients had *KRAS* mutations and should have been excluded from the study [13]. Furthermore, an international study to assess proficiency of 59 European Testing Labs for *KRAS* mutation detection found that 31% of labs made miscalls in at least 10% of the samples [14]. Another reason to avoid using a local laboratory is that it is very likely that the FDA will question the merging of data generated with two different assays to support a filing. Despite these caveats, there may be cases when the use of a local lab for clinical trial assay is acceptable: (1) when the team is sure it does not want to use the data to support drug efficacy, and (2) when the test is an approved *in vitro* diagnostic, for example, when a clinical study's eligibility criteria requires that a patient's tumor harbor certain mutations and there already exists an approved or cleared *in vitro* diagnostic. In general, the risks of using a local lab will usually outweigh the benefits. Thus, it is recommended that molecular pathological analysis be performed at a central lab rather than at the individual clinical sites.

4.3. Cost. The sample analysis cost for a complex predictive marker such as a RNA expression signature or a mutation detection panel in a clinical study can exceed $2000 per sample. Therefore, it is usually imperative that options be explored to reduce costs. This can be particularly challenging, especially for studies in which a clinical team expects that only a few patients will be enrolled per week or per month, which may mean that many samples will be analyzed individually. Therefore, teams should consider (and discuss with the FDA) alternate strategies for assay process controls to reduce the ratio of number of controls to number of samples. Also, if the Testing Lab assay time is 3 days or less, one should consider having the Testing Lab batch samples (e.g., only running the assay twice a week) if that would reduce cost while still providing acceptable TAT. Finally, if enrollment eligibility is dependent on two distinct predictive biomarkers assays, such as a qPCR assay and an IHC assay, one should consider whether there is an opportunity to perform the assays sequentially so that the second assay is performed only if the first indicates the patient is eligible.

4.4. Impact of Screen Failures on Enrollment. The clinical team should estimate and document the expected screen failure rate, and when projecting number of patients it will be necessary to screen, keeping in mind the difference between the percentage of patients deemed ineligible due to the test and the overall clinical study screen failure rate. The Testing Lab may need to know this number to adequately project the number of assays that will need to be performed and the amount of reagents that will need to be qualified. Doing this exercise early may help determine whether the enrollment strategy is appropriate and whether the clinical decision threshold (eligible/not eligible) is set appropriately.

5. Regulatory Considerations

5.1. Predictive Biomarker Tests Are under the Oversight of Centers for Medicare & Medicaid Services (CMS) and State Laws. U.S. Federal laws (CLIA '88) established quality standards for any laboratory that performs testing on human specimens for the purpose of diagnosing, or treating, or assessing patient health. Thus, predictive biomarker tests that are used to balance arms of a study or to select patients for enrollment into a clinical study are under the purview of both the CMS and the U.S. FDA. Labs must be CLIA-certified by the state in which they reside or by a CMS-approved accrediting institution such as the College of American Pathologists (CAP). In addition, some states have additional laws regulating in-state clinical laboratories or the analysis of their residents' samples, independent of where the analysis is conducted. Two states, New York and Washington, developed their own set of regulations for clinical labs, and CMS have deemed their states' clinical laboratories to have met CLIA requirements (i.e., they have been granted "deemed status") because CMS has judged their state-specific regulations as equal to or exceeding CLIA standards. These and other states (CA, FL, MD, RI, and PA) have various regulations that may require one or more of (1) in-person inspection, (2) approval of validation report, (3) approval of laboratory SOPs, (4) proof of adequate lab personnel training and (5) lab

Table 2: Predictive biomarker checklist.

	Team formation
□	Form team; include representatives from assay development, clinical therapeutic area, program management, regulatory affairs and clinical statistics
□	Establish regular team meetings
	Sample collection considerations
□	Determine source tissue for biomarker analysis
□	Minimize amount of specimen required; use non-invasive techniques if possible
□	Allow 1–3 months if sample collection method does not exist
□	Train personnel at clinical site, if needed; create visual aids for training
□	Retain extra specimens for potential bridging studies
□	If utilizing a bridging strategy, initiate sample stability studies
□	If using FFPE specimens, establish minimum percent tumor specification
□	Select clinical sites with licensed pathologist able to mark slides and perform macrodissection
□	Collect extra sections before and after sections being analyzed for H&E staining
□	Perform sample collection experiment to qualify each clinical site, if necessary
	Assay considerations
□	Clearly define and document assay intended use, how positive and negative calls are made and how results determine patient eligibility
□	Select assay technology platform, consider assay output, establish clear requirements
□	Develop validation strategy, validating each sample type or collection method
□	Allow several months to complete vendor agreement
□	Allow time for vendor qualification, if new vendor
□	Obtain clinical specimens for analytical validation and decision-point threshold
□	Allow 1–6 months for assay development for a CTA; at least 24 months for a IVD
	Sample analysis considerations
□	Document anticipated turn around time from patients' perspective
□	Document sample logistics from acquisition to patient test report
□	Request hour-by-hour workflow of assay from vendor
□	Have clinical site send specimen directly to testing lab if possible
□	Ask vendor to accept Saturday shipments, to work weekends or to work longer days
□	Avoid the use of local labs
□	Reduce cost by batching samples, for example, biweekly sample analysis
□	Explore alternate control strategies to reduce cost of running process controls
□	Consider performing assays sequentially if using multiple predictive markers
□	Calculate and document anticipated screen failure rate
	Regulatory considerations
□	Identify CLIA lab with appropriate state licenses or allow 1–6 months for lab to obtain necessary licenses
□	Discuss high complexity assays with FDA before implementing in clinical trials
□	Set up pre-submission meeting with FDA in advance of clinical trial
□	For companion diagnostic development, work closely with partner on timelines

management background checks. These regulations are put in place to protect patients treated in those states, so it matters more where the patients are treated than where the test is performed. New York, California, and Florida are known to have the strictest regulations, so if a planned clinical site is located in one of these states, the team must ensure the Testing Lab has those state certifications. It must be noted that in some cases there is some ambiguity on whether these state-specific regulations apply to clinical studies; the conservative approach is to ensure the lab has the state certification. The practical advice on this point is to engage the laboratory early and to realize that licensure may take up to 6 months. Also, although CLIA applies to laboratories located within the United States, Testing Labs outside the U.S. can request CLIA

certification from various accrediting bodies if they plan to test samples from US citizens.

5.2. Predictive Biomarker Tests Are Laboratory-Developed Tests (LDTs) and Are under the Oversight of the FDA. Historically, LDTs were primarily niche assays, that is, highly specialized, low volume tests that were developed and validated in one clinical laboratory and which were not carefully monitored by the FDA. In FDA language, the FDA exercised enforcement discretion. Today, however, many clinical laboratories have developed predictive biomarker tests that are being used to direct patient treatment. A 2011 guidance document [15] and recent public statements from the FDA commissioner indicate that the agency regards these tests as *in vitro* diagnostics that need to go through the 510 (k) premarket notification or premarket approval (PMA) process. Furthermore, the guidance said the FDA will focus initially on high complexity testing assays, such as Multivariate Index Assays [16], assays which measure multiple analytes and use mathematical algorithms to determine the clinical significance of the test result. Thus, the regulatory compliance of predictive biomarkers involving multigene signatures is likely to be the focus of the most scrutiny by the FDA in the near term. This underscores the wisdom of discussing the assay and its analytical validation with the FDA prior to its use as a patient enrollment assay.

5.3. Laboratory-Developed Tests (LDTs) and In Vitro Diagnostics Devices (IVDs). A comprehensive discussion of LDTs and IVDs is beyond the scope of this paper, so only a few comments will be made here. The FDA recognizes two categories of IVD devices: a "kit" that is shipped from an IVD manufacturer to any appropriate clinical laboratory for use as a diagnostic or a laboratory-developed test (LDT), which can be thought of as a "service" offered by a single specific laboratory, within which the assay was developed, manufactured, and validated using specific equipment. In fact, the FDA considers any test used to direct patient treatment (including selecting patients for enrollment or balancing arms of a study) to be an IVD device that must be reviewed by the FDA [17]. Thus, both types of IVD devices must be reviewed and become either FDA-cleared (if submitted as a 510 (k) application) or FDA-approved (if submitted as a PMA application). Examples of FDA-cleared LDTs include the Tissue of Origin (TOO) test developed by Pathwork Diagnostics and the Mammaprint test developed by Agendia. A presubmission meeting should be planned with the FDA prior to introducing a predictive biomarker assay into a clinical study [17]. The submitted document should include items such as intended use, assay description, and rationale for use and should summarize preclinical studies supporting the assay's use. In addition, it should contain a risk analysis and analytical validation data documenting assay performance characteristics such as accuracy, precision, and linearity.

In summary, it is an exciting time for those involved in predictive biomarker research. Biomarker hypotheses are actively being prospectively tested in clinical studies. Despite the challenges outlined in this paper, stratified medicine is becoming a reality. It is our hope that our suggestions, recommendations and checklist (Table 2) contribute in some small way to the broader effort of fellow translational scientists in the development of stratified treatments that will tangibly benefit our patients.

Acknowledgments

The authors thank Omar Laterza, James Hardwick, Ken Emancipator, Hongyue Dai, Eric Rubin, and members of the Predictive Biomarker Task Force for commenting on an early version of this paper. They thank Usha Signh for providing helpful comments on the final paper.

References

[1] M. Nohaile, "The biomarker is not the end," *Drug Discovery Today*, vol. 16, no. 19-20, pp. 878–883, 2011.

[2] R. Xie, J.-Y. Chung, K. Ylaya et al., "Factors influencing the degradation of archival formalin-fixed paraffin-embedded tissue sections," *Journal of Histochemistry and Cytochemistry*, vol. 59, no. 4, pp. 356–365, 2011.

[3] The cobas 4800 BRAF V600 Mutation Test Product Insert, 2012, http://www.accessdata.fda.gov/cdrh_docs/pdf11/P110020c.pdf.

[4] M. Maak, I. Simon, U. Nitsche et al., "Independent validation of a prognostic genomic signature (ColoPrint) for patients with stage II colon cancer," *Annals of Surgery*, vol. 257, no. 6, pp. 1053–1058, 2013.

[5] D. A. Eberhard, G. Giaccone, and B. E. Johnson, "Biomarkers of response to epidermal growth factor receptor inhibitors in non-small-cell lung cancer working group: standardization for use in the clinical trial setting," *Journal of Clinical Oncology*, vol. 26, no. 6, pp. 983–994, 2008.

[6] W. C. Olson, M. E. Smolkin, E. M. Farris et al., "Shipping blood to a central laboratory in multicenter clinical trials: effect of ambient temperature on specimen temperature, and effects of temperature on mononuclear cell yield, viability and immunologic function," *Journal of Translational Medicine*, vol. 9, article 26, 2011.

[7] S. Duenwald, M. Zhou, Y. Wang et al., "Development of a microarray platform for FFPET profiling: application to the classification of human tumors," *Journal of Translational Medicine*, vol. 7, article 65, 2009.

[8] FDA News Release P07-13, "FDA clears breast cancer specific molecular prognostic test," News & Events, February 2007, http://www.fda.gov/NewsEvents/Newsroom/PressAnnouncements/2007/ucm108836.htm.

[9] FDA News Release, "FDA clears test that helps identify type of cancer in tumor sample," News & Events, February 2007, http://www.fda.gov/NewsEvents/Newsroom/PressAnnouncements/2008/ucm116931.htm.

[10] FDA News Release Approval of Kras test, "FDA approves genetic test to help some colon cancer patients, physicians considering Erbitux therapy," News & Events, July 2012, http://www.fda.gov/NewsEvents/Newsroom/PressAnnouncements/ucm310899.htm.

[11] A. S. Gargis, L. Kalman, M. W. Berry et al., "Assuring the quality of next-generation sequencing in clinical laboratory practice," *Nature Biotechnology*, vol. 30, no. 11, pp. 1033–1036, 2012.

[12] E. A. Perez, V. J. Suman, N. E. Davidson et al., "HER2 testing by local, central, and reference laboratories in specimens from the north central cancer treatment group N9831 intergroup adjuvant trial," *Journal of Clinical Oncology*, vol. 24, no. 19, pp. 3032–3038, 2006.

[13] T. André, H. Blons, M. Mabro et al., "Panitumumab combined with irinotecan for patients with KRAS wild-type metastatic colorectal cancer refractory to standard chemotherapy: a GERCOR efficacy, tolerance, and translational molecular study," *Annals of Oncology*, vol. 24, no. 2, pp. 412–419, 2013.

[14] E. Bellon, M. J. L. Ligtenberg, S. Tejpar et al., "External quality assessment for KRAS testing is needed: setup of a European program and report of the first joined regional quality assessment rounds," *Oncologist*, vol. 16, no. 4, pp. 467–478, 2011.

[15] FDA Draft Guidance for Industry and FDA Staff, "Commercially Distributed in Vitro Diagnostic Products Labeled for Research Use Only or Investigational Use Only: Frequently Asked Questions," June 2011.

[16] FDA Draft Guidance for Industry, Clinical Laboratories, and FDA Staff. In Vitro Diagnostic Multivariate Index Assays, July 2007.

[17] FDA Draft Guidance for Industry and FDA Staff. In Vitro Companion Diagnostic Devices, July 2011.

Hindawi Publishing Corporation
BioMed Research International
Volume 2013, Article ID 241780, 11 pages
http://dx.doi.org/10.1155/2013/241780

Research Article

Circulating microRNAs and Kallikreins before and after Radical Prostatectomy: Are They Really Prostate Cancer Markers?

Maria Giulia Egidi,[1] Giovanni Cochetti,[1] Maria Rita Serva,[1] Gabriella Guelfi,[2] Danilo Zampini,[2] Luca Mechelli,[2] and Ettore Mearini[1]

[1] *Department of Medical-Surgical Sciences and Public Health, Faculty of Medicine and Surgery, University of Perugia, Loc. S. Andrea delle Fratte, 06156 Perugia, Italy*
[2] *Department of Biopathological Science and Hygiene of Food and Animal Production, Faculty of Veterinary Medicine, University of Perugia, Via San Costanzo 4, 06126 Perugia, Italy*

Correspondence should be addressed to Giovanni Cochetti; giovannicochetti@libero.it

Received 10 May 2013; Revised 9 August 2013; Accepted 23 August 2013

Academic Editor: Romonia Renee Reams

The aim of our study was to monitor serum levels of two miRNAs (miR-21 and miR-141) and three KLKs (hK3/PSA, hK11, and hK13) before and 1, 5, and 30 days after radical prostatectomy, in order to characterize their fluctuations after surgery. 38 patients with prostate cancer were included. miR-21 and miR-141 were quantified through real-time PCR, while ELISA assays were used to quantify hK3 (PSA), hK11, and hK13. Both miR-21 and miR-141 showed a significant increase at the 5th postoperative day, after which a gradual return to the preoperative levels was recorded. These findings suggest that miR-21 and miR-141 could be involved in postsurgical inflammatory processes and that radical prostatectomy does not seem to alter their circulating levels. Postoperative serum kallikreins showed a significant decrease, highlighting the potential usefulness of kallikreins apart from PSA as potential prostate cancer markers.

1. Introduction

Prostate cancer (PCa) is the most common male tumor in Europe and USA. The introduction of prostate-specific antigen (PSA, i.e., hK3) in the diagnostic management has allowed an earlier detection and thus the possibility to treat more cancers at a precocious and localized stage, improving the cure rates. Kallikreins are a family of peptidases widely expressed in various tissues, and they rule various physiological events, such as blood pressure homeostasis, skin homeostasis, and semen liquefaction. The proposal of kallikreins besides PSA as cancer biomarkers has been already reported, on the basis of the alterations in expression of many members of this family in several cancers [1–3].

microRNAs (miRNAs) are small noncoding single-stranded RNAs controlling the expression of protein-coding transcripts: each miRNA targets several genes at the posttranscriptional level [4]. About 10–30% of all human genes are regulated by miRNAs [5]. In the last decade, microRNAs have been studied as potential markers for almost every type of cancer [6]: miRNAs locate at cancer-related genomic regions or in fragile sites, and this feature suggests their potential role in tumorigenesis [7]. In 2007, Porkka performed the first profiling of miRNA involved in prostate cancer [8]. miRNAs and KLKs are characterized by a high stability in the serum and for this reason they are both ideal candidates for noninvasive assays.

The first end point of this study was to compare preoperative expression levels of three kallikreins (hK3/PSA, hK11, and hK13) and 2 miRNAs (miR-21, miR-141) with postoperative ones, in order to evaluate if a specific correlation between prostate cancer and these markers exists. The second aim was to evaluate their diagnostic power comparing the preoperative values in prostate cancer patients with healthy ones.

2. Materials and Methods

2.1. Experimental Design. This study was approved by the Institutional Internal Review Board of Santa Maria Hospital,

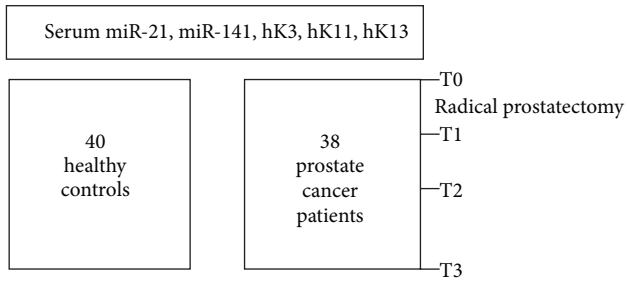

Figure 1: Overview of the experimental design. T0: presurgical phase; T1: 1 day after surgery; T2: 5 days after surgery; T3: 30 days after surgery; C: control.

Table 1: Demographic characteristics of the patients enrolled in the present study.

Clinical parameters	PCa
Median age (range)	62 (54–63 ys)
Median PSA (range)	5.55 (3.11–9 ng/mL)
Clinical stage	
T1c	21 (55.3%)
T2a	6 (15.8%)
T2b	3 (7.9%)
T2c	8 (21%)
Pathological Gleason score	
6 (3 + 3)	20 (52.6%)
7 (3 + 4)	2 (5.3%)
7 (4 + 3)	12 (31.6%)
8 (4 + 4)	4 (10.5%)
Lymph node involvement	6 (15.8%)
Pathological stage	
T2a	6 (15.8%)
T2b	2 (5.3%)
T2c	24 (63.1%)
T3a	4 (10.5%)
T3b	2 (5.3%)

Terni. 38 patients who undergone radical prostatectomy for localized prostate cancer were enrolled consecutively from September 2011 to April 2012. 40 subjects were selected as healthy controls: their mean age was 39 years, mean PSA was 0.56 ng/mL, and they have no history of prostatitis or other urologic pathologies. The demographic characteristics of all prostate cancer patients are reported in Table 1, and the experimental design is shown in Figure 1. Expression levels of miR-21 and miR-141 were measured through real-time PCR, while ELISA assays were conducted on the same serum samples to quantify hK3 (PSA), hK11, and hK13. In prostate cancer patients, serum levels of miRNAs (miR-21 and miR-141) and kallikreins (hK3, hK11, and hK13) were measured at four time points: 1 day before surgery (T0) and 1st (T1), 5th (T2), and 30th (T3) postoperative days (Figure 1).

2.2. Serum Collection and Storage. Serum samples were all obtained from subjects subscribing informed consent. All patients underwent fasting blood withdrawal at one day before surgery (T0) without receiving any drug treatment. Blood was withdrawn into Vacuette Z Serum Sep Clot Activator (Greiner Bio-One). Collection tubes were gently inverted five times to ensure full contact with inner procoagulant surface, and coagulation process was allowed maintaining vacuette for 30 minutes at RT. After centrifugation (2000 ×g, 10 min), aliquots were immediately stored at −80°C until use.

2.3. RNA Isolation. 200 μL of serum was used for the extraction of total RNA with Total Purification Kit (Norgen Biotek Corp., Ontario, Canada), following the instructions for plasma and serum, with minor modifications. Total RNA was quantified by Qubit RNA assay (Life technologies) and stored at −20°C until use.

2.4. Reverse Transcription. 4 μL of purified RNA (20 ng) was reverse-transcribed using the miRCURY LNA Universal RT miR PCR, polyadenylation, and cDNA synthesis kit (Exiqon). RNA spike-in control (UniSp6 RNA template, provided with the cDNA synthesis kit) was introduced in RT mix immediately before retrotranscription in a 20 μL cDNA reaction and served to monitor cDNA synthesis and PCR efficiency.

2.5. Real-Time PCR. Primers were designed based on mature miRNA sequence (miRCURY LNA specific PCR primer set, Exiqon system). Each sample was run in triplicate, and the results were averaged; no-template controls were included in the analysis. Exiqon miRCURY LNA Universal RT microRNA PCR SYBR Green master mix has been used to amplify cDNAs. All PCR reactions were performed on a Bio-Rad iCycler Real-Time PCR system. Three miRNAs (miR-93, -103, -191) were tested for normalization according to the manufacturer's recommendations for serum/plasma applications [9].

2.6. ELISA Assay of hK11 and hK13. 250 μL of serum was used for measurement of hK11 and hK13 with sandwich ELISA (human KLK-11 and KLK-13 pair sets ELISA kits, Sino Biological Inc., Beijing, China). ELISA microplates were separately coated with 100 μL of diluted of affinity-purified rabbit mAbs anti-hK11 or anti-hK13 (2 μg/mL in 5 mM carbonate-bicarbonate), incubated overnight at 4°C, and washed three times with TBS containing Tween 20 0.05% (300 μL/well). Solid phase blocking was performed adding TBST containing BSA 2% (300 μL/well) and incubating 60 min at RT. Wells were then washed three times, and 100 μL/well of serum samples was incubated for 60 min at RT. Plates were washed again as above, and 100 μL/well of anti-rabbit IgG antibody HRP labeled (1 μg/mL) was dispensed and incubated for 60 min at RT. Plates were once more washed, and 100 μL/well of TMB solution (Sigma) was added and incubated for 20 min, before stopping with 100 μL/well of H_2SO_4 1 N and measuring OD at 450 nm on a microplate reader (Infinite 200, Tecan, Männedorf, Switzerland). hK11 and hK13 serum levels were referred to a standard curve of recombinant human kallikreins 11 and 13.

2.7. Total PSA Assay. Total serum PSA measurements were performed through Advia Centaur automated system (Siemens Health Care Diagnostics, Victoria, Australia). The two-site sandwich immunoassay consists of polyclonal goat anti-PSA antibody and a monoclonal mouse anti-PSA antibody.

2.8. Statistical Analysis. Tukey's Multiple Comparison Test was used to compare the serum samples obtained before and after surgery and to compare the difference in the serum miRNA and hKs expression between the cancer group and the healthy control group. The significance was set as $P \leq 0.05$.

Receiver Operating Characteristic (ROC) curve analysis was performed to estimate the diagnostic accuracy of miR-21, miR-141, hK11, and hK13. Logistic regression analysis was performed to evaluate the diagnostic accuracy of the combination of miRNAs.

3. Results

3.1. Serum hK3, hK11, and hK13 before and after Radical Prostatectomy. hK11 levels significantly decreased after surgery (T0 > T1, $P < 0.05$) and remained substantially unmodified at T2 and T3 ($P > 0.05$) (Table 2). The marked decreased of hK11 at the first postoperative day resembled that of PSA (Figure 2). Contrary to PSA which progressively decreased to finally fall down to zero at T3 (Figure 3), hK11 showed a slight increase at T3, although this was not statistically significant ($P > 0.05$).

In contrast, serum hK13 levels significantly increased at T1 (T0 < T1, $P < 0.05$) and finally stabilized at lower levels with respect to preoperative values (T2 < T0, $P < 0.05$) (Figure 2). As seen for hK11, hk13 did not decrease further at T3 (T2 versus T3, $P > 0.05$).

3.1.1. Comparison of Serum hK11 and hK13 between Prostate Cancer Patients before Surgery (T0) and Healthy Controls (C). Serum levels of hK11 and hK13 were significantly higher ($P < 0.05$) in serum from prostate cancer patients at T0 with respect to healthy controls (Figure 4 and Table 3), similarly to PSA (Figure 5).

Serum levels of hK11 and hK13 in control group were also compared with values obtained from prostate cancer group at postoperative sampling times (T1, T2, and T3, see Table 4). Only serum levels of hK13 in patients at the 1st day after surgery differed significantly from controls.

3.2. Serum miR-21 and miR-141 before and after Radical Prostatectomy. For real-time PCR applications, miR-93 exhibited the lowest coefficient of variation in the assay and was chosen as reference gene. The normalized data against miR-93 levels were reported as the mean value ± SD.

Serum levels of miR-21 and miR-141 were analyzed at T0, T1, T2, and T3 (Table 5 and Figure 6). Both miR-21 and miR-141 increased significantly at the fifth postoperative day (T0 < T2, $P < 0.01$ and $P < 0.001$, resp.). At T3, serum miR-21 and miR-141 were not significantly different from preoperative levels (T0 = T3, $P > 0.05$).

3.2.1. Comparison of Serum miR-21 and miR-141 between Patients (T0) and Healthy Controls (C). In prostate cancer patients serum levels of miR-21 preoperatively were not significantly different from healthy controls ($P > 0.05$). On the contrary, serum miR-141 preoperative levels were significantly lower ($P < 0.05$) than healthy controls (Figure 7 and Table 6).

Circulating levels of miR-21 and miR-141 from controls were also compared with prostate cancer group at postoperative sampling times (T1, T2, and T3). Results are shown in Table 7. For miR-21, statistically significant differences were obtained when C was compared with T2 ($P < 0.01$). Comparisons of C with T1 and T2 did not reach significance (C versus T1 and C versus T2, $P > 0.05$). Serum levels of miR-141 in control group were significantly different from those of patients only at the 30th day after surgery (C versus T3, $P < 0.05$; C versus T1 and C versus T2, $P > 0.05$).

3.3. Evaluation of Diagnostic Accuracy of miR-21, miR-141, hK11, and hK13. The diagnostic accuracy of miR-21, miR-141, hK11, and hK13 was evaluated using Receiver Operating Characteristic (ROC) curve analysis. As shown in Figure 8, serum miR-21 displayed the lowest ability (AUC = 0.597, $P > 0.05$) to differentiate between prostate cancer patients and healthy controls, whereas miR-141 reached an AUC of 0.811 ($P < 0.0001$). Serum hK13 showed the highest diagnostic performance (AUC = 0.997, $P < 0.0001$), followed by hK11 (AUC = 0.994, $P < 0.0001$).

Logistic regression analysis was performed to evaluate the probability that the combination of miR-141 and miR-21 could discriminate prostate cancer patients from healthy controls in a better way than miR-141 alone. Area under the curve was 0.811 (which was equal to miR-141 alone) and sensitivity was lower than miR-141 (68.42% versus 78.9%), while specificity increased slightly (85% versus 82.5%).

4. Discussion

4.1. Prostate Cancer Beyond PSA: Postoperative Serum Levels of hK11 and hK13. The main diagnostic tools to detect prostate cancer include digital rectal examination, serum PSA, and transrectal ultrasound guided biopsy. PSA is a quite accurate diagnostic test, but its specificity is too low because PSA is a prostate-specific but not a prostate cancer-specific marker: for this reason, those biopsies requested for altered PSA levels are often negative. When PSA is ranged between 4.0 and 9.9 ng/mL, the first prostate biopsy is positive only up to 37% [10]. PSA belongs to the genetic family of kallikreins, a group of serine proteases widely expressed in various tissues and involved both in many physiological and in pathological processes: the alteration in their expression is related to the onset of various human diseases [11–13]. Since they are circulating proteins, kallikreins are detectable in human body fluids, such as serum, and may be used as molecular assays characterized by a low invasiveness

Table 2: ANOVA showing significance values of hK11 and hK13 for each comparison.

Tukey's multiple comparison test	Groups	Mean difference	q	P value	95% CI	
					Lower	Upper
hK11	T0 versus T1	162.1	7.51	$P < 0.05$	76.28	248.0
	T0 versus T2	174.7	8.09	$P < 0.05$	88.86	260.6
	T0 versus T3	115.5	5.35	$P < 0.05$	29.65	201.4
	T1 versus T2	12.58	0.59	$P > 0.05$	−73.27	98.43
	T1 versus T3	−46.63	2.16	$P > 0.05$	−132.5	39.22
	T2 versus T3	−59.21	2.74	$P > 0.05$	−145.1	26.64
hK13	T0 versus T1	−111.0	9.00	$P < 0.05$	−160.0	−61.99
	T0 versus T2	81.60	6.62	$P < 0.05$	32.59	130.6
	T0 versus T3	62.70	5.08	$P < 0.05$	13.69	111.7
	T1 versus T2	192.6	15.62	$P < 0.05$	143.6	241.6
	T1 versus T3	173.7	14.09	$P < 0.05$	124.7	222.7
	T2 versus T3	−18.90	1.53	$P > 0.05$	−67.91	30.11

T0: preoperative time; T1: 1st postoperative day; T2: 5th postoperative day; T3: 30th postoperative day.

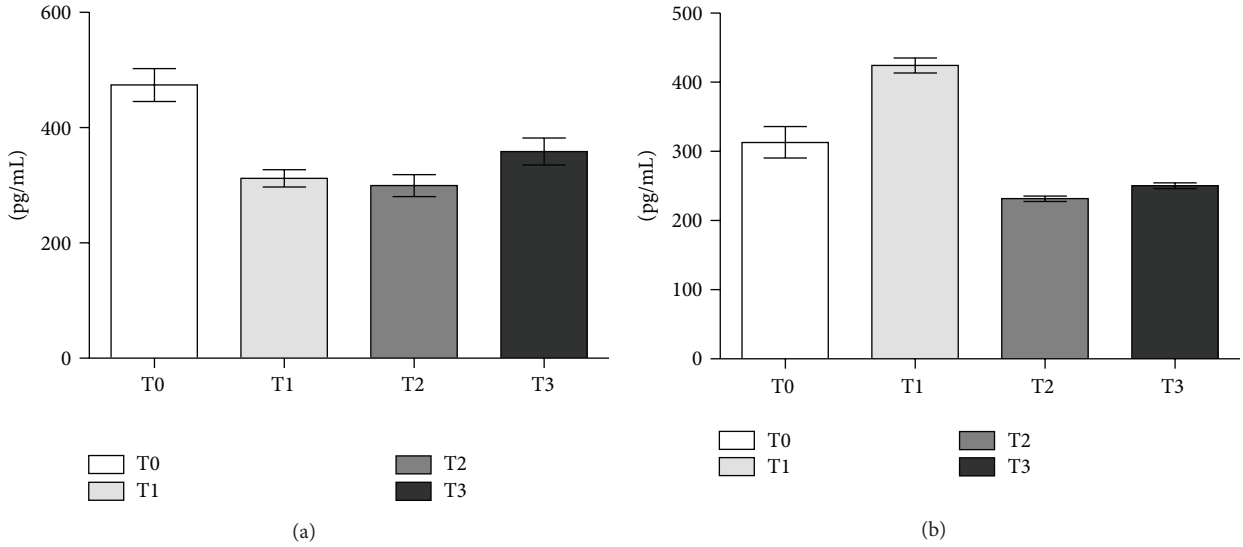

Figure 2: hK11 (Panel a) and hK13 (Panel b) levels (pg/mL ± SE) by ELISA in sera from patients with localized prostate cancer. T0: preoperative time; T1: 1st postoperative day; T2: 5th postoperative day; T3: 30th postoperative day.

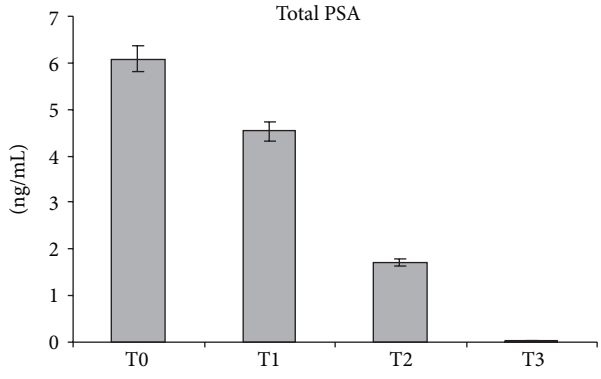

Figure 3: PSA levels expressed as ng/mL ± SE. T0: preoperative time; T1: 1st postoperative day; T2: 5th postoperative day; T3: 30th postoperative day.

and high accuracy. hK2 has been quite recently assayed for its utility in preoperative staging of localized prostate cancer [14]. hK2 was showed to improve the power of total, free, and intact PSA in predicting biopsy outcome in men with PSA levels [15]. Quite recently, the involvement of other kallikreins apart from PSA/hK3 and hK2 in prostate cancerogenesis has been progressively clarified: KLK11 was recently proposed as a new prognostic marker for PCa [16]. The KLK13 protein shares 51% amino acid identity with KLK11, and it is primarily expressed in mammary gland, prostate, salivary gland, and testis. KLK13 gene was found to be regulated by steroid hormones in a human breast cancer cell line so that its expression is an independent favorable prognostic marker for breast carcinoma [17].

PSA is the unique kallikrein whose postsurgical kinetics has been studied: to our knowledge, this is the first report

Table 3: Statistical analysis of serums hK11 and hK13.

Tukey's multiple comparison test	Groups	Mean difference	q	P value	95% CI	
					Lower	Upper
hK11	C versus T0	−176.8	6.532	$P < 0.05$	−284.5	−69.23
hK13	C versus T0	−101.2	6.547	$P < 0.05$	−162.6	−39.76

T0: preoperative time; C: control.

Table 4: ANOVA showing significance values of hK11 and hK13 for each comparison.

Tukey's multiple comparison test	Groups	Mean difference	q	P value	95% CI	
					Lower	Upper
hK11	C versus T1	−14.72	0.544	$P > 0.05$	−122.3	−92.90
	C versus T2	−2.136	0.079	$P > 0.05$	−109.8	105.5
	C versus T3	−61.35	2.266	$P > 0.05$	−169.0	26.27
hK13	C versus T1	−212.2	13.73	$P < 0.05$	−273.6	−150.8
	C versus T2	−19.60	1.268	$P > 0.05$	−81.04	41.84
	C versus T3	−38.50	2.491	$P > 0.05$	−99.94	22.94

C: control; T1: 1st postoperative day; T2: 5th postoperative day; T3: 30th postoperative day.

Table 5: ANOVA showing significance values of miR-21 and miR-141 for each comparison.

Tukey's multiple comparison test	Groups	Mean difference	q	P value	95% CI	
					Lower	Upper
miR-21	T0 versus T1	−0.255	0.75	$P > 0.05$	−1.592	1.082
	T0 versus T2	1.687	4.98	$P < 0.01$	0.350	3.024
	T0 versus T3	0.498	1.47	$P > 0.05$	−0.839	1.835
	T1 versus T2	1.942	5.73	$P < 0.01$	0.605	3.279
	T1 versus T3	0.753	2.22	$P > 0.05$	−0.584	2.090
	T2 versus T3	−1.189	3.51	$P > 0.05$	−2.526	0.148
miR-141	T0 versus T1	0.666	1.75	$P > 0.05$	−0.835	2.167
	T0 versus T2	2.855	7.51	$P < 0.001$	1.354	4.356
	T0 versus T3	−0.237	0.62	$P > 0.05$	−1.738	1.264
	T1 versus T2	2.189	5.76	$P < 0.01$	0.688	3.690
	T1 versus T3	−0.903	2.37	$P > 0.05$	−2.404	0.598
	T2 versus T3	−3.092	8.13	$P < 0.001$	−4.593	−1.591

T0: preoperative time; T1: 1st postoperative day; T2: 5th postoperative day; T3: 30th postoperative day.

Table 6: Statistical analysis showing significance values of miR-21 and miR-141.

Tukey's multiple comparison test	Groups	Mean difference	q	P value	95% CI	
					Lower	Upper
miR-21	C versus T0	0.197	0.59	$P > 0.05$	−1.123	1.517
miR-141	C versus T0	−1.506	4.01	$P < 0.05$	−2.988	−0.024

T0: preoperative time; C: control.

Table 7: ANOVA showing significance values of miR-21 and miR-141 for each comparison.

Tukey's multiple comparison test	Groups	Mean difference	q	P value	95% CI	
					Lower	Upper
miR-21	C versus T1	−0.058	0.17	$P > 0.05$	−1.378	1.262
	C versus T2	1.884	5.63	$P < 0.01$	0.564	3.204
	C versus T3	0.695	2.08	$P > 0.05$	−0.625	2.015
miR-141	C versus T1	−0.840	2.24	$P > 0.05$	−2.322	0.642
	C versus T2	1.349	3.59	$P > 0.05$	−0.133	2.831
	C versus T3	−1.743	4.64	$P < 0.05$	−3.225	−0.261

C: control; T1: 1st postoperative day; T2: 5th postoperative day; T3: 30th postoperative day.

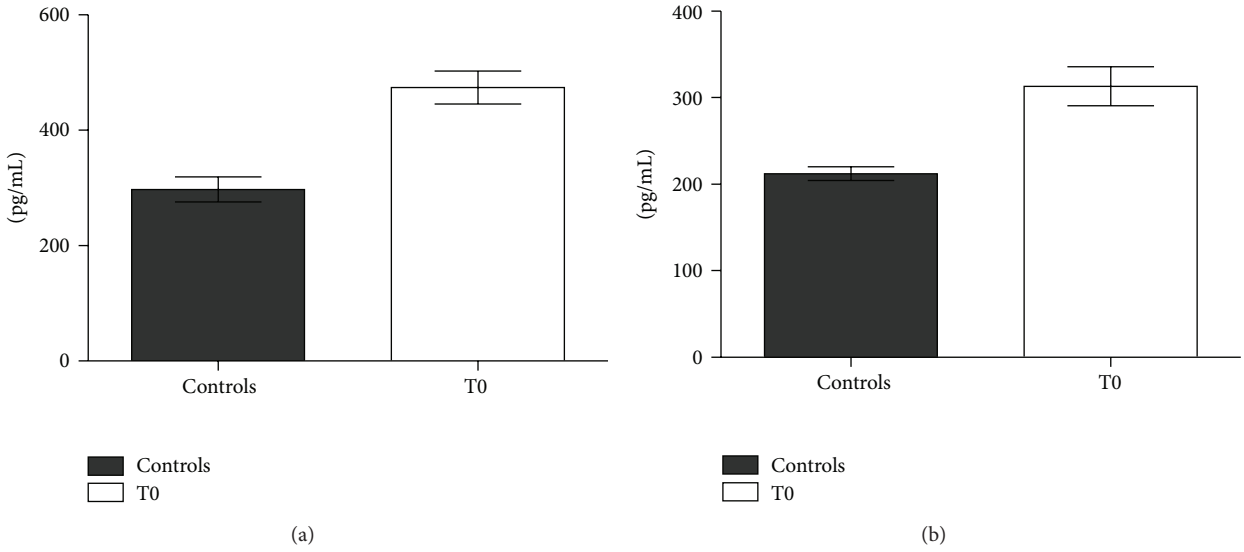

Figure 4: hK11 (Panel a) and hK13 (Panel b) levels (pg/mL ± SE) by ELISA in sera from patients with localized prostate cancer. C: control; T0: preoperative time.

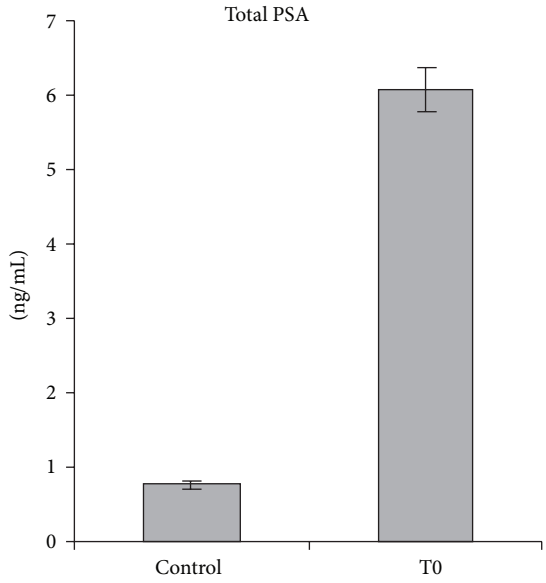

Figure 5: PSA levels expressed as ng/mL ± SE. C: control; T0: preoperative time.

describing postoperative changes in serum levels of other kallikreins at multiple times. Both hK11 and hK13 were significantly higher in prostate cancer patients before surgery and they significantly decreased after surgery. Serum hK13 showed a transient increase at the first day after surgery, suggesting an implication in inflammatory events, whereas serum hK11 immediately decreased after surgery. Both hK11 and hK13 stabilized at lower levels with respect to preoperative values, although they did not fall down to zero such as PSA, which became undetectable 30 days after surgery. hK11 even seemed to increase at the 30th day after radical prostatectomy, although comparisons of T3 with T2 or T1 were not statistically significant. These findings highlighted the direct correlation of these kallikreins to prostate cancer. This was confirmed by the significant difference of hK11 and hK13 serum levels in prostate cancer patients with respect to controls (T0 > C, $P < 0.05$). Serum hK11 and hK13 fluctuations after surgery appeared to have a strong correlation with prostate cancer, since their decrease to lower levels with respect to preoperative values resembles PSA postoperative decay curve.

4.2. Changes in Serums miR-21 and miR-141 after Radical Prostatectomy: Only a Matter of Inflammation? microRNA are progressively emerging as crucial regulators of gene expression, since they affect the tumorigenesis as oncogenes or oncosuppressors [6, 18–20]. The intrinsic stability of miRNAs in human plasma/serum renders these molecules ideal candidates for the development of low invasive diagnostic assays [21]. The involvement of miRNAs in carcinogenesis has been reported elsewhere: this widespread interest on miRNAs led to the development of commercial cancer biomarker assays for pancreatic cancer versus pancreatitis [22], squamous versus nonsquamous lung cancer [23], and malignant pleural mesothelioma versus lung and pleura cancers [24]. miRNAs proved also to be effective in the identification of the unknown primitive cancer of metastasis [25]. Besides being involved in carcinogenesis, several studies have defined mammalian microRNAs as key regulators of the immune system. In fact, inflammation is able to regulate miRNA biogenesis [26].

miR-21 has been recognized as *onco*mir, and it has been demonstrated to target, among others, the following genes: tumor suppressor gene tropomyosin 1 (TPM1), programmed cell death 4 (PDC D4), maspin, phosphatase and tensin homolog (PTEN), and reversion-inducing cysteine-rich protein with kazal motifs (RECK) [26–29]. A recent study aimed

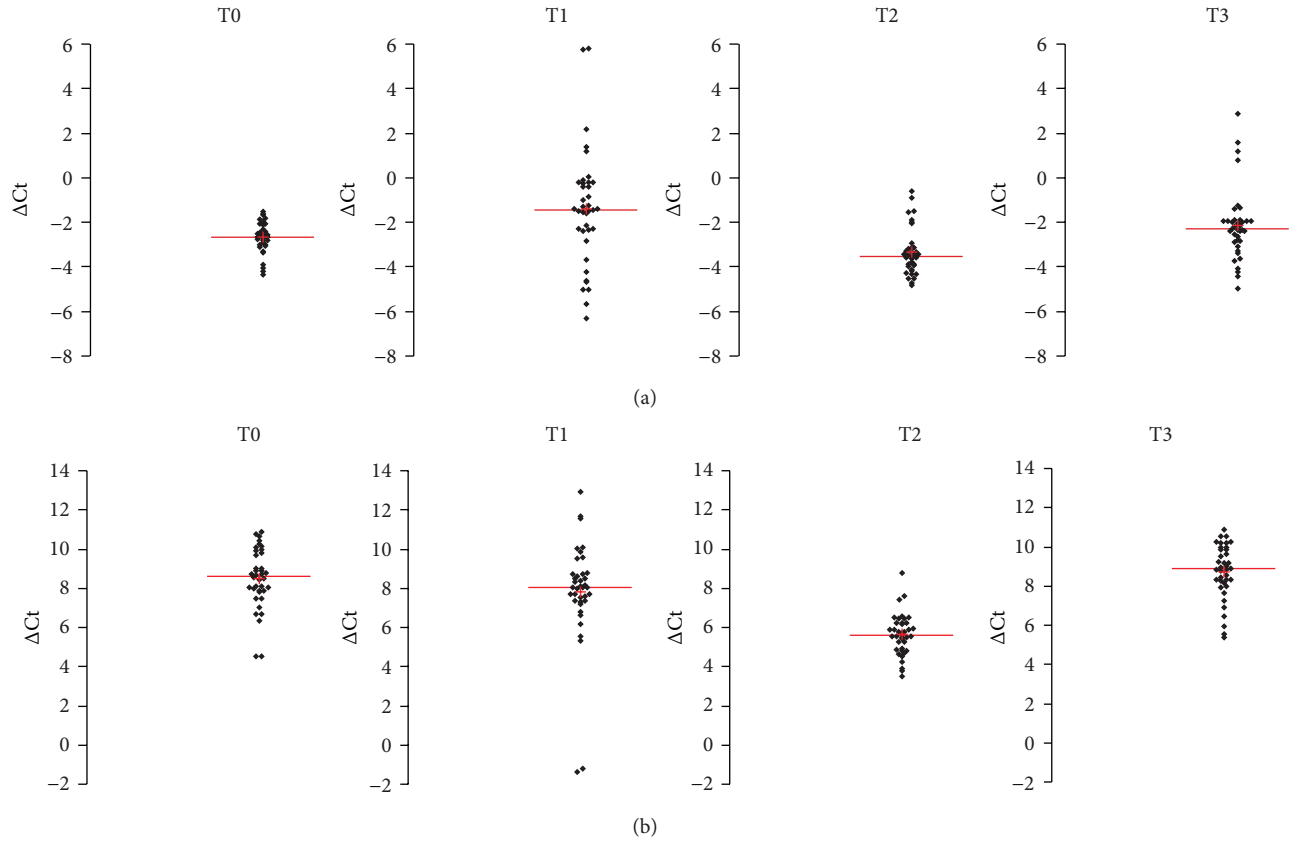

Figure 6: Normalized Ct (ΔCt) of miR-21 (Panel a) and miR-141 (Panel b) in serum from patients with localized prostate cancer. T0: preoperative time; T1: 1st postoperative day; T2: 5th postoperative days; T3: 30th postoperative day.

to assess the expression of circulating miR-21 in serum samples from patients with different types of cancer, but without including prostate cancer because of too few cases [30]. By use of real-time quantitative reverse transcription-PCR, a marked overexpression of circulating miR-21 in 174 patients with solid cancers (breast, esophageal, gastric, colorectal, and lung cancers) with respect to 39 normal control subjects was assessed. Furthermore, miR-21 proved to be associated with the expression of genes that regulated inflammation [31]. miRNAs role in the development, maturation, and function of cells involved in the innate and adaptive immunity has been proved [32, 33]. Chen et al. analyzed the frequent deregulation of serum miRNAs in patients with lung or colorectal carcinoma: they found a quite large portion (38.5%) of the same shared members to be overexpressed also in serum samples from patients with type II diabetes. This is probably attributable to the inflammatory reactions occurring in all the samples under investigation [34]. Thus, although a set of miRNAs specifically associated with inflammation has been characterized [33], the involvement of other members may be hypothesized and still unreported.

miR-141 is representative of epithelial tissue; thus, its expression is not restricted to prostatic epithelium: nonetheless, circulating miR-141 levels in prostate cancer patients were successfully used to screen for metastatic prostate cancer with high sensitivity [6]. Virtually all epithelial cancers overexpress miR-141 (data from literature are mainly available for breast, lung, colon, and prostate cancers) [35]. The convergent deregulation of miR-141 in epithelial cancers suggests that the diagnostic performance of miR-141 in prostate cancer remains to be assessed. Furthermore, miR-141 has been shown to target p38α, thus modulating the oxidative stress response and ultimately affecting tumorigenesis [36].

In the present study, miR-21 and miR-141 levels did not show significant difference with preoperative values ($P > 0.05$) in the first postoperative day. In contrast, a significant increase of both miR-21 and miR-141 was detected at the 5th postoperative day, with respect to the preoperative time. This finding is probably attributable to systemic inflammatory reactions occurring after surgery. We hypothesize that these alterations do not appear immediately at T1 because of a *de novo* production of miRNA from other body districts. At T3, the serum levels of miR-21 and miR-141 decreased to values comparable to preoperative time ($P > 0.05$).

Our findings on serum miR-141 seem to be in contrast with previous data in the literature. So far, miR-141 has been mainly associated with prostate cancer progression [6, 37–39]. The expression levels of circulating miRNAs in low-risk, high-risk, and metastatic castration resistant prostate cancer (mCRPC) have highlighted the characteristic overexpression of miR-141 in mCRPC compared with low-risk disease [40]. On the contrary, our analysis has been conducted on serum samples from patients with localized prostate cancer. Moreover, other discrepancies about circulating levels of

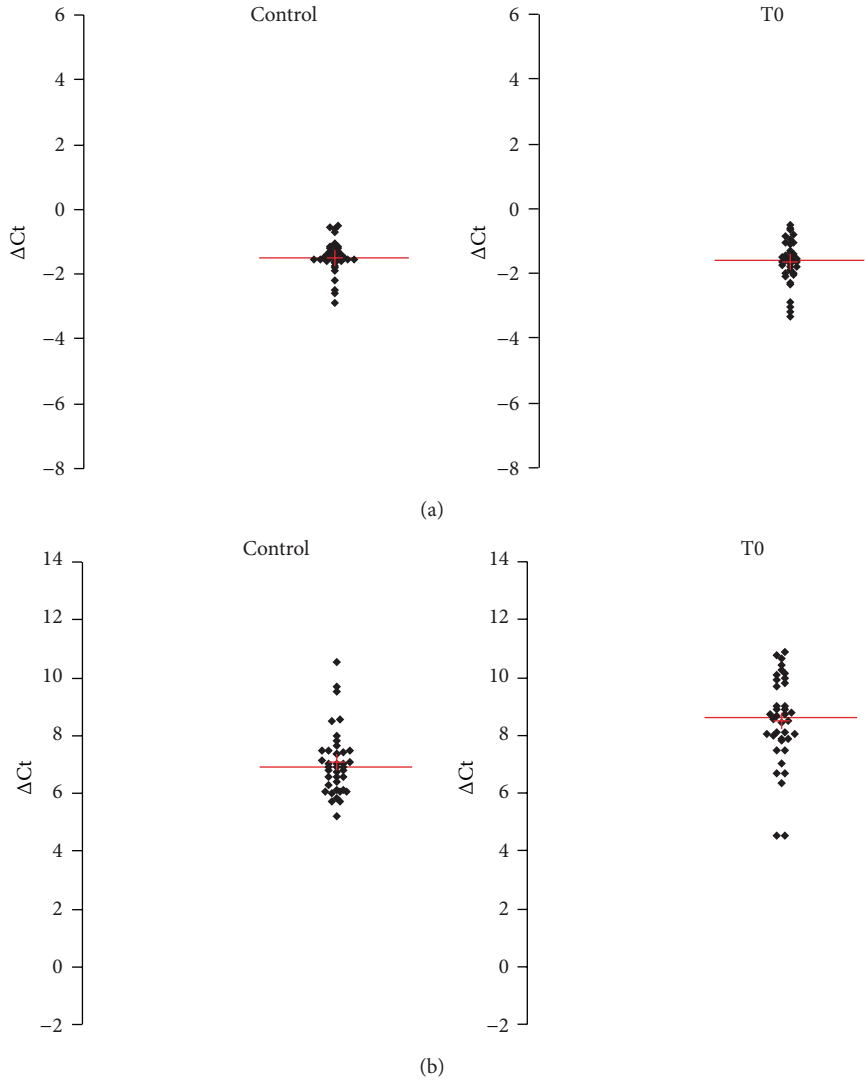

Figure 7: Normalized Ct (ΔCt) of miR-21 (Panel a) and miR-141 (Panel b) in sera from patients with localized prostate cancer with respect to controls. T0: preoperative time; C: control.

miR-141 in prostate cancer have been reported by other researchers. As an example, Agaoglu and colleagues [41] did not find significant differences in circulating levels of miR-141 in prostate cancer (both localized and advanced diseases) with respect to healthy controls. Furthermore, Mahn and coworkers [42] were unable to detect serum miR-141 in localized prostate cancer: the authors hypothesized that this event is due to their patient selection criteria (they did not include patients with metastatic prostate cancer) and to the the lack of a preamplification step to enrich for miRNAs, which was instead performed by Mitchell [6].

Similarly to miR-141, the overexpression of miR-21 has been mainly examined in advanced cancers [43, 44]. A recent study aimed at identifying circulating miRNAs able to discriminate mCRPC from localized prostate cancer revealed a statistically significant upregulation of miR-21 in the former group [45]. On the other hand, Folini [46] found similar expressions of miR-21 in localized tumor and surrounding healthy tissue specimens from 36 patients who undergone radical prostatectomy. In summary, while the upregulation of miR-21 and miR-141 has been established in metastatic prostate cancer, their modulation in localized forms is still controversial. To our knowledge, our report is the first to make serial postoperative measurements of serum miRNAs and analysis of their postoperative kinetics. Single postoperative measurements were successfully performed by other authors, both in prostate cancer patients [42] and in other malignancies [47]. Our results were quite surprising, since both serum miR-21 and miR-141 increased significantly at 5th postoperative day to finally return to the preoperative levels. The observed fluctuations could be explained by a de novo synthesis of miRNAs, suggesting their involvement in postsurgical inflammation.

5. Conclusions

Our study provided innovative information about postoperative changes in the levels of circulating microRNAs and

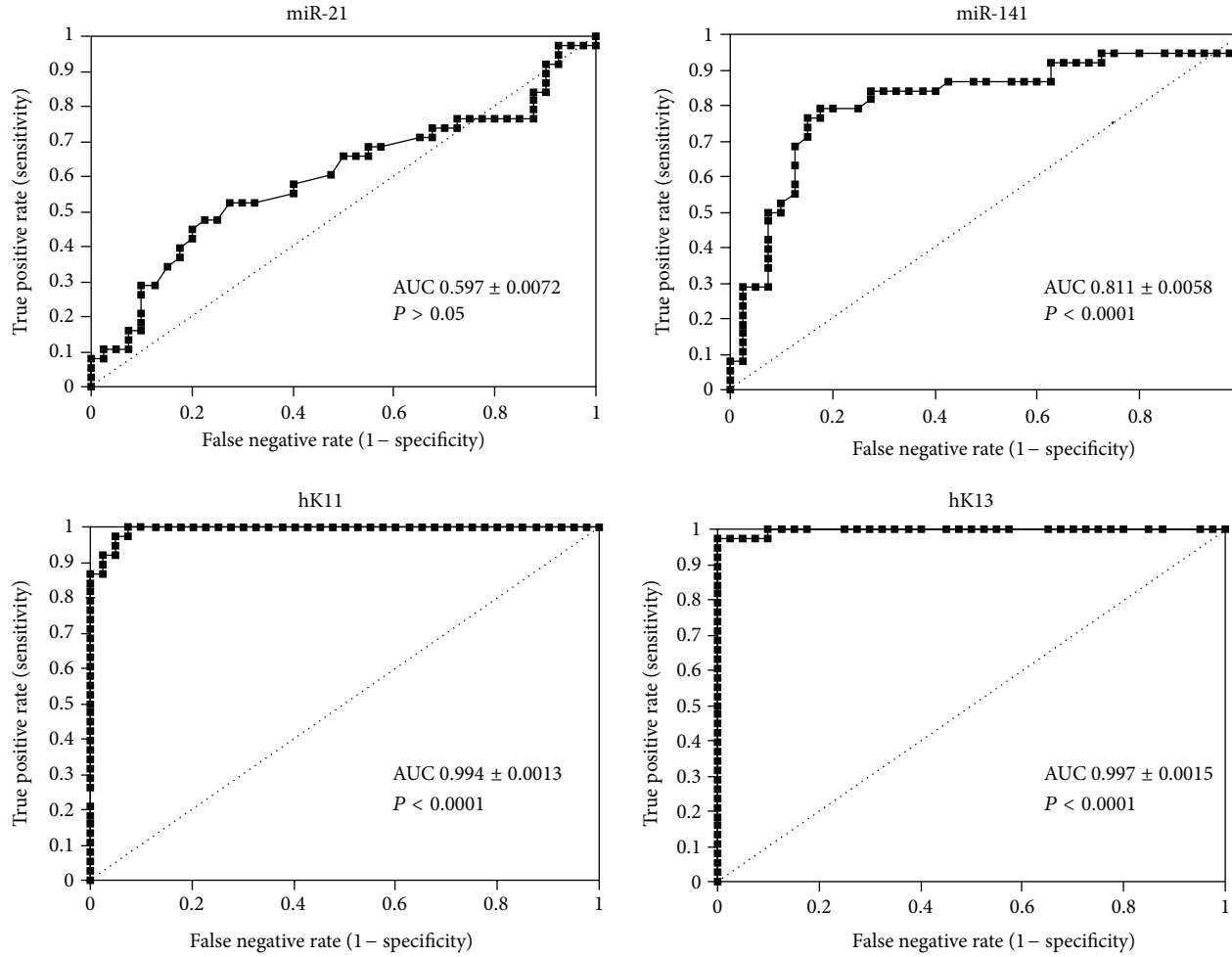

T0 versus control	miR-21	SE	miR-141	SE	hK11	SE	hK13	SE
AUC	0.597		0.811		0.994		0.997	
Sensitivity	0.526	0.0072	0.789	0.0058	1	0.0013	0.974	0.0015
Specificity	0.725		0.825		0.925		1	
95% CI	0.471–0.723		0.712–0.911		0.97–1		0.973–1	

Figure 8: ROC curves and AUCs of serums miR-21, miR-141, hK11, and hK13 between patients (T0) and healthy controls.

kallikreins. This was possible through serial samplings up to 30 days after surgery.

Our results assessed that the interest regarding kallikreins should not be restricted to PSA, since both hK11 and hK13 showed a marked correlation with prostate disease. Indeed, serums hK11 and hK13 showed a statistically significant decrease after surgery, although they did not fall down to zero such as PSA. The delayed increase in expression of serums miR-21 and -141 at the 5th postoperative day could be due to a *de novo* miRNA synthesis induced by systemic inflammatory reactions. At the 30th postoperative day, serums miR-21 and miR-141 were similar to preoperative values. Overall, the results here obtained confirmed that every change in expression of serum markers after surgery should always be taken with caution and confirmed by multiple observations. The diagnostic performance of the markers under examination needs to be confirmed by larger scale studies.

Acknowledgements

This research project was supported by 2007-2013 ESF "Competitiveness and Employment objective" Umbrian Regional Operational Programme (ROP), Avviso pubblico aiuti individuali per la realizzazione di progetti di ricerca.

References

[1] E. P. Diamandis, G. M. Yousef, A. R. Soosaipillai, and P. Bunting, "Human kallikrein 6 (zyme/protease M/neurosin): a new serum biomarker of ovarian carcinoma," *Clinical Biochemistry*, vol. 33, no. 7, pp. 579–583, 2000.

[2] C. V. Obiezu, A. Scorilas, D. Katsaros et al., "Higher human kallikrein gene 4 (KLK4) expression indicates poor prognosis of ovarian cancer patients," *Clinical Cancer Research*, vol. 7, no. 8, pp. 2380–2386, 2001.

[3] G. M. Yousef, A. Scorilas, K. Jung, L. K. Ashworth, and E. P. Diamandis, "Molecular cloning of the human kallikrein 15 gene (KLK15). Up-regulation in prostate cancer," *Journal of Biological Chemistry*, vol. 276, no. 1, pp. 53–61, 2001.

[4] D. P. Bartel, "microRNAs: genomics, biogenesis, mechanism, and function," *Cell*, vol. 116, no. 2, pp. 281–297, 2004.

[5] B. P. Lewis, C. B. Burge, and D. P. Bartel, "Conserved seed pairing, often flanked by adenosines, indicates that thousands of human genes are microRNA targets," *Cell*, vol. 120, no. 1, pp. 15–20, 2005.

[6] P. S. Mitchell, R. K. Parkin, E. M. Kroh et al., "Circulating microRNAs as stable blood-based markers for cancer detection," *Proceedings of the National Academy of Sciences of the United States of America*, vol. 105, no. 30, pp. 10513–10518, 2008.

[7] G. A. Calin, C. Sevignani, C. D. Dumitru et al., "Human microRNA genes are frequently located at fragile sites and genomic regions involved in cancers," *Proceedings of the National Academy of Sciences of the United States of America*, vol. 101, no. 9, pp. 2999–3004, 2004.

[8] K. P. Porkka, M. J. Pfeiffer, K. K. Waltering, R. L. Vessella, T. L. J. Tammela, and T. Visakorpi, "MicroRNA expression profiling in prostate cancer," *Cancer Research*, vol. 67, no. 13, pp. 6130–6135, 2007.

[9] "Profiling of microRNA in serum/plasma and other biofluids-Guidelines for the miRCURY LNATM Universal RT microRNA PCR System, 3rd edition," http://www.exiqon.com/ .

[10] E. Mearini, E. Cottini, G. Cochetti, C. Antognelli, and V. Talesa, "Biomarkers of prostate cancer. A review," *Minerva Urologica e Nefrologica*, vol. 62, no. 2, pp. 163–178, 2010.

[11] E. P. Diamandis and G. M. Yousef, "Human tissue kallikreins: a family of new cancer biomarkers," *Clinical Chemistry*, vol. 48, no. 8, pp. 1198–1205, 2002.

[12] G. Sotiropoulou, V. Rogakos, T. Tsetsenis et al., "Emerging interest in the Kallikrein gene family for understanding and diagnosing cancer," *Oncology Research*, vol. 13, no. 6–10, pp. 381–391, 2002.

[13] I. P. Michael, G. Pampalakis, S. D. Mikolajczyk, J. Malm, G. Sotiropoulou, and E. P. Diamandis, "Human tissue kallikrein 5 is a member of a proteolytic cascade pathway involved in seminal clot liquefaction and potentially in prostate cancer progression," *Journal of Biological Chemistry*, vol. 281, no. 18, pp. 12743–12750, 2006.

[14] C. Becker, T. Piironen, K. Pettersson et al., "Discrimination of men with prostate cancer from those with benign disease by measurements of human glandular kallikrein 2 (HK2) in serum," *Journal of Urology*, vol. 163, no. 1, pp. 311–316, 2000.

[15] A. J. Vickers, A. M. Cronin, G. Aus et al., "A panel of kallikrein markers can reduce unnecessary biopsy for prostate cancer: data from the European Randomized Study of Prostate Cancer Screening in Göteborg, Sweden," *BMC Medicine*, vol. 6, p. 19, 2008.

[16] X. Bi, H. He, Y. Ye et al., "Association of TMPRSS2 and KLK11 gene expression levels with clinical progression of human prostate cancer," *Medical Oncology*, vol. 27, no. 1, pp. 145–151, 2010.

[17] A. Chang, G. M. Yousef, A. Scorilas et al., "Human kallikrein gene 13 (KLK13) expression by quantitative RT-PCR: an independent indicator of favourable prognosis in breast cancer," *British Journal of Cancer*, vol. 86, no. 9, pp. 1457–1464, 2002.

[18] K. M. Nelson and G. J. Weiss, "microRNAs and cancer: past, present, and potential future," *Molecular Cancer Therapeutics*, vol. 7, no. 12, pp. 3655–3660, 2008.

[19] J. W. F. Catto, A. Alcaraz, A. S. Bjartell et al., "MicroRNA in prostate, bladder, and kidney cancer: a systematic review," *European Urology*, vol. 59, no. 5, pp. 671–681, 2011.

[20] C. H. Lawrie, S. Gal, H. M. Dunlop et al., "Detection of elevated levels of tumour-associated microRNAs in serum of patients with diffuse large B-cell lymphoma," *British Journal of Haematology*, vol. 141, no. 5, pp. 672–675, 2008.

[21] N. Kosaka, H. Iguchi, and T. Ochiya, "Circulating microRNA in body fluid: a new potential biomarker for cancer diagnosis and prognosis," *Cancer Science*, vol. 101, no. 10, pp. 2087–2092, 2010.

[22] A. E. Szafranska, T. S. Davison, J. John et al., "MicroRNA expression alterations are linked to tumorigenesis and non-neoplastic processes in pancreatic ductal adenocarcinoma," *Oncogene*, vol. 26, no. 30, pp. 4442–4452, 2007.

[23] D. Lebanony, H. Benjamin, S. Gilad et al., "Diagnostic assay based on hsa-miR-205 expression distinguishes squamous from nonsquamous non-small-cell lung carcinoma," *Journal of Clinical Oncology*, vol. 27, no. 12, pp. 2030–2037, 2009.

[24] H. Benjamin, D. Lebanony, L. Cohen et al., "Differential diagnosis of mesothelioma using a microRNA assay," in *Proceedings of the 44th American Society of Clinical Oncology Annual Meeting*, Chicago, Ill, USA, June 2008, Abstract 22000.

[25] N. Rosenfeld, R. Aharonov, E. Meiri et al., "microRNAs accurately identify cancer tissue origin," *Nature Biotechnology*, vol. 26, no. 4, pp. 462–469, 2008.

[26] F. J. Sheedy and L. A. J. O'Neill, "Adding fuel to fire: microRNAs as a new class of mediators of inflammation," *Annals of the Rheumatic Diseases*, vol. 67, supplement 3, pp. iii50–iii55, 2008.

[27] S. Zhu, M. Si, H. Wu, and Y. Mo, "MicroRNA-21 targets the tumor suppressor gene tropomyosin 1 (TPM1)," *Journal of Biological Chemistry*, vol. 282, no. 19, pp. 14328–14336, 2007.

[28] F. Meng, R. Henson, H. Wehbe-Janek, K. Ghoshal, S. T. Jacob, and T. Patel, "MicroRNA-21 regulates expression of the PTEN tumor suppressor gene in human hepatocellular cancer," *Gastroenterology*, vol. 133, no. 2, pp. 647–658, 2007.

[29] Z. Zhang, Z. Li, C. Gao et al., "miR-21 plays a pivotal role in gastric cancer pathogenesis and progression," *Laboratory Investigation*, vol. 88, no. 12, pp. 1358–1366, 2008.

[30] B. Wang and Q. Zhang, "The expression and clinical significance of circulating microRNA-21 in serum of five solid tumors," *Journal of Cancer Research and Clinical Oncology*, vol. 138, no. 10, pp. 1659–1666, 2012.

[31] F. Wu, M. Zikusoka, A. Trindade et al., "microRNAs are differentially expressed in ulcerative colitis and alter expression of macrophage inflammatory peptide-2 alpha," *Gastroenterology*, vol. 135, no. 5, pp. 1435–1438, 2008.

[32] M. P. Gantier, A. J. Sadler, and B. R. G. Williams, "Fine-tuning of the innate immune response by microRNAs," *Immunology and Cell Biology*, vol. 85, no. 6, pp. 458–462, 2007.

[33] R. M. O'Connell, D. S. Rao, A. A. Chaudhuri, and D. Baltimore, "Physiological and pathological roles for microRNAs in the immune system," *Nature Reviews Immunology*, vol. 10, no. 2, pp. 111–122, 2010.

[34] X. Chen, Y. Ba, L. Ma et al., "Characterization of microRNAs in serum: a novel class of biomarkers for diagnosis of cancer and other diseases," *Cell Research*, vol. 18, no. 10, pp. 997–1006, 2008.

[35] J. Lu, G. Getz, E. A. Miska et al., "MicroRNA expression profiles classify human cancers," *Nature*, vol. 435, no. 7043, pp. 834–838, 2005.

[36] B. Mateescu, L. Batista, M. Cardon et al., "MiR-141 and miR-200a act on ovarian tumorigenesis by controlling oxidative

stress response," *Nature Medicine*, vol. 17, no. 12, pp. 1627–1635, 2011.

[37] J. C. Brase, M. Johannes, T. Schlomm et al., "Circulating miRNAs are correlated with tumor progression in prostate cancer," *International Journal of Cancer*, vol. 128, no. 3, pp. 608–616, 2011.

[38] L. A. Selth, S. Townley, J. L. Gillis et al., "Discovery of circulating microRNAs associated with human prostate cancer using a mouse model of disease," *International Journal of Cancer*, vol. 131, no. 3, pp. 652–661, 2012.

[39] R. J. Bryant, T. Pawlowski, J. W. F. Catto et al., "Changes in circulating microRNA levels associated with prostate cancer," *British Journal of Cancer*, vol. 106, no. 4, pp. 768–774, 2012.

[40] H. C. Nguyen, W. Xie, M. Yang et al., "Expression differences of circulating microRNAs in metastatic castration resistant prostate cancer and low-risk, localized prostate cancer," *The Prostate*, vol. 73, no. 4, pp. 346–354, 2013.

[41] F. Y. Agaoglu, M. Kovancilar, Y. Dizdar et al., "Investigation of miR-21, miR-141, and miR-221 in blood circulation of patients with prostate cancer," *Tumor Biology*, vol. 32, no. 3, pp. 583–588, 2011.

[42] R. Mahn, L. C. Heukamp, S. Rogenhofer, A. Von Ruecker, S. C. Müller, and J. Ellinger, "Circulating microRNAs (miRNA) in serum of patients with prostate cancer," *Urology*, vol. 77, no. 5, pp. 1265–e16, 2011.

[43] F. Meng, R. Henson, M. Lang et al., "Involvement of human micro-RNA in growth and response to chemotherapy in human cholangiocarcinoma cell lines," *Gastroenterology*, vol. 130, no. 7, pp. 2113–2129, 2006.

[44] P. E. Blower, J. Chung, J. S. Verducci et al., "microRNAs modulate the chemosensitivity of tumor cells," *Molecular Cancer Therapeutics*, vol. 7, no. 1, pp. 1–9, 2008.

[45] A. Watahiki, R. J. Macfarlane, M. E. Gleave et al., "Plasma miRNAs as biomarkers to identify patients with castration-resistant metastatic prostate cancer," *International Journal of Molecular Sciences*, vol. 14, no. 4, pp. 7757–7770, 2013.

[46] M. Folini, P. Gandellini, N. Longoni et al., "miR-21: an oncomir on strike in prostate cancer," *Molecular Cancer*, vol. 9, p. 12, 2010.

[47] H. Konishi, D. Ichikawa, S. Komatsu et al., "Detection of gastric cancer-associated microRNAs on microRNA microarray comparing pre- and post-operative plasma," *British Journal of Cancer*, vol. 106, no. 4, pp. 740–747, 2012.

Hindawi Publishing Corporation
BioMed Research International
Volume 2013, Article ID 563751, 14 pages
http://dx.doi.org/10.1155/2013/563751

Research Article

A Novel Differential Predict Model Based on Matrix-Assisted Laser Ionization Time-of-Flight Mass Spectrometry and Serum Ferritin for Acute Graft-versus-Host Disease

Chun-yan Zhang,[1,2] Shu-hong Wang,[3] Wen-rong Huang,[3] Guang-hong Guo,[1] Zhu-hong Zhang,[1,2] Wen-jun Mou,[1,2] Li Yu,[3] and Ya-Ping Tian[1]

[1] *Department of Clinical Biochemistry, Chinese PLA General Hospital, 28 Fu-Xing Road, Beijing 100853, China*
[2] *Department of Immunology, Nankai University School of Medicine, Tianjin 300071, China*
[3] *Department of Hematology, Chinese PLA General Hospital, 28 Fu-Xing Road, Beijing 100853, China*

Correspondence should be addressed to Li Yu; chunhuiliyu@yahoo.com and Ya-Ping Tian; tianyp61@gmail.com

Received 7 May 2013; Accepted 20 August 2013

Academic Editor: Sudhish Mishra

Clinical diagnosis of acute graft-versus-host disease (aGVHD) mainly depends on clinical manifestation and tissue biopsies, leading to a delayed diagnosis and treatment for aGVHD patients when the early symptom is insignificant. Our objective was to investigate the possibility of prewarning the risk of aGVHD before and after allogeneic hematopoietic stem cell transplantation (allo-HSCT) by serum protein profiling combined with serum ferritin. The difference in polypeptide expression before and after transplantation had been compared by using CLINPROT technology, and serum ferritin levels have been analyzed simultaneously. Through combining serum ferritin and MS spectral data, the diagnosis sensitivity and specificity of our model for prewarning severe aGVHD (III~IV°aGVHD) before transplant all increased to 90.0%, while after transplant, the sensitivity and specificity are 78.3% and 86.4%. Our joint prewarning model could predict the risk of aGVHD, especially severe aGVHD before and after transplant, which also provides a reliable method to the continuous monitoring of the condition of patients.

1. Introduction

Allo-HSCT, as a great progress in the medical field for nearly half a century, is the most effective treatment for hematological malignancies. However, aGVHD following allo-HSCT is a major complication of restricting allo-HSCT application and curative effect, with an incidence rate of 35% to 64%. Therefore, early diagnosis and correct treatment of aGVHD have been an important topic in the field of transplantation immunology. At present, the clinical diagnosis of aGVHD mainly is based on pathological, biochemical, and histological symptoms. aGVHD usually occurs in the early stage after allo-HSCT, when most of the patients have a poor constitution and hard to tolerate tissue biopsies. Meanwhile, early performance of aGVHD is not typical, may be only skin itching, rash, mild nausea, or diarrhea, which is difficult to be diagnosed as aGVHD. But once the clinical performance is significant, the immune response has been so strong that it is dangerous and hard to be controlled even by strengthening the immune inhibitor. Therefore, noninvasive early warning and early diagnosis of aGVHD are particularly important to reduce mortality. Cytokines have been reported to be involved in the immune effect of aGVHD [1]. However, they have not yet found a suitable noninvasive blood index or portfolio to help early warning and diagnosis of aGVHD.

The use of immunosuppressive agents after allo-HSCT for treatment and prevention of aGVHD is an empiric therapy. Immune inhibitor combination based on cyclosporine A is used to prevent severe aGVHD [2]. It has been proven clinically that most of the aGVHD occurred in the prophylactic immunosuppression reducing or stop process. Up to now, there are few monitoring indicators, which can provide the basis for clinical medication [3]. Therefore, effective treatment monitoring index of aGVHD is important for early

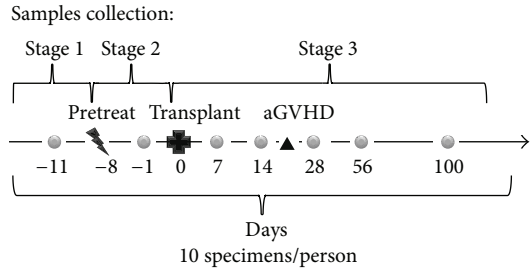

FIGURE 1: Blood specimens collection at the sequential time points.

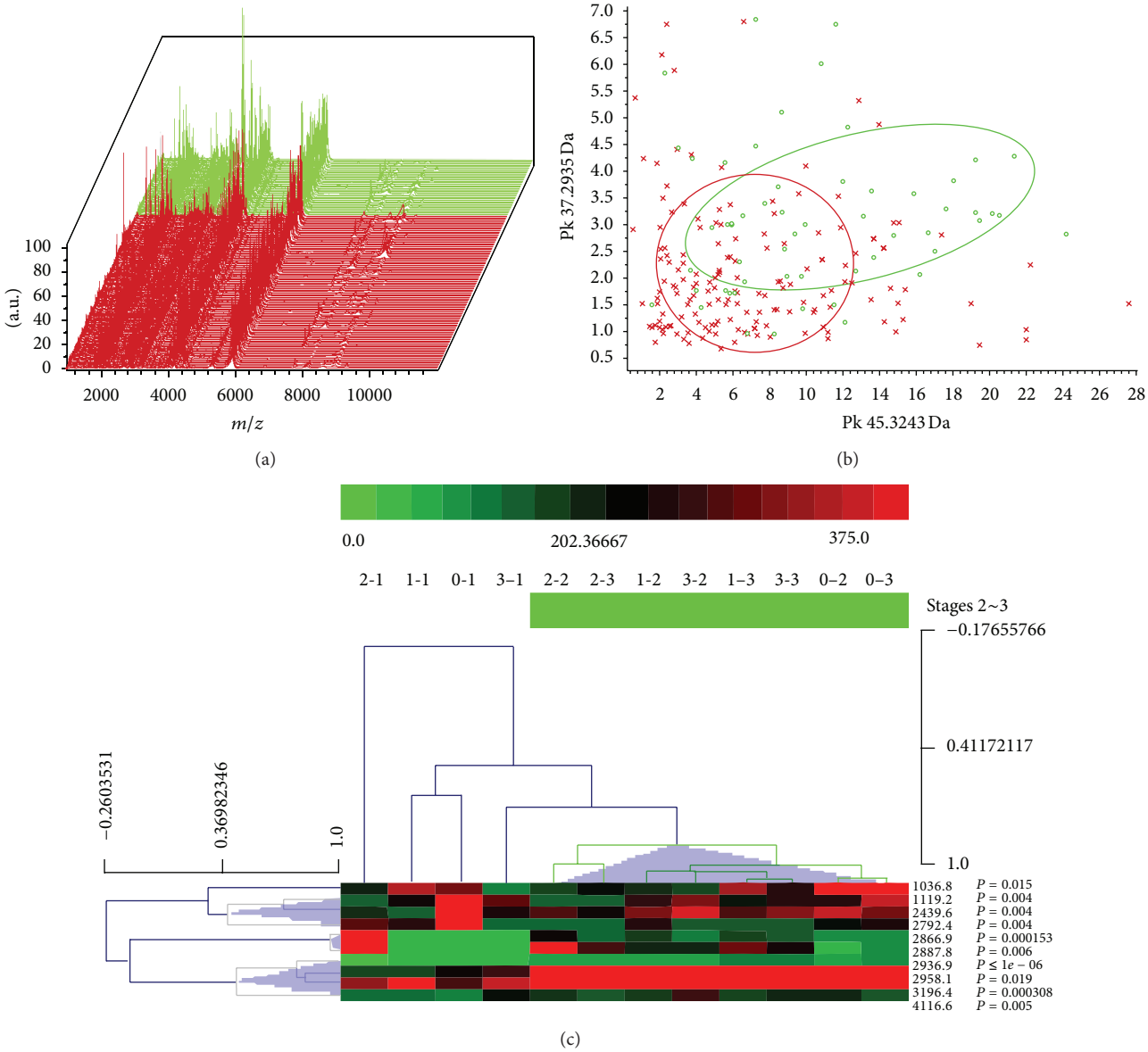

FIGURE 2: The distribution of aGVHD and non-GVHD patients. (a) Three-dimensional m/z ratio-intensity maps of aGVHD (red) and non-GVHD (green) specimens; (b) classification effect of the first two peaks (2935.4 Da and 3245.6 Da) from list of P values (red spots, aGVHD; green spots, non-GVHD); (c) hierarchical cluster analysis of 3-stage specimens with a set of 10 peaks.

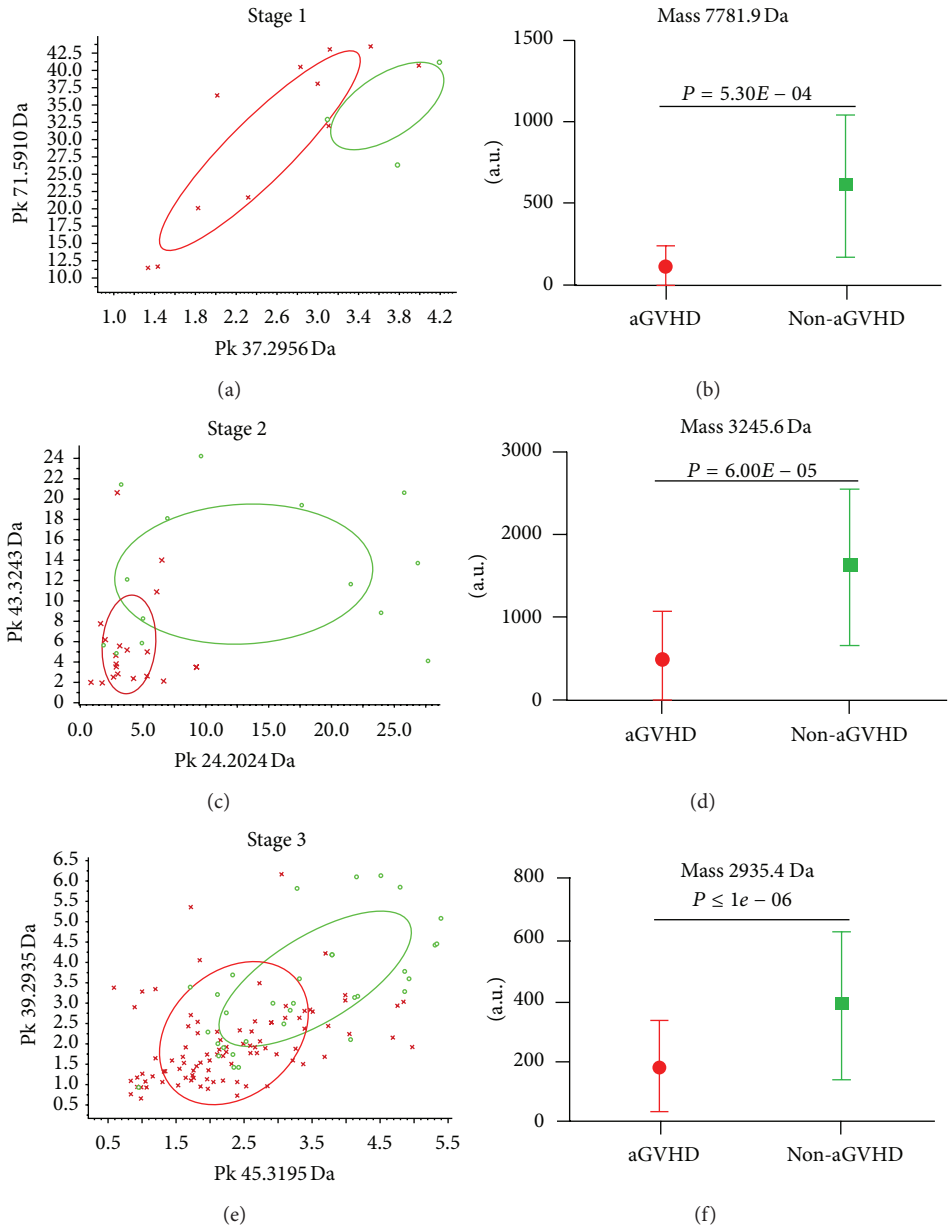

Figure 3: The distribution of aGVHD and non-GVHD patients in stage 1, stage 2, and stage 3 (red, aGVHD; green, non-GVHD). (a) classification effect of the first two peaks (5910 Da; 2957.7 Da) from list of P values in stage 1; (b) comparison of the expression of peak 7781.9 Da between aGVHD and non-GVHD patients in stage 1, $P = 5.30E - 04$; (c) classification effect of the first two peaks (3245.6 Da; 2026 Da) in stage 2; (d) comparison of the expression of peak 3245.6 Da in stage 2, $P = 6.00E - 05$; (e) classification effect of the first two peaks (2935.4 Da; 3195.6 Da) in stage 3; (f) comparison of the expression of peak 2935.4 Da in stage 3, $P < 1e - 06$.

Table 1: Consensus criteria for staging of aGVHD.

Grade	Skin	Liver	Gut
(I) Mild	Maculopapular skin area 25~50% of body	Normal	Diarrhea volume 500–1000 mL/day; nausea and emesis
(II) Moderate	Maculopapular skin area 50~100% of body	Serum bilirubin < 51 μmol/L	Diarrhea volume 1000~1500 mL/day; nausea and emesis
(III) Severe	Maculopapular skin area 50~100% of body	Serum bilirubin 51~256 μmol/L	Diarrhea volume > 1500 mL/day; nausea and emesis
(IV) Life threatening	Generalized exfoliative dermatitis or ulcerative dermatitis, simplex	Serum bilirubin > 256 μmol/L	Severe abdominal pain, with bloody diarrhea or intestinal obstruction

Table 2: Demographic and clinical characteristics of patients with and without acute GVHD.

Case	Age	Recipient gender	Doner gender	Underlying disease	Donor type	Pretreatment	Clinically affected aGVHD organ	aGVHD grade
1	48	M	F	AML	Related	BU + CY	Skin, mouth, gastrointestinal tract	IV
2	36	M	F	AML	Related	BU + CY		0
3	25	M	M	AML	Related	BU + CY		0
4	47	M	M	AML	Related	BU + CY	Skin, mouth	0
5	53	F	F	CML	Related	Flud + BU	Gastrointestinal tract	III
6	14	M	M	ALL	Related	TBI + CY + ATG		0
7	31	F	F	AML	Unrelated	BU + CY	Skin	I
8	15	M	M	AML	Related	BU + CY + ATG	Skin, liver	II
9	40	M	M	MDS	Related	BU + CY + ATG	Skin, mouth, gastrointestinal tract	IV
10	22	M	M	ALL	Related	TBI + CY + ATG	Skin, mouth, liver, gastrointestinal tract	III
11	22	M	M	MDS	Unrelated	BU + CY + ATG	Skin, mouth, gastrointestinal tract	IV
12	44	F	F	AML	Unrelated	BU + CY + ATG	Gastrointestinal tract	II
13	28	M	M	ALL	Unrelated	TBI + CY + ATG		0
14	28	M	M	ALL	Related	TBI + CY		0
16	47	F	F	CML	Related	BU + CY	Skin, liver, gastrointestinal tract	II
17	43	M	M	MDS	Related	BU + CY + ATG	Gastrointestinal tract	II
18	44	M	F	AML	Related	BU + CY	Liver, gastrointestinal tract	III
19	49	F	F	ALL	Unrelated	BU + CY + ATG	Gastrointestinal tract	II
22	15	M	M	ALL	Unrelated	BU + CY + ATG	Skin	I
30	23	M	M	ALL	Related	Flud + BU	Gastrointestinal tract	II
33	16	M	F	MDS	Related	BU + CY + ATG	Gastrointestinal tract	I
36	43	M	M	AML	Unrelated	BU + CY + ATG	Skin	I
39	27	F	F	CML	Unrelated	BU + CY	Skin, mouth	I
40	45	M	M	MDS	Related	BU + CY	Skin	I

M: male; F: female; AML: acute myelogenous leukemia; CML: chronic myelogenous leukemia; MDS: myelodysplastic syndrome; ALL: acute lymophoblastic leukemia; TBI: total body irradiation; BU: busulfan; CY: cyclophosphamide; Flud: fludarabine; ATG: rabbit antithymocyte globulin.

warning aGVHD and monitoring condition of patients after transplant [4].

The emergence and development of serum proteomics make the detection of protein biomarkers become of high throughput and high efficiency. Presently, researchers aboard have begun to investigate the mechanism of aGVHD and the early diagnosis of aGVHD using protein chips and show a good prospect [5, 6], but there are few reports at home. Recently, MALDI-TOF-MS technology has been widely used for the detection and identification of peptides, depending on its high sensitivity and efficiency.

Ferritin, as a principal protein for iron storage, participates in the regulation of hematopoiesis and immune system and is associated with many diseases. Almost all conditions of iron deficiency can cause ferritin reduction. The increase of serum ferritin (SF) level may be caused by blood overtransfusion, inflammation, malignant lesions, or liver diseases. A recent study showed that iron overload increases the risk of hepatic dysfunction and infections after transplantation [7].

Here, we enriched serum polypeptide from the patients with allo-HSCT and compared the difference in polypeptide expression before and after transplantation using CLINPROT technology. We compared the difference in polypeptides expression between aGVHD and non-GVHD patients and held a statistical analysis on serum ferritin levels simultaneously. By combining MS spectrum and serum ferritin, we constructed a novel prewarning model for aGVHD while avoiding invasive tissue biopsies and evaluating therapeutic effect.

2. Patients and Methods

2.1. Patients. Patients in the study were pathologically diagnosed as acute myelocytic leukemia (AML), chronic myeloid leukemia (CML), or myelodysplastic syndrome (MDS) and accepted allo-HSCT at Chinese PLA General Hospital from March 2012 till March 2013. All the patients accepted pretreatment with total body irradiation (TBI)/cyclophosphamide (Cy) scheme or modified busulfan (Bu)/Cy scheme 8~10 days before stem cell transplant. Then, the patients were treated with classic scheme to prevent aGVHD (cyclosporine A+ short-course methotrexate (MTX) + mycophenolate (MMF)). The diagnosis of aGVHD was determined by the clinical and pathologic evaluation of the patient, and aGVHD

Table 3: Statistical information for marker peptides of aGVHD and non-GVHD groups.

Stage	Mass	*P*TTA (*t*)	*P*-WTest	Ave. (aGVHD)	Ave. (non-GVHD)	SD (aGVHD)	SD (non-GVHD)
	7781.9	$5.30E-04$	0.005	127.4	727	101.5	386.2
1	2887.8	0.023	0.021	316.1	187.8	109.5	73.2
	2957.7	0.027	0.04	235.4	428.7	97	219.5
	3245.6	$6.00E-05$	$4.85E-04$	528.3	1614.9	520.8	893.9
	2866.5	0.000143	0.000694	134	483.6	106.1	363.5
	2046.6	0.004	0.051	86.8	212.4	43	183.4
	1781.8	0.004	0.058	139.7	415.5	82.7	410.8
	1351.9	0.005	0.012	60	148.4	29.5	135.9
	2026	0.006	0.048	548.5	1525.9	420.7	1468.8
	2995.1	0.008	0.000984	81.5	348.1	72.9	435.5
	8952.2	0.008	0.005	31.7	117.4	31.7	138.8
	1453.2	0.009	0.05	102.4	277.3	57	290.8
2	4236.6	0.01	0.005	652.5	429.1	286	127.9
	1694.6	0.013	0.06	83.9	230.4	47.2	256.3
	1609.3	0.016	0.036	48.7	125.8	39.7	135.2
	8142.8	0.029	0.111	18.1	133.6	13.2	239.9
	5936.3	0.034	0.031	1183.9	660.4	858.9	257.6
	5928	0.04	0.039	1158.8	649.4	865.9	254.3
	3961	0.041	0.217	248.4	385.9	114	269.3
	2275.3	0.042	0.135	119.5	181.4	61.3	114.7
	1096.4	0.043	0.088	161	86	129.7	36
	4617.8	$4.50E-02$	$5.70E-01$	30.7	124.1	16.5	211.7
	2935.4	$<1e-6$	$3.3E-06$	185.5	384.5	140.9	243
	3195.6	$1.19E-05$	0.000112	145.7	254.3	101.9	156.4
	3474.1	0.000563	0.902	35.6	608.2	16.5	1497.9
	3246	0.000677	0.001	836.9	1477.1	772.7	1224.9
	3455	0.001	0.052	46.8	80.5	20.2	88.3
	3318.4	0.002	0.636	45.2	85.4	22.8	112.1
	4019.4	0.005	0.002	84.5	66.2	36.3	20.6
	3939.6	0.007	0.004	118.3	87.2	63.5	37.5
	1264.6	0.008	0.042	84.7	118.3	47.5	90.8
	2740.8	0.009	0.003	102	72	65.3	29.4
	3493.3	0.01	0.705	34.3	127.4	16	327.6
	5365.9	0.014	0.032	216.8	148.5	158.7	77.8
	2867.3	0.016	0.017	268.8	450.9	279.9	539.9
3	1984.4	0.018	0.016	129.8	100.2	68.1	48.3
	4197.2	0.019	0.023	469	411.4	116.1	138.1
	2958.1	0.022	0.026	266.8	317.9	112.1	110.8
	3506.6	0.023	0.352	47.5	107.9	27.2	240.2
	2815.4	0.026	0.1	163	99.7	166.4	55.2
	3995.6	0.028	0.01	92	65.9	64.6	45.3
	2724.9	0.029	0.013	116.9	82.1	93.4	31.3
	1922.2	0.031	0.263	86.4	118.2	58.1	101.7
	3979.2	0.033	0.007	322.2	214.4	266	223.9
	3687.2	0.035	0.009	93.9	69.3	61.4	50.2
	3211.9	0.035	0.006	91.4	134.8	104.3	99.9
	1890	0.042	0.221	228.2	294.1	120.4	234.1
	1119.5	0.047	0.02	244.8	102.3	415.7	171.3
	5908	0.048	0.075	2074.5	2466.7	1043.6	886.9

Mass: m/z; *P*TTA: *P* value of *t*-test (two classes); *P*WKW: *P* value of Wilcoxon test (>two classes).

Table 4: Parameters in predict models for aGVHD and non-GVHD.

Variables in the equation									Classification table		
Stage	*B*	S.E.	Wald	df	Sig.	Exp (*B*)	95% C.I. for EXP (*B*) Lower	Upper			Percentage correct
Stage 2											
3245.6	−.002	.001	9.105	1	.003	.998	.997	.999	Disease	Non-GVHD	64.3
										aGVHD	86.4
Constant	2.346	.729	10.341	1	.001	10.442			Overall percentage		77.8
Stage 3											
1264.6	−.021	.008	6.762	1	.009	.979	.964	.995	Disease	Non-GVHD	78.1
2740.8	.097	.023	18.145	1	.000	1.101	1.054	1.152		aGVHD	95.3
2935.4	−.012	.003	17.430	1	.000	.989	.983	.994			
Constant	−1.225	.922	1.765	1	.184	.294			Overall percentage		90.6

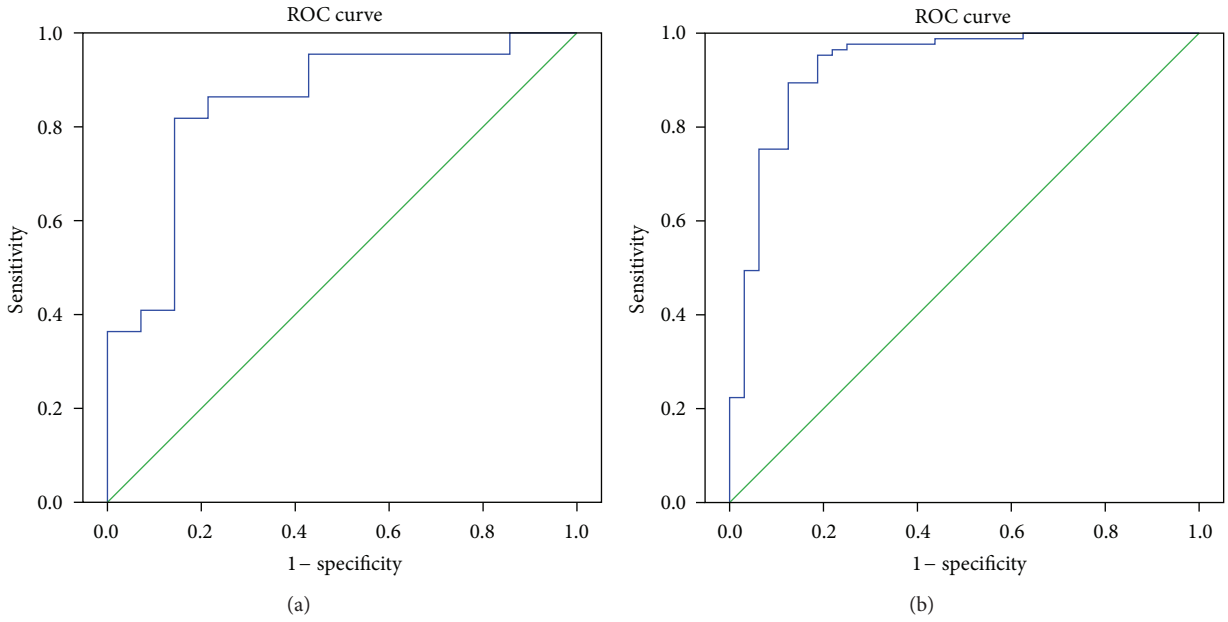

Figure 4: Respective ROC curve of the predicted probability of aGVHD in stage 2 (a) and stage 3 (b) with MS data from logistic regression. The state variable is aGVHD.

was graded according to previously published standard criteria (Table 1).

We used a total of 24 available cases for analysis with complete clinical data, among which there are 18 males, 6 females with age from 14 to 53 years, average 33.5.

Peripheral blood specimens from these patients were collected sequentially before and after allo-HSCT (Figure 1). For the patients of aGVHD, we collected peripheral blood specimens 1 day before treatment and 14, 28 days after treatment. We used a total of 245 specimens in mass spectrometry analysis.

2.2. Serum Ferritin Assay. The fasting blood was taken from cubital vein from every patient at the time point shown in Figure 1. The serum was segregated, and the biochemical parameter serum ferritin (SF) was assayed with commercially available kits (Roche Diagnostic, Penzberg, Germany) using Roche ELC2010 electrochemical luminescence instrument (Roche Diagnostic, Penzberg, Germany).

2.3. Blood Specimens. The blood specimens were collected from each participant within 24 hours. Fast sera were isolated by centrifugation at 4000 rpm for 7 min at 25°C and were frozen in aliquots of 150 μL at −80°C immediately for use.

2.4. MS Analysis. Serum peptides were enriched by weak cation exchange magnetic bead based kits (ClinProt Kits, Bruker Daltonics Inc., Fremont, CA) following the manufacturer's protocol, and spectra was acquired by matrix-assisted laser desorption/ionization time-of-flight mass spectrometry (MALDI-TOF-MS, Autoflex, Bruker Daltonik). Parameters were as follows: source 1,120 kV; ion source 2,186 kV; lens 7.6 kV; positive ion mode; 400 laser shots each sample.

Table 5: Statistical information for marker peptides of I~IV°aGVHD and non-GVHD groups.

Stage	Mass	*P*TTA (*t*)	*P*-KWTest	Ave. (non-GVHD)	SD (non-GVHD)	Ave. (I°aGVHD)	SD (I°aGVHD)	Ave. (II°aGVHD)	SD (II°aGVHD)	Ave. (III~IV°aGVHD)	SD (III~IV°aGVHD)
1	1984.7	1.15*E*−04	0.019	84.3	44.5	83.3	36.4	283	66.6	74	39.5
	3161.8	0.003	0.055	576.8	310.5	393.3	189.5	295.8	89	1167.7	388.4
	3183.8	0.013	0.083	70.8	23.4	80.5	66.8	53.8	31.4	231.3	121.5
	7781.9	0.03	0.036	686	439.5	98	99.4	292.8	290.3	20.7	23.1
	5931.3	0.035	0.127	680.8	266.8	327	300	397.8	277.9	1410.3	864.3
2	2809.6	5.91*E*−05	0.008	117.7	57.4	117.9	71.1	117.3	77.6	408.9	252.4
	5931.3	1.39*E*−04	0.003	641.6	249	644.7	313.9	938.3	298.6	2023.3	1253
	5362.2	5.94*E*−04	0.012	163.3	83.3	127.9	67.3	178	113.2	420.8	259.4
	1119.5	8.73*E*−04	0.02	47.8	20	102.7	63.5	614.8	619.4	113.8	147
	2866.5	0.003	0.005	385.1	271.9	158.1	73.2	107.5	101.5	129.4	120.2
	1781.5	0.007	0.086	459.4	429.4	100.1	64.6	126.5	86.1	157	90.3
	4233.8	0.009	0.015	449	127.6	568.1	245.5	488.1	231.3	800.6	301.9
	2046.6	0.011	0.214	226.4	195.6	70.1	28.6	72.5	21.3	106.8	55.3
	5910.2	0.014	0.026	2381.3	1018.4	2422.2	883	2753.1	728	1287.2	1036.9
	5341	0.015	0.033	605.8	243.3	525.8	264.2	507.1	224	254.4	207.6
	3245.6	0.017	0.008	1490	880.8	938.4	942.1	445.3	359.4	500.1	764.7
	1899.8	0.017	0.069	420.1	279.8	793.2	561.8	303.4	96.9	378.1	180
	2025.1	0.018	0.097	1593	1579.7	323.6	115.3	474.8	278.8	678.9	585.5
	1085.5	0.018	0.12	125.3	62.8	242.8	150.8	153.3	42.6	120.2	59.2
	1969.3	0.018	0.009	262.3	144.4	320.2	179.7	108.5	37.7	237.3	113.4
	1280.8	0.021	0.16	177.8	88.3	373.8	309.5	145.6	63.1	161.4	91.7
	8952.2	0.022	0.048	130.2	146.7	36.1	41.8	24.3	13.3	29.3	26.6
	1069.1	0.023	0.145	404.2	188.9	627.7	322.6	404.4	136.2	320	123.6
	1351.9	0.024	0.067	159.2	144.3	76.2	42.4	48.6	10.2	61.6	33.6
	5827.7	0.026	0.145	84	36.5	136.1	103.1	93.4	46	217.3	168.9
	1453.2	0.027	0.166	304	307.1	114	62.2	88.9	63.5	99.3	52.4
	3976.9	0.028	0.011	157.2	92.5	142	66.9	101.1	52.2	458.1	529.6
	1694.6	0.033	0.157	255	269.9	87.7	42.9	74.9	45.1	82.9	59.6
	5835.9	0.034	0.133	97.3	30.4	145.6	100.5	109.9	37.1	225.4	170.5
	1413.9	0.039	0.08	39.3	19.7	130.2	167.3	30.9	11.9	31.3	17.3
	1053.4	0.042	0.374	265.8	124.1	447.8	280.7	238.4	94.8	241.8	136.4
	3959.6	0.042	0.071	426.3	270.3	354.8	209.5	217.1	95.6	198.6	130.1
	1027.6	0.044	0.075	47.4	23.2	136.6	137.2	151.9	154.5	48.3	32.9
	1096.4	0.047	0.126	84.5	38.1	199.7	153.3	176.9	125.3	103.6	70.2

Table 5: Continued.

Stage	Mass	*P*TTA (*t*)	*P*-KWTest	Ave. (non-GVHD)	SD (non-GVHD)	Ave. (I°aGVHD)	SD (I°aGVHD)	Ave. (II°aGVHD)	SD (II°aGVHD)	Ave. (III~IV°aGVHD)	SD (III~IV°aGVHD)
3	3245.6	2.35*E*−05	6.13*E* − 06	1549.8	1274.7	817.5	742.2	753.3	597.7	349.7	366.2
	5931.3	7.44*E*−05	2.31*E* − 04	647.7	275.3	545.5	271.3	897.3	393.8	1297	864.4
	2935.8	9.42*E*−05	1.65*E* − 04	361.2	233.4	188.7	131.9	132.8	88.8	227.2	226.2
	2815.4	3.30*E*−04	0.007	97.1	49.6	136	74.3	125.9	96.5	260.5	253.7
	3195.6	5.01*E*−04	0.001	243.2	155.9	129.7	94.2	127.5	96.1	128.3	113
	5341.5	5.99*E*−04	9.54*E* − 04	527.7	247.1	616.9	314	750.2	470.4	338.8	276.5
	3976.4	0.001	7.19*E* − 04	236.6	240.4	370.6	267.6	232.3	189.2	493.4	335.1
	5360.6	0.001	4.25*E* − 04	144.6	76.5	155.4	94.6	271.5	150.5	348	384.7
	3995.6	0.003	0.002	68.5	47.9	100	63.1	72.3	47.2	127.9	88.5
	4303.2	0.006	0.002	128.5	110.7	169.3	97.2	116.4	79.5	214.3	128
	1947.6	0.013	0.012	1574.5	1497.1	1608.5	1326.5	673.2	421.5	1106.9	1087.4
	2757.4	0.014	0.008	114.3	84	201.1	258	72.1	39.5	130.6	77.8
	2866.5	0.016	6.31*E* − 04	439.5	541.4	284.2	367.7	230.1	175.1	128.2	62.4
	1609.6	0.016	0.024	54.7	28.5	86.5	93.2	53	30.6	40.6	16.4
	2565.3	0.019	0.27	70.2	31.9	126.8	126.7	63.7	35.4	86.8	82.3
	2370.6	0.021	0.027	109.3	56.1	156.9	110.8	92	71.5	117.8	49.1
	8952.8	0.029	0.035	47.9	38.8	123.8	240.8	33	38.1	32	49.8
	3959.2	0.03	0.007	545.5	407.4	723.7	423	435.9	409.2	415.9	339
	5910.2	0.031	0.068	2351.5	916.7	2397.5	1167	2295.2	877.4	1582.6	1325.7
	2275.3	0.032	0.07	216	176.5	169.2	88.5	124.9	56.5	227.3	177.6
	4094.9	0.035	0.024	437.4	122.7	443.6	97.8	390.2	152.6	354.5	101.2
	3687.2	0.038	0.018	73.7	53.2	106.2	63.6	73.7	47.4	111.4	77.3
	5833.2	0.04	0.029	81	46.6	97.4	68.5	113.8	53.6	137	110.3
	1889.7	0.042	0.045	220.2	118.2	163.3	71	208.2	95	159.2	80
	4253.6	0.044	0.291	124.9	42.2	160.6	85.1	121	41	146.7	51.3
	2107.1	0.046	0.075	188.3	79.8	201.4	83.5	144.1	65.4	164.7	81.8
	5968.7	0.047	0.135	115.8	54.9	121.6	59.6	159.8	81.9	159.1	94.8
	1899.8	0.047	0.1	450.2	305.7	272.4	174.9	330	235.8	311.3	236.3
	1119	0.048	0.004	89.7	152.6	377	638.5	342	486.9	181.3	298.3

2.5. Data Processing. ClinProTools bioinformatics software (ver. 2.0; Bruker Daltonics) was used for statistical analysis and the recognition of peptide patterns. The MS spectra for peaks of 1,000–10,000 m/z (with a signal-to-noise ratio >5) were selected and calculated by t-test P value/analysis using SPSS software (ver.19.0). The proteins/peptides with a P value < 0.05 were confirmed to be significantly different.

3. Results

3.1. The Distribution of aGVHD Group and Non-GVHD Group. The characteristics of the aGVHD and non-GVHD patients are shown in Table 2. The aGVHD patients included 12 males and 6 females, whose median age was 33 years (range: 15–53 years). All 245 serum specimens were analyzed

Table 6: Parameters in predict models for severe aGVHD.

		Variables in the equation								Classification table		
		B	S.E.	Wald	df	Sig.	Exp (B)	95% C.I. for EXP (B)				Percentage correct
								Lower	Upper			
Stage 2	2809.6	.017	.008	4.960	1	.026	1.017	1.002	1.032	Disease Grades 3~4	Non-gvhd, Grade 1, Grade 2	100.0
	3976.9	.015	.009	2.754	1	.097	1.015	.997	1.032		Grades 3~4	80.0
	Constant	−7.305	2.749	7.064	1	.008	.001			Overall percentage		95.0
Stage 3	2815.4	.005	.003	2.902	1	.088	1.005	.999	1.010	Disease Grades 3~4	Non-gvhd, Grade 1, Grade 2	98.8
	3995.6	.004	.007	.328	1	.567	1.004	.990	1.019		Grades 3~4	39.1
	4303.2	.002	.004	.175	1	.676	1.002	.993	1.011			
	5931.3	.001	.001	5.507	1	.019	1.001	1.000	1.003			
	Constant	−3.991	.791	25.470	1	.000	.018			Overall percentage		85.6

Table 7: Parameters in combined models for severe aGVHD.

		Variables in the equation								Classification table		
		B	S.E.	Wald	df	Sig.	Exp (B)	95% C.I. for EXP(B)				Percentage correct
								Lower	Upper			
Stage 2	2809.6	.014	.008	2.960	1	.085	1.014	.998	1.030	Disease Grades 3~4	Non-gvhd, Grade 1, Grade 2	96.7
	3976.9	.009	.008	1.206	1	.272	1.009	.993	1.025		1.00	70.0
	SF	.001	.001	1.141	1	.285	1.001	1.000	1.002			
	Constant	−6.666	2.417	7.607	1	.006	.001			Overall percentage		90.0
Stage 3	2815.4	.004	.003	1.483	1	.223	1.004	.998	1.010	Disease Grades 3~4	Non-gvhd, Grade 1~2	96.3
	3995.6	.004	.008	.232	1	.630	1.004	.988	1.021		Grades 3~4	47.8
	4303.2	.002	.005	.180	1	.671	1.002	.992	1.012			
	5931.3	.001	.001	2.536	1	.111	1.001	1.000	1.002			
	SF	.001	.000	8.998	1	.003	1.001	1.000	1.001			
	Constant	−4.970	.958	26.914	1	.000	.007			Overall percentage		85.6

by MADLI-TOF-MS (mass 1,000~10,000 Da; signal-to-noise ratio >5) (Figure 2(a)) and distributed between non-GVHD and aGVHD by peak 2935.4 Da and 3245.6 Da (Figure 2(b)). All these serum specimens were collected from stage 1 to stage 3 (Figure 1), and a set of 10 peaks that discriminate the 3 stages were used in the hierarchical cluster analysis. As shown in Figure 2(c), serum peptides/proteins in stage 1 are inconsistent with the latter two stages, suggesting that the grouping should be peptides should be grouped and analyzed base on the treatment stages.

Figure 3 compares the different serum proteins/peptides between aGVHD and non-GVHD in stage 1 (before pretreatment), stage 2 (before transplant), and stage 3 (after transplant), respectively. t- and Mann-Whitney U tests were performed to determine significant differences between the aGVHD and non-GVHD groups (Table 3), and we made rough estimate of the patients into aGVHD and non-GVHD group using mass spectrometry results (Figures 3(a), 3(c), and 3(e)). We showed different expression of peptides mass 7781.9 Da ($P = 5.30E - 04$) (Figure 3(b)), 3245.6 Da ($P = 6.00E - 05$) (Figure 3(d)), and 2935.4 Da ($P < 1e - 06$) (Figure 3(f)) between aGVHD and non-GVHD patients in different stages.

3.2. Modeling for aGVHD and Non-GVHD with Mass Spectra Data. For the purposes of prewarning aGVHD, we constructed models in stage 2 and stage 3 using binary logistic regression analyses. Previously, we analyzed the correlation of the peaks selected by ClinProTools software and substituted each peptide into a binary logistic regression (method "Enter") for their contribution to our model (data not shown). The peptides with a significant contribution to the model ($P < 0.01$) and relatively independent to each other ($r < 0.7$, $P < 0.01$) were substituted into the multivariate logistic regression (Table 4). As shown in Figure 4(a),

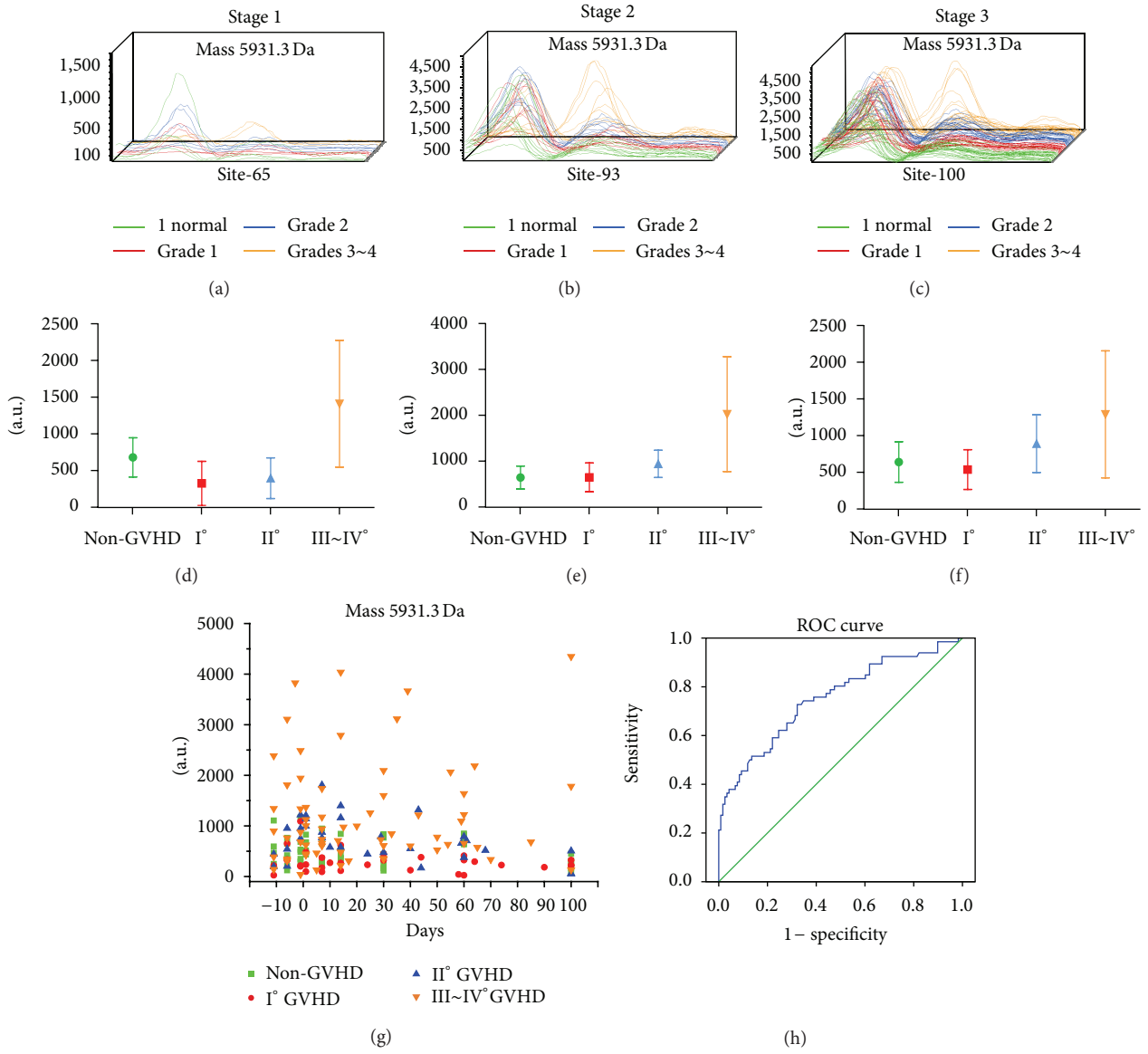

Figure 5: The expression of peak 5931.3 Da in different grades of aGVHD. (green: non-GVHD, red: I°aGVHD, blue: II°aGVHD, and yellow: III~IV°aGVHD). ((a)~(c)) Three-dimensional m/z ratio-intensity maps of peak 5931.3 Da in stage 1(a), stage 2(b), and stage 3(c); ((d)~(f)) bar chart of peak 5931.3 Da intensity in the four different groups, showing an increasing trend in peak 5931.3 Da in severe aGVHD patients in all 3 stages ($P < 0.01$); (g) the expression of peak 5931.3 Da in all the patients through the whole process of allo-HSCT; (h) ROC curve of the predicted probability of severe aGVHD with peak 5931.3 Da from logistic regression.

only one peptide 3245.6 Da enters the model for predicting aGVHD and non-GVHD in stage 2. The area under the curve of ROC curve (AUROC) is 0.851, and accuracy is 77.8%, with a sensitivity of 81.8% and a specificity of 85.7%. Meanwhile, there are 3 peptides (1264.6 Da, 2740.8 Da, and 2935.4 Da) participating in the predict model for aGVHD and non-GVHD during stage 3. AUROC is up to 0.929 (Figure 4(b)), accuracy is 90.6%, while the sensitivity and specificity are 89.4% and 87.5%. These data demonstrate the capability of mass spectra data to predict aGVHD during a certain period. The classification equation for predict aGVHD is as follows:

stage 2: $P = [1 + e^{(-0.002 \times \text{mass3245.6} + 2.346)}]^{-1}$,

stage 3: $P = [1 + (e^{(-0.021 \times \text{mass1264.6} + 0.0979 \times \text{mass2740.8})} \times e^{(-0.012 \times \text{mass2935.4} - 1.225)})]^{-1}$.

3.3. Modeling for Severe aGVHD. Patients with severe aGVHD not responding to treatment with steroids have a poor prognosis [8]. Although the incidence of III~IV°aGVHD is low, clinical data has shown that it almost causes an irrevocable threat to the lives of the patients. Therefore, prewarning severe aGVHD is related to minimizing the incidence and improving the prospects of survival directly [9]. We further refined the groups into I°aGVHD, II°aGVHD, III~IV°aGVHD, and non-GVHD depending on

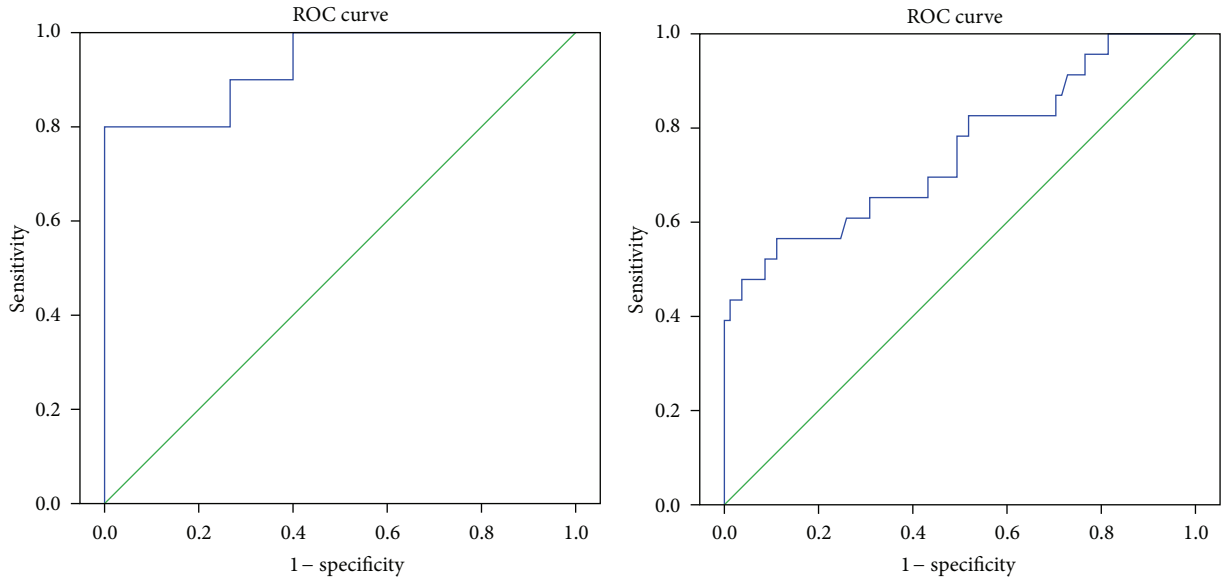

Figure 6: Respective ROC curve of the predicted probability of severe aGVHD in stage 2 (a) and stage 3 (b) with MS data from logistic regression. The state variable is severe aGVHD.

clinical consensus criteria for staging of aGVHD (Table 1) and contrasted the serum peptides/proteins difference of the four groups. In the peaks which showed significant differences analyzed by ClinProTools software (Table 5), the peak 5931.3 Da shows favourable value on prewarning III~IV°aGVHD throughout the whole process of treatment. Figures 5(a)–5(c) show the intuitive peaks of the four groups, and Figures 5(d)–5(f) illustrate the intensities of 5931.3 Da peak separately in 3 stages. Peak 5931.3 Da shows a marked overexpression in III~IV°aGVHD group, compared to non-GVHD group, I°aGVHD group, and II°aGVHD group (Figure 5(g)). When the peptide mass 5931.3 Da was used to distinguish III~IV°aGVHD patients from non-GVHD and I~II°aGVHD patients, AUROC was 0.754 (Figure 5(h)).

Most of the severe aGVHD occurred in the prophylactic immunosuppression reducing or stop process, which caused by empirical drug stop and the lack of effective indicators for early warning aGVHD. Therefore, our models should double as an effective treatment monitoring index of severe aGVHD. We grouped non-GVHD and I~II°aGVHD to distinguish severe aGVHD from them. The correlation of the peaks and their contribution to predict models were analyzed as before, and peptides with a significant effect were substituted into the multivariate logistic regression (Table 6).

During the stage from pretreatment to transplant, the model for III~IV°aGVHD and non-GVHD, I~II°aGVHD, and AUROC of the unite peak, which combined with peaks 2809.6 Da, and 3976.9 Da is up to 0.933. The accuracy is 95.0% with a sensitivity of 80.0% and a specificity of 100.0% (Figure 6(a)). Meanwhile, during the stage from transplant to aGVHD outbreak, AUROC of the unite model (peaks 2815.4 Da, 3995.6 Da, 4303.2 Da, and 5931.3 Da) is 0.750, accuracy is 85.6%, and the sensitivity and specificity of it are 56.5% and 88.9%, separately (Figure 6(b)). The two models can predict the risk of progression to severe aGVHD in stage 2 and stage 3, respectively.

The peptides in our models such as mass 1264.6 Da and 3245.6 Da have been identified, and they belong to fibrinogen alpha chain precursor [10, 11]. The others are still unknown. However, it is essential to verify them, especially 5931.3 Da, which has a high contribution to aGVHD.

3.4. Value of Serum Ferritin to Predict aGVHD. Due to the unavoidable noise of the mass spectra coming from instrument and other external interference, serum ferritin is involved into our models to induce noise and improve the sensitivity. Iron overload is frequently observed in patients with hepatopathy, cancer, and hematologic diseases, and serum ferritin is the most sensitive indicator for iron metabolism. Previous studies have shown that, during allo-HSCT, elevated pretransplant serum ferritin level is associated with a higher incidence of treatment-related complications [7, 12–14]. However, the specificity and sensitivity of sole serum ferritin to aGVHD are very limited due to individual diversity. The normal values of serum ferritin in biochemical tests are male (20~60 years old) 30~400 ng/mL; female (17~60 years old) 13–150 ng/mL. As shown in Figure 7(a), statistics suggests that I°aGVHD and III~IV°aGVHD groups, especially the latter, have an elevated serum ferritin level before and after transplant. Therefore, we used serum ferritin to predict severe aGVHD instead of all grades of aGVHD. During stage 2, AUROC of single SF is 0.802 (Figure 7(b)), with a sensitivity of 66.7% and a specificity of 90.3%; in stage 3, AUROC of single SF is 0.814 (Figure 7(c)), with a sensitivity of 78.3% and a specificity of 77.8%.

3.5. The Combination Model for Prewarning Severe aGVHD. To improve the prewarning value of mass spectrometry and

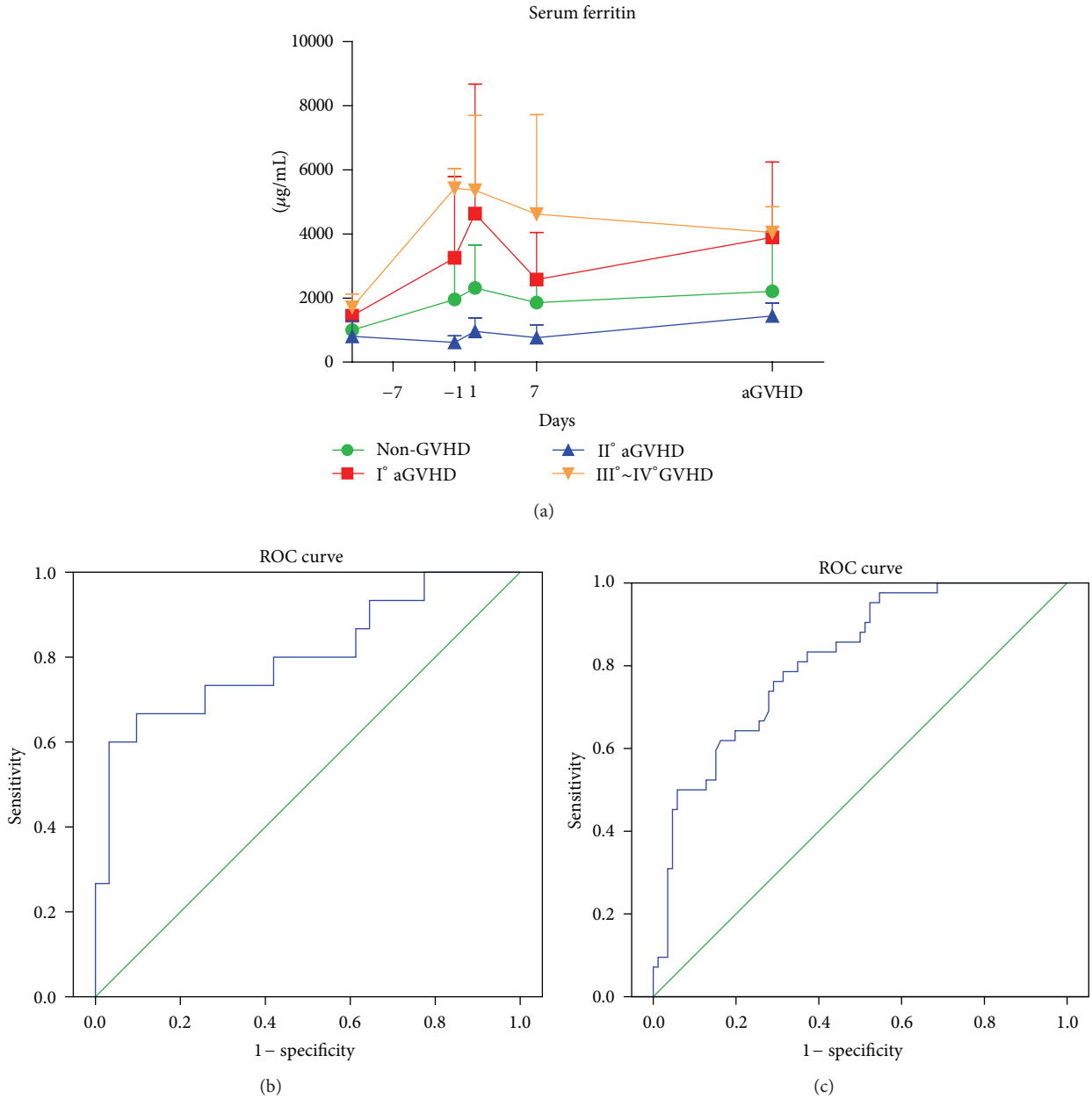

Figure 7: The effect of serum ferritin level on predicting severe aGVHD. (a) The level of serum ferritin in non-GVHD (green), I°aGVHD (red), II°aGVHD (blue), and III~IV°aGVHD (yellow); ((b)~(c)) respective ROC curve of the predicted probability of severe aGVHD with single serum ferritin in stage 2 (b) and stage 3 (c) from logistic regression. The state variable is severe aGVHD.

serum ferritin to aGVHD, we conjointly analyzed the two noninvasive indicators (Table 7). Figures 8(a) and 8(b) illuminate that the sensitivity and specificity are obviously elevated using added method. During the period from pretreatment to transplant, AUROC of combination is 0.920 and accuracy is 90%, with a sensitivity of 90.0% and a specificity of 90.0% (Figure 8(a)). After transplant, the conjoint analysis of mass spectrometry and serum ferritin also has an elevated early-warning value. AUROC of it is 0.855 and accuracy is 85.6%, the sensitivity and specificity of it are 78.3% and 86.4% (Figure 8(b)). This further develops the potential of our data and supports our methods that are robust for raw MS data preprocessing.

The classification equation combined with mass spectrometry and serum ferritin for predicting severe aGVHD is as follows:

$$\text{stage 2: } P = [1 + (e^{(0.014\times \text{mass2809.6}+0.009\times \text{mass3976.9})} \times e^{(+0.001\times \text{SF}-6.666)})]^{-1},$$

$$\text{stage 3: } P = [1 + (e^{(0.004\times \text{mass2815.4}+0.004\times \text{mass3995.6})} \times e^{(+0.002\times \text{mass4303.2}+0.001\times \text{mass5931.3}+0.001\times \text{SF}-4.970)})]^{-1}.$$

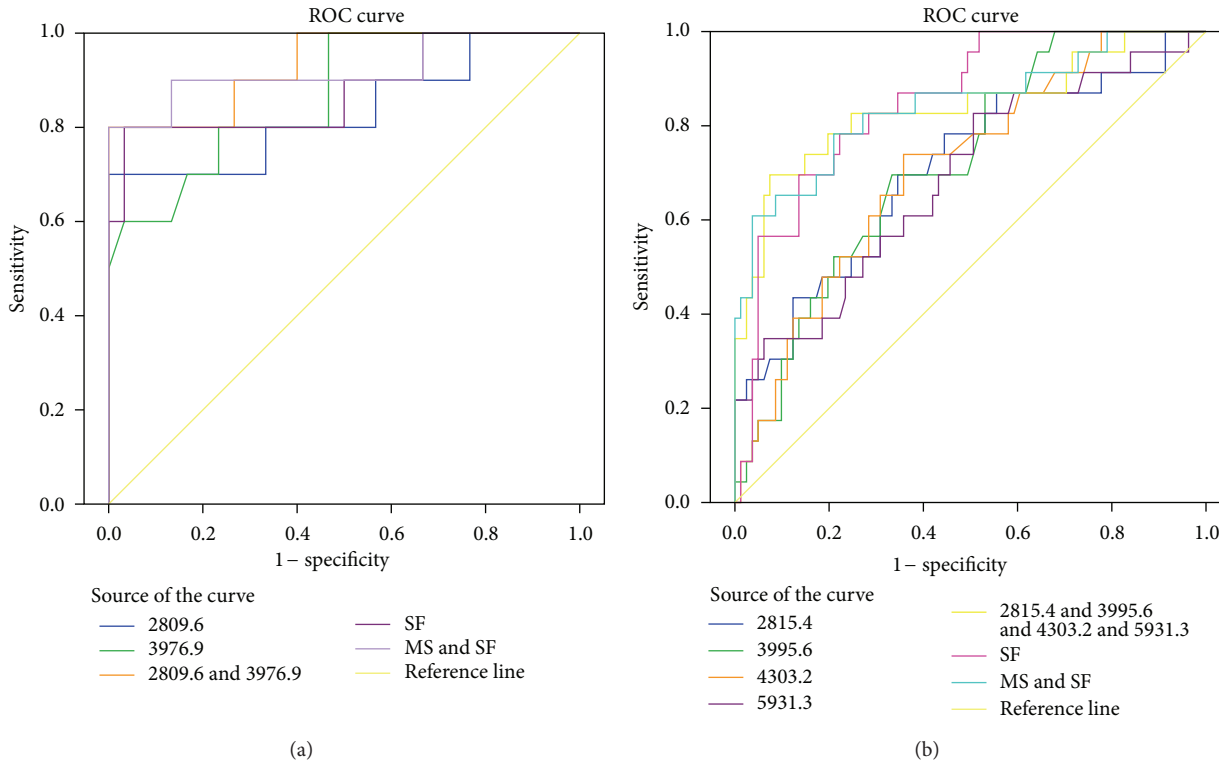

Figure 8: Respective ROC curve of the predicted probability of severe aGVHD with "MS+SF" combination in stage 2 (a) and stage 3 (b) from logistic regression. The state variable is severe aGVHD.

4. Discussion

Although the pathophysiology of acute GVHD is complex, accumulating evidence suggests that most of the effectors participating in aGVHD immune responses are serum peptides/proteins [4]. Most previous investigations focused on cytokine in aGVHD and made it as biomarker [6, 15–17], which is reliable, stable, but lagging. In another words, cytokine is not effective enough for prewarning aGVHD. Therefore, we collected blood samples from the patients at sequential points from the very beginning of the treatment to aGVHD occurrence for our research.

Currently, MALDI-TOF-MS has been one of the sensitive and effective approaches for identifying potential biomarkers of health and disease [18]. Here, we enriched the serum low abundance peptides/proteins by WCX magnetic beads and got serum protein profiling by MALDI-TOF-MS, which offers wide selection, and at the same time it is a noninvasive detection avoiding tissue biopsies.

In this study, we analyzed the difference between aGVHD and non-GVHD group before and after transplantation. During the stage from pretreatment to transplant, our MS spectral data shows prewarning potential to aGVHD. Before transplant, the sensitivity and specificity of our model are 81.8% and 85.7%, which serve as an early warning of aGVHD, giving therapists plenty of time to make preventive measures. After transplant, the accuracy of our model is 90.6%, while the sensitivity and specificity are 89.4% and 87.5%.

Due to individual diversity and instrument noise, raw MALDI-TOF MS spectra need to be analyzed based on clinical features. Therefore, we constructed the models combined with serum ferritin. Iron overload increases the risk of infections, venoocclusive disease and hepatic dysfunction in posttransplant period [12], which is also proved by our statistical data. Our statistics reports that SF concentrations of our patients all exceed the upper line. Moreover, SF levels of the patients with aGVHD, especially severe aGVHD (III~IV°aGVHD) are much higher than those of non-GVHD group, whether before transplant or after transplant. Clinical statistics have reported that severe intestinal aGVHD was often difficult to reverse and sometime rapidly lead to death. Through combining serum ferritin and MS spectral data, the sensitivity and specificity of our model for prewarning severe aGVHD before transplant increased to 90.0%. The warning during this stage will provide sufficient time for therapists to observe the patient closely; to start, stop, or change the dosage of any medicine; to delay or stop transplant; and to enhance preparedness and aGVHD protection.

After transplant, there is also joint scheme that suggests a risk for severe aGVHD, the sensitivity and specificity of which are 78.3% and 86.4%. In clinically work, the dosage of immunosuppressive drugs prone to be insufficient or excessive, since of that treatment response and monitoring indicators are insufficient at present. Short dosage would cause disease, like aGVHD, while excess drugs would lead to a tumor recurrence. [3]. Our model can realize continuous

monitoring to the condition of patients and prewarning the risk for severe aGVHD, which threatens the lives of the patients.

An interesting phenomenon in our models was that the peak 3245.6 Da, which is a fragment of fibrinogen alpha chain precursor, was more highly expressed in non-GVHD than in aGVHD patients before transplant. This suggested the potential of 3245.6 Da as a biomarker for aGVHD and the possible relationship between fibrinolysis and aGVHD, which would be explored in our further work. The peak 5931.3 Da in the original MALDI-TOF profiles showed its trend to severe aGVHD through the entire course of allo-HSCT. Further identification is needed for this biomarker for severe aGVHD, and intensive study remains to be continued.

Taken together, all of the evidences reveal a novel prewarning model for aGVHD while avoiding invasive tissue biopsies and improving long-term effect of transplantation. Furthermore, more studies are needed to verify the special serum peptides expression and the roles they play.

5. Conclusions

Our models can predict aGVHD and non-GVHD based on MS spectral data while avoiding invasive tissue biopsies. The sensitivities of the models are 81.8% and 89.4% before and after transplant. Moreover, through combining serum ferritin and MS spectral data, the sensitivity and specificity of our model for prewarning severe aGVHD (III~IV°aGVHD) before transplant all increased to 90.0%, while after transplant the sensitivity and specificity are 78.3% and 86.4%.

Authors' Contribution

Chun-yan Zhang and Shu-hong Wang contributed equally to this work.

Acknowledgments

The authors would like to thank the staff in the Department of Clinical Biochemistry and Department of Hematology at the Chinese PLA General Hospital for their support and guidance. This research was supported by the National Natural Science Foundation of China (81071413), the National High Technology Research and Development Program of China (863 Program) (2011AA 02A 111), and the Capital Health Research and Development of Special (2011-5001-07). Written consent for publication was obtained from either the patients or their relatives.

References

[1] A. Bacigalupo, "Acute graft-versus-host disease," *Immunotherapy*, vol. 3, no. 12, pp. 1419–1422, 2011.

[2] L. Perez, C. Anasetti, and J. Pidala, "Have we improved in preventing and treating acute graft-versus-host disease?" *Current Opinion in Hematology*, vol. 18, no. 6, pp. 408–413, 2011.

[3] R. Korngold and J. H. Antin, "Biology and management of acute graft-versus-host disease," *Cancer Treatment and Research*, vol. 144, pp. 257–275, 2009.

[4] T. Toubai, J. Tanaka, S. Paczesny, Y. Shono, P. Reddy, and M. Imamura, "Role of cytokines in the pathophysiology of acute graft-versus-host disease (GVHD) are serum/plasma cytokines potential biomarkers for diagnosis of acute GVHD following allogeneic hematopoietic cell transplantation (Allo-HCT)?" *Current Stem Cell Research and Therapy*, vol. 7, no. 3, pp. 229–239, 2012.

[5] G. Socié, "Graft-versus-host disease: proteomics comes of age," *Blood*, vol. 113, no. 2, pp. 271–272, 2009.

[6] S. Paczesny, O. I. Krijanovski, T. M. Braun et al., "A biomarker panel for acute graft-versus-host disease," *Blood*, vol. 113, no. 2, pp. 273–278, 2009.

[7] S. Sakamoto, H. Kawabata, J. Kanda et al., "Differing impacts of pretransplant serum ferritin and C-reactive protein levels on the incidence of chronic graft-versus-host disease after allogeneic hematopoietic stem cell transplantation," *International Journal of Hematology*, vol. 97, pp. 109–116, 2013.

[8] G. Kobbe, P. Schneider, U. Rohr et al., "Treatment of severe steroid refractory acute graft-versus-host disease with infliximab, a chimeric human/mouse antiTNFα antibody," *Bone Marrow Transplantation*, vol. 28, no. 1, pp. 47–49, 2001.

[9] A. R. Rezvani, B. E. Storer, R. F. Storb et al., "Decreased serum albumin as a biomarker for severe acute graft-versus-host disease after reduced-intensity allogeneic hematopoietic cell transplantation," *Biology of Blood and Marrow Transplantation*, vol. 17, no. 11, pp. 1594–1601, 2011.

[10] Y. L. Tao, Y. Li, J. Gao et al., "Identifying FGA peptides as nasopharyngeal carcinoma-associated biomarkers by magnetic beads," *Journal of Cellular Biochemistry*, vol. 113, no. 7, pp. 2268–2278, 2012.

[11] N. Kaneshiro, Y. Xiang, K. Nagai et al., "Comprehensive analysis of short peptides in sera from patients with IgA nephropathy," *Rapid Communications in Mass Spectrometry*, vol. 23, no. 23, pp. 3720–3728, 2009.

[12] S. Sivgin, S. Baldane, L. Kaynar et al., "Pretransplant serum ferritin level may be a predictive marker for outcomes in patients having undergone allogeneic hematopoietic stem cell transplantation," *Neoplasma*, vol. 59, no. 2, pp. 183–190, 2012.

[13] N. S. Majhail, H. M. Lazarus, and L. J. Burns, "Iron overload in hematopoietic cell transplantation," *Bone Marrow Transplantation*, vol. 41, no. 12, pp. 997–1003, 2008.

[14] P. Armand, H. T. Kim, C. S. Cutler et al., "Prognostic impact of elevated pretransplantation serum ferritin in patients undergoing myeloablative stem cell transplantation," *Blood*, vol. 109, no. 10, pp. 4586–4588, 2007.

[15] R. G. Resende, J. D. Correia-Silva, T. A. Silva et al., "Saliva and blood interferon gamma levels and IFNG genotypes in acute graft-versus-host disease," *Oral Diseases*, vol. 18, no. 8, pp. 816–822, 2012.

[16] I. Tawara, M. Koyama, C. Liu et al., "Interleukin-6 modulates graft-versus-host responses after experimental allogeneic bone marrow transplantation," *Clinical Cancer Research*, vol. 17, no. 1, pp. 77–88, 2011.

[17] A. Bouazzaoui, E. Spacenko, G. Mueller et al., "Chemokine and chemokine receptor expression analysis in target organs of acute graft-versus-host disease," *Genes and Immunity*, vol. 10, no. 8, pp. 687–701, 2009.

[18] S. Aldred, M. M. Grant, and H. R. Griffiths, "The use of proteomics for the assessment of clinical samples in research," *Clinical Biochemistry*, vol. 37, no. 11, pp. 943–952, 2004.

Hindawi Publishing Corporation
BioMed Research International
Volume 2013, Article ID 798054, 6 pages
http://dx.doi.org/10.1155/2013/798054

Research Article

The use of Multidimensional Data to Identify the Molecular Biomarker for Pancreatic Ductal Adenocarcinoma

Liwei Zhuang,[1,2] Yue Qi,[2] Yun Wu,[2] Nannan Liu,[2] and Yili Fu[1]

[1] *State Key Laboratory of Robotics and System, Bio-X Centre, Harbin Institute of Technology, Harbin, Heilongjiang 150001, China*
[2] *Department of Gastroenterology, The Fourth Affiliated Hospital of Harbin Medical University, Harbin, Heilongjiang 150001, China*

Correspondence should be addressed to Liwei Zhuang; zhuangliweiyd@126.com and Yili Fu; meylfu@hit.edu.cn

Received 28 June 2013; Accepted 23 August 2013

Academic Editor: Romonia Renee Reams

Pancreatic ductal adenocarcinoma (PDAC) is a lethal disease, and the patient has an extremely poor overall survival with a less than 5% 5-year survival rate. Development of potential biomarkers provides a critical foundation for the diagnosis of PDAC. In this project, we have adopted an integrative approach to simultaneously identify biomarker and generate testable hypothesis from multidimensional omics data. We first examine genes for which expression levels are correlated with survival data. The gene list was screened with TF regulation, predicted miRNA targets information, and KEGG pathways. We identified that 273 candidate genes are correlated with patient survival data. 12 TF regulation gene sets, 11 miRNAs targets gene sets, and 15 KEGG pathways are enriched with these survival genes. Notably, CEBPA/miRNA32/PER2 signaling to the clock rhythm qualifies this pathway as a suitable target for therapeutic intervention in PDAC. PER2 expression was highly associated with survival data, thus representing a novel biomarker for earlier detection of PDAC.

1. Introduction

Pancreatic ductal adenocarcinoma (PDAC) is a leading cause of cancer-related deaths both in China and the United States [1, 2]. The patients with advanced stage PDAC have a median survival of less than 1 year [2]. Surgery followed by cytotoxic chemotherapy or radiation is the standard treatment for PDAC. Unfortunately, this adjuvant therapy has only a modest impact on survival time [3, 4]. This situation highlights the importance of developing diagnostic biomarker for earlier detection of PDAC.

In recent years, high throughput technologies, such as expression profiling, have provided new insights for biomarker development of pancreatic cancer [5–7]. These investigations have shown that pancreatic cancer is fundamentally a heterogenetic disease, and multiple molecular mechanisms, including the tumor microenvironment, cell adhesion-mediated drug resistance, and pancreatic cancer stem cells, contribute to PDAC progression. Although such molecular profiling analyses have produced several potential biomarkers, most of which are the lack of adequate functional significance with PDAC. Thus how those findings could be applied in daily clinical practice remains unknown. Furthermore, the remarkable genomic heterogeneity of PDAC and the small number of patients studied have hindered the advances in our understanding of PDAC.

In this study, we have proposed an integrative approach to mining novel biomarker from multidimensional omics data. This approach effectively combines patients expression profiling data with known transcriptional factor binding data, miRNAs targeting data, and KEGG pathway knowledge. This approach can produce novel biomarkers together with testable hypothesis on molecular mechanism. We have analyzed over one hundred of PDAC expression profiling arrays and large collections of TF, miRNA, and KEGG pathway gene sets. We validated several previously implicated genes with clinical significance based on literature survey and also proposed a novel biomarker for further study.

2. Materials and Methods

2.1. Gene Datasets. The gene expression data and the corresponding clinical data (GSE21501) were obtained from NCBI Gene Expression Omnibus (GEO) database, available at http://www.ncbi.nlm.nih.gov/geo/. This dataset comprises

molecular profiling from 132 PDAC cancer patients in Agilent-014850 Whole Human Genome Microarray 4x44K G4112F microarray platform. Thirty samples were not analyzed in this study since the clinical data are not provided. The raw signals were normalized by quintile normalization to produce expression values.

2.2. Survival Analysis. Univariate Cox proportional hazards model was used to correlate gene expression data with survival data (censor status and survival days). This computation was done on all genes to genome-wide select candidate survival related genes (at $P < 0.0001$ level). Kaplan-Meier survival product-limit method and log-rank test were used to assess the differences between the survival curves of the good and poor survival patients.

2.3. Gene Sets Enrichment Analysis. Gene sets can be classified into the following 3 categories (1) Genes regulated by one transcriptional factor (TF). All genes in each gene set have been experimentally verified as targets of the same TF. This curation information is collected from TRANSFAC database [8]. One hundred and six experimentally verified gene sets were used in this study. (2) Genes are predicted to be targeted by miRNA. There are many programs used to predicts miRNA targets. Previous study indicate that the intersection of PicTar and TargetScanS prediction could achieve both high sensitivity and specificity compared to other programs [9]. The update intersection of PicTar and TargetScanS predictions was used in this study. We totally obtained 715 miRNA targets gene sets. (3) Genes are included in KEGG pathway. We use the compiled human KEGG pathway, which is a collection of hundreds of manually curated pathway maps classified into subsections such as metabolism, drug development, and human disease [10]. The gene sets data can be found in Supplementary Table 1 available online at http://dx.doi.org/10.1155/2013/798054.

Enrichment analysis of gene list is a statistical technique used to reveal higher levels of functional modular changes and elucidating underlying functional mechanisms. In this study, we used enrichment analysis to correlate the TF, miRNAs and KEGG pathway with survival genes. All survival correlated genes were matched to their corresponding TF, miRNAs, and KEGG pathways. The probability for the survival gene in every gene sets was calculated using hypergeometric function as follows:

$$p = 1 - \sum_{i=0}^{x-1} \frac{\binom{K}{i}\binom{M-K}{N-i}}{\binom{M}{N}}. \quad (1)$$

x_i is the number of altered genes in a given patient in gene sets i, K_j the number of altered genes in patient j, M the total number of genes tested, and N_i the total number of genes in gene sets i.

The result is the probability of extracting up to x of possible K genes in N drawings. P value for every gene sets was then calculated using Fisher's test. Multiple statistical tests were controlled by false discovery rate (FDR). All of the above computations were conducted in R statistical package (http://www.r-project.org/).

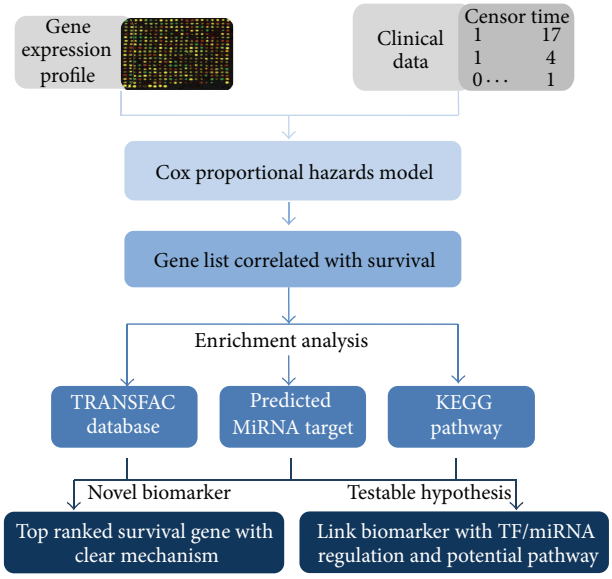

Figure 1: Framework of the analysis.

3. Results

The overall strategy of our approach is outlined in Figure 1. To identify survival biomarker in PDAC and its potential mechanism related with cancer progression, we initially extracted survival correlated gene by Cox proportional hazards model from microarray dataset. This gene list was simultaneously examined with TF regulation, predicted miRNA targets information, and KEGG pathways. Finally, based on the above evidence, the top ranked survival gene with clear molecular mechanism was identified as novel biomarker. Applying enrichment analysis on large-scale annotations data enables us to link potential biomarker with significantly altered TFs, miRNAs, and signal pathways. Notably, testable hypothesis can also be generated simultaneously, which greatly facilitate further functional experiments. This approach can refine survival genes with biologic significance and identify core TF, predicted miRNA, and KEGG pathways, which regulated PDAC progression.

3.1. Gene Expression Microarray Analysis to Identify Genes Correlated with Survival Data. We compared gene expression profile of 102 pairs of PDAC samples assayed in Agilent-014850 Whole Human Genome Microarray 4x44K G4112F microarray platform. Using univariate Cox proportional hazards model, 273 genes were found significantly correlated with patients' survival data (at $P < 0.0001$ level). These survival correlated genes (hereafter referred to as survival genes) were list in Supplementary Table 2. Inspecting this list, we found several genes, such as thymidine phosphorylase (TYMP), apoptosis-related cysteine peptidase (CASP10), and notch 4 (NOTCH4), have been implicated in cancer cells, but most of the gene are novel ones [11–13].

Table 1: Significant TF, miRNA, and KEGG pathway that are enriched with survival genes.

Transcription factor gene sets	FDR	References
TP53	0.0141	[14, 15]
CEBPA	0.0187	Novel
STAT6	0.0194	Novel
PGR	0.0225	Novel
E2F1	0.0329	[16, 17]
MicroRNA gene sets		
hsa-miR-543	0.0001	Novel
hsa-miR-576	0.0004	[18]
hsa-miR-32	0.0008	Novel
hsa-miR-545	0.0021	Novel
hsa-miR-608	0.0072	[19]
KEGG pathways		
Glycolysis/gluconeogenesis	0.0001	[33, 34]
Circadian rhythm	0.0001	[20, 21]
Phosphatidylinositol signaling system	0.0001	[29, 30]
Hedgehog signaling pathway	0.0007	[31, 32]
Insulin signaling pathway	0.0007	[35, 36]

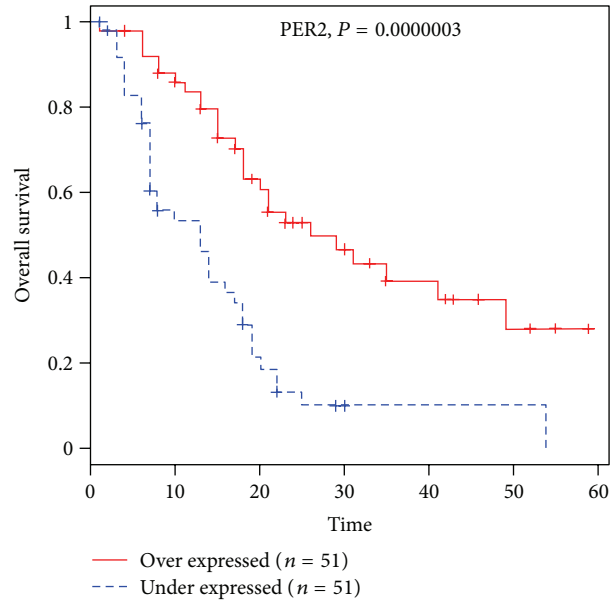

Figure 2: Kaplan-Meier overall survival of PDAC patients classified by high and low PER2 gene expression.

3.2. Multidimensional Analysis of Survival Genes Reveals Core TFs, miRNAs, and Pathways Contribute to PDAC

3.2.1. TF Regulation Analysis of Survival Genes. In order to identify the transcriptional programs governing the expression of these survival genes, we extract the experimentally verified targets information of TFs from TRANSFAC database, and to test if the survival gene are enriched with targets genes of one specific TF. With a cutoff of FDR < 0.05, we identified 12 TFs regulation gene sets are enriched with survival gene (Supplementary Table 3). The top 5 significant TFs are summarized in Table 1. TP53 and E2F1, two well-characterized master TFs in pancreatic cancer, were successfully identified. In pancreatic cancer, these two TFs have been found to play a crucial role in diverse cellular stresses such as driving metastasis, overcoming senescence, and cell cycle arresting [14–17]. We also found three TFs, that is, signal transducer and activator of transcription 6 (STAT6), CCAAT/enhancer binding protein, and alpha (CEBPA) and progesterone receptor (PGR), are related with PDAC survival data. The molecular mechanism and functional significance of these TFs remain elusive in pancreatic cancer cells.

3.2.2. miRNAs Target Analysis of Survival Genes. The list of 273 genes was then subjected to miRNAs target enrichment analysis. Eleven miRNAs gene sets were found to be enriched with survival genes (Supplementary Table 3). Top five miRNAs involved in PDAC survival are hsa-miR-543, hsa-miR-576, hsa-miR-32, hsa-miR-545, and hsa-miR-608 (Table 1). None of them have been reported to be involved in pancreatic cancers. But hsa-miR-576 and hsa-miR-608 have been implicated in digestive system cancers. For example, hsa-miR-576 was found over-expressed in brain metastases of colorectal cancers [18]. In another report, one SNP, rs4919510 in pre-miR-608, was also associated with altered recurrence-free survival in Chinese colorectal cancer patients [19].

3.2.3. Pathway-Based Analysis of Survival Genes. Discovering biologically meaningful gene patterns is highly important in analyzing genome-wide transcription profiles. Totally, we found 15 KEGG pathways enriched for survival-correlated genes (Supplementary Table 3). Many of the identified pathways in our analysis have already been implicated in pancreatic cancer. Beside, we identified circadian rhythms as a potential survival related pathway, which is consistent with recent findings that circadian transcriptional rhythms are necessary for metabolic homeostasis [20, 21].

3.3. Link Potential Biomarker with TF Regulation, miRNAs Targeting Information, and KEGG Pathway. Kaplan-Meier overall survival analysis of PDAC patients expression profile revealed that PER2 was the most significantly survival gene (Figure 2. $P < 0.0000003$). PER2 gene is a key player in controlling the circadian rhythm and plays an essential role in tumor suppression. In our survival analysis, low expression of PER2 is clearly correlated with poor survival time. This is consistent with the report that overexpression of PER2 in human pancreatic cancer cells lines reduced cellular proliferation, inhibited cell-cycle progression, and induced apoptotic cell death and arrest [22].

Based on our enrichment analyses, we found that PER2 is regulated by transcriptional factor CEBPA and predicted to be a target of miR-32. Interestingly, CEBPA, miR-32, and circadian rhythm signaling pathways are all top ranked (Table 1). Thus candidate biomarker PER2 may be regulated by CEBPA at transcriptional level and fine-tuned by miR-32 at posttranscriptional level (Figure 3.). CEBPA is a bZIP

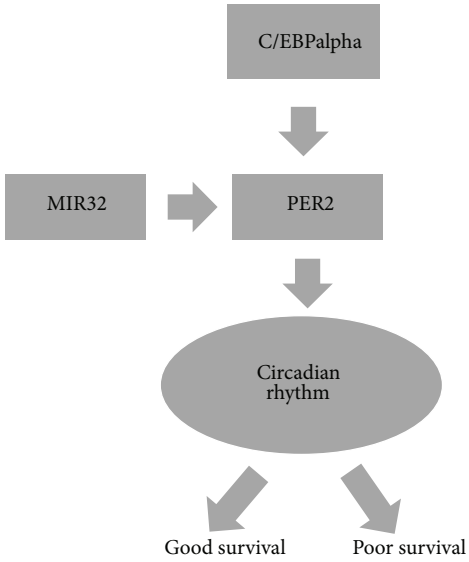

Figure 3: Link potential biomarker with TF regulation, miRNA targeting, and KEGG pathway. The diagram depicts putative interactions of PER2 with CEBPA, miR32 and Circadian rhythm pathway.

transcription factor which can bind as a homodimer or form heterodimers with the related proteins CEBP-beta and CEBP-gamma. Previous study has shown that CEBPA can bind to the promoter of leptin that plays an important role in body weight homeostasis [23]. Also, the encoded protein can interact with CDK2 and CDK4, thereby inhibiting these kinases and causing growth arrest in cultured cells [24]. In pancreatic cancer cells, Kumagai et al. found epigenetic silencing, as well as, inappropriate cytoplasmic localization of CEBPA disrupt its biological function [25]. Recently, Thoennissen et al. demonstrated direct regulation of PER2 by CEBPA in diffuse large B-cell lymphoma (DLBCL) [26]. Currently there is no report on the direct regulation of PER2 by miR-32, but miR-32 can target phosphatase and tensin homologue (PTEN) and promote growth, migration, and invasion in colorectal carcinoma cells [27]. The regulation by CEBPA and miR-32 will converge on circadian rhythms signaling pathway (Figure 3.). Mammalian circadian rhythms are an array of autonomous and autoregulatory transcriptional architecture [21]. The basic helix-loop-helix-PER-ARNT-SIM (PAS) transcriptional activators BMAL1, CLOCK, and NPAS2 activate the Period (PER1 and PER2) and cryptochrome (CRY1 and CRY2) genes, forming the core components. The deregulation of metabolic process is key event during multistage carcinogenesis. Circadian disruption accelerates cancer progression; possible due to circadian transcriptional rhythms are necessary for metabolic homeostasis. Thus, targeting circadian clocks represents a novel potential challenge for cancer therapeutics [22].

4. Discussion

PDAC accounts over 90% of pancreatic cancer and is a lethal malignancy with very high mortality rates. However better outcomes have been observed for smaller tumors detected at an earlier stage. For example, according to a recent analysis, the 5-year survival rates were significantly inversely correlated with tumor size [28]. This clearly indicates that detecting the PDAC at earlier stage can alter the fate of PC patients. Recently the large scale omics data present both significant challenges and opportunities for improving our understanding and treatment of this highly aggressive and lethal disease. We have adopted an integrative approach to prioritize genes of potential importance in PDAC.

Our survival-based approach involved multidimensional analysis of gene expression, transcriptional regulation level, and miRNA level mechanisms. This novel strategy allows us successfully to discovere several known cellular mechanisms related to PDAC progression. For example, a literature survey of the top 5 pathways significantly enriched with survival genes indicated that all of them have been associated with PDAC (Table 1). It is well known that mutations in KRAS oncogene accumulate early in the disease progression and occur in almost all of pancreatic ductal adenocarcinoma (PDAC). A key downstream target of the Ras family is phosphoinositide 3-kinase (PI3K), the enzyme responsible for the generation of 3-phosphorylated phosphoinositides and the activation of Akt (protein kinase B/Akt). The PI3K/Akt pathway is responsive for the stimulation of cell proliferation and inhibition of apoptosis. Abnormal regulation of this pathway was found in at least 50% of all cancer types [29, 30]. Hedgehog signaling pathway is normally involved in patterning processes in the developing embryo, but this pathway is frequent deregulation and correlated with the mutation of the KRAS in pancreatic ductal adenocarcinoma (PDAC) [31, 32]. Glycolysis/gluconeogenesis and insulin signaling pathways, two signaling pathways related with the metabolic change, are also significantly associated with survival genes. Recent investigations suggested that strengthened glycolysis under hypoxia metabolic adaptive processes favors hypoxic and normoxic cancer cell survival and correlates with pancreatic ductal adenocarcinoma aggressiveness [33]. Furthermore, oncogenic KRAS mutation promotes metabolic reprogramming in native tumors, indicating that glucose metabolism can be exploited for therapeutic benefit in PDAC [34]. A possible association between insulin use with cancer risk has long been speculated. Recently, multiple epidemiological studies and meta-analysis revealed that pancreatic cancer risk was increased among new users of insulin or insulin glargine. Increased risk is also observed with established diabetes or new-onset diabetes [35, 36].

More importantly, our approach can link potential biomarker with TF regulation, miRNAs targeting information, and pathway mechanism into one testable hypothesis, which would not have been done based on one dataset. Specifically, we show that CEBPA/miRNA32/PER2 signaling to the clock rhythm qualifies this pathway as a suitable target for therapeutic intervention in PDAC. Our approach offers a paradigm for future larger and more complex multidimensional studies seeking to link clinical phenotype with the highly diverse molecular alterations that define PDAC or other cancer types. Although our study is a preliminary analysis of PDAC and need further verification, it provides

a new avenue to find additional molecular diagnostic and prognostic markers in PDAC.

5. Conclusion

PER2 may represent putative clinical biomarkers and possible targets of individualized therapy in PDAC. These results provided new insights for understanding the potential mechanisms that govern the PDAC progression.

Authors' Contribution

Liwei Zhuang and Yue Qi contributed equally to this work.

Acknowledgment

This work was supported by the Natural Science Foundation of Heilongjiang Province of China (D201139).

References

[1] R. Siegel, D. Naishadham, and A. Jemal, "Cancer statistics, 2013," *CA: A Cancer Journal for Clinicians*, vol. 63, no. 1, pp. 11–30, 2013.

[2] A. Stathis and M. J. Moore, "Advanced pancreatic carcinoma: current treatment and future challenges," *Nature Reviews Clinical Oncology*, vol. 7, no. 3, pp. 163–172, 2010.

[3] F. Giovinazzo, G. Turri, S. Zanini, G. Butturini, A. Scarpa, and C. Bassi, "Clinical implications of biological markers in pancreatic ductal adenocarcinoma," *Surgical Oncology*, vol. 21, no. 4, pp. e171–e182, 2012.

[4] S. Kaur, M. J. Baine, M. Jain, A. R. Sasson, and S. K. Batra, "Early diagnosis of pancreatic cancer: challenges and new developments," *Biomarkers in Medicine*, vol. 6, no. 5, pp. 597–612, 2012.

[5] R. Grützmann, H. Boriss, O. Ammerpohl et al., "Meta-analysis of microarray data on pancreatic cancer defines a set of commonly dysregulated genes," *Oncogene*, vol. 24, no. 32, pp. 5079–5088, 2005.

[6] M. Hidalgo and D. D. von Hoff, "Translational therapeutic opportunities in ductal adenocarcinoma of the pancreas," *Clinical Cancer Research*, vol. 18, no. 16, pp. 4249–4256, 2012.

[7] J. K. Stratford, D. J. Bentrem, J. M. Anderson et al., "A six-gene signature predicts survival of patients with localized pancreatic ductal adenocarcinoma," *PLoS Medicine*, vol. 7, no. 7, Article ID e1000307, 2010.

[8] S. Gama-Castro, V. Jiménez-Jacinto, M. Peralta-Gil et al., "RegulonDB (version 6.0): gene regulation model of Escherichia coli K-12 beyond transcription, active (experimental) annotated promoters and Textpresso navigation," *Nucleic Acids Research*, vol. 36, no. 1, pp. D120–D124, 2008.

[9] P. Sethupathy, M. Megraw, and A. G. Hatzigeorgiou, "A guide through present computational approaches for the identification of mammalian microRNA targets," *Nature Methods*, vol. 3, no. 11, pp. 881–886, 2006.

[10] M. Kanehisa, S. Goto, Y. Sato, M. Furumichi, and M. Tanabe, "KEGG for integration and interpretation of large-scale molecular data sets," *Nucleic Acids Research*, vol. 40, no. D1, pp. D109–D114, 2012.

[11] F. Qi, Y. Inagaki, B. Gao et al., "Bufalin and cinobufagin induce apoptosis of human hepatocellular carcinoma cells via Fas- and mitochondria-mediated pathways," *Cancer Science*, vol. 102, no. 5, pp. 951–958, 2011.

[12] M. W. Saif, S. Hashmi, D. Bell, and R. B. Diasio, "Prognostication of pancreatic adenocarcinoma by expression of thymidine phosphorylase/dihydropyrimidine dehydrogenase ratio and its correlation with survival," *Expert Opinion on Drug Safety*, vol. 8, no. 5, pp. 507–514, 2009.

[13] K. Vo, B. Amarasinghe, K. Washington, A. Gonzalez, J. Berlin, and T. P. Dang, "Targeting notch pathway enhances rapamycin antitumor activity in pancreas cancers through PTEN phosphorylation," *Molecular Cancer*, vol. 10, article 138, 2011.

[14] J. P. Morton, P. Timpson, S. A. Karim et al., "Mutant p53 drives metastasis and overcomes growth arrest/senescence in pancreatic cancer," *Proceedings of the National Academy of Sciences of the United States of America*, vol. 107, no. 1, pp. 246–251, 2010.

[15] L. F. Grochola, H. Taubert, T. Greither, U. Bhanot, A. Udelnow, and P. Würl, "Elevated transcript levels from the MDM2 P1 promoter and low p53 transcript levels are associated with poor prognosis in human pancreatic ductal adenocarcinoma," *Pancreas*, vol. 40, no. 2, pp. 265–270, 2011.

[16] M. Reichert, D. Saur, R. Hamacher, R. M. Schmid, and G. Schneider, "Phosphoinositide-3-kinase signaling controls S-phase kinase-associated protein 2 transcription via E2F1 in pancreatic ductal adenocarcinoma cells," *Cancer Research*, vol. 67, no. 9, pp. 4149–4156, 2007.

[17] C. Schild, M. Wirth, M. Reichert, R. M. Schmid, D. Saur, and G. Schneider, "PI3K signaling maintains c-myc expression to regulate transcription of E2F1 in pancreatic cancer cells," *Molecular Carcinogenesis*, vol. 48, no. 12, pp. 1149–1158, 2009.

[18] Z. Li, X. Gu, Y. Fang, J. Xiang, and Z. Chen, "microRNA expression profiles in human colorectal cancers with brain metastases," *Oncology Letters*, vol. 3, no. 2, pp. 346–350, 2012.

[19] J. Xing, S. Wan, F. Zhou et al., "Genetic polymorphisms in pre-microRNA genes as prognostic markers of colorectal cancer," *Cancer Epidemiology Biomarkers and Prevention*, vol. 21, no. 1, pp. 217–227, 2012.

[20] G. Asher and U. Schibler, "Crosstalk between components of circadian and metabolic cycles in mammals," *Cell Metabolism*, vol. 13, no. 2, pp. 125–137, 2011.

[21] J. Bass and J. S. Takahashi, "Circadian integration of metabolism and energetics," *Science*, vol. 330, no. 6009, pp. 1349–1354, 2010.

[22] A. Oda, Y. Katayose, S. Yabuuchi et al., "Clock gene mouse period2 overexpression inhibits growth of human pancreatic cancer cells and has synergistic effect with cisplatin," *Anticancer Research*, vol. 29, no. 4, pp. 1201–1210, 2009.

[23] R. F. Morrison and S. R. Farmer, "Hormonal signaling and transcriptional control of adipocyte differentiation," *Journal of Nutrition*, vol. 130, no. 12, pp. 3116S–3121S, 2000.

[24] F. Krempler, D. Breban, H. Oberkofler et al., "Leptin, peroxisome proliferator-activated receptor-γ, and CCAAT/enhancer binding protein-α mRNA expression in adipose tissue of humans and their relation to cardiovascular risk factors," *Arteriosclerosis, Thrombosis, and Vascular Biology*, vol. 20, no. 2, pp. 443–449, 2000.

[25] T. Kumagai, T. Akagi, J. C. Desmond et al., "Epigenetic regulation and molecular characterization of C/EBPalpha in pancreatic cancer cells," *International Journal of Cancer*, vol. 124, no. 4, pp. 827–833, 2009.

[26] N. H. Thoennissen, G. B. Thoennissen, S. Abbassi et al., "Transcription factor CCAAT/enhancer-binding protein alpha and critical circadian clock downstream target gene PER2 are highly

deregulated in diffuse large B-cell lymphoma," *Leukemia & Lymphoma*, vol. 53, no. 8, pp. 1577–1585, 2012.

[27] W. Wu, J. Yang, X. Feng et al., "MicroRNA-32 (miR-32) regulates phosphatase and tensin homologue (PTEN) expression and promotes growth, migration, and invasion in colorectal carcinoma cells," *Molecular Cancer*, vol. 12, article 30, 2013.

[28] D. Chu, W. Kohlmann, and D. G. Adler, "Identification and screening of individuals at increased risk for pancreatic cancer with emphasis on known environmental and genetic factors and hereditary syndromes," *Journal of the Pancreas*, vol. 11, no. 3, pp. 203–212, 2010.

[29] M. Falasca, F. Selvaggi, R. Buus, S. Sulpizio, and C. E. Edling, "Targeting phosphoinositide 3-kinase pathways in pancreatic cancer—from molecular signalling to clinical trials," *Anti-Cancer Agents in Medicinal Chemistry*, vol. 11, no. 5, pp. 455–463, 2011.

[30] C. Sun, A. H. Rosendahl, R. Andersson, D. Wu, and X. Wang, "The role of phosphatidylinositol 3-kinase signaling pathways in pancreatic cancer," *Pancreatology*, vol. 11, no. 2, pp. 252–260, 2011.

[31] M. Lauth and R. Toftgård, "Hedgehog signaling and pancreatic tumor development," *Advances in Cancer Research*, vol. 110, pp. 1–17, 2011.

[32] J. P. Morris, S. C. Wang, and M. Hebrok, "KRAS, Hedgehog, Wnt and the twisted developmental biology of pancreatic ductal adenocarcinoma," *Nature Reviews Cancer*, vol. 10, no. 10, pp. 683–695, 2010.

[33] F. Guillaumond, J. Leca, O. Olivares et al., "Strengthened glycolysis under hypoxia supports tumor symbiosis and hexosamine biosynthesis in pancreatic adenocarcinoma," *Proceedings of the National Academy of Sciences of the United States of America*, vol. 110, no. 10, pp. 3919–3924, 2013.

[34] H. Ying, A. C. Kimmelman, C. A. Lyssiotis et al., "Oncogenic Kras maintains pancreatic tumors through regulation of anabolic glucose metabolism," *Cell*, vol. 149, no. 3, pp. 656–670, 2012.

[35] C. Bosetti, V. Rosato, D. Buniato et al., "Cancer risk for patients using thiazolidinediones for type 2 diabetes: a meta-analysis," *Oncologist*, vol. 18, no. 2, pp. 148–156, 2013.

[36] I. N. Colmers, S. L. Bowker, L. A. Tjosvold, and J. A. Johnson, "Insulin use and cancer risk in patients with type 2 diabetes: a systematic review and meta-analysis of observational studies," *Diabetes & Metabolism*, vol. 38, no. 6, pp. 485–506, 2012.

Hindawi Publishing Corporation
BioMed Research International
Volume 2013, Article ID 195692, 7 pages
http://dx.doi.org/10.1155/2013/195692

Research Article

Clinical Evaluation and Cost-Effectiveness Analysis of Serum Tumor Markers in Lung Cancer

Rong Wang,[1] Guoqing Wang,[1,2] Nan Zhang,[1] Xue Li,[1] and Yunde Liu[1]

[1] *School of Laboratory Medicine, Tianjin Medical University, No. 1 Guangdong Road, Hexi District, Tianjin 300203, China*
[2] *Department of Clinical Laboratory, Tianjin Stomatological Hospital, Tianjin 300041, China*

Correspondence should be addressed to Yunde Liu; yundeliu@126.com

Received 30 April 2013; Accepted 22 August 2013

Academic Editor: Romonia Renee Reams

The detection of serum tumor markers is valuable for the early diagnosis of lung cancer. Tumor markers are frequently used for the management of cancer patients. However, single markers are less efficient but marker combinations increase the cost, which is troublesome for clinics. To find an optimal serum marker combination panel that benefits the patients and the medical management system as well, four routine lung cancer serum markers (SCCA, NSE, CEA, and CYFRA21-1) were evaluated individually and in combination. Meanwhile, the costs and effects of these markers in clinical practice in China were assessed by cost-effectiveness analysis. As expected, combinations of these tumor markers improved their sensitivity for lung cancer and different combination panels had their own usefulness. NSE + CEA + CYFRA21-1 was the optimal combination panel with highest Youden's index (0.64), higher sensitivity (75.76%), and specificity (88.57%), which can aid the clinical diagnosis of lung cancer. Nevertheless, the most cost-effective combination was SCCA + CEA, which can be used to screen the high-risk group.

1. Introduction

Lung cancer has the highest incidence and mortality of any cancer worldwide. In 2008, 1.61 million new cases were reported, and 1.38 million deaths were attributed to lung cancer. The highest rates are in Europe and North America. In contrast to the declining mortality rate in men, lung cancer mortality rates in women have been rising over the recent decades [1]. In China, lung cancer has the highest incidence, and it is the leading cause of mortality of all cancers. This cancer is increasing at a rapid rate, and both incidence and mortality are steadily growing. China will drive up global rates of lung cancer in the foreseeable future [2].

Lung cancer patients often do not exhibit specific symptoms, particularly in early stages. Therefore, the majority of lung cancer patients are diagnosed at an advanced stage, which undermines their effective treatment. Currently, conventional diagnostic tests such as chest radiographs, computed tomography (CT) scans, and fiber optic bronchoscopy (FB) are not sensitive enough for effective early detection. Meanwhile, the benign pulmonary nodules and malignant tumors cannot be distinguished by imaging methods currently [3, 4]. Whereas, the pathological and cytological detections needed to obtain biopsy samples are invasive and difficult to repeat. Serum tumor markers are proteins that can be found in the blood, and their higher-than-normal concentrations have resulted in their widespread use in oncology [5, 6].

Early studies have illustrated the significance of serum tumor markers in the detection, prognosis, and follow-up of lung cancer [7–9]. Serum tumor markers such as carcinoembryonic antigen (CEA), squamous carcinoma antigen (SCCA), neuron specific enolase (NSE), and cytokeratin fragment (CYFRA21-1) have been investigated in patients with lung cancer. SCCA is a tumor-associated antigen originally isolated from squamous cell carcinoma of the uterine cervix [10]. Serum antigen levels have been used to follow the tumor status of squamous cell carcinomas, including those of the head and neck, oral cavity, esophagus, and lung [6]. NSE is the $\gamma\gamma$ dimer (isoenzyme) of enolase, which was first found in brain tissue extract and has been shown to be present in neuroendocrine cells and tumors [11]. NSE is a selective

Table 1: Patient characteristics.

	Lung cancer group (132)	Pulmonary benign disease group (48)	Normal group (92)
Gender			
Male	88	28	48
Female	44	20	44
Age	28~81 (54.6)	22~82 (56.3)	18~82 (53.5)
Lung cancer			
Histology			
Adenocarcinoma	68		
Squamous cell lung cancer	56		
Small cell lung cancer	8		
NSCLC stages			
I/II	73		
III/IV	51		
SCLC stages			
Limited disease	3		
Extensive disease	5		
Pulmonary benign disease			
Pneumonia		14	
Pleural effusion		12	
Bronchiectasia		4	
Pulmonary abscess		2	
Phthisis		16	

marker for small-cell carcinoma [12]. CEA was first identified by GOLD and FREEDMAN in 1965 as an antigen specific for digestive tract adenocarcinomas [13]. In comparative studies [14–16], CYFRA 21-1 has proven to be the marker of choice in nonsmall cell lung cancer and also exhibits independent prognostic value [17]. Serum biomarkers are useful for physicians to screen, diagnose, and treat lung cancer.

However, the diagnostic value of a single marker is limited by its sensitivity and specificity [12, 18]. Therefore, combination marker panel is frequently chosen in the clinic. However, combination panel has increased costs. China is a developing country with a large population where nearly 70% of the people live in poor rural areas. Hence, the cost-effectiveness of each assay is an important consideration.

Aims of this study were (1) to further evaluate the clinical value of four common serum markers (SCCA, NSE, CEA, and CYFRA21-1) in our cohort and (2) to find an optimal serum marker combination panel that benefits both patients and the medical insurance system.

2. Materials and Methods

2.1. Patient Population. Three groups of people were selected between March 2008 and December 2008 from the Tianjin Medical University Cancer Institute and Hospital. The first group comprised lung cancer patients. The diagnosis of each patient was confirmed by clinical outcome, imaging diagnosis and histological examinations. Stage and histological classification were evaluated according to the World Health Organization (WHO) 1999 lung cancer classification. All samples were collected before treatment. The second group was composed of patients with benign pulmonary diseases. In-patients with pneumonia, pleural effusion, bronchiectasia, and pulmonary abscess diagnoses were randomly selected. Patients were confirmed by routine standard diagnostic methods or histological examination, those patients with a history of malignant disease, digestive or kidney disease, or two or more concomitant lung diseases were excluded. The third group served as the healthy control group. Healthy people who took a physical examination and all the examination in the normal range were included, except for those with a family history of lung cancer. Detailed patient characteristics are described in Table 1.

2.2. Sample Collection and Detection. A 3 mL fasting venous blood sample was collected from each patient in the morning into a sterile tube. The samples were then centrifuged at 2,500 rpm for 20 min. The serums were stored at +4°C and at −70°C on the longterm. The SCCA concentration was determined by a microparticle enzyme immunoassay using Abbott reagent sets (Abbott, USA) and measured by a chemical luminescence analyzer (ARCHITECT i2000SR, Abbott, USA). The NSE, CEA, and CYFRA21-1 concentrations were detected by electrochemical luminescence (Roche Diagnostics, Shanghai, China). According to each manufacturer's recommendations, the positive cut-off values for each marker were 1.5 ng/mL for SCCA, 5.0 ng/mL for CEA, 3.3 ng/mL for CYFRA21-1, and 15.2 ng/mL for NSE. A positive sample was considered to be a sample with at least one positive serum marker in the marker combination panel.

2.3. Cost-Effectiveness Analysis. The cost-effectiveness of the combination marker panel was evaluated in lung cancer

Table 2: Concentrations of SCCA, NSE, CEA, and CYFRA21-1 in serum (ng/mL, $\overline{x} \pm s$).

Group	Number	SCCA	NSE	CEA	CYFRA21-1
Lung cancer	132	$1.73 \pm 3.98^{*}$	$19.45 \pm 14.47^{*\star}$	$17.81 \pm 35.79^{*\star}$	$6.54 \pm 7.36^{*\star}$
Pulmonary benign disease	48	0.38 ± 0.55	10.88 ± 1.87	$1.13 \pm 0.24^{**}$	$1.72 \pm 0.83^{**}$
Healthy control	92	0.17 ± 0.10	9.09 ± 2.81	0.78 ± 0.30	1.03 ± 0.52

P value was calculated by Student's t-test *compared to healthy control, $P < 0.05$; **compared to healthy control, $P < 0.01$.
*compared to pulmonary benign disease, $P < 0.05$; **compared to pulmonary benign disease, $P < 0.01$.

Table 3: The relationship between SCCA, NSE, CEA, and CYFRA21-1 and the clinicopathological factors (ng/mL, $\overline{x} \pm s$).

Clinicopathological characteristics	N	SCCA	NSE	CEA	CYFRA21-1
Histological classification					
Adenocarcinoma	68	0.22 ± 0.26	17.95 ± 8.30	$30.76 \pm 46.78^{*}$	4.00 ± 3.76
Squamous cell lung cancer	56	$3.79 \pm 5.56^{*}$	16.83 ± 5.66	4.49 ± 2.49	$10.34 \pm 9.38^{*}$
Small cell lung cancer	8	0.15 ± 0.07	$50.80 \pm 22.60^{*}$	1.81 ± 1.05	1.31 ± 0.30
NSCLC TNM stage					
I/II	73	2.59 ± 4.92	15.21 ± 4.53	7.44 ± 8.36	7.32 ± 9.01
III/IV	51	0.70 ± 1.03	21.94 ± 19.15	$33.71 \pm 50.04^{*}$	5.65 ± 3.99
SCLC stage					
Limited disease (LD)	3	2.06 ± 1.87	23.43 ± 16.74	7.27 ± 6.12	7.11 ± 5.23
Extensive disease (ED)	5	0.86 ± 0.79	25.02 ± 10.90	$33.51 \pm 29.63^{*}$	5.92 ± 3.80

P value was calculated by Student's t-test $^{*}P < 0.05$.

group. The effectiveness is determined by the tumor marker sensitivity, and the cost depends on the expense that patients incur for the detection. According to the charge fee in the third class A level hospital in Tianjin, the cost for SCCA detection was ¥77, and detections for the other three markers (NSE, CEA, CYFRA21-1) were each ¥100.

2.4. Statistical Analysis. Statistical analysis was performed using SPSS Statistics 19.0 (SPSS, Inc., Chicago, IL). The association between serum markers and lung cancer characteristics including stage and histological classification were compared by Student's t-test. The data were described by means ± standard deviation. The sensitivity, specificity, and Youden's index of single markers and combination markers were calculated. Receiver operation characteristic (ROC) curves were used to estimate the diagnostic efficiency of each marker. Three levels are stratified into no diagnostic value (<0.5), lower accuracy (0.5–0.7), higher accuracy (0.7–0.9), and highest accuracy (>0.9). Based on the statistics, the accuracy of the diagnostic assay is enhanced as the area under the ROC curve increases [19, 20]. A similar trend is exhibited by Youden's index [21]; the accuracy of the diagnostic strength increases with the index. Cost-effectiveness was analyzed by a cost-benefit ratio.

3. Results

3.1. Comparison of the SCCA, NSE, CEA, and CYFRA21-1 Concentrations in the Lung Cancer Group, Benign Lung Disease Group, and Healthy Control Group. Table 2 showed that the four markers were more abundant in the lung cancer group than in the healthy control group; NSE, CEA, and CYFRA21-1 were dramatically increased ($P < 0.01$). The concentrations of CEA and CYFRA21-1 were higher in the benign disease group than in the healthy group ($P < 0.01$). The SCCA concentration was not significantly different between the cancer and benign disease groups, but the remaining three markers were significantly different in the two groups.

3.2. Comparison of the SCCA, NSE, CEA, and CYFRA21-1 Concentrations among Each Clinicopathological Factor in the Cancer Group. Table 3 showed a significant increase in the concentrations of SCCA and CYFRA21-1 in squamous cell carcinoma, an increased NSE concentration in small cell carcinoma, and an increased CEA concentration in adenocarcinoma ($P < 0.05$).

With respect to TNM stage, only CEA was dramatically increased in stages III/IV when compared to stages I/II ($P < 0.05$), while no differences were observed in the concentrations of the SCCA, NSE, and CYFRA21-1 markers between the two stages. Similar to the trend in TNM stage, CEA demonstrated a higher concentration in the extensive disease group than in the limited disease. No significant difference was observed in the remaining three markers.

3.3. Comparison on ROC Curves of SCCA, NSE, CEA, and CYFRA21-1. Figure 1 demonstrated that the sensitivities of NSE, CEA, and CYFRA21-1 ($P < 0.05$) were better than those of SCCA. The areas under the curves of NSE, CEA, and CYFRA21-1 were 0.928 ± 0.034, 0.957 ± 0.026, and 0.964 ± 0.023, respectively.

3.4. Comparison of the Sensitivity, Specificity, and Youden's Index of the Four Markers Individually and in Combination.

Table 4: The sensitivity, specificity, and Youden's index of the four markers individually and in combination.

Tumor markers	Sensitivity (%)				Specificity (%)	Youden's index
	Adenocarcinoma	Squamous cell lung cancer	Small cell lung cancer	Lung cancer		
SCCA	7.35 (5/68)	50.00 (28/56)	12.50 (1/8)	25.76 (34/132)	94.29 (132/140)	0.20
NSE	47.06 (32/68)	50.00 (28/56)	50.00 (4/8)	48.48 (64/132)	91.43 (128/140)	0.40
CEA	58.82 (40/68)	35.71 (20/56)	0.00 (0/8)	45.45 (60/132)	89.29 (125/140)	0.35
CYFRA21-1	29.41 (20/68)	71.43 (40/56)	12.50 (1/8)	46.21 (61/132)	97.14 (136/140)	0.43
SCCA + NSE	47.06 (32/68)	67.86 (38/56)	62.50 (5/8)	56.82 (75/132)	91.43 (128/140)	0.48
SCCA + CEA	58.82 (40/68)	69.64 (39/56)	12.50 (1/8)	60.61 (80/132)	89.29 (125/140)	0.50
SCCA + CYFRA21-1	29.41 (20/68)	71.43 (40/56)	25.00 (2/8)	46.97 (62/132)	90.71 (127/140)	0.38
NSE + CEA	66.18 (45/68)	71.43 (40/56)	50.00 (4/8)	67.42 (89/132)	89.29 (125/140)	0.57
NSE + CYFRA21-1	52.94 (36/68)	78.57 (44/56)	62.50 (5/8)	64.39 (85/132)	88.57 (124/140)	0.53
CEA + CYFRA21-1	58.82 (40/68)	78.57 (44/56)	12.50 (1/8)	64.39 (85/132)	89.29 (125/140)	0.54
SCCA + NSE + CEA	67.65 (46/68)	75.00 (42/56)	62.50 (5/8)	70.45 (93/132)	89.29 (125/140)	0.60
SCCA + NSE + CYFRA21-1	52.94 (36/68)	78.57 (44/56)	75.00 (6/8)	65.15 (86/132)	88.57 (124/140)	0.54
SCCA + CEA + CYFRA21-1	58.82 (40/68)	91.07 (51/56)	25.00 (2/8)	70.45 (93/132)	89.29 (125/140)	0.60
NSE + CEA + CYFRA21-1	66.18 (45/68)	89.29 (50/56)	62.50 (5/8)	75.76 (100/132)	88.57 (124/140)	0.64
SCCA + NSE + CEA + CYFRA21-1	67.65 (46/68)	91.07 (51/56)	75.00 (6/8)	78.03 (103/132)	85.00 (119/140)	0.63

In descending order of individual sensitivity, the tumor markers were NSE (48.48%) > CYFRA21-1(46.21%) > CEA (45.45%) > SCCA (25.76%) (Table 4). The combination of tumor markers can improve the sensitivity, and the combination of NSE + CEA + CYFRA21-1 ranked the highest in Youden's index (0.64) with higher sensitivity (75.76%) and specificity (88.57%).

3.5. Cost-Effectiveness Analysis. In the cost-effectiveness analysis, only the combination markers whose sensitivity exceeded 50% were included. The combination of SCCA and NSE was taken as the healthy control group because it exhibited the lowest sensitivity and the lowest cost. Table 5 demonstrated that the most cost-effective combination was SCCA + CEA given that its cost was the lowest; furthermore, its cost was the lowest per 1% of sensitivity. When the cost of the assays was decreased by 10%, the cost of the SCCA + CEA combination was still the lowest as well as the ratio of cost to sensitivity.

4. Discussion

In this study, four common serum markers (SCCA, NSE, CEA, and CYFRA21-1) in lung cancer were evaluated individually and in combination. In addition to sensitivity and specificity, the ROC curve and Youden's index were applied, which are more accurate, effective, and comprehensive indexes for validation. Compared to SCCA, the markers NSE, CEA, and CYFRA21-1 were more accurate according to both higher Youden's indexes (0.40, 0.35, 0.43) and larger areas under ROC curves (0.928 ± 0.034, 0.957 ± 0.026, and 0.964 ± 0.023). However, the sensitivities of all four individual markers in our investigation were lower than 50%. Table 4 demonstrates that the combination of tumor markers is one way to improve their sensitivities. The combination of NSE + CEA + CYFRA21-1 might be an optimal choice due to the highest Youden's index (0.64) with higher sensitivity (75.76%) and specificity (88.57%). Furthermore, different combination panels can assist to differentiate histological subtype of lung cancer. The combination of SCCA, NSE, and CEA with the highest sensitivity (67.65%) and higher specificity (89.29%) can help in the diagnosis of AC; SCCA, CEA, and CYFRA21-1 (91.07% and 89.29%) can aid to the diagnosis of SCC; and SCCA, NSE, and CYFRA21-1 (75.00% and 88.57%) can assist in the diagnosis of SCLC. These results are associated to the unique function of each marker in previous reports.

Enolase molecules in mammalian tissues are dimers composed of three immunologically distinct subunits (α, β and γ). The γ subunit, which has been designated as neuron-specific enolase (NSE), is highly concentrated in neurons, neuroendocrine cells, and neurogenic tumors [11]. NSE can be taken as a distinguishing marker between SCLC and NSCLC given that SCLC is a neurosecretion tumor that results in NSE expressing highly in SCLC patients [22, 23]. High serum levels of NSE in patients with suspicion of malignancy suggest the presence of SCLC with high probability. Previous studies have indicated that approximately 70% of 450 SCLC patients have elevated serum concentrations of NSE while only 14% of 190 NSCLC patients show this [6]. Consistent with this conclusion, the concentration of NSE in SCLC is higher than that in SCC and AC ($P < 0.05$) in our study. Contrary to our results, no difference was observed between LD and ED, high pretreatment values of NSE were noted in 38–71% of SCLC patients with LD and in 83–98% of those with ED and were summarized in Ferrigno's review [6].

Compared to NSE, the CEA, CYFRA21-1, and SCCA are more specific to NSCLC in our investigation. CEA is

Table 5: Cost-effectiveness analysis of different combinations of tumor markers at the current cost and with a 10% decrease in cost.

Group	Cost (C)/¥	Effectiveness (E)/%	C/E	$\Delta C/\Delta E$
SCCA + NSE	177 (159.3)	56.82	3.12 (2.80)	0.00 (0.00)
SCCA + CEA	177 (159.3)	60.61	2.92 (2.63)	0.00 (0.00)
NSE + CEA	200 (180)	67.42	2.97 (2.67)	2.17 (1.95)
NSE + CYFRA21-1	200 (180)	64.39	3.11 (2.80)	3.04 (2.73)
CEA + CYFRA21-1	200 (180)	64.39	3.11 (2.80)	3.04 (2.73)
SCCA + NSE + CEA	277 (249.3)	70.45	3.93 (3.54)	7.34 (6.60)
SCCA + NSE + CYFRA21-1	277 (249.3)	65.15	4.25 (3.83)	12.00 (10.80)
SCCA + CEA + CYFRA21-1	277 (249.3)	70.45	3.93 (3.54)	7.34 (6.60)
NSE + CEA + CYFRA21-1	300 (270)	75.76	3.96 (3.56)	6.49 (5.84)
SCCA + NSE + CEA + CYFRA21-1	377 (339.3)	78.03	4.83 (4.35)	9.43 (8.49)

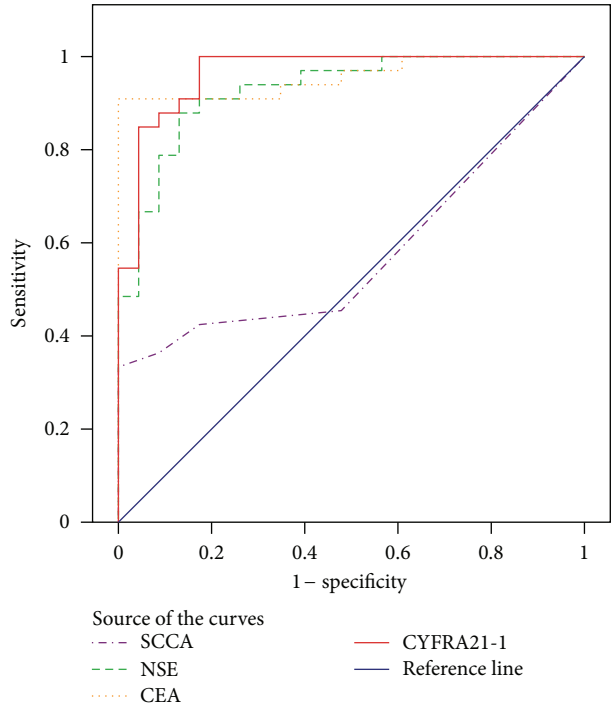

Figure 1: Receiver operation characteristic curves (ROCs) for the tumor markers in serum for the discrimination between lung cancer and healthy control. SCCA 0.578 ± 0.077 (95% CI 0.427~0.728), NSE 0.928 ± 0.034 (95% CI 0.861~0.994), CEA 0.957 ± 0.026 (95% CI 0.905~1.008), and CYFRA21-1 0.964 ± 0.023 (95% CI 0.919~1.01).

produced by the secretion cells of the normal adult gastrointestinal tract [24]. It is a marker for monitoring colon and rectal cancers. Recently, CEA has become the marker of choice for lung AC [25]. Meanwhile, several studies have reported increased CEA values in advanced bronchogenic cancers of various histological types [26, 27]. Generally, CEA levels vary in accordance with obvious changes in disease status, or they may precede their clinical recognition. Our data show that CEA has elevated levels ($P < 0.05$) and higher sensitivity (58.82%) in lung AC. Furthermore, it may have a role in monitoring therapy in advanced stages. In the present study, CEA is correlated with TNM stage and tumor invasion. In stages III/IV, CEA is observed at higher levels than in stages I/II. The same event occurs to the extensive lung cancer. However, the SCCA, NSE, and CYFRA21-1 do not show the correlation with TNM stage and extent of disease. In addition, the AUC for CEA in our study is higher than those in the literature where they range from 0.69 to 0.79 [28–31], which might be caused by samples in advanced stages or those including distant metastases.

CYFRA 21-1 is a sensitive tumor marker for NSCLC, particularly in squamous cell tumors. Because CYFRA 21-1 determines only fragments of cytokeratin 19, the test shows a higher specificity than tissue polypeptide antigen (TPA), which determines a mixture of cytokeratins 8, 18, and 19. CK-19 is a protein component of the intermediate filament protein in epithelial cells [32]. When epithelial cells transform into malignant cells, the keratin content is increased. Due to necrosis of tumor cells, the soluble fragment CYFRA21-1 of CK-19 is released into the blood. However, no organ tissue-specific and tumor-specific epithelial cytokeratins exist; therefore, it cannot be used as a tumor diagnosis indicator. However, CYFRA21-1 in serum will increase when epithelial cells transform into cancerous tumor cells, especially squamous epithelial cells of the lung and bladder transitional cells [32]. The results of this study indicate that the CYFRA21-1 concentration in the lung cancer group was significantly higher than that in the normal control and benign lung disease groups ($P < 0.01$), and the concentration in the benign lung disease group was significantly higher than that in the normal control group ($P < 0.01$). Therefore, its measurement may be helpful in the differential diagnosis of suspicious lung masses, but it can also be used as a good indicator for distinguishing between benign lung disease and normal group. Moreover, Table 3 shows that the expression of CYFRA21-1 in NSCLC was higher than that in SCLC. CYFRA21-1 and SCCA in SCC were more sensitive than those in AC and SCLC ($P < 0.05$) which is consistent with other reports [33, 34]. In descending order of CYFRA21-1 sensitivity, each pathological types are SCC (71.43%) > AC (29.41%) > SCLC (12.50%). This might be caused by the CK-19 expression in SCC and AC, while CK-18 is always expressed in SCLC. Taken together, CYFRA21-1 has a high diagnostic value in SCC.

SCCA is a purified subfraction of the tumor antigen. Elevated SCCA serum levels were found in many types of SCC, including the uterine cervix, bronchus, and nasopharynx

[6, 10]. In 1988, Mino et al. [35] found higher SCCA serum levels in patients with lung squamous carcinoma compared to healthy subjects or those with benign pulmonary diseases. Our data are in partial agreement with this result; a higher level of SCCA is found in lung cancer, but it is only significantly different from the healthy control group and not different from the benign pulmonary group. Moreover, given that SCCA yielded the lowest sensitivity (25.76%) and the lowest Youden's index (0.20) in addition to exhibiting no significant difference from the control group by the ROC curve, SCCA may not be a good marker for lung cancer screening, but it might be useful as a marker for histological subtyping. However, because of its significantly reduced sensitivity, SCCA would preferably be used in combination with CYFRA 21-1, which is also specific for SCC.

Although the combination of tumor markers can improve the sensitivity, the specificity will decrease with increasing sensitivity, meanwhile, the cost will increase as well. Presently, some hospitals and clinics prefer to take the four markers together (SCCA + NSE + CEA + CYFRA21-1). In reality, our results indicate that Youden's index and specificity of four marker panel are lower than three marker panel (NSE + CEA + CYFRA21-1) for the diagnosis of lung cancer. China is a developing country, and therefore, the optimal cost should be considered. The best marker combination panel is useful not only for promoting the efficiency of diagnosis, but also for reducing the economic load for the patient and health management department. Some reports [36–38] indicate that an analysis of cost-effectiveness is an appropriate evaluation of tumor marker combinations. In this study, we perform an analysis of cost-effectiveness for the tumor marker combinations. The results demonstrate that the cost of SCCA + CEA is the lowest per 1% sensitivity. However, many variables will affect the cost-effectiveness analysis. For instance, cost, discount rate, and depreciation of fixed assets may contribute to cost-effectiveness. If one of the variables varies, the result may change. Therefore, $\Delta C/\Delta E$ (C: cost, E: effectiveness) is applied to evaluate the result due to the variables. With the advancement of laboratory medicine and instruments, the cost will decrease. We decreased the expense by 10%, and reassessed the tumor marker cost-effectiveness. The results remained unchanged. Hence, compared to other panels, the combination of SCCA and CEA is the best choice to implement screening program in high-risk group.

5. Conclusions

Lung cancer is the most common and lethal malignant neoplasm in most of the western countries, and it is becoming one of the major health problems in undeveloped countries. The above data may explain several limitations in the clinical use of serum tumor markers. Although the four markers in our investigation are quick, objective, comparable, and reproducible, none of the single serum markers has sufficient sensitivity for the screening and diagnosis of lung cancer. Combination tumor markers could be a choice to improve the clinical effectiveness in the diagnosis of lung cancer. Furthermore, different combination panels have their own usefulness. In our investigation, the optimal marker panel with NSE, CEA, and CYFRA21-1 can assist to the diagnosis of lung cancer, and SCCA + NSE + CEA can help in the diagnosis of AC; SCCA + CEA + CYFRA21-1 can aid to the diagnosis of SCC; and SCCA + NSE + CYFRA21-1 can assist in the diagnosis of SCLC. In addition, from an economic viewpoint, SCCA + CEA might be a cost-effective combination for screening program. However, a large cohort validation and other tumor markers would be valuable research undertakings in the future.

List of Abbreviations

CEA: Carcinoembryonic antigen
NSE: Neuron-specific enolase
SCCA: Squamous cell carcinoma antigen
NSCLC: Non-small cell lung cancer
SCLC: Small cell lung cancer
SCC: Squamous cell carcinoma
AC: Adenocarcinoma
ED: Extensive disease
LD: Limited disease
ROC: Receiver operating characteristic
AUC: Area under ROC curve
TNM: TNM classification of malignant tumors.

Authors' Contribution

Rong Wang and Guoqing Wang contributed equally to this article.

Acknowledgment

This work was supported by the Tianjin Municipal Health Bureau Project (09KZ04).

References

[1] J. Ferlay, H.-R. Shin, F. Bray, D. Forman, C. Mathers, and D. M. Parkin, "Estimates of worldwide burden of cancer in 2008: GLOBOCAN 2008," *International Journal of Cancer*, vol. 127, no. 12, pp. 2893–2917, 2010.

[2] S. Chang, M. Dai, J. S. Ren, Y. H. Chen, and L. W. Guo, "Estimates and prediction on incidence, mortality and prevalence of lung cancer in China in 2008," *Zhonghua Liu Xing Bing Xue Za Zhi*, vol. 33, no. 4, pp. 391–394, 2012.

[3] X. Xie, Y. Zhao, R. A. Snijder et al., "Sensitivity and accuracy of volumetry of pulmonary nodules on low-dose 16- and 64-row multi-detector CT: an anthropomorphic phantom study," *European Radiology*, vol. 23, no. 1, pp. 139–147, 2013.

[4] C. I. Henschke and D. F. Yankelevitz, "CT screening for lung cancer: update 2007," *Oncologist*, vol. 13, no. 1, pp. 65–78, 2008.

[5] R. J. Pamies and D. R. Crawford, "Tumor markers: an update," *Medical Clinics of North America*, vol. 80, no. 1, pp. 185–199, 1996.

[6] D. Ferrigno, G. Buccheri, and A. Biggi, "Serum tumour markers in lung cancer: history, biology and clinical applications," *European Respiratory Journal*, vol. 7, no. 1, pp. 186–197, 1994.

[7] J. S. de Cos Escuin and J. H. Hernandez, "Tumor markers and lung cancer. What's new?" *Archivos de Bronconeumología*, vol. 40, supplement 6, pp. 35–40, 2004.

[8] D. E. Niewoehner and J. B. Rubins, "Clinical utility of tumor markers in the management of non-small cell lung cancer," *Methods in Molecular Medicine*, vol. 75, pp. 135–141, 2003.

[9] N. Viñolas, R. Molina, M. C. Galán et al., "Tumor markers in response monitoring and prognosis of non-small cell lung cancer: preliminary report," *Anticancer Research*, vol. 18, no. 1B, pp. 631–634, 1998.

[10] H. Kato, K. Tamai, T. Magaya et al., "Clinical value of SCC-antigen, a subfraction of tumor antigen TA-4, in the management of cervical cancer," *Gan no Rinshos*, vol. 31, supplement 6, pp. 594–599, 1985.

[11] E. H. Cooper, T. A. Splinter, D. A. Brown, M. F. Muers, M. D. Peake, and S. L. Pearson, "Evaluation of a radioimmunoassay for neuron specific enolase in small cell lung cancer," *British Journal of Cancer*, vol. 52, no. 3, pp. 333–338, 1985.

[12] L. G. M. Jørgensen, K. Osterlind, J. Genollá et al., "Serum neuron-specific enolase (S-NSE) and the prognosis in small-cell lung cancer (SCLC): a combined multivariable analysis on data from nine centres," *British Journal of Cancer*, vol. 74, no. 3, pp. 463–467, 1996.

[13] S. Hammarström, "The carcinoembryonic antigen (CEA) family: structures, suggested functions and expression in normal and malignant tissues," *Seminars in Cancer Biology*, vol. 9, no. 2, pp. 67–81, 1999.

[14] J. Grenier, J. L. Pujol, F. Guilleux, J. P. Daures, H. Pujol, and F. B. Michel, "Cyfra 21-1, a new marker of lung cancer," *Nuclear Medicine and Biology*, vol. 21, no. 3, pp. 471–476, 1994.

[15] M. Muraki, Y. Tohda, T. Iwanaga, H. Uejima, Y. Nagasaka, and S. Nakajima, "Assessment of serum CYFRA 21-1 in lung cancer," *Cancer*, vol. 77, no. 7, pp. 1274–1277, 1996.

[16] A. van der Gaast, C. H. H. Schoenmakers, T. C. Kok, B. G. Blijenberg, F. Cornillie, and T. A. W. Splinter, "Evaluation of a new tumour marker in patients with non-small-cell lung cancer: Cyfra 21.1," *British Journal of Cancer*, vol. 69, no. 3, pp. 525–528, 1994.

[17] H.-J. Yan, R.-B. Wang, K.-L. Zhu et al., "Cytokeratin 19 fragment antigen 21-1 as an independent predictor for definitive chemoradiotherapy sensitivity in esophageal squamous cell carcinoma," *Chinese Medical Journal*, vol. 125, no. 8, pp. 1410–1415, 2012.

[18] M. Plebani, D. Basso, F. Navaglia, M. de Paoli, A. Tommasini, and A. Cipriani, "Clinical evaluation of seven tumour markers in lung cancer diagnosis: can any combination improve the results?" *British Journal of Cancer*, vol. 72, no. 1, pp. 170–173, 1995.

[19] B. J. McNeil, E. Keeler, and S. J. Adelstein, "Primer on certain elements of medical decision making," *The New England Journal of Medicine*, vol. 293, no. 5, pp. 211–215, 1975.

[20] J. A. Hanley and B. J. McNeil, "The meaning and use of the area under a receiver operating characteristic (ROC) curve," *Radiology*, vol. 143, no. 1, pp. 29–36, 1982.

[21] N. J. Perkins and E. F. Schisterman, "The inconsistency of "optimal" cutpoints obtained using two criteria based on the receiver operating characteristic curve," *American Journal of Epidemiology*, vol. 163, no. 7, pp. 670–675, 2006.

[22] H. Satoh, H. Ishikawa, K. Kurishima, Y. T. Yamashita, M. Ohtsuka, and K. Sekizawa, "Cut-off levels of NSE to differentiate SCLC from NSCLC," *Oncology Reports*, vol. 9, no. 3, pp. 581–583, 2002.

[23] S. Ando, H. Kimura, N. Iwai et al., "Optimal combination of seven tumour markers in prediction of advanced stage at first examination of patients with non-small cell lung cancer," *Anticancer Research*, vol. 21, no. 4B, pp. 3085–3092, 2001.

[24] V. L. Go, H. V. Ammon, K. H. Holtermuller, E. Krag, and S. F. Phillips, "Quantification of carcinoembryonic antigen like activities in normal human gastrointestinal secretions," *Cancer*, vol. 36, supplement 6, pp. 2346–2350, 1975.

[25] P. Foa, M. Fornier, R. Miceli et al., "Tumour markers CEA, NSE, SCC, TPA and CYFRA 21.1 in resectable non-small cell lung cancer," *Anticancer Research*, vol. 19, no. 4C, pp. 3613–3618, 1999.

[26] G. Plavec, M. Ninković, G. Kozlovacki, A. Lazarov, and V. Tatić, "Tumor markers in pleural effusions in bronchogenic carcinoma and tuberculosis," *Vojnosanitetski Pregled*, vol. 59, no. 1, pp. 23–28, 2002.

[27] T. Rasmuson, G. R. Bjork, L. Damber et al., "Tumor markers in bronchogenic carcinoma. An evaluation of carcinoembryonic antigen, tissue polypeptide antigen, placental alkaline phosphatase and pseudouridine," *Acta Radiologica*, vol. 22, no. 3, pp. 209–214, 1983.

[28] B. Nisman, J. Lafair, N. Heching et al., "Evaluation of tissue polypeptide specific antigen, CYFRA 21-1, and carcinoembryonic antigen in nonsmall cell lung carcinoma: does the combined use of cytokeratin markers give any additional information?" *Cancer*, vol. 82, no. 10, pp. 1850–1859, 1998.

[29] M. Takada, N. Masuda, E. Matsuura et al., "Measurement of cytokeratin 19 fragments as a marker of lung cancer by CYFRA 21-1 enzyme immunoassay," *British Journal of Cancer*, vol. 71, no. 1, pp. 160–165, 1995.

[30] B. Bergman, F.-T. Brezicka, C.-P. Engstrom, and S. Larsson, "Clinical usefulness of serum assays of neuron-specific enolase, carcinoembryonic antigen and CA-50 antigen in the diagnosis of lung cancer," *European Journal of Cancer A*, vol. 29, no. 2, pp. 198–202, 1993.

[31] D. Moro, D. Villemain, J. P. Vuillez, C. A. Delord, and C. Brambilla, "CEA, CYFRA21-1 and SCC in non-small cell lung cancer," *Lung Cancer*, vol. 13, no. 2, pp. 169–176, 1995.

[32] P. Stieber, H. Dienemann, U. Hasholzner et al., "Comparison of CYFRA 21-1, TPA and TPS in lung cancer, urinary bladder cancer and benign diseases," *International Journal of Biological Markers*, vol. 9, no. 2, pp. 82–88, 1994.

[33] M. Tomita, T. Shimizu, T. Ayabe, A. Yonei, and T. Onitsuka, "Prognostic significance of tumour marker index based on preoperative CEA and CYFRA 21-1 in non-small cell lung cancer," *Anticancer Research*, vol. 30, no. 7, pp. 3099–3102, 2010.

[34] R.-S. Lai, H.-K. Hsu, J.-Y. Lu, L.-P. Ger, and N.-S. Lai, "CYFRA 21-1 enzyme-linked immunosorbent assay: evaluation as a tumor marker in non-small cell lung cancer," *Chest*, vol. 109, no. 4, pp. 995–1000, 1996.

[35] N. Mino, A. Iio, and K. Hamamoto, "Availability of tumor-antigen 4 as a marker of squamous cell carcinoma of the lung and other organs," *Cancer*, vol. 62, no. 4, pp. 730–734, 1988.

[36] A. J. Atherly and D. R. Camidge, "The cost-effectiveness of screening lung cancer patients for targeted drug sensitivity markers," *British Journal of Cancer*, vol. 106, no. 6, pp. 1100–1106, 2012.

[37] J.-X. Hou, X.-Q. Yang, C. Chen, Q. Jiang, G.-L. Yang, and Y. Li, "Screening the gastric cancer related tumor markers from multi-tumor markers protein chip with kappa coefficient and cost-effectiveness analysis," *Hepato-Gastroenterology*, vol. 58, no. 106, pp. 632–636, 2011.

[38] W. F. McGhan, C. R. Rowland, and J. L. Bootman, "Cost-benefit and cost-effectiveness: methodologies for evaluating innovative pharmaceutical services," *American Journal of Hospital Pharmacy*, vol. 35, no. 2, pp. 133–140, 1978.

Hindawi Publishing Corporation
BioMed Research International
Volume 2013, Article ID 107940, 13 pages
http://dx.doi.org/10.1155/2013/107940

Research Article

Immune Parameters in The Prognosis and Therapy Monitoring of Cutaneous Melanoma Patients: Experience, Role, and Limitations

Monica Neagu,[1] Carolina Constantin,[1] and Sabina Zurac[2]

[1] *Immunobiology Laboratory, "Victor Babes" National Institute of Pathology, 99-101 Splaiul Independentei, 050096 Bucharest, Romania*
[2] *Department of Pathology, University of Medicine and Pharmacy Carol Davila, Colentina University Hospital, 21 Stefan cel Mare, 020125 Bucharest, Romania*

Correspondence should be addressed to Carolina Constantin; caroconstantin@gmail.com

Received 9 May 2013; Accepted 1 August 2013

Academic Editor: Tiziano Verri

Cutaneous melanoma is an immune-dependent aggressive tumour. Up to our knowledge, there are no reports regarding immune parameters monitoring in longitudinal followup of melanoma patients. We report a followup for 36 months of the immune parameters of patients diagnosed in stages I–IV. The circulatory immune parameters comprised presurgery and postsurgery immune circulating peripheral cells and circulating intercommunicating cytokines. Based on our analysis, the prototype of the intratumor inflammatory infiltrate in a melanoma with good prognosis is composed of numerous T cells CD3+, few or even absent B cells CD20+, few or absent plasma cells CD138+, and present Langerhans cells CD1a+ or langerin+. Regarding circulatory immune cells, a marker that correlates with stage is CD4+/CD8+ ratio, and its decrease clearly indicates a worse prognosis of the disease. Moreover, even in advanced stages, patients that have an increased overall survival rate prove the increase of this ratio. The decrease in the circulating B lymphocytes with stage is balanced by an increase in circulating NK cells, a phenomenon observed in stage III. Out of all the tested cytokines in the followup, IL-6 level correlated with the patient's survival, while in our study, IL-8, IL-10, and IL-12 did not correlate statistically in a significant way with overall survival, or relapse-free survival.

1. Introduction

Melanoma is one of the most aggressive forms of human cancer [1], although it represents only 4% of all skin cancers, it accounts for 80% of skin cancer deaths, and it is placed second after adult leukemia in terms of potential productive life-years loss [2]. The updated figures show that in 2012 only in the United States there are 76,250 new cases accompanied by 9,180 deaths due this cancer [3]. As shown in various neoplasias, tumorigenesis can be an immune-mediated disease, melanoma being sustained by a clear immune defective background. Thus, the tumour cells are not eliminated due to the activation of immune suppressive functions. Tumor initiation and progression are sustained by maintaining a chronic inflammatory state and polarized immunosuppressive regulatory cells that generate a procarcinogenesis cellular microenvironment [4].

Among the huge amount of published studies that deals with immune markers in cutaneous melanoma in the past 5 years, there are actually only tens that focus on circulatory immune markers that prove a diagnostic/prognostic value. Up to our knowledge, immune-related markers were not proficient for distinguishing benign skin disease from cutaneous melanoma. They were used for their prognostic value, whether at tumoral site or characterizing the overall immune status of the treated/untreated patient, a domain that is still insufficiently explored. Taking into account the close interrelation of the skin's resident cells with the immune cells (Figure 1) and our day-to-day experience in cutaneous melanoma, we felt that the patient's quantifiable immune parameters, namely the immune status, are important tools to be exploited in the continuous effort to improve the patient's clinical management [5]. Therefore, the present paper shows the acquired immune data in a longitudinal

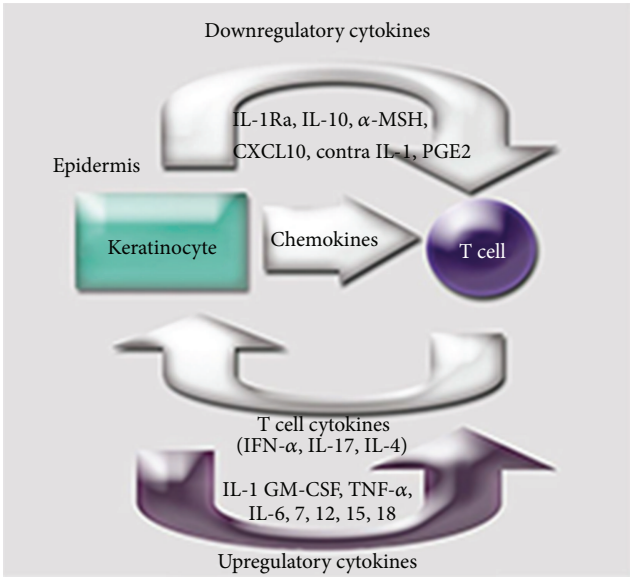

Figure 1: Interrelation mediated by humoral factors between keratinocytes and T cells. Keratinocytes up-regulates T cell functions by IL-1, GM-CSF, TNF-alpha, IL-6, 7, 12, 15, and 18 and down-regulates them by IL-1Ra, IL-10, α-MSH, CXCL10, Contra IL-1, and PGE2. T cell produces IFN-alpha, IL-17, and IL-4 that influences keratinocyte's functions. Keratinocyte's chemoattractant cytokines influences T cell trafficking: IL-1, IL-8, CCL27, CCL5, CCL17, CXCL10, MIG, IP9, and CCL20 [5].

study in cutaneous melanoma diagnosed patients followed for 36 months during their clinical evolution. The immune parameters comprised presurgery and postsurgery immune circulating peripheral cells and the circulatory form of intercommunicating cytokines. The immune tumour infiltrating cell populations were investigated in relation to stage and further correlated with the circulatory immune cells.

2. Materials and Methods

2.1. Patients. 143 patients staged according to the American Joint Committee on Cancer (AJCC) [6] were included in the study; patients entering the study in the early stages were diagnosed only with cutaneous primaries, excluding ocular melanoma or melanoma of soft parts. All melanoma patients gave written informed consent prior to their participation in this study. The standard parameters that were followed are WBC, serum LDH, S100, MIA, and routine biochemistry. Pre- and postsurgery immune parameters evaluation was performed for all patients; therefore, we registered at least two determinations of peripheral blood immune parameters.

102 patients were followed up from April 2008 to January 2012 and besides their overall clinical assessments and standard parameters, they were monitored for their immune parameters. Patients that had low WBC count displayed a mean less than 6.8×10^9/liter, and lymphopenia was considered when the absolute lymphocyte count was less than 800/μL.

2.2. Controls. 270 subjects (matching gender and age) were tested for immune parameters. In the longitudinal study along with the patients, we had a group of 150 healthy subjects that agreed to follow the patient's visits; thus, we have tried to minimize the individual normal variation of the tested parameters. The selection of the constant group of donors was performed randomly on the basis of age and gender matching.

The study had all the ethical approvals as mentioned in the acknowledgment part.

2.3. Peripheral Immune Cells. From peripheral blood immediately after withdraw CD3+, CD4+, CD8+, CD16, CD19+, Treg CD4+CD25+FOX3+; early activation marker CD4+/CD19+ for CD69+ were identified. Becton Dickinson kits: Multitest IMK Kit for In vitro Diagnostic Enumeration of Lymphocyte Subsets; OncoMark CD4 FITC/CD25 PE/CD3 PerCP-Cy5.5, FASTIMMUNE Assay System for early activation CD69+ marker on CD4, CD8, and CD19 were used. Biolegend kit: One Step Staining Human Treg Flow Kit (FOXP3 Alexa Fluor 488/CD25 PE/CD4 PerCP) was used. Evaluation was done with CELLQuest Software.

2.4. Plasma Immune-Related Cytokines. From patients' plasma immune-related cytokines/chemokines were quantified using the Luminex xMAP technology. Cytokine multiplexing for IL-1 beta; IL-6; IL-8; IL-10; IL-12 p40; and TNF-alpha kit (Human Cytokine/Chemokine Premixed 6 Plex Millipore). Acknowledging our hands-on experience, an increased number of simultaneously quantified cytokines can give false results, mainly due to the crossreactivity of labeling antibodies.

2.5. Tissue Samples—Immune Markers. Immunohistochemical analysis of inflammatory infiltrate within the tumor was performed on paraffin-embedded fragments of tumor harvested from surgical specimens. Several markers were investigated in order to identify T and B cells, plasma cells, and dendritic and antigen presenting cells (see Table 1). detection system used: Novolink Polymer (Leica/Novocastra) and DAB chromogen. Positive cells were analyzed in three parts of tumor: (a) main tumor mass in melanomas without regression, (b) nonregressed tumor mass in melanoma with regression, and (c) areas of regression in melanoma with regression. Results were registered as "absent" (no positive cells), "rare" cells (less than 20 positive cells/high power field HPF), and "frequent" cells (positive cells 20 or more/HPF). In case of CD1a and Langerin, only one melanoma without regression showed 23 and, respectively, 21 positive cells/HPF within the main tumor mass. For this reason, for CD1a and Langerin analysis, we used two categories "absent" and "present."

2.6. Followup and Statistics. At periodically scheduled visits, patients were clinically checked, disease progression registered by their physicians, and bled for monitoring their immune parameters. For statistical analyses, mean values ± SD was performed, a two-tailed Student's t-test was used, and

Table 1: Immunohistochemical markers.

Antibody	Source	Clone	Host	Working dilution	Pretreatment*
CD3	Leica/Novocastra	PS1	Mouse	0.3/200	HIER, buffer citrate, and pH 6
CD5	idem	4C7	idem	1/200	idem
CD4	idem	4B12	idem	5/200	idem
CD23	idem	1B12	idem	RTU	idem
Langerin	idem	12D6	idem	0.5/200	idem
CD1a	idem	JPM30	idem	2/160	idem
CD7	Thermo Scientific/Neomarkers	272	idem	RTU	idem
CD8	idem	C8/144B	idem	2/200	idem
CD20	Cell Marque	L26		RTU	idem
CD138	Invitrogen	—	Rabbit	1/200	HIER, EDTA citrate, and pH 8

Table 2: Cutaneous melanoma patients' characteristics at presentation, percentage of patients diagnosed in different stages, age, and gender.

Stage at presentation (% out of the total group)	I (34%)	II (40%)	III (15%)	IV (11%)
Age (mean ± SD years)	57 ± 3	51 ± 4	59 ± 1	67 ± 4
Age range (years)	18–72	20–68	22–89	35–70
Gender (% women)	89%	72%	33%	66%

significance was defined as $P < 0.05$ when comparing various groups or parameters.

3. Results and Discussion

3.1. Melanoma Patients' Characterization. The investigated groups comprised subjects diagnosed in all AJCC stages (Table 2). The majority of the investigated patients were diagnosed in stages I and II (74% out of the total number of patients), while the rest of patients (26%) were diagnosed at presentation in stages III and IV. The overall age range of investigated patients was 18–89 years with an overall predominance in female patients. Out of the total group of patients, 13 were registered at presentation with lymphopenia (absolute lymphocyte count < 800/μL). In all the patients, the circulating percentage of lymphocytes population/subpopulations was calculated upon the absolute lymphocyte counts.

3.2. Immune Parameters before Melanoma Treatment

3.2.1. Peripheral Immune Cells. Besides standard evaluation (laboratory and clinical parameters), patients were evaluated for peripheral immune parameters before surgery/treatment and 1 month after. Taking into account our experience regarding postsurgery immediately tested parameters (existence of normal regenerative and inflammation processes), we did not consider these data meaningful in the context of the presented results. Thus, patients that agreed to be followed were tested one month after surgery and thereafter followed up for two-three years regularly.

Before tumour surgery or any other treatment for advanced melanoma stages, patients had an interesting

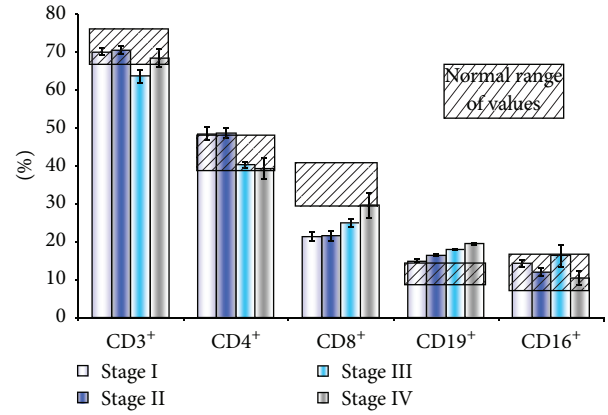

Figure 2: Peripheral blood lymphocytes in cutaneous melanoma patients in comparison to normal ranges (% from CD45+ pan leukocytic antigen)—CD8+ in stages I and II compared to normal values $P < 0.005$, CD19+ in stages III and IV compared to normal values $P < 0.005$.

immune cellular pattern (Figure 2). The total circulating T lymphocytes do not display abnormal values no matter the stage. The circulating CD4+ T cells have a tendency to decrease in more advanced stages but are not statistically different from normal ranges. The most interesting pattern was found in stages I and II where there is statistically significant lower percentage of CD8+CD3+ T lymphocytes and normal values for B CD19+ and NK cells. In advanced stages (III and IV), normal CD8+ T and NK cells were registered, while statistically higher B lymphocytes were registered. In advanced stages there is a decrease of the classic T-CD4+/T-CD8+ ratio [5], based mainly on the increase of the circulating T-CD8+ subpopulation. We have additionally investigated the total serum immunoglobulins (Igs), and we found no correlation between the levels of the circulating Igs, classes, or total Igs with the high circulating percentage of B lymphocytes. The levels of circulating B lymphocytes showed a reverse correlation with the level of circulating NK cells, as previously reported by us [7].

We have noticed that in more advanced stages there is a doubling of cells with CD4+CD25+FOXP3 phenotype (Figure 3). Interestingly, we found the percentage of

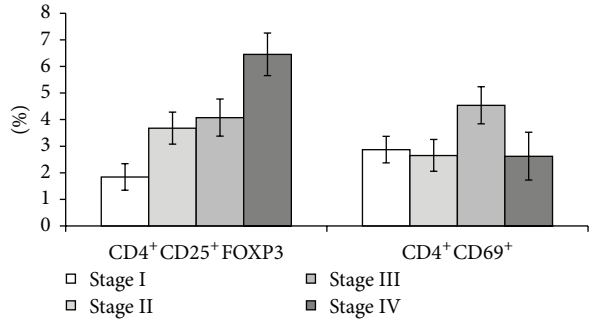

Figure 3: Circulating CD4+ T cells in cutaneous melanoma patients.

circulating CD4+ T lymphocytes expressing early activation marker CD69+ slightly higher in stage III and no statistical differences in early or late stage patients. Tregs (CD4+CD25+FOXP3+) were registered in normal donors in the range of 2–4% out of the total circulating CD4+ T cells. Up to our knowledge, there is no reporting of the circulating Tregs in normal Romanian population. In international references, the reported values of circulating Tregs can range from 4.4 to 13.0% out of the total circulating CD4+ T cells in one study [8], while 1 to 6% in another [9]. The differences with the already published results regarding normal circulatory Tregs can be sustained by different types of detection methods or even by differences among cellular tested population of healthy individuals.

Circulating Tregs in patients diagnosed in stages I–III when compared to normal values do not display statistically significant differences, while we have obtained an increase in the circulatory Tregs in stage IV.

An interesting finding was in stage III where we have registered an activation pattern for circulating CD4+ T cells, while the other stages did not register any statistical differences.

Early activation antigen on T cells, CD69, is expressed transiently, and it was reported that in the periphery, it down regulates sphingosine-1-phosphate. This leads to the inhibition of lymphocyte circulating from the lymph node and the retention of T lymphocytes in the lymph node [10, 11]. These arguments come in favor of the detection in stage III (before any treatment) of a statistically relevant CD4+CD69+ circulatory population, that is prone to elicit an antitumoral response in an already invaded lymph node. However, in a study published several years ago, it was shown that before therapy, patients that had low proportions of circulating CD3+CD4+CD69+ and CD3+CD56+ proved an increased interval of disease-free survival compared to those with high proportions. This study strengthened the prognostic potential of circulating T cells displaying the early activation marker in melanoma [12].

3.2.2. Circulating Levels of Cytokines. Testing concomitantly the panel of circulating cytokines/chemokines from the diagnosed patients, we have seen several statistically altered levels compared to controls. Circulating IL-6 (Figure 4(a)) is statistically different from controls only in advanced stages ($P < 0.005$), while for stage II, we have evaluated a slight statistically significant increase in the circulatory IL-6 ($P = 0.5$). It is known that skin cells, like keratinocytes, produce cytokines that upregulate T-cell functions [5]. Finding an increased circulatory IL-6 can account for the immune system upregulation done by keratinocytes to enhance the T cells antitumoral activity. The same explanation can account for the circulatory high values of TNF-alpha. All the stages displayed statistically higher values compared to controls (Figure 4(b)). As expected, the highest circulatory TNF level was found in advanced stages, a mean of two-fold increase compared to early stages (I and II). Although not statistically different, we can note an interesting elevation of circulatory TNF in stage I compared to stage II.

Circulatory IL-10 was found strongly elevated in late stages of melanoma (Figure 4(c)) and had a good positive correlation (PC = 0.94) with the circulatory elevated T lymphocytes CD4+CD25+ with FOXP3 expression (Figure 3). In a previously published study focusing on metastatic melanoma patients, circulating Tregs were reported as specific for tumour antigens like gp100, TRP1 NY-ESO-1, survivin, and so on. In that study, Tregs from peripheral blood mononuclear cells (PBMC) cultures were found proliferating and producing preferentially IL-10 [13]. Thus, the correlation between the high plasma values of IL-10 found by us in melanoma advanced stages can account for the increased circulating Tregs. Although a previous study has stated that IL-10 was not detectable in melanoma serum patients [14], we do not exclude the existence of differences regarding the multiplexing method *versus* classical ELISA; moreover, we have used plasma that offers an increased availability for detecting lower concentration of cytokines.

Circulatory IL-12 was found undoubtedly high in all patients no matter the diagnosis stage (Figure 4(d)). Note that we have detected IL-12 subunit p40 in the patients' plasma and that IL-12p40 is known as a component of the bioactive interleukins IL-12 and IL-23 [15]. IL-12 is secreted by a plethora of cells like antigen presenting cells (monocyte/macrophages, dendritic cells, and B lymphocytes), mast cells, and nonimmune cells such as keratinocytes. In addition, IL-12 has receptors on NK and T lymphocytes that increase their proliferation and cytotoxic capacity [16]. Thus, the finding that IL-12 is enhanced in the circulation of melanoma patients can be accounted for by an active immune response. Although not statistically different, we can recognize an increase of IL-12 level in early melanoma stages, followed by a decrease in more advanced ones.

IL-8 present in patients' plasma is statistically elevated only in advanced melanoma stages, a 2.5-fold increase compared to controls (Figure 4(d)). Thoroughly revised by Dewing et al. [17], IL-8 has a chemokine function, actively secreted by macrophages, endothelial cells, and tumour cells, favoring metastatic processes. An increase of this chemokine in the later stages of disease was somewhat to be expected. Only patients in stage I showed a slight correlation of IL-8 level with the circulatory percentage of CD16+ and CD8+ (PC = 0.75) and no other significant correlation. Overall, high IL-8 levels have been registered in patients with metastatic melanoma,

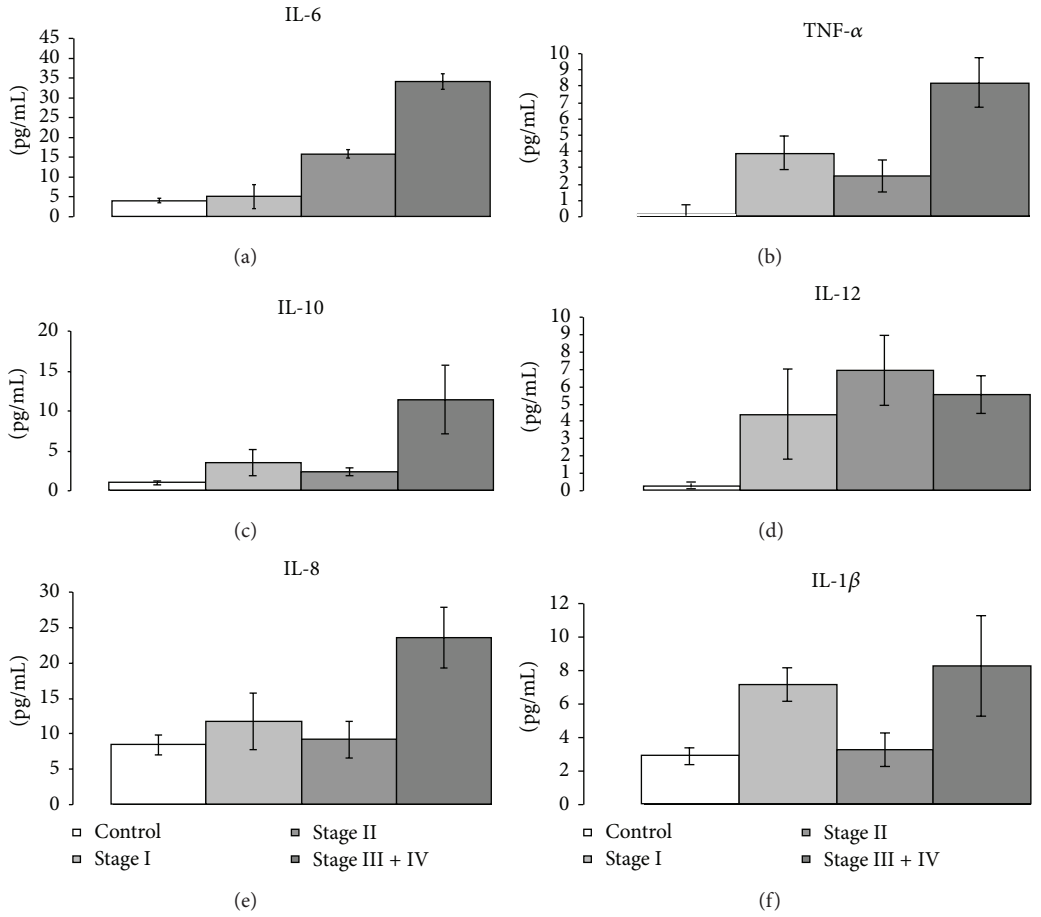

Figure 4: Plasma level of IL-6 (a), TNF-α (b), IL-10 (c), IL-12 (d), IL-8 (e), and IL-1β (f) in melanoma patients compared to control.

and a decrease of serum IL-8 level has been described as a result of chemotherapy or immune therapy [18, 19].

One of the most interesting circulatory cytokines in terms of the plasma level in association to staging is IL-1beta. We have chosen to focus on the beta form of IL-1 due to various reasons: some human melanoma cells can spontaneously produce functional IL-1beta [20], the paracrine function of IL-1beta is known [21], and its involvement in tumour growth and inflammation is well proven [22]. Thus, stage I has a two fold increase in the circulating level compared to control, while stage II has no difference from the normal values. Advanced stages (III and IV) display a circulating IL-1beta at the same level as stage I. Previous data have shown that at the tumoral level, the expression of IL-1beta increases in primary tumour versus normal/benign tissue and increases once more in the metastatic tumour [20]. Therefore, we have identified the circulating levels of IL-1beta that can indicate the evolution of the metastatic processes. The patients that we have enrolled were not tested for the existence of BRAF (V600E) mutation in the excised primary or metastatic tumours. Knowing that the expression of BRAF (V600E) can induce both the transcription of IL-1alpha and beta in melanocytes and melanoma cell lines [23], we can account that, at least for a part of the patients, the enhanced level of circulatory cytokine can be due to BRAF (V600E) mutation.

We found very low levels of IFN-gamma with no statistical relevance between either of the investigated groups, matching an older study showing that the levels of IFN-gamma were less elevated in patients while detectable IFN-gamma patients had higher risk for recurrence [24].

3.2.3. Tumour Inflammatory Infiltrate. Our lot includes 62 superficial spreading melanomas (SSMs), 31 nodular melanomas (NMs) and 9 acral-lentiginous melanomas (ALMs) (Figure 5(a)). Some SSM and ALM cases presented regression (64.79%), in different proportion for each type of tumor (SSM: 62.90%; ALM: 77.78%) (Figure 5(b)). We analyzed the inflammatory infiltrate separately, in both regressed and nonregressed component, due to the obvious differences in appearance and distribution of inflammatory cells in these areas.

Inflammatory infiltrate mainly consisted in T lymphocytes (CD3+). When analyzing the presence of CD3+ cells within tumor mass (quantified as absent, rare, and frequent) versus tumor-infiltrating lymphocytes (TIL) (quantified as absent, nonbrisk, and brisk), we found a perfect match between these categories. These findings were similar with other authors' data [25, 26].

We identified a significant association between high pT level and the presence of frequent CD3+ T cells

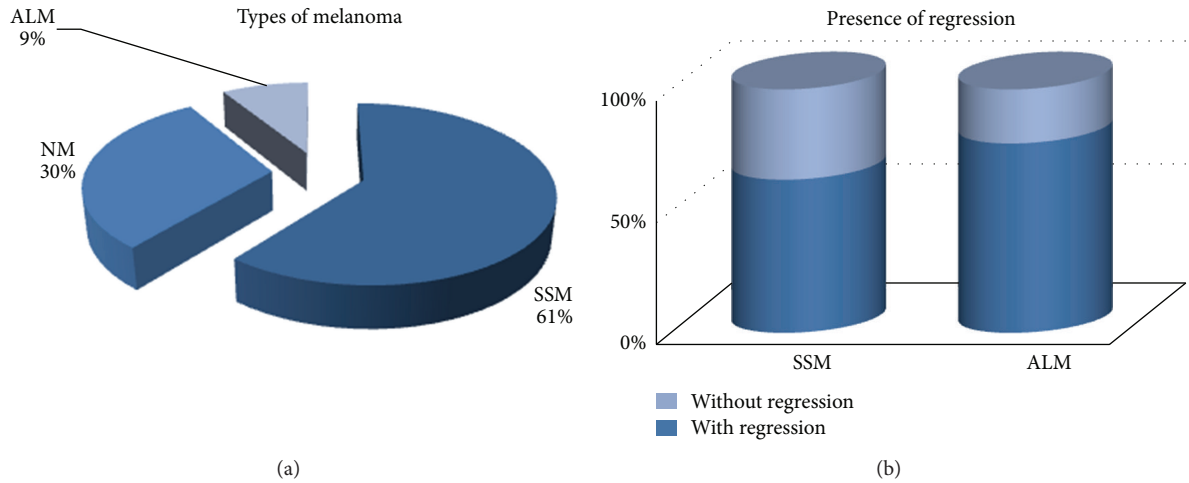

Figure 5: (a) Types of melanoma. (b) Presence of regression according to melanoma type.

($P_{\text{frequent versus absent CD3+}} = 0.002$; $P_{\text{frequent versus absent CD3+}} < 0.001$) (Figure 6(a)) and ulceration and presence of frequent CD3+ cells ($P_{\text{frequent versus absent CD3+}} = 0.01$; $P_{\text{frequent versus absent CD3+}} < 0.001$) (Figure 6(b)). Nonulcerated tumors have similar distributions of CD3+ cells irrespective of pT level; significantly more numerous cases with ulceration presented frequent CD3+ cells in association with high pT levels ($P_{\text{frequent versus absent CD3+}} = 0.007$; $P_{\text{frequent versus absent CD3+}} = 0.0001$) (Figure 6(c)). These findings are surprising, considering the overall favorable prognostic significance associated with brisk TIL [27–33], our data indicates the presence of abundant TILs within thick ulcerated tumors (unfavorable prognosis). More likely, our results represent the reflection of a normal increasing of the inflammatory infiltrate within an ulcerated tumor as a physiologic reaction to ulceration.

All regressed areas presented very numerous CD3+ cells (over 200 cells/HPF). No significant differences occurred in the density of CD3+ cells within the tumor mass between nonregressed areas in cases with regression and cases without regression, irrespective of tumor type (SSM and/or ALM).

CD5 presented a similar distribution as CD3. There were some differences when analyzing CD7 (overall tendency of loosing CD7 expression in inflammatory infiltrate both intratumor and in regression areas), but the differences were minor.

Analyzing CD4+ and CD8+ T cells, we identified a slight predominance of CD4+ cells in most cases (CD4 : CD8 > 1 : 1) without differences when correlating with pT level, ulceration, or regression. Also, there was a slight tendency of increasing CD4+ cells number in cases with higher pT levels. There was no correlation between the data obtained by evaluating circulating immune cells and tumor associated ones. This apparent inconsistency between specific T cells found both in the same patients' tumor tissue and blood is well documented [34].

We analyzed the presence of B lymphocytes (CD20+). We recorded an increased number of B cells in pT4 tumors and almost statistically significant predominance of B cells in ulcerated tumors ($P = 0.06$) (Figure 7(a)). Less numerous CD20+ cells were present in the nonregressed component of tumor with regression than in tumors without regression, but the results had no statistical significance ($P = 0.07$) (Figure 7(b)). The presence of B cells within TIL was previously identified [35] in other tumors being correlated with better prognosis [36]. In our cases, the presence of more numerous B cells in ulcerated tumors may be secondary to ulceration (as part of subsequent inflammatory reaction) and therefore should not be regarded as an indicator of bad prognosis.

CD138+ cells (plasma cells) were present in almost all areas of regression (95.23%) and, when present, they were frequent, irrespective of the type of regression or ulceration. More numerous CD138+ cells were present in areas of regression in tumors with high pT, especially in ulcerated ones, but the data lacks statistical significance (Figures 8(a) and 8(b)).

CD23+ cells were absent in tumors without regression; they were present in 34.88% of cases in areas of regression and in only two cases in nonregressed areas.

Interesting results occurred when evaluating the presence of Langerhans cells (LC) (CD1a+ Langerin+). Within the tumor mass, LC was either absent or scarce (isolated cells, less than 20 cells/HPF in all cases but one). SSM presented LC within tumor mass more frequent than NM ($P < 0.001$) or ALM ($P = 0.003$) (Figure 9(a)). The presence of LC within tumor mass correlates with Breslow index (higher pT level, more probable absence of LC—$P = 0.007$) (Figure 9(b)) but not with ulceration (more numerous non-ulcerated tumors have LC but not statistically significant) (Figure 9(c)). However, when correlating LC and pT level separately in ulcerated and nonulcerated tumors, we identified their presence in thinner tumors (Figure 9(d) nonulcerated tumors, $P = 0.01$,

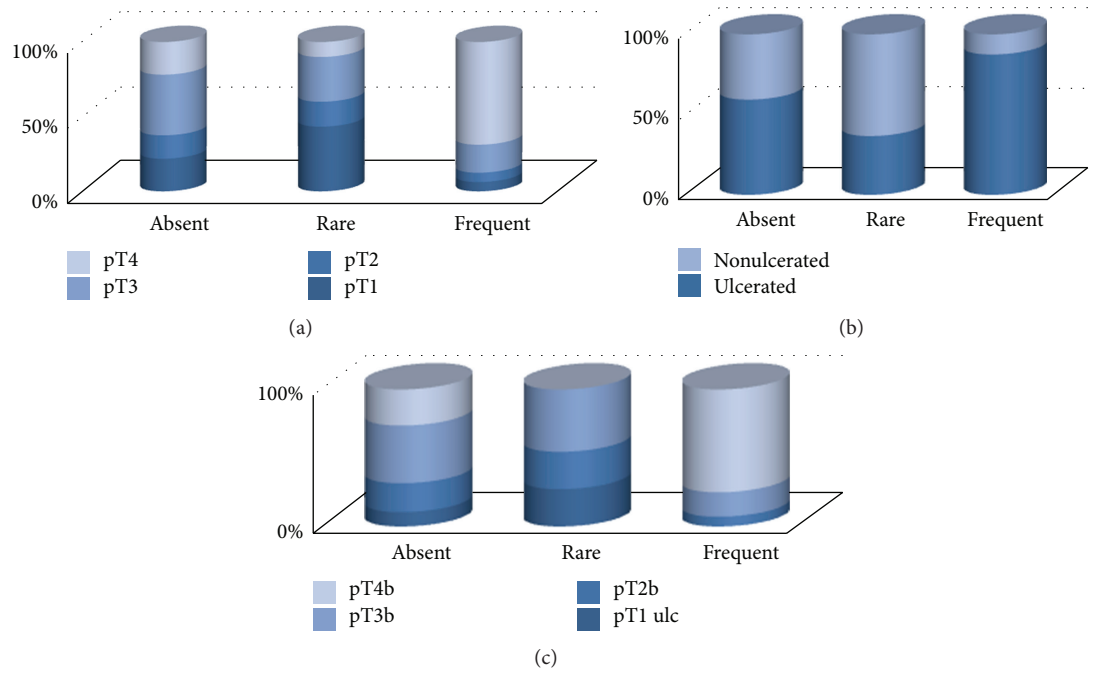

Figure 6: (a) Correlation between CD3+ cells density and pT level. (b) Correlation between CD3+ cells density and ulceration. (c) Correlation between CD3+ cells density and pT level in ulcerated tumors.

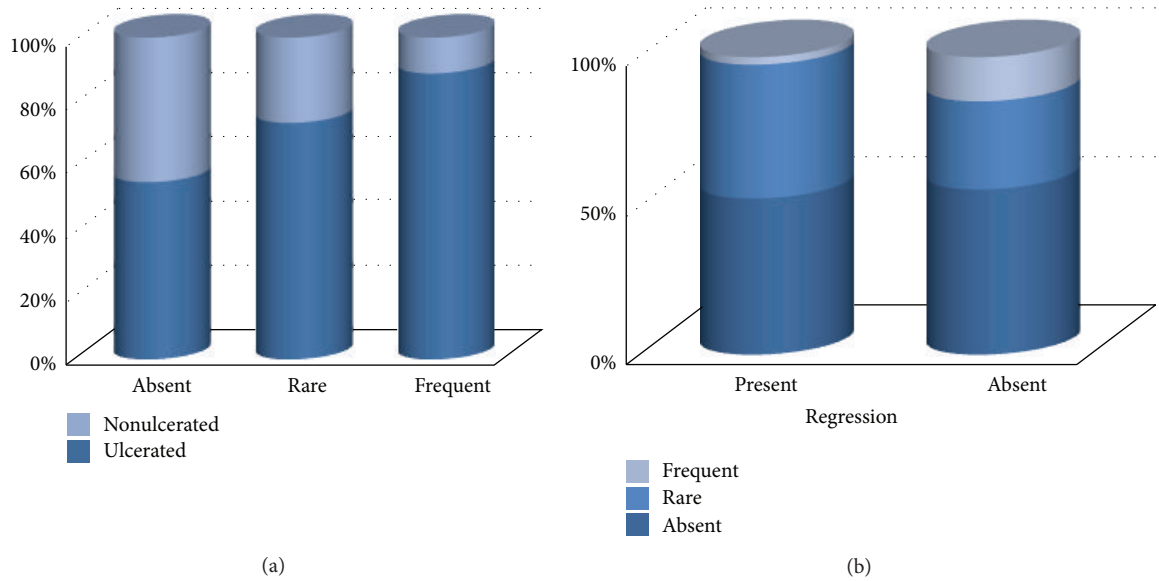

Figure 7: (a) Correlation between density of CD20+ cells and presence of ulceration. (b) Correlation between density of CD20+ cells within the tumor mass and presence of regression.

and Figure 9(e) ulcerated tumors, $P = 0.02$). The presence of LC within the tumor is associated with the factors of better prognosis (thinner tumors), most likely these cells being involved in antitumor host defense by presenting antigens to CD8+ cells [37, 38].

3.3. Immune Parameters Evaluated in Longitudinal Study. Reports of long-term monitoring of immune parameters do not abound in this type of cancer. We have studied in the longitudinal study 102 patients, 74 in stages I and II and 28 in stages III and IV. The overall survival rate of patients at the time of publication is as follows: 100% for stage I, 92% for stage II, 70% for stage III, and 30% for stage IV. Apart from primary tumour surgery with wide margin excision, stages I and II did not receive any other therapy intervention. Stage III was surgically treated for tumour and lymph nodes resection, and postsurgery therapy consisted

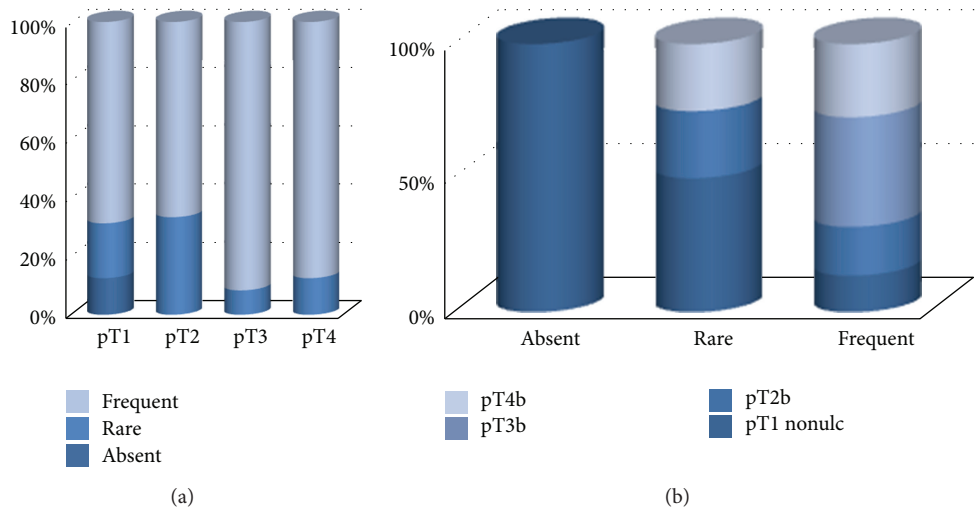

Figure 8: (a) Correlations between the presence of CD138+ cells and pT level. (b) Correlations between the presence of CD138+ cells and pT level in ulcerated tumors.

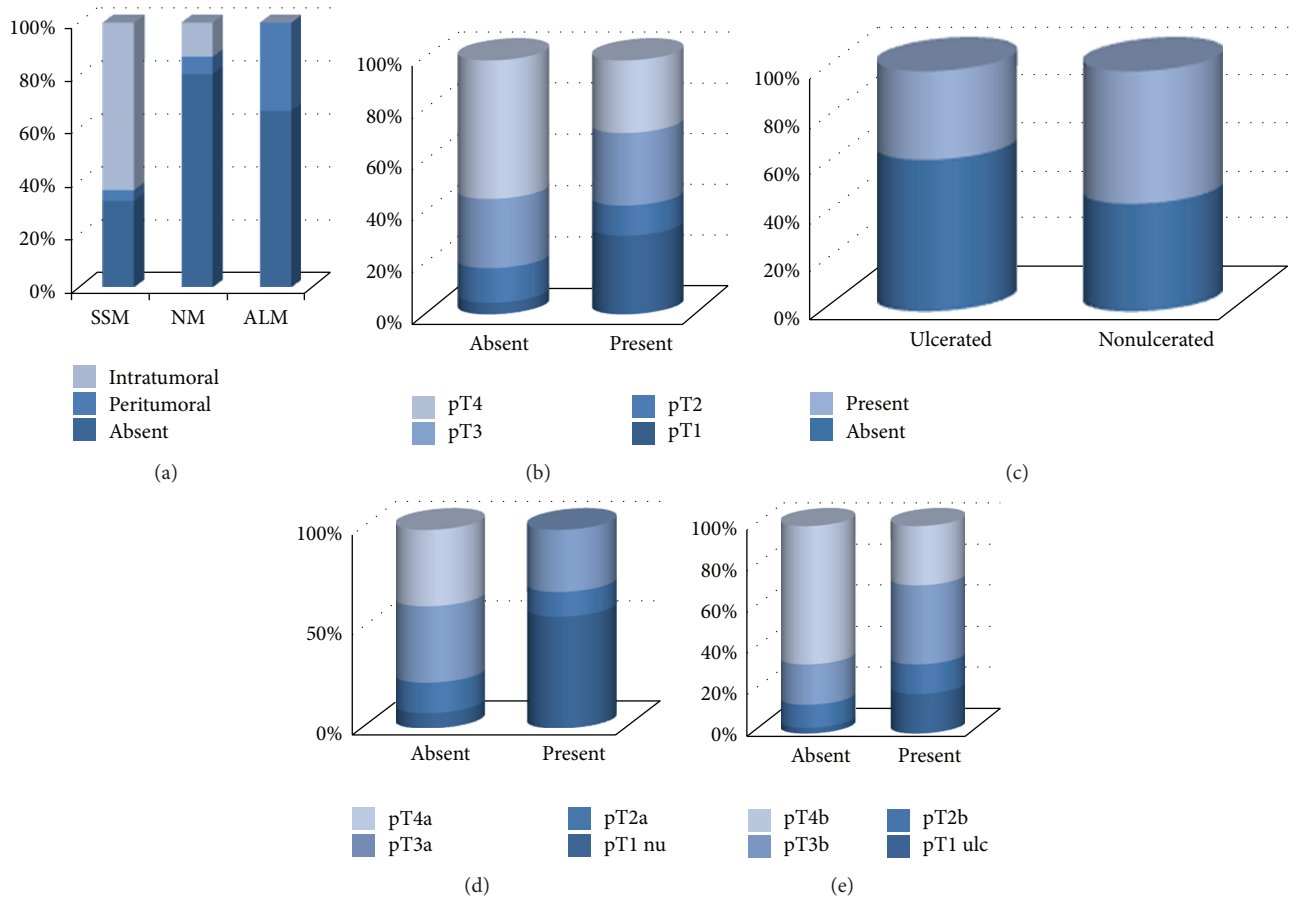

Figure 9: (a) The presence of Langerhans cells within tumor mass correlated with tumor type. (b) The presence of CD1a+ cells within tumor mass correlated with pT level. (c) The presence of CD1a+ cells correlated with the presence of ulceration. (d) The presence of CD1a+ cells correlated with pT level in nonulcerated tumors. (e) The presence of CD1a+ cells correlated with pT level in ulcerated tumors.

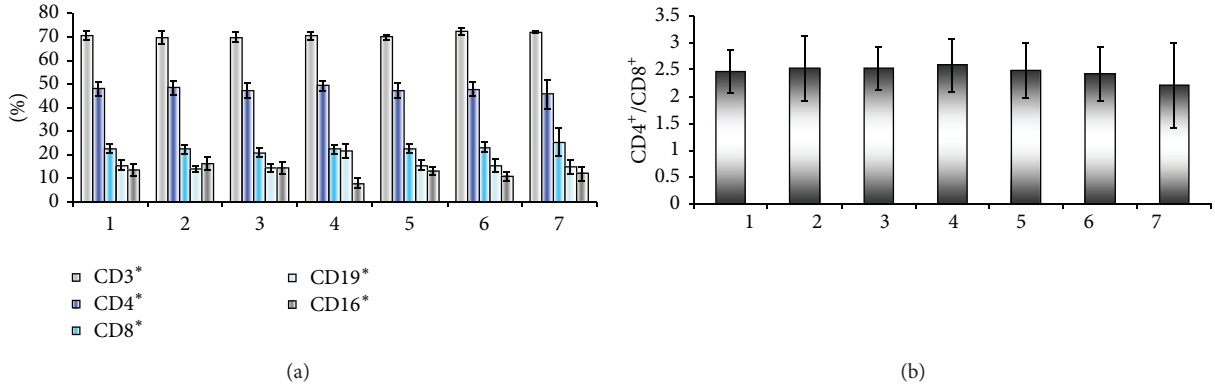

Figure 10: Peripheral blood immune populations evaluated in stage I patients before surgery (1) and 36 months followup in 6 visits (2–7). Percentage of circulating immune subpopulations (a) and CD4/CD8 ratio (b).

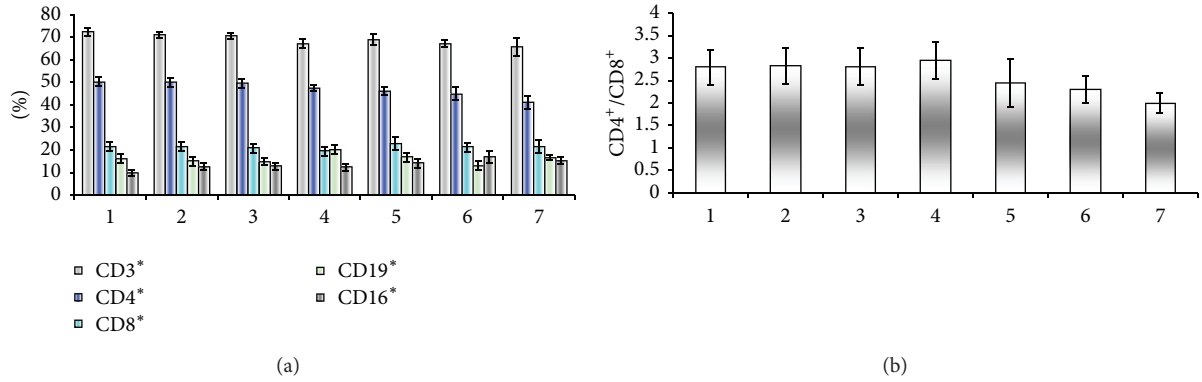

Figure 11: Peripheral blood immune populations evaluated in patients stage II before surgery (1) and 36 months followup in 6 visits (2–7). Percentage of circulating immune subpopulations (a) and CD4/CD8 ratio (b).

of high doses of IFN-alpha-2b and/or dacarbazine-based combination chemotherapy regimens. Stage IV patients were treated with surgery reintervention if metastasis was approachable, and postsurgery treatment included dacarbazine or temozolomide-based combination chemotherapy regimens. None of the presented patients had any kind of vaccine-based immunotherapy.

Patients that were studied in dynamics in the longitudinal evaluation showed various patterns. In stage I (Figure 10), there is an unchanged level of CD3+ in peripheral circulation (a) and a tendency for the CD4/CD8 ratio to drop after 3 years of followup (b).

The registered tendency to drop the CD4/CD8 ratio in stage I (Figure 10(b)) is more evident in stage II (Figures 11(a) and 11(b)).

In stage III, the same decrease of CD4/CD8 ratio was identified (Figures 12(a) and 12(b)), and then an increase of this ratio (marked in red line). This marking identifies the time when patients diagnosed at presentation with the disease started to exit the study due to natural causes: death, impossibility to follow up due to the low quality of life, and so on.

Moreover, it is noticeable that the SD of the results increased as the actual number of enrolled patients drops. The decrease in circulating B lymphocytes is balanced by an increase in circulating NK cells (Figure 12(a)). We can note this regulatory mechanism between immune circulating populations in stage III mechanism that probably compensates between the two arms of the immune response.

In stage IV patients at presentation (Figure 13(b)), the patients' cell number drops earlier in the followup, and it is more obvious the increase of CD4/CD8 ratio for patients that survive more than a few months. We can postulate that the shown increased SD resides in the actual number of enrolled patients that is decreased. The compensatory mechanism between B and NK is not as obvious as in stage III probably due to a generally impaired immune response.

During followup, the plasma IL-6 proved to be a good prognosticator of the overall survival. When we applied for IL-6 the 10 pg/mL cutoff value that was obtained from the first quartile of the values registered at first presentation in all patients, a clear correspondence of IL-6 level with survival appeared (Figure 14). A study published by the Italian Melanoma Intergroup evaluating chemotherapy versus biochemotherapy showed that higher values of IL-6 correlated with a worse survival [39]. An experimental mouse model has demonstrated that IL-6 is involved in both the development and progression of skin melanoma

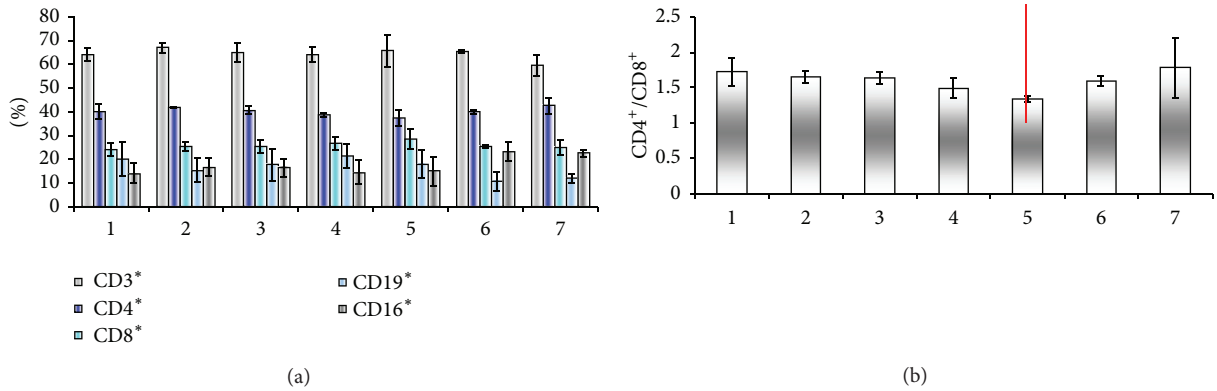

Figure 12: Peripheral blood immune populations evaluated in patients stage III before surgery/therapy (1) and 36 months followup in 6 visits (2–7). Percentage of circulating immune subpopulations (a) and CD4/CD8 ratio (b).

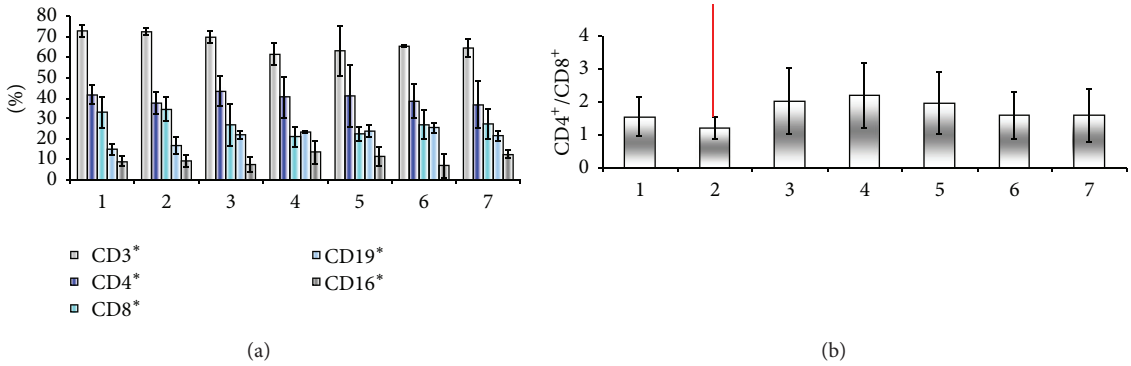

Figure 13: Peripheral blood immune populations evaluated in patients stage IV before surgery/therapy (1) and 36 months followup in 6 visits (2–7). Percentage of circulating immune subpopulations (a) and CD4/CD8 ratio (b).

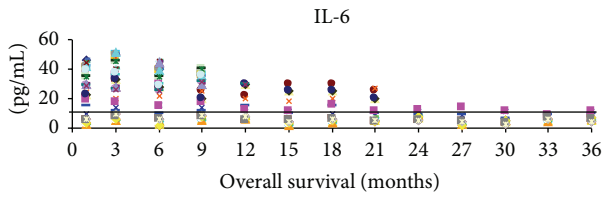

Figure 14: Plasma level of IL-6 for all the investigated patients during follow-up, cross-line depicts the 10 pg/mL cut-off.

[40]. Furthermore, a review [41] summarized recent clinical studies focusing on IL-6 and melanoma. In the light of our findings, it could be possible to stratify patients with high IL-6 levels to be treated with an anti-IL-6 receptor monoclonal antibody like tocilizumab.

For IL-12 found statistically elevated in all the patients no matter the stage, we did not find these clear-cut results as we did in IL-6, although the previously cited study by the Italian Melanoma Intergroup indicated IL-12 as a good prognosticator. The same case was for IL-8 and IL-10, meaning no correlation with overall survival or relapse-free survival.

4. Conclusion—"The Good, the Bad, and the Insensitive"

Immunohistochemical phenotype of TIL in melanoma is comparable to the circulating immune cells without a perfect overlapping, with some differences occurring mainly due to the systemic immune response depicted in the blood circulating cells, the lymph node trafficking to and from the tumor, and so on.

Intratumoral CD3+ cells were frequent in advanced stages and ulcerated tumors, more likely as an inflammatory response towards ulceration and not a host defense against tumor. In regressed areas, we found both CD4+ and CD8+ cells with a CD4/CD8 supraunitary ratio but no correlation with pT level in presence of ulceration or regression.

Similarly to peripheral blood, more numerous B cells were present in advanced stages and/or ulcerated cases. Langerhans cells were not frequent within the tumor mass but, when present, they were associated with the histopathologic parameters of proven favorable prognosis such as thin tumor, irrespective of absence or presence of ulceration. Based on our analysis, the prototype of the intratumor inflammatory infiltrate in a melanoma with good prognosis is composed of numerous T cells CD3+, few/absent B cells

CD20+, few/absent plasma cells, and present Langerhans cells.

When drawing the circulatory immune parameters of a melanoma patient first of all, testing the absolute count of lymphocytes will provide the correct data for detecting the actual circulating subpopulations. CD3+ total T lymphocytes is a parameter that will change during the followup just in advanced stages and will not give an early prognosticator, while the CD4/CD8 ratio will indicate the evolution of disease and will prognosticate the overall survival of the patient, no matter the stage and the applied therapy. We found an increase only in stage III of the circulating percentage of T cells with CD4+CD69+ phenotype indicating a lymph node-related antitumoral activity. We had no correlation to the other stages or to the clinical evolution of patient, although there are statements that pretreatment percentages of circulating CD3+CD4+CD69+ cells can be an independent prognostic factor for overall survival [42]. Peripheral Tregs increase with stage, but we could not establish a correlation between the degree of metastasis and the percentages of circulatory Tregs as previously published [43]. Advanced stages show statistically higher circulating CD19+ B lymphocytes with no increase in plasma level of total and/or subclasses Igs. There is a negative correlation between the level of circulating B lymphocytes and NK cells in melanoma patients.

Circulatory cytokines have different patterns matching the cutaneous melanoma stages. Thus, IL-6 increases with stage, as do TNF-alpha and IL-8. We found plasma IL-6 strongly positively correlated with other serum markers tested in our patients, like S100 and MIA.

IL-6 can pinpoint the overall survival of the patient, and the circulating levels of IL-1beta can indicate the evolving of metastatic processes. Some other cytokines like TNF-alpha, IL-8, and IL-10 increased only in advanced stage not proving, at least in our group, any discrimination power for early stages. Out of all the tested cytokines in the followup, IL-6 level correlated with the patient's survival, while IL-8, IL-10, and IL-12 did not correlate with overall survival or relapse-free survival.

A panel of circulatory immune markers can complete the immune status of the patient and can bring added value to the overall prognosis of the patient and thus direct/redirect the therapy choice. The future lies within establishing low-cost, affordable/available, and easily reproducible assays that will complete the preclinical parameters of the patient.

Abbreviations

AJCC: American Joint Committee on Cancer
ALMs: Acral-lentiginous melanoma
Alpha-MSH: Alpha-Melanocyte-stimulating hormone
CCL: Chemokine ligands
CXCL: Chemokine (C-X-C motif) ligand
GM-CSF: Granulocyte macrophage colony-stimulating factor
gp100: Glycoprotein100
HIER: Heat induced epitope retrieval
HPF: High power field
IFN: Interferon
Igs: Immunoglobulins
IL: Interleukin
IP9: CXCL11
LDH: Lactate dehydrogenase
MIA: Melanoma inhibitory activity
MIG: Monokine induced by gamma interferon
Nk: Natural killer cells
NM: Nodular melanomas
NY-ESO-1: New York esophageal squamous cell Carcinoma 1
PBMC: Peripheral blood mononuclear cells
PGE2: Prostaglandin E2
S100: Calcium-binding protein soluble in 100% saturated ammonium sulfate
SSM: Superficial spreading melanoma
TIL: Tumor infiltrating lymphocytes
TNF-alpha: Tumor necrosis factor alpha
Treg: T regulatory cells
TRP1: Tyrosinase-related protein 1
WBC: White blood cells.

Ethical Approval

The authors state that they have obtained appropriate institutional review board approval and have followed the principles outlined in the Declaration of Helsinki for all human experimental investigations. In addition, for investigations involving human subjects, informed consent has been obtained from the participants involved.

Acknowledgments

Authors had equally contributed to designing the experimental approaches, performing the tests, obtaining the presented results and writing the paper. The authors would like to thank physicians from the Military Hospital Bucharest, the Colentina Hospital, Bucharest, and the Dermato-oncology Excellence Centre, Bucharest, for cutaneous melanoma diagnosed patients, clinically monitoring them, and constant help for developing the presented research. The work was supported from the following Grants: NATO Project SfP 982838/2007, PN 0933-01-01/2008, PN-II-ID-PCE-2011-3-0918, and Postdoctoral Program POSDRU/89/1.5/S/60746.

References

[1] L. Chin, L. A. Garraway, and D. E. Fisher, "Malignant melanoma: genetics and therapeutics in the genomic era," *Genes and Development*, vol. 20, no. 16, pp. 2149–2182, 2006.

[2] M. Neagu, C. Constantin, G. Manda, and I. Margaritescu, "Biomarkers of metastatic melanoma," *Biomarkers in Medicine*, vol. 3, no. 1, pp. 71–89, 2009.

[3] American Cancer Society, *Cancer Facts and Figures 2012*, American Cancer Society, Atlanta, Ga, USA, 2012.

[4] M. R. Shurin, "Cancer as an immune-mediated disease," *ImmunoTargets and Therapy*, vol. 1, pp. 1–6, 2012.

[5] M. Neagu, "Chapter 5-the immune system-a hidden treasure for biomarker discovery in cutaneous melanoma," in *Advances in Clinical Chemistry*, G. S. Makowski, Ed., vol. 58, pp. 89–140, Academic Press, Burlington, Canada, 2012.

[6] NCCN, *Clinical Practice Guidelines in Oncology: Melanoma, Version 3. 2012*, National Comprehensive Cancer Network, Washington, Pa, USA, 2012.

[7] M. Costache, M. Neagu, A. Petrescu et al., "Statistical correlations between peripheral blood lymphocyte subpopulations and tumor inflammatory infiltrate in stage I of skin melanoma," *Romanian Journal of Morphology and Embryology*, vol. 51, no. 4, pp. 693–699, 2010.

[8] S. Klein, C. C. Kretz, P. H. Krammer, and A. Kuhn, "CD127 low/and FoxP3 expression levels characterize different regulatory T-cell populations in human peripheral blood," *Journal of Investigative Dermatology*, vol. 130, no. 2, pp. 492–499, 2010.

[9] L. Michel, L. Berthelot, S. Pettré et al., "Patients with relapsing-remitting multiple sclerosis have normal Treg function when cells expressing IL-7 receptor α-chain are excluded from the analysis," *Journal of Clinical Investigation*, vol. 118, no. 10, pp. 3411–3419, 2008.

[10] L. R. Shiow, D. B. Rosen, N. Brdičková et al., "CD69 acts downstream of interferon-α/β to inhibit S1P 1 and lymphocyte egress from lymphoid organs," *Nature*, vol. 440, no. 7083, pp. 540–544, 2006.

[11] M. Tomura, K. Itoh, and O. Kanagawa, "Naive CD4+ T lymphocytes circulate through lymphoid organs to interact with endogenous antigens and upregulate their function," *Journal of Immunology*, vol. 184, no. 9, pp. 4646–4653, 2010.

[12] M. Hernberg, P. S. Mattila, M. Rissanen et al., "The prognostic role of blood lymphocyte subset distribution in patients with resected high-risk primary or regionally metastatic melanoma," *Journal of Immunotherapy*, vol. 30, no. 7, pp. 773–779, 2007.

[13] L. Vence, A. K. Palucka, J. W. Fay et al., "Circulating tumor antigen-specific regulatory T cells in patients with metastatic melanoma," *Proceedings of the National Academy of Sciences of the United States of America*, vol. 104, no. 52, pp. 20884–20889, 2007.

[14] M. D. McCarter, J. Baumgartner, G. A. Escobar et al., "Immunosuppressive dendritic and regulatory T cells are upregulated in melanoma patients," *Annals of Surgical Oncology*, vol. 14, no. 10, pp. 2854–2860, 2007.

[15] A. M. Cooper and S. A. Khader, "IL-12p40: an inherently agonistic cytokine," *Trends in Immunology*, vol. 28, no. 1, pp. 33–38, 2007.

[16] Y. Sun, K. Jurgovsky, P. Möller et al., "Vaccination with IL-12 gene-modified autologous melanoma cells: preclinical results and a first clinical phase I study," *Gene Therapy*, vol. 5, no. 4, pp. 481–490, 1998.

[17] D. Dewing, M. Emmett, and R. Pritchard Jones, "The roles of angiogenesis in malignant melanoma: trends in basic science research over the last 100 years," *ISRN Oncology*, vol. 2012, Article ID 546927, 7 pages, 2012.

[18] C. Scheibenbogen, T. Mohler, J. Haefele, W. Hunstein, and U. Keilholz, "Serum interleukin-8 (IL-8) is elevated in patients with metastatic melanoma and correlates with tumour load," *Melanoma Research*, vol. 5, no. 3, pp. 179–181, 1995.

[19] S. Brennecke, M. Deichmann, H. Naeher, and H. Kurzen, "Decline in angiogenic factors, such as interleukin-8, indicates response to chemotherapy of metastatic melanoma," *Melanoma Research*, vol. 15, no. 6, pp. 515–522, 2005.

[20] M. Okamoto, W. Liu, Y. Luo et al., "Constitutively active inflammasome in human melanoma cells mediating autoinflammation via caspase-1 processing and secretion of interleukin-1β," *Journal of Biological Chemistry*, vol. 285, no. 9, pp. 6477–6488, 2010.

[21] D. S. Tyler, G. M. Francis, M. Frederick et al., "Interleukin-1 production in tumor cells of human melanoma surgical specimens," *Journal of Interferon and Cytokine Research*, vol. 15, no. 4, pp. 331–340, 1995.

[22] Y. Qin, S. Ekmekcioglu, P. Liu et al., "Constitutive aberrant endogenous interleukin-1 facilitates inflammation and growth in human melanoma," *Molecular Cancer Research*, vol. 9, no. 11, pp. 1537–1550, 2011.

[23] J. S. Khalili, S. Liu, T. G. Rodríguez-Cruz et al., "Oncogenic BRAF(V600E) promotes stromal cell-mediated immunosuppression via induction of interleukin-1 in melanoma," *Clinical Cancer Research*, vol. 18, no. 19, pp. 5329–5340, 2012.

[24] G. A. Porter, J. Abdalla, M. Lu et al., "Significance of plasma cytokine levels in melanoma patients with histologically negative sentinel lymph nodes," *Annals of Surgical Oncology*, vol. 8, no. 2, pp. 116–122, 2001.

[25] L. T. Nguyen, P. H. Yen, J. Nie et al., "Expansion and characterization of human melanoma tumor-infiltrating lymphocytes (TILs)," *PLoS One*, vol. 5, no. 11, Article ID e13940, 2010.

[26] M. R. Hussein, D. A. H. Elsers, S. A. Fadel, and A.-E. M. Omar, "Immunohistological characterisation of tumour infiltrating lymphocytes in melanocytic skin lesions," *Journal of Clinical Pathology*, vol. 59, no. 3, pp. 316–324, 2006.

[27] F. Azimi, R. A. Scolyer, P. Rumcheva et al., "Tumor-infiltrating lymphocyte grade is an independent predictor of sentinel lymph node status and survival in patients with cutaneous melanoma," *Journal of Clinical Oncology*, vol. 30, no. 21, pp. 2678–2683, 2012.

[28] M. C. Mihm Jr., C. G. Clemente, and N. Cascinelli, "Tumor infiltrating lymphocytes in lymph node melanoma metastases: a histopathologic prognostic indicator and an expression of local immune response," *Laboratory Investigation*, vol. 74, no. 1, pp. 43–47, 1996.

[29] C. G. Clemente, M. C. Mihm Jr., R. Bufalino, S. Zurrida, P. Collini, and N. Cascinelli, "Prognostic value of tumor infiltrating lymphocytes in the vertical growth phase of primary cutaneous melanoma," *Cancer*, vol. 77, no. 7, pp. 1303–1310, 1996.

[30] C. M. Balch, S.-J. Soong, J. E. Gershenwald et al., "Prognostic factors analysis of 17,600 melanoma patients: validation of the American Joint Committee on Cancer melanoma staging system," *Journal of Clinical Oncology*, vol. 19, no. 16, pp. 3622–3634, 2001.

[31] R. C. Taylor, A. Patel, K. S. Panageas, K. J. Busam, and M. S. Brady, "Tumor-infiltrating lymphocytes predict sentinel lymph node positivity in patients with cutaneous melanoma," *Journal of Clinical Oncology*, vol. 25, no. 7, pp. 869–875, 2007.

[32] A. L. Burton, B. A. Roach, M. P. Mays et al., "Prognostic significance of tumor infiltrating lymphocytes in melanoma," *American Surgeon*, vol. 77, no. 2, pp. 188–192, 2011.

[33] D. A. Oble, R. Loewe, P. Yu, and M. C. Mihm Jr., "Focus on TILs: prognostic significance of tumor infiltrating lymphocytes in human melanoma," *Cancer Immunity*, vol. 9, p. 3, 2009.

[34] J. B. Haanen, A. Baars, R. Gomez et al., "Melanoma-specific tumor-infiltrating lymphocytes but not circulating melanoma-specific T cells may predict survival in resected advanced-stage melanoma patients," *Cancer Immunology, Immunotherapy*, vol. 55, no. 4, pp. 451–458, 2006.

[35] S. H. Chiou, B. C. Sheu, W. C. Chang, S. C. Huang, and H. Hong-Nerng, "Current concepts of tumor-infiltrating lymphocytes in human malignancies," *Journal of Reproductive Immunology*, vol. 67, no. 1-2, pp. 35–50, 2005.

[36] E. Pavoni, G. Monteriù, D. Santapaola et al., "Tumor-infiltrating B lymphocytes as an efficient source of highly specific immunoglobulins recognizing tumor cells," *BMC Biotechnology*, vol. 7, p. 70, 2007.

[37] G. M. Woods, R. C. Malley, and H. K. Muller, "The skin immune system and the challenge of tumour immunosurveillance," *European Journal of Dermatology*, vol. 15, no. 2, pp. 63–69, 2005.

[38] S. Zurac, G. Negroiu, S. Petrescu et al., "Matrix metalloproteinases underexpression in melanoma with regression," *Virchows Archiv*, vol. 461, supplement 1, p. S40, 2012.

[39] M. Guida, A. Riccobon, G. Biasco et al., "Basal level and behaviour of cytokines in a randomized outpatient trial comparing chemotherapy and biochemotherapy in metastatic melanoma," *Melanoma Research*, vol. 16, no. 4, pp. 317–323, 2006.

[40] V. von Felbert, F. Córdoba, J. Weissenberger et al., "Interleukin-6 gene ablation in a transgenic mouse model of malignant skin melanoma," *American Journal of Pathology*, vol. 166, no. 3, pp. 831–841, 2005.

[41] L. Hoejberg, L. Bastholt, and H. Schmidt, "Interleukin-6 and melanoma," *Melanoma Research*, vol. 22, no. 5, pp. 327–333, 2012.

[42] M. Hernberg, P. S. Mattila, M. Rissanen et al., "The prognostic role of blood lymphocyte subset distribution in patients with resected high-risk primary or regionally metastatic melanoma," *Journal of Immunotherapy*, vol. 30, no. 7, pp. 773–779, 2007.

[43] W. Wang, H. D. Edington, U. N. M. Rao et al., "Effects of high-dose IFNα.2b on regional lymph node metastases of human melanoma: modulation of STAT5, FOXP3, and IL-17," *Clinical Cancer Research*, vol. 14, no. 24, pp. 8314–8320, 2008.

Hindawi Publishing Corporation
BioMed Research International
Volume 2013, Article ID 354582, 13 pages
http://dx.doi.org/10.1155/2013/354582

Research Article

Comparative Gene Expression Profiling in Human Cumulus Cells according to Ovarian Gonadotropin Treatments

Said Assou,[1,2] Delphine Haouzi,[2] Hervé Dechaud,[1,2,3] Anna Gala,[1,2,3] Alice Ferrières,[1,2,3] and Samir Hamamah[1,2,3]

[1] *Université Montpellier 1, UFR de Médecine, Montpellier, France*
[2] *CHU Montpellier, Institute for Research in Biotherapy, Hôpital Saint-Eloi, INSERM U1040, 34295 Montpellier, France*
[3] *ART-PGD Department, CHU Montpellier, Hôpital Arnaud de Villeneuve, 34295 Montpellier, France*

Correspondence should be addressed to Samir Hamamah; s-hamamah@chu-montpellier.fr

Received 7 June 2013; Accepted 8 August 2013

Academic Editor: Shivani Soni

In *in vitro* fertilization cycles, both HP-hMG and rFSH gonadotropin treatments are widely used to control human follicle development. The objectives of this study are (i) to characterize and compare gene expression profiles in cumulus cells (CCs) of periovulatory follicles obtained from patients stimulated with HP-hMG or rFSH in a GnRH antagonist cycle and (ii) to examine their relationship with *in vitro* embryo development, using Human Genome U133 Plus 2.0 microarrays. Genes that were upregulated in HP-hMG-treated CCs are involved in lipid metabolism (*GM2A*) and cell-to-cell interactions (*GJA5*). Conversely, genes upregulated in rFSH-treated CCs are implicated in cell assembly and organization (*COL1A1* and *COL3A1*). Interestingly, some genes specific to each gonadotropin treatment (*NPY1R* and *GM2A* for HP-hMG; *GREM1* and *OSBPL6* for rFSH) were associated with day 3 embryo quality and blastocyst grade at day 5, while others (*STC2* and *PTX3*) were related to *in vitro* embryo quality in both gonadotropin treatments. These genes may prove valuable as biomarkers of *in vitro* embryo quality.

1. Introduction

The gonadotropin-releasing hormone (GnRH) antagonist and agonist protocols with either highly purified human menopausal gonadotropin (HP-hMG) or recombinant FSH (rFSH) preparations are the most widely used protocols for controlled ovarian stimulation (COS) for both intracytoplasmic sperm injection (ICSI) and *in vitro* fertilization (IVF) [1–3]. At present, most of the mature oocytes retrieved after COS are capable of fertilization; however, only half of them develop into good embryos and only a few implants. There is increasing evidence that cumulus cells (CCs), which are somatic cells that surround the oocyte, play a crucial role in folliculogenesis and oocyte developmental competence acquisition [4, 5]. Several authors propose the use of CC gene expression as a noninvasive approach to predict oocyte aneuploidy, and oocyte competence, as well as embryo and pregnancy outcomes during assisted reproductive technology (ART) procedures [6–17]. Despite the recent molecular advances in the knowledge of human CCs, our understanding is far from complete. We believe that the characterization of the biology of these cells following COS might explain observed changes in *in vitro* embryo development. Several studies have compared the effects of HP-hMG and rFSH on oocyte and embryo quality, follicular fluid biochemical profile, and pregnancy rate [18–23]. However, their specific effects on the gene expression profile of individual CC samples have not been investigated. To date, only two such studies have been reported. They compared the gene expression profiles of pooled human granulosa cells (GCs) from periovulatory follicles of six patients in one study and eight patients in the other study. In both studies, the patients were treated with HP-hMG or rFSH in a GnRH agonist long protocol. Significant differences have been observed [24, 25]. The aims of the present study were (i) to compare the gene expression profiles of large cohorts of individual CCs isolated from periovulatory follicles of patients stimulated with HP-hMG or rFSH in a GnRH antagonist protocol and (ii) to determine

the relationship between *in vitro* embryo development and expression profiles of CCs isolated from mature oocytes after COS.

2. Materials and Methods

2.1. Study Oversight. This research was approved by our Institutional Review Board. All patients provided their written informed consent for the use of CC samples for research.

2.2. Sample Collection and Treatment Cycle. This study is a retrospective analysis of data from of a subgroup of eleven randomly selected patients, who participated in an open-label, assessor-blind, parallel groups, multicenter trial (ClinicalTrials.gov Identifier: NCT00884221) that was previously described [26]. CCs ($n = 146$) were collected from all oocytes retrieved from four patients treated with HP-hMG (Menopur, Ferring Pharmaceuticals) and seven patients treated with rFSH (Follitropin beta, Puregon; MSD) following a GnRH antagonist protocol (Ganirelix Acetate, Orgalutran; MSD), respectively. Stimulation with HP-hMG or rFSH was started at a dose of 150 IU/day (first 5 days of the COS protocol), and the patients' follicular response during stimulation was monitored by transvaginal ultrasound. The GnRH antagonist (daily dose of 0.25 mg) was initiated at day 6 and continued throughout the stimulation period. Transvaginal ultrasound echo guidance, FSH, LH, and estradiol levels were used to monitor the ovarian response. A single injection of 250 μg human chorionic gonadotropin (hCG) (choriogonadotropin alfa, Ovitrelle; Merck Serono) was administered to induce the final follicular maturation when three or more follicles ≥17 mm in diameter were observed. Cumulus-oocyte-complexes were collected 36 h after hCG administration (day 0). Supplemental Table SI (see Supplementary Materials available online at http://dx.doi.org/10.1155/2013/354582) shows a summary of the patients' clinical features, end-of-stimulation data, and the number of retrieved oocytes/patients. All CCs were mechanically removed shortly after oocyte retrieval, washed in culture medium, and frozen immediately prior to total RNA extraction. MII oocytes were used for ICSI. All embryos and blastocysts were assessed daily by the embryologists until 5 days after oocyte retrieval. Embryo quality was assessed at 26 ± 2 and 92 ± 2 hours after insemination. On day 5, the quality evaluations of blastocysts consisted of expansion and hatching status, inner cell mass grading (grade A-C), and trophectoderm grading (grade A-C) [26–28]. Each CC sample included only CCs from a single oocyte. The number of CCs isolated from oocytes at GV, MI, and MII stages and the *in vitro* embryo outcome for the two patients' groups (HP-hMG or rFSH) are reported in (Figure 1).

2.3. Cumulus Cells RNA Extraction. The RNeasy Micro kit (ref. 74004, Qiagen) was used to extract total RNA from each CCs sample ($n = 146$) according to the manufacturers' recommended protocols. The quantity and purity of the total RNAs were determined by using a NanoDrop ND-1000 spectrophotometer (NanoDrop ND-Thermo Fisher Scientific, Wilmington, DE, USA) and their integrity by using the Agilent 2100 Bioanalyzer (Agilent Technologies, Palo Alto, CA, http://www.agilent.com/). All RNA samples were stored at −80°C until the microarray experiments.

2.4. Preparation of cRNA and Microarray Hybridization. Total RNA (50 ng) was used to prepare cRNA (one cycle of amplification) using the Affymetrix 3′ IVT express protocol. An oligo-dT primer with a T7 promoter sequence was used to synthesize the first-strand cDNA. After generating the second strand, the complete cDNA was amplified by *in vitro* transcription (linear amplification) with a T7 RNA polymerase. The amplified RNA (aRNA) was generated and quantified by using a NanoDrop ND-1000 spectrophotometer (NanoDrop ND-Thermo Fisher Scientific, Wilmington, DE, USA), and biotinylated nucleotide analog was incorporated during *in vitro* transcription step. RNA from the GeneChip Eukaryotic Poly-A RNA Control Kit (Affymetrix, Santa Clara, CA), which contains mRNAs from *Bacillus subtilis* genes (*lys*, *phe*, *thr*, and *dap*), was amplified and labeled under the same conditions as positive controls. After fragmentation, the labeled antisense aRNA (15 μg) was hybridized to HG-U133 Plus 2.0 GeneChip pan-genomic oligonucleotide arrays (Affymetrix) containing 54,675 sets of oligonucleotide probes (probeset) which correspond to ≈25,000 unique human genes or predicted genes. Each cumulus cell sample was put individually on a microarray chip. Microarray experiments were performed in DNA microarray platform of our Institute of Research in Biotherapy at the Montpellier University Hospital.

2.5. Data Processing and Gene Expression Profile Analysis. After image processing with the Affymetrix GeneChip Operating 1.4 software (GCOS), the CEL files were analyzed using the Affymetrix Expression Console Software v1.3.1 and normalized with the MAS5.0 algorithm by scaling each array to a target value (TGT) of 100 using the global scaling method to obtain an intensity value signal for each probe set. This algorithm also determines whether a gene is expressed with a defined confidence level or not ("detection call"). This "call" can either be "present" (when the perfect match probes are significantly more hybridized than the mismatch probes, $P < 0.04$), "marginal" (for P values of >0.04 and <0.06) or "absent" ($P > 0.06$). Gene annotation was performed using NetAffx (http://www.affymetrix.com/, March 2009). A first selection of microarray data was based on the detection call (present in at least 50% of the CC samples of each group). Then, the Significant Analysis of Microarrays (SAM) (http://www-stat.stanford.edu/~tibs/SAM/) with the Wilcoxon test and sample label permutation ($n = 300$) was used to identify genes of which expression varied significantly between the HP-hMG and rFSH CC samples. The lists of significant genes (fold change, FC ≥1.5 and false discovery rate, FDR ≤5%) as well as common genes were analyzed using the Ingenuity Pathway Analysis (IPA) software (http://www.ingenuity.com/) to identify the biological functions that were specific of each CC group and in common between the two treatments, respectively. Only annotations with significant P value ($P < 0.05$) were considered.

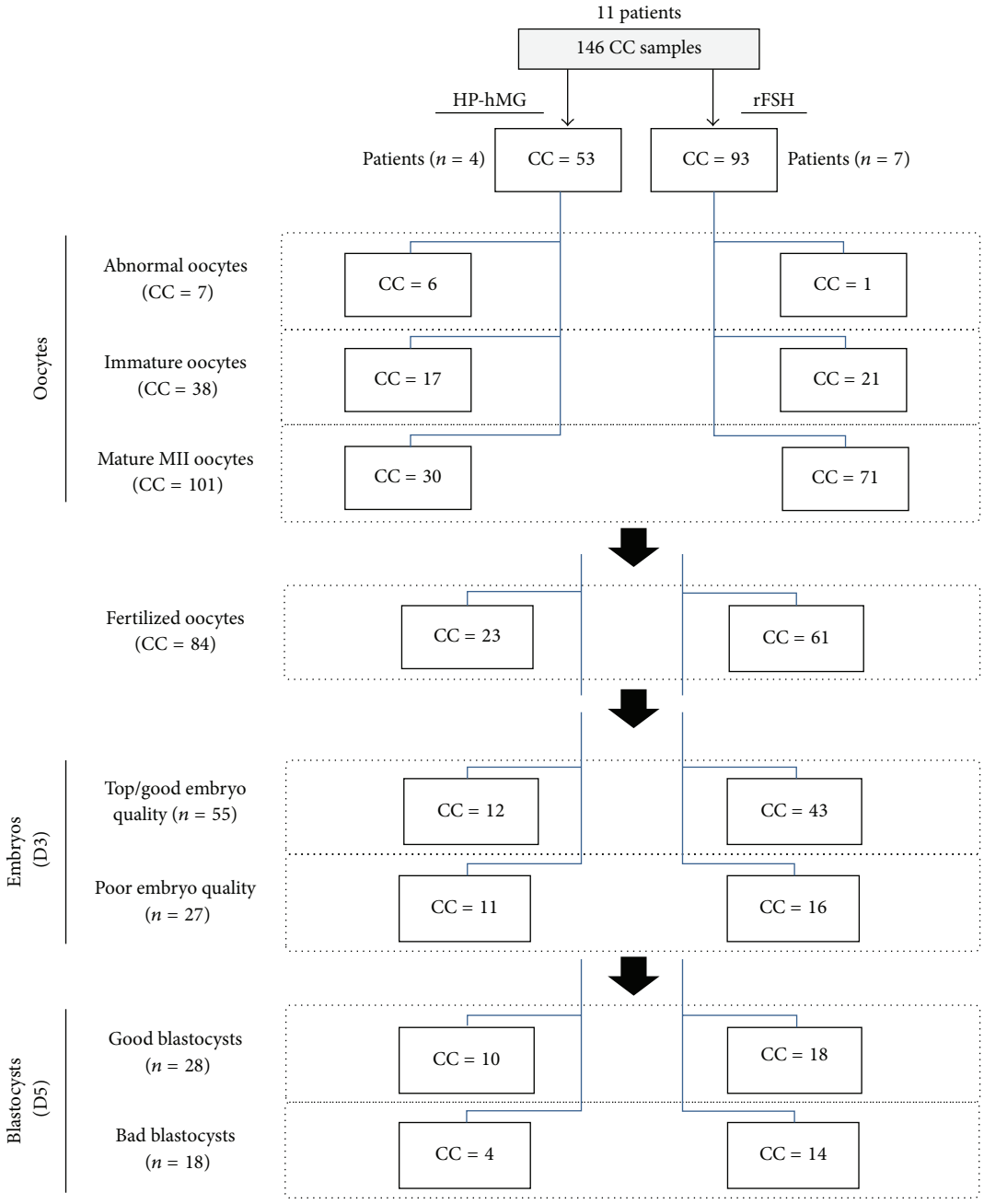

Figure 1: Distribution tree of cumulus cell (CC) samples and embryo outcome relative to the used COS protocol.

Then, the SAM analysis (FC ≥1.5, FDR ≤5%) was used to link gonadotropin-specific genes in CCs or those that are irrespective of gonadotropin treatment to subsequent embryo outcome at day 3 (top, good embryo versus poor) or day 5 (good blastocyst versus bad). Hierarchical clustering analyses based on the expression levels of the differentially expressed genes were performed by using the Cluster and Treeview software packages [29]. Box-and-whisker plots depicted the comparisons of the expression levels of candidate genes carried out using SPSS 12.0 (SPSS, Chicago, IL, USA) software.

2.6. Microarray Data Validation by Quantitative RT-PCR. Quantitative RT-PCR was performed to validate the expression of selected genes identified as differentially expressed between the two CC groups by using mRNAs from HP-hMG ($n = 4$) and rFSH ($n = 4$) CC samples as described in [30]. The primer sequences are shown in (Supplementary data, Table SII). Briefly, cDNA was reverse transcribed (RT) following the manufacturer's instructions using 500 ng of amplified RNA in a 20 μL reaction volume that included Superscript II (ref. 18064-014, Invitrogen), oligo-dT primer,

dNTP mixture, $MgCl_2$, and RNase inhibitor. Quantitative PCR was performed using a LightCycler 480 apparatus with the LC480 SYBR Green I Master kit (Roche Diagnostics, Mannheim, Germany) and 2 μL of diluted cDNA (1/25) and 0.6 mMol primers in a total volume of 10 μL. After 10 min of activation at 95°C, cycling conditions were 10 s at 95°C, 30 s at 63°C, and 1 s at 72°C for 45 cycles. Gene expression levels were normalized to the housekeeping gene glyceraldehyde 3-phosphate dehydrogenase (*GAPDH*), because its expression was stable between all CC groups using the following formula $100/2^{\Delta\Delta Ct}$, where $\Delta\Delta Ct = \Delta Ct$ unknown $- \Delta Ct$ positive control.

2.7. Statistical Analysis. Statistical analyses were performed with SPSS 12.0 software. A repartition difference between sample groups was considered significant when the Kruskal-Wallis nonparametric test and Wilcoxon test gave a P value ≤ 0.05. For q-RT-PCR, a statistical analysis was performed with the GraphPad InStat software (Mann-Whitney U test; GraphPad, San Diego, CA). A value of $P \leq 0.05$ was considered to be statistically significant.

3. Results

3.1. Identification of Differentially Expressed Genes in Human CCs following Stimulation with HP-hMG or rFSH. A first selection is based on the detection call between all the CC samples from patients stimulated with HP-hMG or rFSH delineated 9,899 genes. Then, using SAM, 94 genes that significantly differentiated between HP-hMG and rFSH CCs were identified. Among them, 45 and 49 genes were upregulated in HP-hMG and rFSH CC samples, respectively (fold-change, FDR, and annotation are in Tables 1 and 2). The HP-hMG CC list included genes implicated in lipid metabolism such as *GM2A* (x2.3, FDR = 0), *AKR1C1* (x1.5, FDR = 0), *AKR1C2* (x1.6, FDR = 0.005), and in cell-to-cell interaction like *GJA5* (x1.9, FDR = 0), *NTS* (x1.8, FDR = 0.005), *FOS* (x1.6, FDR = 0), and *NPY1R* (x2.1, FDR = 0), *NPY2R* (x1.6, FDR = 0). Conversely, the rFSH CC list was significantly enriched in genes important for cellular assembly and organization such as *COL3A1* (x2, FDR = 0.015), *COL1A1* (x1.5; FDR = 0), *MT3* (x1.5; FDR = 0), and *CAMK1D* (x1.5; FDR = 0). Other genes of the rFSH list are members of the tumour necrosis factor (*TNF*) family such as *TNFAIP6* (x1.7; FDR = 0.01) and *TNFAIP8* (x1.6, FDR = 0.005). The clustering based on these 94 genes segregates the majority of the HP-hMG (85%) from the rFSH CC samples (Figure 2). RT-qPCR validated the differential expression of some of these genes (Supplementary data, Figure SI).

3.2. Common Transcriptional Gene Profile in HP-hMG/rFSH CCs. In view of few differences between the two gonadotropin treatments, we examined the list of genes in common to HP-hMG and rFSH groups (list of 9,805 genes; see Supplementary data, Table SIII). We used IPA software to explore the specific functional properties of this common molecular signature. Estrogen receptor signaling (83 genes) (P value = $8.17E-08$) was one of the top canonical pathways related to this molecular signature. On the other hand, the top network involving 35 genes was articulated around the "cell death and survival, DNA replication, recombination, and repair" functions. The detailed list of genes involved in this network can be found in (Supplementary data, Table SIV). Interestingly, the most common HP-hMG/rFSH genes were associated with multiple signaling pathways including *FGF* signaling (*FGFR and GRB2*), *IGF* signaling (*IGF1R* and *IGFBP3*), *EGF* signaling (*EGFR* and *MAPK1*), and *PDGF* signaling (*PDGFRA* and *PDGFD*). It is important to note that no difference was observed in the mRNA CC level between treatments for receptors (*LHCGR* and *BMPR2*), aromatase (*CYP19A1*), cytochrome *P450* (*CYP11A1*), or steroidogenic genes (*StAR*, *HSD3B2*, *ACVR1*, *ACVR1B*, *INHBC*, and *INHBB*).

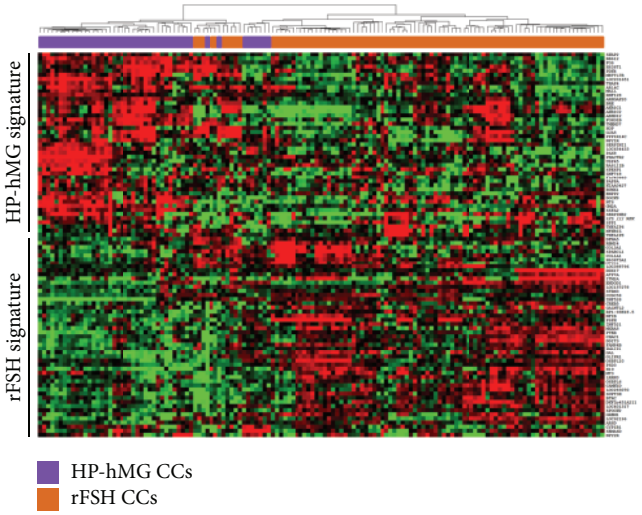

Figure 2: Gene expression patterns of the HP-hMG and rFSH CC samples. Supervised hierarchical clustering of CC samples based on the 94 genes that are differentially expressed between the two treatment groups (HP-hMG and rFSH). We can see a distinct signature in each CCs category. The color intensity indicates the level of gene expression (red for upregulated genes and green for downregulated genes).

3.3. Relationship between the HP-hMG or rFSH CC Expression Profiles and In Vitro Embryo Development. Of the 146 CC samples, 101 were isolated from MII mature oocytes which underwent ICSI. In the HP-hMG group, 77% of injected oocytes were fertilized and 61% achieved blastocyst stage at day 5. In the rFSH group, these values were, respectively, 86% and 52%. Fertilized MII oocytes ($n = 23$ in the HP-hMG and $n = 61$ in the rFSH group) were divided into oocytes that developed into (i) top/good quality (52% in the HP-hMG and 70% in the rFSH group, no significant difference ($\varepsilon = 1.65$)) or poor quality embryos at day 3; and then into (ii) good (AA and AB) (43% for the HP-hMG and 29% for the rFSH group, no significant difference ($\varepsilon = 1.28$)) or bad grade (AC, BC, CC, and CB) blastocysts at day 5 (Figure 1). Then, the transcription profile of the cumulus cell samples isolated from these 101 MII oocytes was evaluated relative to day 3 embryo quality and blastocyst

Table 1: List of genes that were significantly upregulated in HP-hMG CCs compared with rFSH CCs.

Gene name	Gene title	Probesets	Fold change	FDR (%)
PHACTR2	Phosphatase and actin regulator 2	244774_at	2.9	0
GM2A	GM2 ganglioside activator	235678_at	2.3	0
LOC654433	*Homo sapiens*, clone IMAGE:4826696, mRNA	228425_at	2.2	0
LOC201651	Similar to esterase/N-deacetylase (EC 3.5.1.-), 50 K hepatic-rabbit	1569582_at	2.1	0
PAX8	Transcribed locus, moderately similar to XP_375099.1 hypothetical protein LOC283585 (*Homo sapiens*)	227474_at	2.1	0
NPY1R	Neuropeptide Y receptor Y1	205440_s_at	2.1	0
GJA5	Gap junction protein, alpha 5, 40 kDa (connexin 40)	226701_at	1.9	0
FOXG1B	Forkhead box G1B	206018_at	1.9	0
SPP1	Secreted phosphoprotein 1	209875_s_at	1.9	0.58
NTS	Neurotensin	206291_at	1.8	0.58
THAP4	THAP domain containing 4	220417_s_at	1.8	0
SPESP1	Sperm equatorial segment protein 1	229352_at	1.8	0.58
SEMA6D	Sema domain, transmembrane domain (TM), and cytoplasmic domain, (semaphorin) 6D	233882_s_at	1.8	0.58
DOCK8	Dedicator of cytokinesis 8	225502_at	1.8	0.58
SERPINB2	Serine (or cysteine) proteinase inhibitor, clade B (ovalbumin), member 2	204614_at	1.7	0.58
PPP1R14C	Protein phosphatase 1, regulatory (inhibitor) subunit 14C	226907_at	1.7	0
CTIF	CBP80/20-dependent translation initiation factor	243090_at	1.7	0
SSFA2	Sperm-specific antigen 2	236207_at	1.7	0
HS3ST1	Heparan sulfate (glucosamine) 3-O-sulfotransferase 1	205466_s_at	1.7	0
CYP1B1	Cytochrome P450, family 1, subfamily B, polypeptide 1	202437_s_at	1.7	0
TMEM37	Transmembrane protein 37	1554485_s_at	1.6	0
BBS12	Hypothetical protein FLJ35630	229603_at	1.6	0
AKR1C2	Aldo-keto reductase family 1, member C2	211653_x_at	1.6	0.58
MALL	BENE protein	209373_at	1.6	0
NPY2R	Neuropeptide Y receptor Y2	210729_at	1.6	0
METTL7B	Hypothetical protein MGC17301	227055_at	1.6	0
RNF128	Ring finger protein 128	219263_at	1.6	0
ARL4C	ADP-ribosylation factor-like 7	202207_at	1.6	0
PAPPA	Pregnancy-associated plasma protein A, pappalysin 1	240450_at	1.6	0
USP45	Ubiquitin-specific protease 45	224441_s_at	1.6	0
FOS	v-fos FBJ murine osteosarcoma viral oncogene homolog	209189_at	1.6	0
PDK4	Pyruvate dehydrogenase kinase, isozyme 4	225207_at	1.6	0
ZNF718	Hypothetical protein FLJ90036	1553269_at	1.6	0
ARHGAP20	Rho GTPase activating protein 20	228368_at	1.5	0
FLJ43663	CDNA FLJ26188 fis, clone ADG04821	238619_at	1.5	0
HOP	Homeodomain-only protein	211597_s_at	1.5	0
ENPP2	Ectonucleotide pyrophosphatase/phosphodiesterase 2 (autotaxin)	209392_at	1.5	2.95
LYZ	Lysozyme (renal amyloidosis)	213975_s_at	1.5	1.05
SKAP2	src family associated phosphoprotein 2	204361_s_at	1.5	0
ABHD12	Chromosome 20 open reading frame 22	228124_at	1.5	0
RUNX1	Runt-related transcription factor 1	236114_at	1.5	0
AKR1C1	Aldo-keto reductase family 1, member C2	216594_x_at	1.5	0
BRE	Brain and reproductiveorgan-expressed (TNFRSF1A modulator)	211566_x_at	1.5	0
SERPINI1	Serine (or cysteine) proteinase inhibitor, clade I (neuroserpin), member 1	205352_at	1.5	0
RASL11B	RAS-like, family 11, member B	219142_at	1.5	0

Table 2: List of genes that were significantly upregulated in rFSH CCs compared with HP-hMG CCs.

Gene name	Gene title	Probesets	Fold change	FDR (%)
ITM2A	Integral membrane protein 2A	202746_at	4.2	0
H19	H19, imprinted maternally expressed transcript (nonprotein coding)	224646_x_at	3.8	0
PSPH	Phosphoserine phosphatase	205048_s_at	2.4	0
GAL	Galanin	214240_at	2.4	0
ZNF528	Zinc finger-like	232315_at	2.3	0
NFKBIZ	Nuclear factor of kappa light polypeptide gene enhancer in B-cell inhibitor, zeta	223217_s_at	2.2	4.73
FAM84B	Breast cancer membrane protein 101	225864_at	2	0
COL3A1	Collagen, type III, alpha 1 (Ehlers-Danlos syndrome type IV, autosomal dominant)	211161_s_at	2	1.53
DKFZp451A211	DKFZp451A211 protein	1556114_a_at	1.8	0
SPARCL1	SPARC-like 1 (mast9, hevin)	200795_at	1.8	0
PTER	Phosphotriesterase related	222798_at	1.8	0
NFIB	Nuclear factor I/B	213032_at	1.8	0
MXRA5	Adlican	209596_at	1.8	0
GALNTL2	UDP-N-acetyl-alpha-D-galactosamine:polypeptide N-acetylgalactosaminyltransferase-like 2	228501_at	1.8	0
SUPT3H	Suppressor of Ty 3 homolog (*S. cerevisiae*)	211106_at	1.7	0
DDX17	DEAD (Asp-Glu-Ala-Asp) box polypeptide 17 /// DEAD (Asp-Glu-Ala-Asp) box polypeptide 17	208151_x_at	1.7	4.15
TNFAIP6	Tumor necrosis factor, alpha-induced protein 6	206026_s_at	1.7	1.05
MTUS1	Mitochondrial tumor suppressor 1	212096_s_at	1.7	4.73
RP1-93H18.5	Similar to RIKEN cDNA A630077B13 gene, RIKEN cDNA 2810048G17	229390_at	1.7	0
LOC92196	Hypothetical LOC92196 (uncharacterized)	229290_at	1.6	0
LOC401317	Hypothetical LOC402472 (uncharacterized)	242329_at	1.6	0
CHAC1	Hypothetical protein MGC4504	219270_at	1.6	0
STRN3	Striatin, calmodulin binding protein 3	215505_s_at	1.6	0
OSBPL10	Oxysterol binding protein-like 10	219073_s_at	1.6	0
GLIPR1	HIV-1 rev binding protein 2	214085_x_at	1.6	0
BTRC	Beta-transducin repeat containing E3 ubiquitin protein ligase	237862_at	1.6	0
TNFAIP8	Tumor necrosis factor, alpha-induced protein 8	208296_x_at	1.6	0.54
PMAIP1	Phorbol-12-myristate-13-acetate-induced protein 1	204286_s_at	1.6	0
RBM24	RNA binding motif protein 24	235004_at	1.6	1.53
LOC388796	Hypothetical LOC388796 (uncharacterized)	65588_at	1.6	0
LOC157278	*Homo sapiens*, clone IMAGE:5285282, mRNA (uncharacterized)	238716_at	1.6	0
GREM1	Gremlin 1	218468_s_at	1.6	0
OSBPL6	Oxysterol binding protein-like 6	223805_at	1.6	0
CREB5	cAMP responsive element binding protein 5	205931_s_at	1.5	0
CAMK1D	Calcium/calmodulin-dependent protein kinase ID	235626_at	1.5	0
CCDC58	Hypothetical LOC131076	235244_at	1.5	0
LRRN3	Leucine-rich repeat neuronal 3	209840_s_at	1.5	0
HS3ST3A1	Heparan sulfate (glucosamine) 3-O-sulfotransferase 3A1	219985_at	1.5	0
ARSD	Arylsulfatase D	232423_at	1.5	0
ENDOD1	KIAA0830 protein	212570_at	1.5	0
ZNF521	Zinc finger protein 521	226676_at	1.5	0
DFNA5	Deafness, autosomal dominant 5	203695_s_at	1.5	0

Table 2: Continued.

Gene name	Gene title	Probesets	Fold change	FDR (%)
PSD3	Pleckstrin and Sec7 domain containing 3	203354_s_at	1.5	0
LOC283070	Hypothetical protein LOC283070 (uncharacterized)	226382_at	1.5	0
COL1A1	Collagen, type I, alpha 1	1556499_s_at	1.5	0
SPOCK2	Sparc/osteonectin, cwcv and kazal-like domains proteoglycan (testican) 2	202523_s_at	1.5	0
ATP7A	ATPase, Cu++ transporting, alpha polypeptide (Menkes syndrome)	205197_s_at	1.5	0
MT3	Metallothionein 3 (growth inhibitory factor (neurotrophic))	205970_at	1.5	0
DDIT3	DNA-damage-inducible transcript 3	209383_at	1.5	0

grading at day 5. In the HP-hMG group, *NPY1R* (x1.58, FDR = 0.0004) and *NPY2R* (x1.67, FDR = 0.0004) upregulation was observed in CCs isolated from MII oocytes that developed into top/good day 3 embryos, whereas *GM2A* (x2.10, FDR = 0.0005) and *USP45* (x2.32, FDR = 0.0005) were upregulated in cumulus cells from MII oocytes with good blastocyst grading (Figure 3(a)). After rFSH treatment, upregulation of *GREM1* (x1.59, FDR = 0) and *PSPH* (x1.6, FDR = 0) was significantly associated with top/good quality day 3 embryos; *OSBPL6* (x1.59, FDR = 0) upregulation was found in CCs from oocytes that developed into good blastocyst at day 5 (Figure 3(b)). In the two gonadotropin groups, *PTX3* (x-1.81, FDR = 0) downregulation and *STC2* (x1.76, FDR = 0) upregulation were observed in CCs isolated from MII oocytes that developed into top/good day 3 embryos, whereas *TRIM65* (x-1.62, FDR = 0) and *GSTM2* (x-1.67, FDR = 0) expressions were downregulated in CCs associated with good blastocyst grading (Figure 3(c)).

3.4. CC mRNA Content and In Vitro Blastocyst Outcome at Day 5. Independently of the type of gonadotropin treatment used, the relation between amplified mRNA content of CC samples and *in vitro* blastocyst development at day 5 was also investigated. Seventeen CC samples, isolated from MII oocytes that developed into top quality 8-cell embryos at day 3, were selected and divided in three groups: (i) CCs from MII oocytes that developed into good quality (grade AA-AB, $n = 7$), (ii) intermediary (grade BB, $n = 6$), and (iii) bad (grade CC and others, $n = 4$) blastocysts. The amount (mean ± SEM) of amplified mRNA from CCs from MII oocytes leading to good quality blastocysts was 1044.28 ± 159.18 ng/μL. This value decreased to 796.66 ± 150 ng/μL in the intermediary group and to 627.50 ± 76.25 ng/μL in the bad blastocyst grade group (Figure 4).

4. Discussion

Following global genomic assessment of 146 human CCs transcriptome under HP-hMG and rFSH treatments, the present study revealed a small but significant distinct molecular signature of 94 genes between the two treatments, suggesting that these treatments impact differentially the CC gene expression profile. This may be accounted for by the differences in the origin of the two pharmaceutical preparations. More precisely, overexpression of genes involved in the metabolism of lipids such as *GM2A*, *AKR1C1* and *AKR1C2,* as well as genes related to the intercellular signaling (*GJA5* and *FOS*) was observed in the CCs treated with HP-hMG, while genes involved in "cellular assembly and organization" (*COL1A1*, *COL3A1*, *MT3, TNFAIP6,* and *TNFAIP8*) were overexpressed in the rFSH CCs. Each of these functions plays a central role in oocyte maturation and/or oocyte competence [31–33]. Indeed, the metabolism of lipids represents the main energy source for protein synthesis during oocyte nuclear maturation and early embryo development [34, 35]. Simultaneously, adequate communication between oocyte and CCs and appropriate assembly and organization of the CC matrix are required for both oocyte maturation and competence [36–38]. Most of the genes, identified in the present investigation as differentially expressed in CCs treated with HP-hMG and rFSH, were reported for the first time, except for *TNFAIP6* and *GJA5* (connexin 40) which have been previously identified as potential markers of oocyte competence in CCs from bovine preovulatory follicles [39] and biomarker of oocyte maturation in canine cumulus-oocyte complexes matured *in vitro*, respectively [38].

Furthermore, the comparison of our data with the two other transcriptomic studies comparing the same gonadotropin treatment in granulosa cells (GCs) using the GnRH agonist long protocols [24, 25] indicates that *GM2* ganglioside activator is upregulated in HP-hMG CCs (this study) and rFSH GCs [24]. *GM2A* is known to play an important role in the hydrolysis of phospholipids or small glycolipids [40]. In addition, among the 9 common genes of our study and the one by Brannian et al. [25], six genes (*ATP7A*, *BTRC*, *LRRN3*, *STRN3*, *PTER*, and *SUPT3*) are upregulated in both CCs and GCs after rFSH treatment; one (*H19*) was upregulated in both rFSH CCs and HP-hMG GCs and the two others (*SERPINI1* and *SSFA2*) in HP-hMG CCs and rFSH. The use of different GnRH analogs might explain these discrepancies, but we cannot exclude the possibility that gonadotropin stimulation might have different effects on CCs and GCs. More investigations are required to address this issue.

On the other hand, we reported an important common CC molecular signature revealing the preservation of numerous growth factor signaling between the two types of treatments including the *IGF*, *PDGF*, *FGF*, and *EGF* pathways (See Figure SIII). These signaling pathways have been previously reported to play a central role in the control of the intrafollicular androgen/estrogen ratio for the *IGF*

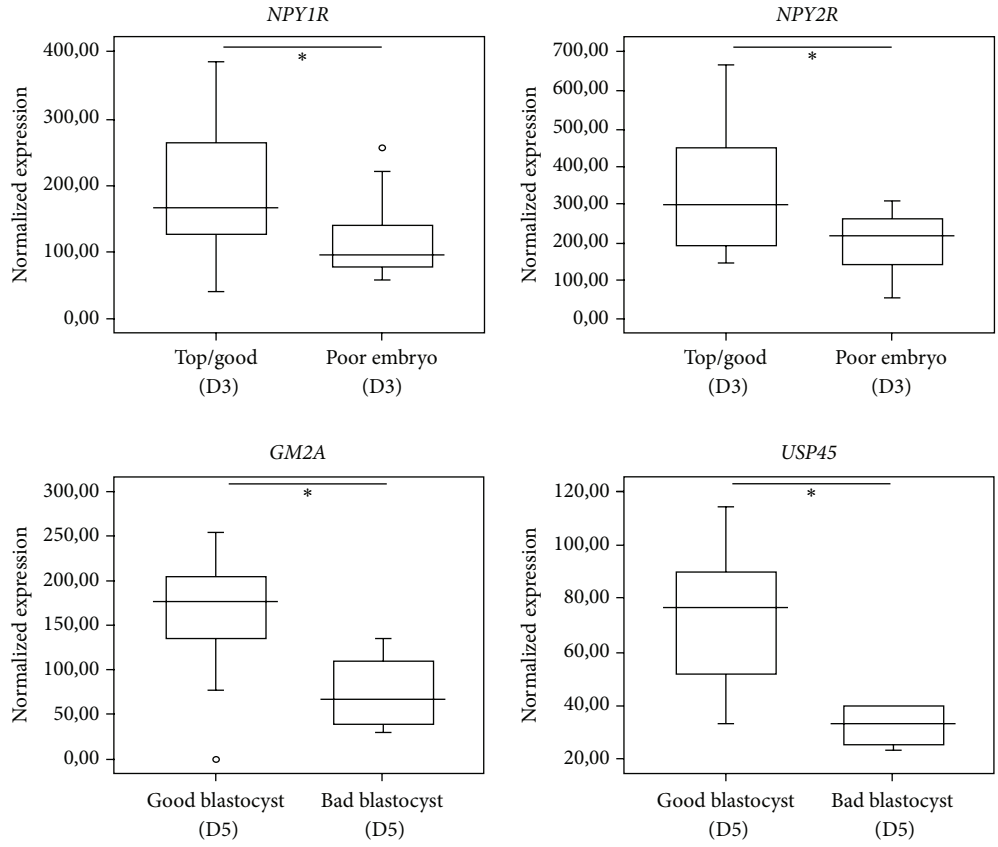

(a) HP-hMG treatment

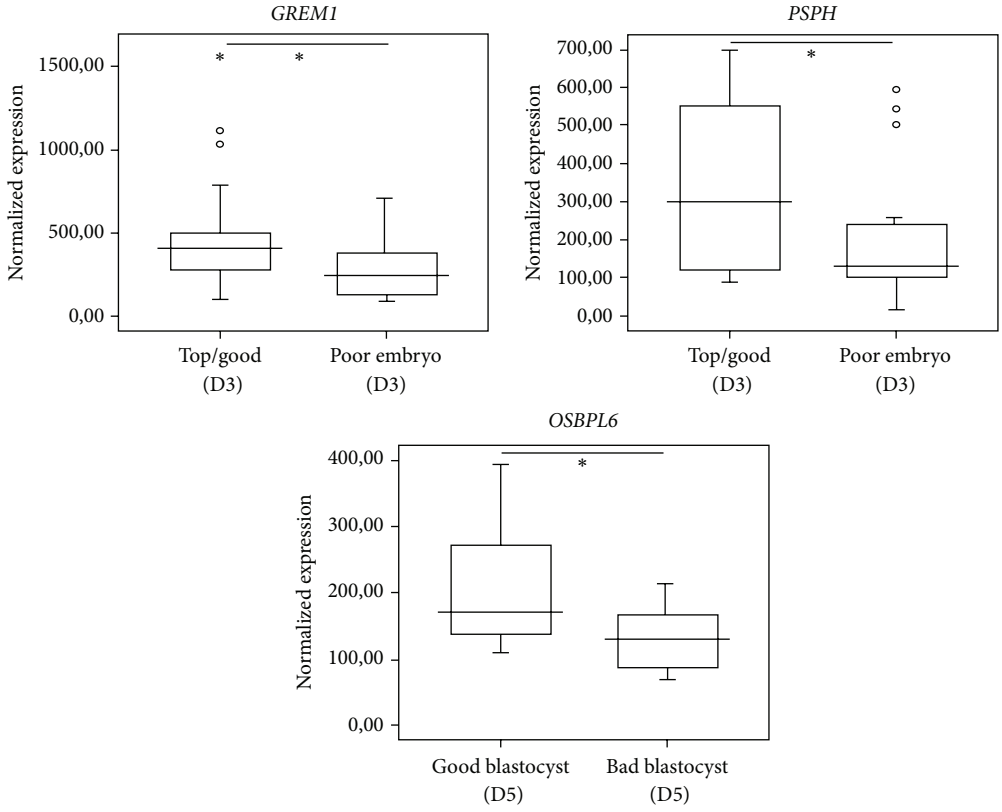

(b) rFSH treatment

Figure 3: Continued.

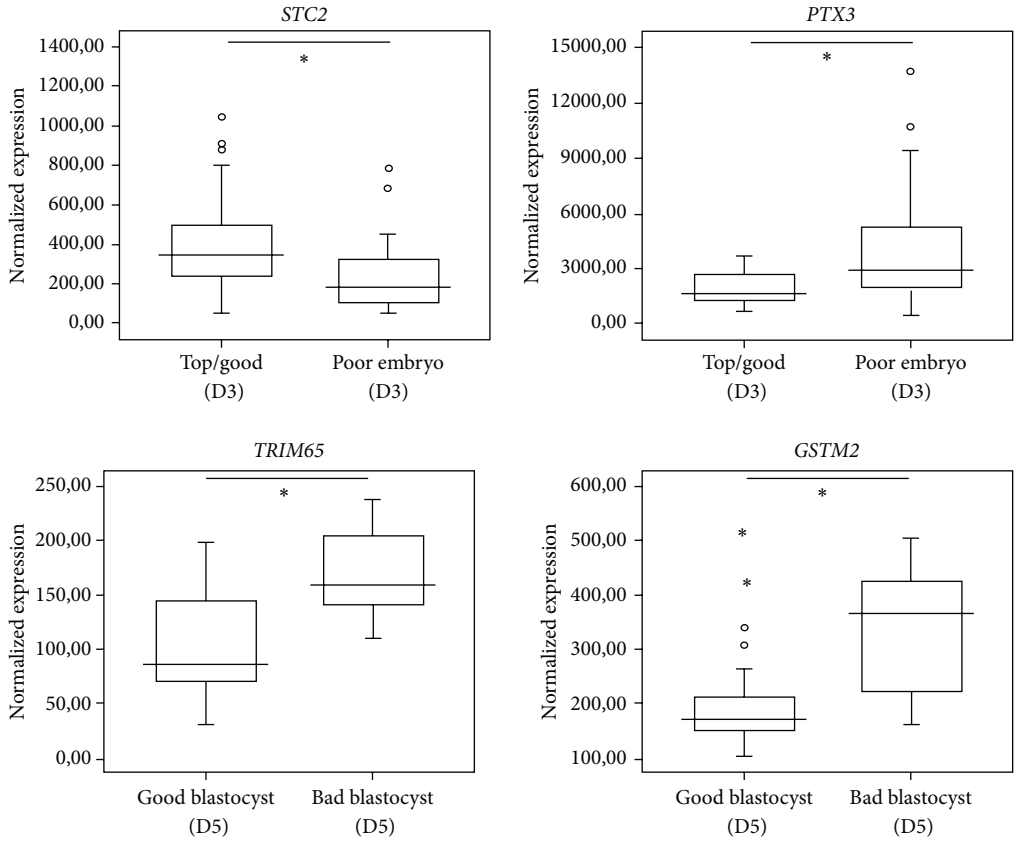

(c) Common to both HP-hMG/rFSH treatments

Figure 3: Gonadotropin gene expression associated with *in vitro* embryo development. (a) and (b) Box-and-whisker plots comparing the expression level of gonadotropin-specific gene in CCs from oocytes that developed into top/good quality embryos ($n = 43$ in the rFSH and $n = 12$ in the HP-hMG group) or poor quality embryos ($n = 16$ in the rFSH and $n = 11$ in the HP-hMG group) and into good blastocysts ($n = 18$ in the rFSH and $n = 10$ in the HP-hMG group) or bad blastocysts ($n = 14$ in the rFSH and $n = 4$ in the HP-hMG group). (c) Box-and-whisker plots comparing the expression level of gonadotropin common genes in CCs from oocytes that developed into top/good quality embryos ($n = 55$ CCs) or poor quality embryos ($n = 27$ CCs) and into good blastocysts ($n = 28$ CCs) or bad blastocysts ($n = 18$ CCs). The signal intensity for each gene is shown on the y-axis as arbitrary units determined by the Affymetrix GCOS software. * A significant difference with FDR ≤0.05.

members [41], in angiogenesis and embryo development for the *FGF* and *PDGF* members [42] and in oocyte maturation for the members of the *EGF* family [43–45]. The interactions between these signaling pathways in CCs under COS will be a precious itinerary to explore in future works in order to complete the oocyte competence puzzle.

Another important finding of this study is that the mRNA level for key genes involved in ovulation process including hormonal receptors (*LHCGR* and *BMPR2*) and regulators of steroidogenesis (*StAR*, *HSD3B2*, *Activins*, and *Inhibins*) was comparable in the HP-hMG and rFSH CC groups. This suggests a similar potency of the two protocols to induce hormonal receptors and similar estrogenic capacity of the CC samples stimulated by HP-hMG and rFSH. This is in line with several studies reporting that CCs *in vitro* were able to secrete estradiol during COCs culture from patients undergoing stimulated cycles, probably as a consequence of the action of gonadotropins [46].

We also identified a significant relationship between some CC genes that were specifically upregulated following stimulation with HP-hMG or rFSH and *in vitro* embryo development. In the HP-hMG group, upregulation of *NPY1R* and *NPY2R* in CCs was associated with top/good embryo quality at day 3. *NPY* modulates steroid production through *NPY* receptors [47] and plays a role in human ovarian steroidogenesis directly at the level of the granulosa cells of the follicles in the early stage of luteinization [48, 49]. Additionally, the association of ubiquitin specific protease 45 (*USP45*) with good blastocyst quality suggests the requirement of proteasomal activity in HP-hMG-treated CCs. Proteasomal activity has been reported to have multiple functions in CCs expansion, in oocyte meiosis, and in the modification of cumulus-oocyte communication [50].

In the rFSH group, upregulation of gremlin 1 (*GREM1*) in CCs was associated with top/good embryo quality at day 3 and *OSBPL6* upregulation with good blastocyst grading at day 5. Only CC expression of *GREM1*, a member of the bone morphogenic protein (*BMP*) antagonist family, has been reported as positively correlated with embryo quality [7, 12, 51]. The regulation of *BMP* through *GREM1* is thought

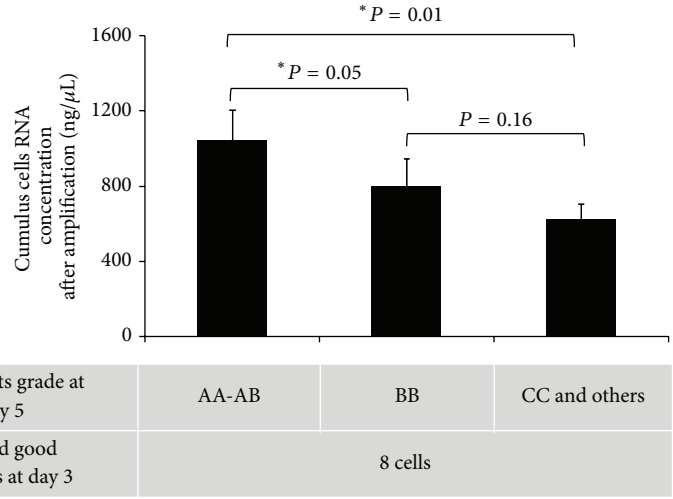

Figure 4: Relationship between amount of amplified CCs mRNA and blastocyst quality. Three groups of blastocysts (good, intermediary, or bad quality) were obtained from top and good 8-cell embryos at day 3. The Kruskal-Wallis test was used to indicate that at least one of the groups is different from the others ($P = 0.011$, Kruskal-Wallis test), and the Wilcoxon test was used to establish whether group AA-AB is significantly different from group BB and/or group CC. * A significant difference in the concentration of amplified CC mRNA between two groups of blastocysts. CC samples ($n = 17$) were from oocytes that developed in top and good 8-cell embryos at day 3. AA-AB: good blastocyst grades ($n = 7$); BB: intermediary blastocyst grades ($n = 6$); CC and others: bad blastocyst grades ($n = 4$). Bars represent the mean ± SEM.

to contribute to CCs expansion and therefore to the final maturation of oocytes [52]. The gene *OSBPL6* codes for the oxysterol binding protein-like-6 receptor. Oxysterols, which bind to this receptor, are potent modulators of expression of cholesterol synthesis in human granulosa cells [53]. Recently, Watanabe et al. [54] reported that variation in cholesterol contents in cumulus-oocyte complexes during *in vitro* maturation of porcine oocytes affected their ability to be fertilized, suggesting that, under rFSH regime, cholesterogenesis at a nearby site of oocyte growth and maturation might also be involved in *in vitro* blastocyst outcome.

On the other hand, we also identified CC genes associated with day 3 embryo quality and blastocyst grading at day 5, independently of the type of gonadotropins. Among these genes, we report for the first time the expression of *STC2*, *GSTM2*, and *TRIM65*, as well as *PTX3* which has been shown in previous studies to either be associated with fertilization rate [55] or to have no relationship with high-quality embryo on day 3 [51]. A possible reason for higher stanniocalcin 2 (*STC2*) expression in the CCs isolated from MII oocytes that developed into top/good day 3 is the modulation of the angiogenic [56] or steroidogentic pathways [57] or principal processes in ovarian function [58–60]. Conversely, we observed an increased expression of *GSTM2* and *TRIM65* in CCs from oocytes that developed into bad blastocyst grading. *GSTM2* and *TRIM65* play a role in the protection against lipid peroxidation [61] and in DNA repair [62] respectively, suggesting an increase in cellular resistance against oxidative stress and damaged DNA. The implications of these genes, at the CC level, deserve to be addressed in future studies in order to understand their function in follicular growth.

Furthermore, independently of the type of gonadotropin treatment, we found an association between blastocyst grading at day 5 and the amount of amplified mRNA in CC samples from MII mature oocytes with comparable top/good embryo quality at day 3. Lower mRNA values were detected in CCs from MII oocytes that developed into bad blastocysts as compared to CC samples from oocytes that developed into intermediary or good quality blastocysts at day 5. This suggests that CCs surrounding an incompetent oocyte are less transcriptionally active.

These results are in line with our previously published data showing a general reduction in transcriptomic activity of CCs associated with poor oocyte competence and negative clinical outcome [6].

5. Conclusion

Analysis of the microarray data of CCs from patients, who underwent GnRH-antagonist COS, highlights a significant difference in the gene expression profile of CCs following treatment with HP-hMG or rFSH. Components of signaling pathways (the *EGF*, *IGF*, *FGF*, and *PDGF* cascades) were conserved in CCs under the two gonadotropin stimulation regimens. Some genes specific to each gonadotropin treatment or commonly expressed in both groups were associated with *in vitro* embryo development. Moreover, independently of the gonadotropin preparation used, the amount of amplified mRNA in each CC was associated with blastocyst grading at day 5. These genes may prove valuable as biomarkers of *in vitro* embryo quality and can be useful for understanding the biology of stimulation.

Acknowledgments

This work was supported by Ferring Pharmaceuticals A/S. The authors thank the direction of the Montpellier 1 University, University Hospital of Montpellier for their support, and

Dr. Aït-ahmed Ounissa for the insightful discussions and the critical review of the paper.

References

[1] G. H. Trew, A. P. Brown, S. Gillard et al., "In vitro fertilisation with recombinant follicle stimulating hormone requires less IU usage compared with highly purified human menopausal gonadotrophin: results from a European retrospective observational chart review," *Reproductive Biology and Endocrinology*, vol. 8, article 137, 2010.

[2] M. van Wely, I. Kwan, A. L. Burt et al., "Recombinant versus urinary gonadotrophin for ovarian stimulation in assisted reproductive technology cycles. A cochrane review," *Human Reproduction Update*, vol. 18, no. 2, p. 111, 2012.

[3] M. van Wely, I. Kwan, A. L. Burt et al., "Recombinant versus urinary gonadotrophin for ovarian stimulation in assisted reproductive technology cycles," *Cochrane Database of Systematic Reviews*, no. 2, Article ID CD005354, 2011.

[4] K. J. Hutt and D. F. Albertini, "An oocentric view of folliculogenesis and embryogenesis," *Reproductive BioMedicine Online*, vol. 14, no. 6, pp. 758–764, 2007.

[5] D. F. Albertini, C. M. H. Combelles, E. Benecchi, and M. J. Carabatsos, "Cellular basis for paracrine regulation of ovarian follicle development," *Reproduction*, vol. 121, no. 5, pp. 647–653, 2001.

[6] S. Assou, D. Haouzi, K. Mahmoud et al., "A non-invasive test for assessing embryo potential by gene expression profiles of human cumulus cells: a proof of concept study," *Molecular Human Reproduction*, vol. 14, no. 12, pp. 711–719, 2008.

[7] L. J. McKenzie, S. A. Pangas, S. A. Carson et al., "Human cumulus granulosa cell gene expression: a predictor of fertilization and embryo selection in women undergoing IVF," *Human Reproduction*, vol. 19, no. 12, pp. 2869–2874, 2004.

[8] A. P. A. van Montfoort, J. P. M. Geraedts, J. C. M. Dumoulin, A. P. M. Stassen, J. L. H. Evers, and T. A. Y. Ayoubi, "Differential gene expression in cumulus cells as a prognostic indicator of embryo viability: a microarray analysis," *Molecular Human Reproduction*, vol. 14, no. 3, pp. 157–168, 2008.

[9] K. M. Gebhardt, D. K. Feil, K. R. Dunning, M. Lane, and D. L. Russell, "Human cumulus cell gene expression as a biomarker of pregnancy outcome after single embryo transfer," *Fertility and Sterility*, vol. 96, no. 1, pp. 47.e2–52.e2, 2011.

[10] M. Hamel, I. Dufort, C. Robert et al., "Identification of differentially expressed markers in human follicular cells associated with competent oocytes," *Human Reproduction*, vol. 23, no. 5, pp. 1118–1127, 2008.

[11] S. Assou, I. Boumela, D. Haouzi et al., "Dynamic changes in gene expression during human early embryo development: from fundamental aspects to clinical applications," *Human Reproduction Update*, vol. 17, no. 2, pp. 272–290, 2011.

[12] R. A. Anderson, R. Sciorio, H. Kinnell et al., "Cumulus gene expression as a predictor of human oocyte fertilisation, embryo development and competence to establish a pregnancy," *Reproduction*, vol. 138, no. 4, pp. 629–637, 2009.

[13] T. Adriaenssens, S. Wathlet, I. Segers et al., "Cumulus cell gene expression is associated with oocyte developmental quality and influenced by patient and treatment characteristics," *Human Reproduction*, vol. 25, no. 5, pp. 1259–1270, 2010.

[14] Z. G. Ouandaogo, D. Haouzi, S. Assou et al., "Human cumulus cells molecular signature in relation to oocyte nuclear maturity stage," *PLoS One*, vol. 6, no. 11, Article ID e27179, 2011.

[15] S. Assou, T. Anahory, V. Pantesco et al., "The human cumulus-oocyte complex gene-expression profile," *Human Reproduction*, vol. 21, no. 7, pp. 1705–1719, 2006.

[16] E. Fragouli, D. Wells, A. E. Iager, U. A. Kayisli, and P. Patrizio, "Alteration of gene expression in human cumulus cells as a potential indicator of oocyte aneuploidy," *Human Reproduction*, vol. 27, pp. 2559–2568, 2012.

[17] S. Assou, D. Haouzi, J. de Vos, and S. Hamamah, "Human cumulus cells as biomarkers for embryo and pregnancy outcomes," *Molecular Human Reproduction*, vol. 16, no. 8, pp. 531–538, 2010.

[18] J. Balasch, J. Peñarrubia, F. Fábregues et al., "Ovarian responses to recombinant FSH or HMG in normogonadotrophic women following pituitary desensitization by a depot GnRH agonist for assisted reproduction," *Reproductive BioMedicine Online*, vol. 7, no. 1, pp. 35–42, 2003.

[19] Z. Kilani, A. Dakkak, S. Ghunaim et al., "A prospective, randomized, controlled trial comparing highly purified hMG with recombinant FSH in women undergoing ICSI: ovarian response and clinical outcomes," *Human Reproduction*, vol. 18, no. 6, pp. 1194–1199, 2003.

[20] P. Platteau, A. N. Andersen, A. Balen et al., "Similar ovulation rates, but different follicular development with highly purified menotrophin compared with recombinant FSH in WHO Group II anovulatory infertility: a randomized controlled study," *Human Reproduction*, vol. 21, no. 7, pp. 1798–1804, 2006.

[21] S. Daya, "Updated meta-analysis of recombinant follicle-stimulating hormone (FSH) versus urinary FSH for ovarian stimulation in assisted reproduction," *Fertility and Sterility*, vol. 77, no. 4, pp. 711–714, 2002.

[22] A. Coomarasamy, M. Afnan, D. Cheema, F. van der Veen, P. M. M. Bossuyt, and M. van Wely, "Urinary hMG versus recombinant FSH for controlled ovarian hyperstimulation following an agonist long down-regulation protocol in IVF or ICSI treatment: a systematic review and meta-analysis," *Human Reproduction*, vol. 23, no. 2, pp. 310–315, 2008.

[23] S. Ziebe, K. Lundin, R. Janssens, L. Helmgaard, and J.-C. Arce, "Influence of ovarian stimulation with HP-hMG or recombinant FSH on embryo quality parameters in patients undergoing IVF," *Human Reproduction*, vol. 22, no. 9, pp. 2404–2413, 2007.

[24] M. L. Grøndahl, R. Borup, Y. B. Lee, V. Myrhøj, H. Meinertz, and S. Sørensen, "Differences in gene expression of granulosa cells from women undergoing controlled ovarian hyperstimulation with either recombinant follicle-stimulating hormone or highly purified human menopausal gonadotropin," *Fertility and Sterility*, vol. 91, no. 5, pp. 1820–1830, 2009.

[25] J. Brannian, K. Eyster, B. A. Mueller, M. G. Bietz, and K. Hansen, "Differential gene expression in human granulosa cells from recombinant FSH versus human menopausal gonadotropin ovarian stimulation protocols," *Reproductive Biology and Endocrinology*, vol. 8, article 25, 2010.

[26] P. Devroey, A. Pellicer, A. Nyboe Andersen, and J.-C. Arce, "A randomized assessor-blind trial comparing highly purified hMG and recombinant FSH in a GnRH antagonist cycle with compulsory single-blastocyst transfer," *Fertility and Sterility*, vol. 97, no. 3, pp. 561–571, 2012.

[27] D. K. Gardner and W. B. Schoolcraft, "Culture and transfer of human blastocysts," *Current Opinion in Obstetrics and Gynecology*, vol. 11, no. 3, pp. 307–311, 1999.

[28] D. K. Gardner, W. B. Schoolcraft, L. Wagley, T. Schlenker, J. Stevens, and J. Hesla, "A prospective randomized trial of blastocyst culture and transfer in in-vitro fertilization," *Human Reproduction*, vol. 13, no. 12, pp. 3434–3440, 1998.

[29] M. B. Eisen, P. T. Spellman, P. O. Brown, and D. Botstein, "Cluster analysis and display of genome-wide expression patterns," *Proceedings of the National Academy of Sciences of the United States of America*, vol. 95, no. 25, pp. 14863–14868, 1998.

[30] S. Assou, I. Boumela, D. Haouzi et al., "Transcriptome analysis during human trophectoderm specification suggests new roles of metabolic and epigenetic genes," *PLoS One*, vol. 7, no. 6, Article ID e39306, 2012.

[31] B. L. Dozier, K. Watanabe, and D. M. Duffy, "Two pathways for prostaglandin F2α synthesis by the primate periovulatory follicle," *Reproduction*, vol. 136, no. 1, pp. 53–63, 2008.

[32] A. Regassa, F. Rings, M. Hoelker et al., "Transcriptome dynamics and molecular cross-talk between bovine oocyte and its companion cumulus cells," *BMC Genomics*, vol. 12, article no. 57, 2011.

[33] D. Szöllösi, "On the role of gap junctions between follicle cells and oocyte in the mammalian ovarian follicle," *Research Communications in Chemical Pathology and Pharmacology*, vol. 10, no. 2, pp. 3–4, 1978.

[34] K. R. Dunning, K. Cashman, D. L. Russell, J. G. Thompson, R. J. Norman, and R. L. Robker, "Beta-oxidation is essential for mouse oocyte developmental competence and early embryo development," *Biology of Reproduction*, vol. 83, no. 6, pp. 909–918, 2010.

[35] T. G. McEvoy, G. D. Coull, P. J. Broadbent, J. S. M. Hutchinson, and B. K. Speake, "Fatty acid composition of lipids in immature cattle, pig and sheep oocytes with intact zona pellucida," *Journal of Reproduction and Fertility*, vol. 118, no. 1, pp. 163–170, 2000.

[36] D. L. Russell and R. L. Robker, "Molecular mechanisms of ovulation: co-ordination through the cumulus complex," *Human Reproduction Update*, vol. 13, no. 3, pp. 289–312, 2007.

[37] C. Fülöp, S. Szántó, D. Mukhopadhyay et al., "Impaired cumulus mucification and female sterility in tumor necrosis factor-induced protein-6 deficient mice," *Development*, vol. 130, no. 10, pp. 2253–2261, 2003.

[38] H. J. Song, E. J. Kang, G. H. Maeng et al., "Influence of epidermal growth factor supplementation during in vitro maturation on nuclear status and gene expression of canine oocytes," *Research in Veterinary Science*, vol. 91, no. 3, pp. 439–445, 2011.

[39] M. Assidi, S. J. Dieleman, and M.-A. Sirard, "Cumulus cell gene expression following the LH surge in bovine preovulatory follicles: potential early markers of oocyte competence," *Reproduction*, vol. 140, no. 6, pp. 835–852, 2010.

[40] Y. Shimada, Y.-T. Li, and S.-C. Li, "Effect of GM2 activator protein on the enzymatic hydrolysis of phospholipids and sphingomyelin," *Journal of Lipid Research*, vol. 44, no. 2, pp. 342–348, 2003.

[41] G. F. Erickson, V. G. Garzo, and D. A. Magoffin, "Insulin-like growth factor-I regulates aromatase activity in human granulosa and granulosa luteal cells," *Journal of Clinical Endocrinology and Metabolism*, vol. 69, no. 4, pp. 716–724, 1989.

[42] C. I. Friedman, D. B. Seifer, E. A. Kennard, L. Arbogast, B. Alak, and D. R. Danforth, "Elevated level of follicular fluid vascular endothelial growth factor is a marker of diminished pregnancy potential," *Fertility and Sterility*, vol. 70, no. 5, pp. 836–839, 1998.

[43] J.-Y. Park, Y.-Q. Su, M. Ariga, E. Law, S.-L. C. Jin, and M. Conti, "EGF-like growth factors as mediators of LH action in the ovulatory follicle," *Science*, vol. 303, no. 5658, pp. 682–684, 2004.

[44] H. Ashkenazi, X. Cao, S. Motola, M. Popliker, M. Conti, and A. Tsafriri, "Epidermal growth factor family members: endogenous mediators of the ovulatory response," *Endocrinology*, vol. 146, no. 1, pp. 77–84, 2005.

[45] Z. G. Ouandaogo, N. Frydman, L. Hesters et al., "Differences in transcriptomic profiles of human cumulus cells isolated from oocytes at GV, MI and MII stages after in vivo and in vitro oocyte maturation," *Human Reproduction*, vol. 27, pp. 2438–2447, 2012.

[46] R.-C. Chian, A. Ao, H. J. Clarke, T. Tulandi, and S.-L. Tan, "Production of steroids from human cumulus cells treated with different concentrations of gonadotropins during culture in vitro," *Fertility and Sterility*, vol. 71, no. 1, pp. 61–66, 1999.

[47] P. Kempná, M. Körner, B. Waser et al., "Neuropeptide Y modulates steroid production of human adrenal H295R cells through Y1 receptors," *Molecular and Cellular Endocrinology*, vol. 314, no. 1, pp. 101–109, 2010.

[48] A. Barreca, B. Valli, A. Cesarone et al., "Effects of the neuropeptide Y on estradiol and progesterone secretion by human granulosa cells in culture," *Fertility and Sterility*, vol. 70, no. 2, pp. 320–325, 1998.

[49] M. Körner, B. Waser, and J. C. Reubi, "Neuropeptide Y receptor expression in human primary ovarian neoplasms," *Laboratory Investigation*, vol. 84, no. 1, pp. 71–80, 2004.

[50] Y.-J. Yi, E. Nagyova, G. Manandhar et al., "Proteolytic activity of the 26S proteasome is required for the meiotic resumption, germinal vesicle breakdown, and cumulus expansion of porcine cumulus-oocyte complexes matured in vitro," *Biology of Reproduction*, vol. 78, no. 1, pp. 115–126, 2008.

[51] F. Cillo, T. A. L. Brevini, S. Antonini, A. Paffoni, G. Ragni, and F. Gandolfi, "Association between human oocyte developmental competence and expression levels of some cumulus genes," *Reproduction*, vol. 134, no. 5, pp. 645–650, 2007.

[52] S. A. Pangas, C. J. Jorgez, and M. M. Matzuk, "Growth differentiation factor 9 regulates expression of the bone morphogenetic protein antagonist gremlin," *Journal of Biological Chemistry*, vol. 279, no. 31, pp. 32281–32286, 2004.

[53] T. G. Golos and J. F. Strauss III, "8-Bromoadenosine cyclic 3′5′-phosphate rapidly increases 3-hydoxy-3-methylglutaryl coenzyme a reductase mRNA in human granulosa cells: role of cellular sterol balance in controlling the response to tropic stimulation," *Biochemistry*, vol. 27, no. 9, pp. 3503–3506, 1988.

[54] H. Watanabe, S. Hirai, H. Tateno, and Y. Fukui, "Variation of cholesterol contents in porcine cumulus-oocyte complexes is a key factor in regulation of fertilizing capacity," *Theriogenology*, vol. 79, pp. 680–686, 2013.

[55] X. Zhang, N. Jafari, R. B. Barnes, E. Confino, M. Milad, and R. R. Kazer, "Studies of gene expression in human cumulus cells indicate pentraxin 3 as a possible marker for oocyte quality," *Fertility and Sterility*, vol. 83, no. 4, supplement 1, pp. 1169–1179, 2005.

[56] A. Chakraborty, H. Brooks, P. Zhang et al., "Stanniocalcin-1 regulates endothelial gene expression and modulates transendothelial migration of leukocytes," *American Journal of Physiology—Renal Physiology*, vol. 292, no. 2, pp. F895–F904, 2007.

[57] M. Paciga, C. R. McCudden, C. Londos, G. E. DiMattia, and G. F. Wagner, "Targeting of big stanniocalcin and its receptor to lipid storage droplets of ovarian steroidogenic cells," *The Journal of Biological Chemistry*, vol. 278, no. 49, pp. 49549–49554, 2003.

[58] G. Basini, S. Bussolati, S. E. Santini et al., "Antiangiogenesis in swine ovarian follicle: a potential role for 2-methoxyestradiol," *Steroids*, vol. 72, no. 8, pp. 660–665, 2007.

[59] G. Basini, L. Baioni, S. Bussolati et al., "Expression and localization of stanniocalcin 1 in swine ovary," *General and Comparative Endocrinology*, vol. 166, no. 2, pp. 404–408, 2010.

[60] G. Basini, S. Bussolati, S. E. Santini et al., "Hydroxyestrogens inhibit angiogenesis in swine ovarian follicles," *Journal of Endocrinology*, vol. 199, no. 1, pp. 127–135, 2008.

[61] J. Lim and U. Luderer, "Oxidative damage increases and antioxidant gene expression decreases with aging in the mouse ovary," *Biology of Reproduction*, vol. 84, no. 4, pp. 775–782, 2011.

[62] Y. Ziv, D. Bielopolski, Y. Galanty et al., "Chromatin relaxation in response to DNA double-strand breaks is modulated by a novel ATM-and KAP-1 dependent pathway," *Nature Cell Biology*, vol. 8, no. 8, pp. 870–876, 2006.

Hindawi Publishing Corporation
BioMed Research International
Volume 2013, Article ID 731516, 7 pages
http://dx.doi.org/10.1155/2013/731516

Review Article

Aptamers: Novel Molecules as Diagnostic Markers in Bacterial and Viral Infections?

Flávia M. Zimbres,[1] Attila Tárnok,[2] Henning Ulrich,[3] and Carsten Wrenger[1]

[1] *Unit for Drug Discovery, Department of Parasitology, Institute of Biomedical Science, University of São Paulo, Avenida Professor Lineu Prestes 1374, 05508-000 São Paulo, SP, Brazil*
[2] *Department of Pediatric Cardiology, Heart Centre Leipzig, Translational Centre for Regenerative Medicine (TRM), University of Leipzig, Strümpellstraße 39, 04289 Leipzig, Germany*
[3] *Department of Biochemistry, Institute of Chemistry, University of São Paulo, Avenida Professor Lineu Prestes 748, 05508-900 São Paulo, SP, Brazil*

Correspondence should be addressed to Henning Ulrich; henning@iq.usp.br and Carsten Wrenger; cwrenger@icb.usp.br

Received 6 June 2013; Accepted 30 July 2013

Academic Editor: Sudhish Mishra

Worldwide the entire human population is at risk of infectious diseases of which a high degree is caused by pathogenic protozoans, worms, bacteria, and virus infections. Moreover the current medications against pathogenic agents are losing their efficacy due to increasing and even further spreading drug resistance. Therefore, there is an urgent need to discover novel diagnostic as well as therapeutic tools against infectious agents. In view of that, the Systematic Evolution of Ligands by Exponential Enrichment (SELEX) represents a powerful technology to target selectively pathogenic factors as well as entire bacteria or viruses. SELEX uses a large combinatorial oligonucleic acid library (DNA or RNA) which is processed a by high-flux *in vitro* screen of iterative cycles. The selected ligands, termed aptamers, are characterized by high specificity and affinity to their target molecule, which are already exploited in diagnostic and therapeutic applications. In this minireview we will discuss the current status of the SELEX technique applied on bacterial and viral pathogens.

1. Introduction

Due to the continuously rising number of the population as well as the emergence of resistances of human pathogenic organisms against the current treatment, there is an urgent need to develop novel diagnostic and—even further—therapeutic tools to deal with the upcoming problems in the near future. Not only the development of new tools is mandatory but also—and becoming an even more prominent issue—the commercial value in terms of their costs. In this sense the discovery of novel technologies and moreover their subsequent applications have become important in laboratory and field studies. As an example, innovations in high-throughput single cell analysis for diagnostic purposes but also for functional analysis and drug discovery are today available in order to analyze pathogenic organisms such as the viruses Hepatitis C [1], influenza [2], or HIV [3] as well as bacteria like *Mycobacterium tuberculosis* [4] or *Staphylococcus aureus* [5]. The SELEX technique (Systematic Evolution of Ligands by Exponential Enrichment) was originally discovered by Gold and Szostak [6, 7]. They were using reiterative *in vitro* selection for high-affinity oligonucleotide ligands (aptamers) against almost any kind of molecules which is of biological or therapeutic interest (for illustration see Figure 1). RNA and DNA aptamers recognize their targets with high specificity and affinity. These high-affinity ligands can be developed against almost any target through iterative cycles of *in vitro* screening of a combinatorial oligonucleotide library for target binding followed by their PCR amplification. SELEX procedures are characterised by employing random oligonucleotide libraries of up to 10^{12}–10^{15} different nucleic acid molecules, revealing an at least equivalent number of secondary and tertiary structures of their respective single-stranded nucleic acid molecules [8]. After their first round of *in vitro* selection against a chosen target molecule, the

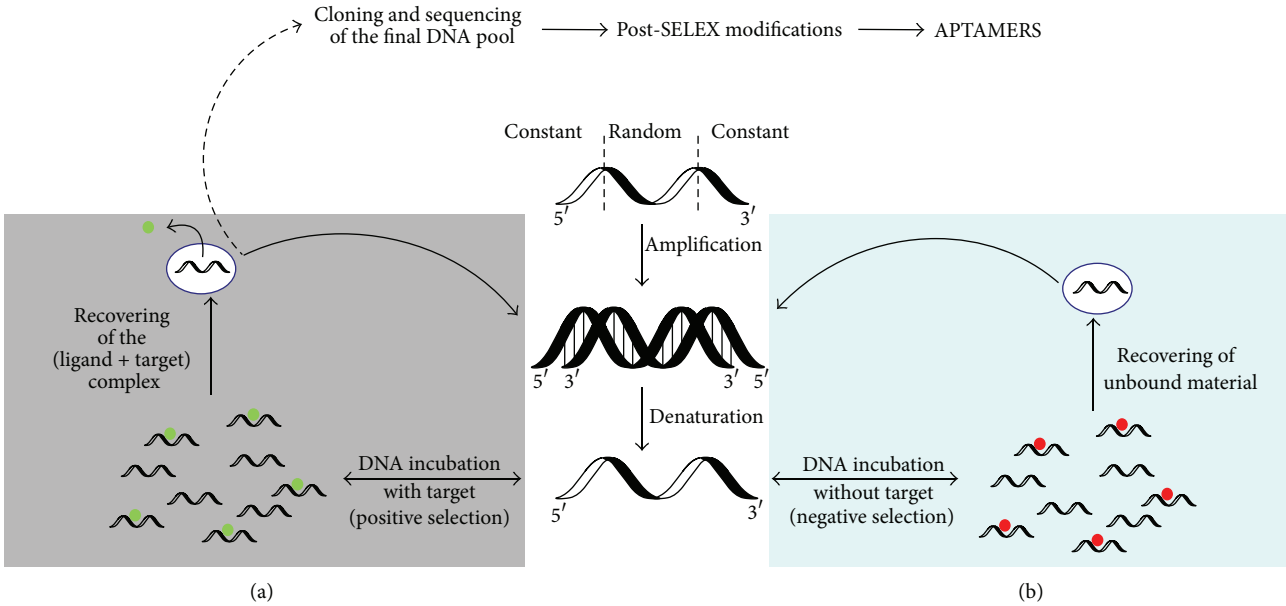

Figure 1: Schematic illustration of the SELEX methodology. The SELEX technique uses a large combinatorial oligonucleic acid library (DNA or RNA) consisting of an inner random region flanked by two constant regions. In the following, attention has solely been drawn on the development of DNA aptamers. The DNA library consisting of partially randomised DNA sequences (inner random region flanked on both sites by constant sequences) is amplified by conventional PCR. The derived double-stranded DNA is denatured and separated into single-stranded DNA by gel electrophoresis, the single-stranded DNA isolated and subsequently incubated with the respective target molecules ((a), positive selection). After incubation step, the formed target-aptamer-complex is separated from nonbinding aptamers and applied to PCR for amplification of the target-bound aptamers (grey panel). Eventually, (b) negatives cycles (blue panel) are also carried out to remove aptamers which bind unspecifically or not to the desired target molecules. As a resulting consequence, the unbound aptamers are recovered, amplified via PCR, and applied in the next (positive) selection cycle. Subsequently, from final selected library aptamer sequences are identified and aligned for the verification of consensus sequence motifs. If required post-SELEX modifications such as truncations, stabilizations, and covalent attachment of fluorescence reporters can be applied to optimize aptamers for any desired purpose.

eluted aptamers are amplified by PCR procedures to restore the DNA library for the next SELEX cycle. The number of cycles depends mainly on the affinity of the aptamer-target interactions as well as on the stringency imposed to each round of selection. After several rounds of iterative SELEX cycles, the aptamers are selected via their target molecules (positive selection step) (Figure 1). In case of not using highly pure target molecules, the library needs to be exposed to different or contaminating molecules for counterselection in order to discard these molecules (negative selection step) (Figure 1). Subsequently, the final selected library of high affinity aptamers are cloned and sequenced to identify respective consensus motifs, which are responsible for the secondary/tertiary structures interacting with the target molecule [9]. These structures comprise a variety of different conformations which include—among others—stem-loop structures. Comparisons between DNA or RNA stem-loops suggest that the structure of the DNA molecules can be slightly less stable. On the other hand—due the lacking ribose 2′-hydroxyl group—DNA is characterised by a greater flexibility and, consequently, leading to a higher diversity of structural conformations [10]. In contrast to DNA aptamers, RNA aptamers require reverse transcription prior amplification by PCR and in terms of their stability they might need modifications such as substitution of the 2′-OH group of ribose by 2′-amino, 2′-fluoride, or O-methylene functions, to prolong their half-life in biological fluids [11, 12]. Unlike RNA aptamers which are obliged to modifications in order to prevent RNAse accessibility, DNA aptamers do not need any modifications for their stability in various applications. Moreover, the latter one can be easily modified for the attachment of reporter molecules such as fluorescence dyes or biotin [13]. Those biotinylated aptamers can subsequently be applied in pull-down experiments using streptavidin-coated magnetic beads [14, 15] or to visualise targets using fluorescent reporters [16]. The binding properties of an aptamer are dictated by its sequence and the deriving folding into stem-loop structures (Figure 2) [13, 17]. Aptamer-target complexes often reveal low dissociation constants that range from nanomolar to picomolar levels [9, 18], which is comparable to those of monoclonal antibodies.

Moreover, aptamers are capable of distinguishing between protein isoforms [19] as well as different conformational forms of the same protein [20]. Furthermore, aptamers can be denatured and renatured by changing the temperature. Additionally they are generated by an iterative *in vitro* instead of an *in vivo* process as it is the case for animal-derived antibodies [16].

In the near future oligonucleotide-based high-affinity aptamers are expected to substitute antibodies in many applications, mostly due to their stability, nonpeptide character, and their independency from animal resources. Moreover, the beneficial characteristics of aptamers have already been

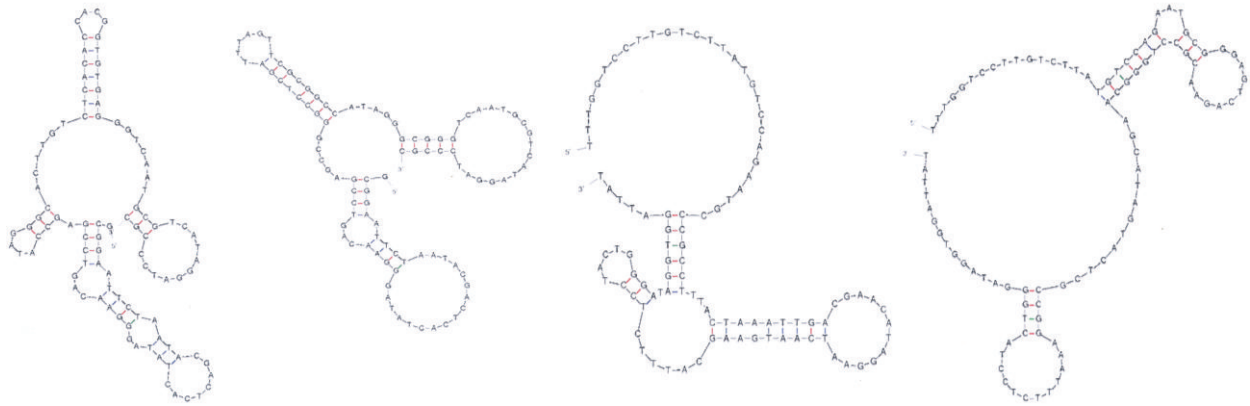

(a) (b)

Figure 2: Predicted folding of selected single-stranded DNA aptamers. Stem-loop structures of aptamers play a fundamental role in target molecule binding. Respective consensus sequences of aptamers binding to (a) Hepatitis C virus (HCV) E2 glycoprotein on the cell surface [24] and (b) S. Typhimurium outer membrane proteins (OMPs) [25] were analyzed using the MFold programme [26] for secondary structure predictions.

exploited in the fight against infectious diseases as outlined below.

2. Overview of Aptamer Applications in Human Infection Diseases

Infectious diseases affect almost the entire mankind as well as animals. Furthermore, increasing levels of pathogen resistance against available drugs aggravate the state of health worldwide, particularly in developing countries, where infectious diseases are responsible for a high level of mortality and morbidity [21]. Moreover, the continuously growing population combined with the ongoing drug resistance forces scientific research to discover novel diagnostic tools as well as chemotherapeutics to deal with the future problems caused by pathogenic agents. Here, we will focus on the status of SELEX applications for combating bacterial and viral human infections.

3. Aptamers and Bacterial Infections

Tuberculosis, along with malaria and HIV, is a major public health problem affecting millions of people worldwide. Currently, only one vaccine against tuberculosis is existing which is the attenuated strain of *Mycobacterium bovis* "BCG—bacillus Calmette-Guėrin"; however, the vaccine has only limited efficacy in tuberculosis-endemic regions [22]. In 2007 Chen et al. [23] isolated an aptamer entitled NK2 with high affinity and specificity against membrane proteins that are present on the surface of the virulent *M. tuberculosis* stain H37Rv while not existing on BCG. Furthermore, the binding of the NK2 aptamer to H37Rv led CD4+ T cells to produce an increased level of IFN-γ, which is known to be a protective cytokine against *M. tuberculosis* infections. Analysis of the spleen of mice treated with the NK2 aptamer showed a lower bacterial number as the control [23]. These results underline the potency of the NK2 aptamer as an antimycobacterial agent (Table 1).

Another common bacterial infection is caused by Salmonellae which are significantly involved in food-borne illness. About 25% of all food-borne diarrhoea patients need hospitalisation. A major problem is salmonellosis caused by multidrug-resistant (MDR) strains such as *Salmonella enterica* serovar Typhimurium DT104 or *S. enterica* serovar Newport [27]. Salmonellae are also important bacterial pathogens in food animal species including cows [28], pigs [29], chickens [30], and turkeys [31]. In order to evaluate the potential of aptamers against *S. enterica* serovar Typhimurium multidrug-resistant (MDR) strains, the SELEX method using DNA aptamers was applied to the bacterial outer membrane proteins (OMPs) by performing counter-selection against *Escherichia coli* OMPs and lipopolysaccharides (LPS) (negative selection step). Subsequently aptamers were identified which selectively interact only with the bacterial OMPs [25] (Table 1).

It is known that the invasion of IVB piliated *S. enterica* serovar Typhimurium A21-6 into human THP-1 monocytic cells reveals higher efficacy than that of a nonpiliated *S. enterica* serovar Typhimurium mutant strain. Consequently, approaches have been undertaken to interfere with the formation and accessibility of the type IVB pili. Thus, the SELEX technique was applied and single-stranded RNA aptamers were discovered that selectively bind to the pili and thereby hamper the infection of human THP-1 cells [32]. Analysis of the consensus sequence identified a stem-loop structure, which might be the possible binding site of the aptamer [32]. In summary, these RNA aptamers are considered as a novel agent for blocking bacterial pathogenesis (Table 1).

Bacteria such as *S. aureus* or *E. coli* are naturally present in humans. For example, *S. aureus* colonises permanently about 20% of healthy adults and up to 50% transiently. Its pathogenicity plays an important role in nosocomial infections affecting immunosuppressed patients. This pathogenic agent is responsible for a wide spectrum of diseases, which

Table 1: Summary of aptamers against bacterial and viral human pathogens.

Aptamers	Type of aptamer	Organism	Target	Reference
NK2	DNA aptamer	*Mycobacterium tuberculosis* (strain H37Rv)	Membrane proteins	[23]
33	DNA aptamer	*Salmonella enterica* serovar Typhimurium	Outer membrane proteins (OMPs)	[25]
S-PS8.4	RNA aptamer	*Salmonella enterica* serovar Typhimurium	Type IVB pili	[32]
SA20, SA23, SA31, SA34 and SA43	DNA aptamer	*Staphylococcus aureus* (strain MRSA)	Whole bacteria	[33]
ZE2	DNA aptamer	Hepatitis C virus	HCV envelope surface glycoprotein E2	[24]
Sequence (1), aptamer sequence (2), and aptamer sequence (3)	DNA aptamer	Avian influenza virus H5N1	Hemagglutinin	[34]
FO21 and FO24	DNA aptamer	Rabies virus (RABV)	RABV-infected BHK-21 cells	[35]
A-1 and Ch A-1	RNA aptamer	Human immunodeficiency virus type 1 (HIV-1)	gp120	[36]
RT1t49	DNA aptamer	Human immunodeficiency virus type 1 (HIV-1)	Viral reverse transcriptase	[37]
70.5, 70.8, 80.55, 80.93 and T1.1	RNA aptamer			[38]
TPK isolates, TPK-like isolates and non-TPK isolates	RNA aptamer			[39]
70.8, 13, 70.15, 80.55, 65, 70.28, 70.28t34 and 1.1	RNA aptamer			[40]
1.1 and 1.3a	RNA aptamer			[41]

includes life-threatening conditions like pneumonia or endocarditis [42], and emerges as a major human pathogen due to methicillin-resistant *S. aureus* (MRSA) strains. These bacteria are known to produce potent protein toxins and to express cell-surface proteins that can bind to antibodies and thereby inactivate their function [43]. It is well established that bacteria can express different sets of molecules to precisely control their proliferation at different growth states [44, 45]. They can even undergo antigenic variations to escape the immune response of its host [46, 47]. In order to deal with these bacterial mechanisms, a whole set of specific markers have been developed by Cao and coworkers [33]. They obtained a panel of single-stranded DNA aptamers with high specificity and sensitivity against *S. aureus*. The derived aptamers were grouped into different families on the basis of sequence homology as well as similarity in their predicted secondary structure. Subsequently five aptamers were identified that recognised different molecular targets, and a combination of them had a much better effect than the application of individual aptamers in detecting different *S. aureus* strains. These results clearly demonstrate that a set of aptamers specific to one bacterium can be used as a highly selective diagnostic tool or even potentially to block the growth cycle of the pathogen [33].

4. Aptamers in Viral Infections

Hepatitis C is an infectious disease caused by the hepatitis C virus (HCV), which has infected about 3% of the world's population and induces in 80% of the infected people dysfunction of the liver, like cirrhosis. Presently, there is no efficient vaccine available, and the treatment of the infectious disease relies on the use of alpha interferon (IFN-α) alone or in combination with ribavirin [48–50]. However, the rate of success is limited, and such treatments are expensive and bear the risk of serious side effects [48, 49, 51]. In order to discover new modes of detection and selective interference with the proliferation of the virus, the alive Cell Surface-Systematic Evolution of Ligands by Exponential Enrichment (CS-SELEX) technique has been developed and subsequently used for selection of single-stranded DNA aptamers directed to the HCV envelope surface glycoprotein E2 [24]. A single-stranded DNA aptamer that specifically binds to the HCV-E2 envelope glycoprotein was named ZE2. It is believed that the ZE2 aptamer competitively inhibits the HCV-E2 envelope glycoprotein by binding to CD81, an important HCV receptor, and significantly blocks HCV cell culture infection of human hepatocytes. Thereby, the ZE2 aptamer emphasizes its potency to act as a possible novel diagnostic and therapeutic candidate in HCV infections.

Avian influenza virus (AIV) H5N1, also known as "bird flu," is a type A influenza virus, responsible for major epidemics and pandemics. Therefore attention has been drawn—besides the use of other therapeutic tools—on the selection of aptamers against the H5N1 virus. Wang et al. [34] started with a single-stranded DNA library and performed the first rounds of selection cycles using purified hemagglutinin (HA) from AIV H5N1, and afterwards the

entire H5N1 virus was used as a target. After various SELEX rounds of positive target selection and clearance of selected pools of oligonucleotides binding to nontarget AIV subtypes (H5N2, H5N3, H5N9, H7N2, H2N2, and H9N2), aptamers were cloned and sequenced. The found consensus sequences were analysed for predicted secondary structures, which led to the identification of hairpin loops and bulge loops that are suggested to play an important role in target binding. By using surface plasmon resonance, one aptamer was identified possessing a high binding capability with a dissociation constant of less than 5 nM to the H5N1 virus.

Rabies is a zoonotic disease, which is caused by the rabies virus (RABV), and is transmitted through exposure to infected saliva during either a bite or direct contact with mucosal tissues. Infection with this virus results in an acute fatal encephalitis, leading to coma and death. This disease affects many warm-blooded mammals. Currently, no approved therapy is available once the clinical signs have appeared. By being a fatal disease in all instances, there is a strong incentive to develop a cheap and effective drug. In this sense aptamers were selected against RABV-infected cells using the Cell-SELEX technique [35]. These aptamers were subsequently applied to viral titre assays, which clearly demonstrated an inhibition of RABV-infected cell, while an inhibition of the canine distemper virus or canine parvovirus was not observed. Furthermore, in *in vivo* tests aptamers could protect mice to a certain extent from RABV infection. Interestingly, the selected aptamers were of protective nature because when mice were inoculated with aptamers before inoculation with CVS-11, only about 15% of the animals died, whereas almost no mice survived when aptamers were used for treatment [35].

Such as other pathogens, HIV is also characterised by the appearance of drug-resistant viruses. About 30 years ago, it was discovered that HIV contains several small RNA sequences or regions which can specifically bind to viral or cellular proteins with high affinity. Functional studies indicated that these viral RNA-protein complexes could be exploited in therapeutic approaches as demonstrated for small HIV RNA regions, termed TAR, that could be used to inhibit HIV virus replication in cellular models [52]. The envelope glycoprotein gp120 of the HIV-1 virus plays a fundamental role during infection of CD4-positive cells. Cell fusion is initiated by the interaction between gp120 and CD4 (Table 1). In view of this mechanism, RNA aptamers were generated, which bind selectively to the gp120 glycoprotein [53, 54]. In a humanized mouse model where HIV-1 replication and T-cell depletion mimic the human situation, Neff and colleagues [36] found that the anti-gp120 aptamer suppressed HIV-1 replication and prevented thereby the viral-mediated T-cell reduction.

The SELEX technique was also applied to the viral reverse transcriptase, which is essential for replication, and thereby RNA and DNA aptamers were identified that bound to multiple epitopes of the viral reverse transcriptase with high affinity and specificity [37, 38, 55]. Among those aptamers, pseudoknot RNAs have received attention which bind to the HIV-1 reverse transcriptase at a nanomolar level [39–41], abolish its catalytic activity [38], and inhibit HIV replication in cell culture [40, 56, 57]. These results clearly emphasize that aptamers binding to the HIV-1 reverse transcriptase are promising novel tools to be used in therapeutic interventions.

5. Conclusion

As outlined above bacterial and viral infection diseases are a major threat to humans. Considering that the current therapeutics are losing their efficacy, there is an urgent need to discover and develop novel medication and rapid diagnostic to deal with these diseases. In this sense the SELEX technology by using aptamers provides a powerful tool not only to identify novel diagnostic markers but also to interfere with the proliferation of these human pathogens [16]. The aptamer technique is already subject to a variety of clinical trials in human-related diseases [58]. A VEGF165-binding aptamer, Macugen, was recently commercialised as an antiangiogenic therapeutic agent for neovascular age-related macular eye disease [59, 60]. Macugen has been a breakthrough in the therapeutic use of aptamers and encourages the development of further aptamers against infectious disease targets as outlined in this minireview and summarized in Table 1.

Acknowledgments

This work was financially supported by the Grants 2009/54325-2, 2010/20647-0, and 2011/19703-6 as well as the German-Brazilian Network project (Grant 2012/50393-6) of the Fundação de Amparo à Pesquisa do Estado de São Paulo (FAPESP) and the German Federal Ministry of Education and Research (BMBF, PtJ-Bio, 1315883).

References

[1] G. Shi, F. Yagyu, Y. Shimizu et al., "Flow cytometric assay using two fluorescent proteins for the function of the internal ribosome entry site of hepatitis C virus," *Cytometry Part A*, vol. 79, no. 8, pp. 653–660, 2011.

[2] F. Gondois-Rey, S. Granjeaud, S. L. T. Kieu, D. Herrera, I. Hirsch, and D. Olive, "Multiparametric cytometry for exploration of complex cellular dynamics," *Cytometry Part A*, vol. 81, no. 4, pp. 332–342, 2012.

[3] J. Pollara, L. Hart, F. Brewer et al., "High-throughput quantitative analysis of HIV-1 and SIV-specific ADCC-mediating antibody responses," *Cytometry Part A*, vol. 79, no. 8, pp. 603–612, 2011.

[4] J. M. Mateos-Pérez, R. Redondo, R. Nava et al., "Comparative evaluation of autofocus algorithms for a real-time system for automatic detection of Mycobacterium tuberculosis," *Cytometry Part A*, vol. 81, no. 3, pp. 213–221, 2012.

[5] M. Ruger, G. Bensch, R. Tungler, and U. Reichl, "A flow cytometric method for viability assessment of *Staphylococcus aureus* and Burkholderia cepacia in mixed culture," *Cytometry Part A*, vol. 81, pp. 1055–1066, 2012.

[6] A. D. Ellington and J. W. Szostak, "In vitro selection of RNA molecules that bind specific ligands," *Nature*, vol. 346, no. 6287, pp. 818–822, 1990.

[7] C. Tuerk and L. Gold, "Systemic evolution of ligands by exponential enrichment: RNA ligands to bacteriophage T4 DNA polymerase," *Science*, vol. 249, no. 4968, pp. 505–510, 1990.

[8] H. Ulrich, A. H. B. Martins, and J. B. Pesquero, "RNA and DNA aptamers in cytomics analysis," *Current Protocols in Cytometry*, vol. 7, pp. 1–39, 2005.

[9] H. Ulrich, A. H. B. Martins, and J. B. Pesquero, "RNA and DNA aptamers in cytomics analysis," *Cytometry Part A*, vol. 59, no. 2, pp. 220–231, 2004.

[10] K. Harada and A. D. Frankel, "Identification of two novel arginine binding DNAs," *The EMBO Journal*, vol. 14, no. 23, pp. 5798–5811, 1995.

[11] A. S. Davydova, M. A. Vorobjeva, and A. G. Venyaminova, "Escort aptamers: new tools for the targeted delivery of therapeutics into cells," *Acta Naturae*, vol. 3, pp. 12–29, 2011.

[12] E. W. M. Ng, D. T. Shima, P. Calias, E. T. Cunningham Jr., D. R. Guyer, and A. P. Adamis, "Pegaptanib, a targeted anti-VEGF aptamer for ocular vascular disease," *Nature Reviews Drug Discovery*, vol. 5, no. 2, pp. 123–132, 2006.

[13] A. A. Nery, C. Wrenger, and H. Ulrich, "Recognition of biomarkers and cell-specific molecular signatures: aptamers as capture agents," *Journal of Separation Science*, vol. 32, no. 10, pp. 1523–1530, 2009.

[14] M. B. Murphy, S. T. Fuller, P. M. Richardson, and S. A. Doyle, "An improved method for the in vitro evolution of aptamers and applications in protein detection and purification," *Nucleic Acids Research*, vol. 31, no. 18, p. e110, 2003.

[15] J.-N. Rybak, S. B. Scheurer, D. Neri, and G. Elia, "Purification of biotinylated proteins on streptavidin resin: a protocol for quantitative elution," *Proteomics*, vol. 4, no. 8, pp. 2296–2299, 2004.

[16] H. Ulrich and C. Wrenger, "Disease-specific biomarker discovery by aptamers," *Cytometry Part A*, vol. 75, no. 9, pp. 727–733, 2009.

[17] M. Famulok, G. Mayer, and M. Blind, "Nucleic acid aptamers—from selection in vitro to applications in vivo," *Accounts of Chemical Research*, vol. 33, no. 9, pp. 591–599, 2000.

[18] S. Tombelli, M. Minunni, and M. Mascini, "Analytical applications of aptamers," *Biosensors and Bioelectronics*, vol. 20, no. 12, pp. 2424–2434, 2005.

[19] R. Conrad and A. D. Ellington, "Detecting immobilized protein kinase C isozymes with RNA aptamers," *Analytical Biochemistry*, vol. 242, no. 2, pp. 261–265, 1996.

[20] S. Sekiya, F. Nishikawa, K. Noda, P. K. Kumar, T. Yokoyama, and S. Nishikawa, "In vitro selection of RNA aptamers against cellular and abnormal isoform of mouse prion protein," *Nucleic Acids Symposium Series*, no. 49, pp. 361–362, 2005.

[21] A. R. Renslo and J. H. McKerrow, "Drug discovery and development for neglected parasitic diseases," *Nature Chemical Biology*, vol. 2, no. 12, pp. 701–710, 2006.

[22] B. Bloom and P. Fine, "The BCG experience: implications for future vaccines against tuberculosis," in *Tuberculosis: Pathogenesis, Protection and Control*, B. R. Bloom, Ed., pp. 531–557, ASM Press, Washington, DC, USA, 1994.

[23] F. Chen, J. Zhou, F. Luo, A.-B. Mohammed, and X.-L. Zhang, "Aptamer from whole-bacterium SELEX as new therapeutic reagent against virulent Mycobacterium tuberculosis," *Biochemical and Biophysical Research Communications*, vol. 357, no. 3, pp. 743–748, 2007.

[24] F. Chen, Y. Hu, D. Li, H. Chen, and X.-L. Zhang, "CS-SELEX generates high-affinity ssDNA aptamers as molecular probes for hepatitis C virus envelope glycoprotein E2," *PLoS ONE*, vol. 4, no. 12, Article ID e8142, 2009.

[25] R. Joshi, H. Janagama, H. P. Dwivedi et al., "Selection, characterization, and application of DNA aptamers for the capture and detection of *Salmonella enterica* serovars," *Molecular and Cellular Probes*, vol. 23, no. 1, pp. 20–28, 2009.

[26] M. Zuker, "Mfold web server for nucleic acid folding and hybridization prediction," *Nucleic Acids Research*, vol. 31, no. 13, pp. 3406–3415, 2003.

[27] A. Gupta, J. Fontana, C. Crowe et al., "Emergence of multidrug-resistant *Salmonella enterica* serotype Newport infections resistant to expanded-spectrum cephalosporins in the United States," *Journal of Infectious Diseases*, vol. 188, no. 11, pp. 1707–1716, 2003.

[28] S. J. Wells, P. J. Fedorka-Cray, D. A. Dargatz, K. Ferris, and A. Green, "Fecal shedding of *Salmonella* spp. by dairy cows on farm and at cull cow markets," *Journal of Food Protection*, vol. 64, no. 1, pp. 3–11, 2001.

[29] B. Malorny and J. Hoorfar, "Toward standardization of diagnostic PCR testing of fecal samples: lessons from the detection of salmonellae in pigs," *Journal of Clinical Microbiology*, vol. 43, no. 7, pp. 3033–3037, 2005.

[30] K. T. Carli, A. Eyigor, and V. Caner, "Prevalence of Salmonella serovars in chickens in Turkey," *Journal of Food Protection*, vol. 64, no. 11, pp. 1832–1835, 2001.

[31] R. Nayak, P. B. Kenney, J. Keswani, and C. Ritz, "Isolation and characterisation of *Salmonella* in a turkey production facility," *British Poultry Science*, vol. 44, no. 2, pp. 192–202, 2003.

[32] Q. Pan, X.-L. Zhang, H.-Y. Wu et al., "Aptamers that preferentially bind type IVB pili and inhibit human monocytic-cell invasion by *Salmonella enterica* serovar typhi," *Antimicrobial Agents and Chemotherapy*, vol. 49, no. 10, pp. 4052–4060, 2005.

[33] X. Cao, S. Li, L. Chen et al., "Combining use of a panel of ssDNA aptamers in the detection of *Staphylococcus aureus*," *Nucleic Acids Research*, vol. 37, no. 14, pp. 4621–4628, 2009.

[34] R. Wang, J. Zhao, T. Jiang et al., "Selection and characterization of DNA aptamers for use in detection of avian influenza virus H5N1," *Journal of Virological Methods*, vol. 189, pp. 362–369, 2013.

[35] H. R. Liang, Q. Liu, X. X. Zheng et al., "Aptamers targeting rabies virus-infected cells inhibit viral replication both in vitro and in vivo," *Virus Research*, vol. 173, no. 2, pp. 398–403, 2013.

[36] C. P. Neff, J. Zhou, L. Remling et al., "An aptamer-siRNA chimera suppresses HIV-1 viral loads and protects from helper $CD4^+$ T cell decline in humanized mice," *Science Translational Medicine*, vol. 3, no. 66, Article ID 66ra6, 2011.

[37] T. S. Fisher, P. Joshi, and V. R. Prasad, "Mutations that confer resistance to template-analog inhibitors of human immunodeficiency virus (HIV) type 1 reverse transcriptase lead to severe defects in HIV replication," *Journal of Virology*, vol. 76, no. 8, pp. 4068–4072, 2002.

[38] D. M. Held, J. D. Kissel, D. Saran, D. Michalowski, and D. H. Burke, "Differential susceptibility of HIV-1 reverse transcriptase to inhibition by RNA aptamers in enzymatic reactions monitoring specific steps during genome replication," *Journal of Biological Chemistry*, vol. 281, no. 35, pp. 25712–25722, 2006.

[39] D. H. Burke, L. Scates, K. Andrews, and L. Gold, "Bent pseudoknots and novel RNA inhibitors of type 1 human immunodeficiency virus (HIV-1) reverse transcriptase," *Journal of Molecular Biology*, vol. 264, no. 4, pp. 650–666, 1996.

[40] P. Joshi and V. R. Prasad, "Potent inhibition of human immunodeficiency virus type 1 replication by template analog reverse transcriptase inhibitors derived by SELEX (systematic evolution

of ligands by exponential enrichment)," *Journal of Virology*, vol. 76, no. 13, pp. 6545–6557, 2002.

[41] C. Tuerk, S. MacDougal, and L. Gold, "RNA pseudoknots that inhibit human immunodeficiency virus type 1 reverse transcriptase," *Proceedings of the National Academy of Sciences of the United States of America*, vol. 89, no. 15, pp. 6988–6992, 1992.

[42] F. D. Lowy, "Medical progress: *Staphylococcus aureus* infections," *The New England Journal of Medicine*, vol. 339, no. 8, pp. 520–532, 1998.

[43] N. M. Qtaishat, H. A. Gussin, and D. R. Pepperberg, "Cysteine-terminated B-domain of *Staphylococcus aureus* protein A as a scaffold for targeting GABA(A) receptors," *Analytical Biochemistry*, vol. 432, pp. 49–57, 2013.

[44] D. Beier and R. Gross, "Regulation of bacterial virulence by two-component systems," *Current Opinion in Microbiology*, vol. 9, no. 2, pp. 143–152, 2006.

[45] S. Bronner, H. Monteil, and G. Prévost, "Regulation of virulence determinants in *Staphylococcus aureus*: complexity and applications," *FEMS Microbiology Reviews*, vol. 28, no. 2, pp. 183–200, 2004.

[46] A. Loughman, T. Sweeney, F. M. Keane, G. Pietrocola, P. Speziale, and T. J. Foster, "Sequence diversity in the A domain of *Staphylococcus aureus* fibronectin-binding protein A," *BMC Microbiology*, vol. 8, article 74, 2008.

[47] M. W. van der Woude and A. J. Bäumler, "Phase and antigenic variation in bacteria," *Clinical Microbiology Reviews*, vol. 17, no. 3, pp. 581–611, 2004.

[48] P. Bellecave and D. Moradpour, "A fresh look at interferon-alpha signaling and treatment outcomes in chronic hepatitis C," *Hepatology*, vol. 48, pp. 1330–1333, 2008.

[49] N. Boyer and P. Marcellin, "Pathogenesis, diagnosis and management of hepatitis C," *Journal of Hepatology*, vol. 32, no. 1, pp. 98–112, 2000.

[50] C. H. Liu, C. J. Liu, C. L. Lin et al., "Pegylated interferon-alpha-2a plus ribavirin for treatment-naive Asian patients with hepatitis C virus genotype 1 infection: a multicenter, randomized controlled trial," *Clinical Infectious Diseases*, vol. 47, pp. 1260–1269, 2008.

[51] M. Sarasin-Filipowicz, E. J. Oakeley, F. H. T. Duong et al., "Interferon signaling and treatment outcome in chronic hepatitis C," *Proceedings of the National Academy of Sciences of the United States of America*, vol. 105, no. 19, pp. 7034–7039, 2008.

[52] B. A. Sullenger, H. F. Gallardo, G. E. Ungers, and E. Gilboa, "Overexpression of TAR sequences renders cells resistant to human immunodeficiency virus replication," *Cell*, vol. 63, no. 3, pp. 601–608, 1990.

[53] A. K. Dey, M. Khati, M. Tang, R. Wyatt, S. M. Lea, and W. James, "An aptamer that neutralizes R5 strains of human immunodeficiency virus type 1 blocks gp120-CCR5 interaction," *Journal of Virology*, vol. 79, no. 21, pp. 13806–13810, 2005.

[54] M. Khati, M. Schüman, J. Ibrahim, Q. Sattentau, S. Gordon, and W. James, "Neutralization of infectivity of diverse R5 clinical isolates of human immunodeficiency virus type 1 by gp120-binding 2′F-RNA aptamers," *Journal of Virology*, vol. 77, no. 23, pp. 12692–12698, 2003.

[55] J. Jaeger, T. Restle, and T. A. Steitz, "The structure of HIV-1 reverse transcriptase complexed with an RNA pseudoknot inhibitor," *The EMBO Journal*, vol. 17, no. 15, pp. 4535–4542, 1998.

[56] L. Chaloin, M. J. Lehmann, G. Sczakiel, and T. Restle, "Endogenous expression of a high-affinity pseudoknot RNA aptamer suppresses replication of HIV-1," *Nucleic Acids Research*, vol. 30, no. 18, pp. 4001–4008, 2002.

[57] M. J. Lange, T. K. Sharma, A. S. Whatley et al., "Robust suppression of HIV replication by intracellularly expressed reverse transcriptase aptamers is independent of ribozyme processing," *Molecular Therapy*, vol. 20, pp. 2304–2314, 2012.

[58] H. Ulrich and C. Wrenger, "Identification of aptamers as specific binders and modulators of cell-surface receptor activity," *Methods in Molecular Biology*, vol. 986, pp. 17–39, 2013.

[59] N. Ferrara, H.-P. Gerber, and J. LeCouter, "The biology of VEGF and its receptors," *Nature Medicine*, vol. 9, no. 6, pp. 669–676, 2003.

[60] J. Ruckman, L. S. Green, J. Beeson et al., "2′-fluoropyrimidine RNA-based aptamers to the 165-amino acid form of vascular endothelial growth factor (VEGF165): inhibition of receptor binding and VEGF-induced vascular permeability through interactions requiring the exon 7-encoded domain," *Journal of Biological Chemistry*, vol. 273, no. 32, pp. 20556–20567, 1998.

Hindawi Publishing Corporation
BioMed Research International
Volume 2013, Article ID 782941, 5 pages
http://dx.doi.org/10.1155/2013/782941

Research Article

Distribution of ABO Blood Group and Major Cardiovascular Risk Factors with Coronary Heart Disease

Santanu Biswas,[1] Pradip K. Ghoshal,[2] Bhubaneswar Halder,[2] and Nripendranath Mandal[1]

[1] *Division of Molecular Medicine, Bose Institute, P-1/12 CIT Scheme VIIM, Kolkata 700054, India*
[2] *Department of Cardiology, N.R.S. Medical College & Hospital, 138 A.J.C. Bose Road, Kolkata 700014, India*

Correspondence should be addressed to Nripendranath Mandal; mandaln@rediffmail.com

Received 24 April 2013; Revised 11 July 2013; Accepted 17 July 2013

Academic Editor: Sudhish Mishra

The purpose of this study is to establish whether ABO blood group is related to coronary heart disease in an individual in Asian Indian Bengali population of eastern part of India. Two hundred and fifty (250) CHD patients and two hundred and fifty (250) age and sex matched healthy subjects were enrolled in the study. ABO blood group distribution in patients was compared with control group. Frequency of major cardiac risk factors was determined to find any correlation between blood groups and cardiovascular risk factors. The distribution of ABO blood groups in patients versus control group was A in 24.00 versus 21.60%, B in 30.80 versus 32.40%, O in 38.40 versus 21.60%, and AB in 6.80 versus 24.40%. The analysis showed significant difference in frequency of O (OR = 1.857, 95%CI = 1.112–3.100, $P = 0.018$) and AB (OR = 0.447, 95%CI = 0.227–0.882, $P = 0.020$) blood group between healthy controls and CHD individuals. Our results may suggest that the AB blood group decreases the risk of CHD in healthy controls, and it might be due to the higher concentration of high density lipoprotein cholesterol (HDL-c), while the O blood group increases the risk of CHD due to lower HDL-c levels in Bengali population of eastern part of India.

1. Introduction

Coronary heart disease (CHD) is a multifactorial disease. The etiology of CHD is complex and appears to involve interactions between genetic and environmental factors. Blood is an individual's complete and unchangeable identity. Although almost 400 blood group antigens have been reported, the ABO and Rh have been recognized as the major clinically significant blood group antigens [1]. Research on ABO group system has been of immense interest, due to its medical importance in different diseases [2–7], though the explanation for the association between ABO blood groups and some disease is still unclear. Clinical studies have shown that individuals of the A phenotype blood group are more susceptible to cardiovascular disease [8, 9]. In British men, the incidence of ischemic heart disease is higher in patients with blood group A [10]. Likewise, in the Hungarian population, again blood group A is more common in patients with CHD [11]. In a most recent study carried out in Copenhagen, Denmark, the Lewis blood phenotype Le (a-b-) was found to be associated with an increased risk for CHD in men; this appears independent of conventional cardiovascular risk factors like smoking, obesity, diabetes mellitus, high cholesterol, triglycerides, and so forth [12].

The present study was designed to explore the relation between ABO blood group and coronary heart disease in Asian Indian Bengali population of eastern part of India. We also examined the relation between ABO blood group and cardiovascular risk factors.

2. Methods

All subjects are Indian Bengali adults. The criteria for selecting the patients ($n = 250$) and controls ($n = 250$) have been presented in detail previously [13]. Briefly, patients having typical angina and evidence of ischemia or infarction after electrocardiographic study, tread mill test, stress echo

and echocardiographic study; on the other hand, controls comprised the spouses, neighbors, and people from same work place of the patients, with the same sociocultural background, in whom the clinical history, the objective search for signals of CHD, and the electrocardiographic as well as echocardiographic examinations did not suggest the presence of that disease. All patients and controls with ancestral origin were from the Bengali eastern part of India. All patients were admitted to the hospital within 12 hours of the onset of chest pain. Blood samples for biochemical analysis were taken at the time of admission. Blood samples were collected by vein puncture into vacuum tubes containing EDTA. Any patients or controls found to have taken any lipid-lowering drugs were excluded from the study. Plasma samples were processed on the day of sample collection by centrifugation at 3000 rpm for 10 min at room temperature using tabletop centrifuge (Remi Pvt. Ltd., Mumbai, India), divided into aliquots, and stored in cryovials at −80°C until further analysis. Patients and controls were fully informed of the aim of this study. All subjects included gave their informed consent to participation in the study. The study was approved by the ethics committee of the institute involved.

Standard slide method was adopted: a drop of each of the monoclonal antisera (Anti-A, Anti-B and Anti-D) (manufactured by Agappe Diagnostics Ltd., Kerala, India) was taken on glass slides. The blood cells subjects of whose blood group is to be determined were mixed with each blood separately with the help of separate glass rods. Blood groups were determined on the basis of agglutination reaction within 5 minutes of mixing. Total cholesterol (TC) was determined enzymatically using CHOD/POD-Phosphotungstate reagent. High density lipoprotein cholesterol (HDL-c) was determined with CHOD/POD-Phosphotungstante reagent (Accurex Biomedical Pvt. Ltd., India), after precipitation with phosphotungstic acid. Triglyceride (TG) was determined using GOP-POD reagent (Accurex Biomedical Pvt. Ltd., India). Besides values of low density lipoprotein cholesterol (LDL-c) were estimated using the formulae LDL-c = TC − (HDL-c + FTG/5) [14].

After the completion of each experiment, the data were recorded on predesigned proforma and managed with Microsoft Excel software. Data entry was double checked for any human error. All calculations were performed using SPSS version 10.0 software package for Windows. Continuous variables are expressed as mean (standard deviations) and as percentages for categorical variables. Comparisons between groups were done using unpaired Student's t-test or chi-square (χ^2) test as appropriate. An allele frequency of the antigens was computed by application of the Hardy-Weinberg Law [15] on the basis of the number of subjects with different blood groups. ABO differences in cardiovascular risk factors were examined using post hoc analysis, after correcting the P value for multiple comparisons by using Bonferroni's correction. The association between different parameters and risk of CHD was examined by estimating odd ratios (ORs) with corresponding 95% confidence intervals (CIs), using univariate logistic regression analysis. Multivariate analysis was performed using multiple logistic regression (Enter method) to assess the independent adjusted relationship between different variables and CHD with independent variables being those with $P \leq 0.05$ in univariate logistic regression analysis. The P value < 0.05 was considered statistically significant.

Table 1: Characteristic of Asian Indian Bengalee population in eastern part of India in the case and control groups.

Variable	Case ($N = 250$)	Control ($N = 250$)	P value
No. (%) of smokers	150 (60%)	70 (28%)	<0.0001
No. (%) of alcohol users	61 (24.4%)	35 (14%)	0.003
No. (%) of cases with hypertension	119 (47.6%)	84 (33.6%)	0.001
No. (%) of cases with family history	81 (32.4%)	38 (15.2%)	<0.0001
WC (cm)	87.24 (6.37)	85.28 (5.30)	<0.0001
TC (mg/dL)	191.11 (40.37)	168.51 (42.83)	<0.0001
TG (mg/dL)	183.09 (55.16)	141.47 (57.75)	<0.0001
HDL-c (mg/dL)	28.81 (7.28)	34.60 (8.52)	<0.0001
LDL-c (mg/dL)	125.49 (37.60)	105.62 (37.89)	<0.0001

Continuos variable are expressed as mean (SD) and compared by Student's t-test. Categorical variables were expressed as percentage (%) and compared by chi-square test.
TC: total cholesterol, SD: standard deviation, TG: triglycerides, HDL-c: high density lipoprotein cholesterol, LDL-c: low density lipoprotein cholesterol, WC: waist circumference.

3. Results

During the period of this study, April 2009 to February 2011, 250 CHD patients and 250 healthy controls, participated in this study. Females constituted 18.4% of the cases and 16.8% of the controls and males constituted 81.6% of cases and 83.2% of the controls ($P > 0.05$). No significant difference was observed in mean age between cases (mean: 54.71 years) and controls (mean: 54.49 years) ($P = 0.375$).

As shown in Table 1, smoking, being an alcohol user, hypertension, family history, and increased waist circumference were highly prevalent in the group with CHD as compared to control. The mean value of TC, LDL-c, and TG was significantly higher in CHD patient compared to control; on the contrary, the mean value of HDL-c was significantly lower in patient than control.

In Table 2 the distribution of ABO blood types in patients with CHD and controls is shown. Blood group O is more common (38.40%) in patients than controls (21.60%) ($P < 0.0001$). Blood group A is also found more often in patients (24.00%) than controls (21.60%) ($P = 0.522$). But in blood group AB, the controls are more numerous (24.40%) than patients (6.80%) ($P < 0.0001$). In blood group B also, the controls outnumber (32.40%) the patients (30.80%) ($P =$

Table 2: Distribution of the ABO blood types in patients with CHD and controls.

Sample	n		Phenotype frequency				Allele frequency		
			A	B	O	AB	A	B	O
Patients	250	Abs. no.	60	77	96	17	0.193	0.238	0.567
		%	24.00	30.80	38.40	6.80			
Controls	250	Abs. no.	54	81	54	61	0.265	0.337	0.398
		%	21.60	32.40	21.60	24.40			

Table 3: Distribution of major cardiovascular risk factors in all samples ($n = 500$) in accordance with ABO blood groups.

Variables (mean (SD))	Blood group				Test for heterogeneity[1]
	AB ($n = 78$)	A ($n = 114$)	B ($n = 158$)	O ($n = 150$)	
TC (mg/dL)	174.08 (44.52)[2]	181.24 (36.29)	185.28 (49.77)	174.96 (38.43)	$P = 0.117$
TG (mg/dL)	163.11 (39.02)	159.24 (64.28)	164.01 (66.02)	161.38 (59.03)	$P = 0.928$
HDL-c (mg/dL)	36.65 (12.04)	30.81 (5.78)[5]	32.13 (7.39)[5]	29.56 (8.11)[5]	$P < 0.0001$
LDL-c (mg/dL)	104.80 (40.71)	118.58 (32.29)	120.34 (44.05)[4]	112.78 (35.79)	$P = 0.025$
WC (cm)	85.55 (4.03)	86.62 (6.93)	86.04 (6.08)	86.56 (5.72)	$P = 0.557$
Smoker	25 (32.1%)[3]	41 (36%)	78 (49.4%)	78 (52%)[4]	$P = 0.007$
Alcohol user	9 (11.5%)	40 (35.1%)[5]	36 (22.8%)	14 (9.3%)	$P < 0.0001$
Hypertension	25 (32.1%)	46 (40.9%)	66 (41.8%)	67 (44.7%)	$P = 0.457$
Family history	8 (10.3%)	27 (23.7%)	41 (25.9%)	43 (28.7%)[4]	$P = 0.037$

[1]Derived from analysis of covariance that evaluated the associations between major cardiovascular risk factors (dependent factor) and blood group (independent factor), after adjustment for age (in years) and sex.
[2]Mean (SD) (all such values).
[3]Number (percentage in individual group) (all such values).
[4,5]Significantly different from AB blood group (ANOVA with Bonferroni's correction): [4]$P < 0.05$, [5]$P < 0.01$.
A indicates A blood group; B indicates B blood group; O indicates O blood group; AB indicates AB blood group; TC: total cholesterol; TG: triglycerides; HDL-c: high density lipoprotein cholesterol; LDL-c: low density lipoprotein cholesterol; WC: waist circumference.

0.271). The allele frequencies in both the patients and the controls are in order A < B < O.

We examined the contribution of major cardiovascular risk factors in subjects with ABO blood groups to all 500 patients (Table 3). We found from the analysis that HDL-c and LDL-c had significantly different mean value in the blood groups. The mean value of HDL-c was highest among AB group (36.65 mg/dL) and in O group was lowest (29.56 mg/dL) compared to other groups. But on the other hand, the LDL-c concentration was higher in O group (112.78 mg/dL) than AB group (104.80 mg/dL). In this analysis we also found that 28.7% of blood group O population had CHD in their family history. Post hoc analysis revealed significant difference of ABO blood group. In particular, compared with AB blood group, the A, B, and O groups were associated with substantial decrease of HDL-c levels. With regard to smoking and family history, differences were significant when we compared O blood group with AB blood group. There was no such significant difference of LDL-c levels found when we compared the AB blood group and O blood group but significant difference was found only when we compared the B blood group with AB blood group.

In Table 4, the univariate analysis showed significant difference in O blood group between the patient and control groups (OR = 2.263, 95% CI = 1.525–3.357. $P < 0.0001$). In addition, a significant association was found between AB blood group and CHD (OR = 0.226, 95% CI = 0.128–0.400, $P < 0.0001$). No significant difference in blood groups A and B was observed between cases and controls ($P > 0.05$); other biochemical and conventional risk factors were also significantly associated with the disease.

Table 4: Risk of coronary heart disease (CHD) by ABO blood group and other risk factors in the study patients as compared to study controls.

Variables	Odd ratio	95% CI	P value
A	1.146	0.754–1.742	0.523
B	0.834	0.574–1.212	0.341
O	2.263	1.525–3.357	0.000
AB	0.226	0.128–0.400	0.000
TC	0.987	0.982–0.991	0.000
TG	0.986	0.983–0.990	0.000
HDL-c	1.102	1.073–1.132	0.000
LDL-c	0.986	0.981–0.991	0.000
Smoker	1.851	1.294–2.647	0.001
Hypertension	1.795	1.251–2.576	0.001
Alcohol user	1.983	1.253–3.138	0.003
WC	0.945	0.916–0.974	0.000
Family history	2.674	1.730–4.132	0.000

Odd ratio (OR) calculated by univariate logistic regression analysis. A indicates A blood group; B indicates B blood group; O indicates O blood group; AB indicate AB blood group; TC: total cholesterol; TG: triglycerides; HDL-c: high density lipoprotein cholesterol; LDL-c: low density lipoprotein cholesterol; WC: waist circumference.

Table 5: Multivariate logistic regression analysis of different variables of coronary heart disease among Asian Indian Bengalee population in the eastern part of India.

Variables	Odd ratio	95% CI	*P* value
TC	0.990	0.984–0.996	0.001
TG	0.990	0.985–0.994	<0.0001
HDL-c	1.097	1.063–1.132	<0.0001
AB	0.447	0.227–0.882	0.020
O	1.857	1.112–3.100	0.018
Smoker	1.340	0.897–2.003	0.153
Hypertension	1.772	1.130–2.779	0.013
Alcohol user	2.004	1.100–3.650	0.023
WC	0.917	0.882–0.954	<0.0001
Family history	1.430	0.821–2.490	0.206

Odd ratio (OR) calculated by multiple logistic regression analysis. O indicates O blood group, AB indicates AB blood group; TC: total cholesterol; TG: triglycerides; HDL-c: high density lipoprotein cholesterol; WC: waist circumference.

Multivariate analysis was performed including the variables which revealed statistically significant difference in the univariate analysis. In this analysis, LDL-c was set to be zero because it is redundant. In the end point of this analysis, AB and O blood groups along with TC, TG, HDL-c, and other conventional risk factors (i.e., hypertension, being an alcohol user, and waist circumference) remained significant, but the smoking and family history lost their significance (Table 5).

4. Discussions

The ABO blood group system is the most important system for blood group compatibility. However, as suggested elsewhere, ABO blood group may have additional consequences on other factors that might also contribute to the risk of thrombosis [16, 17] and deserve additional investigation particularly to explain the CHD risk. The data generated in the present study may be useful for health planners, while making efforts to face the future health challenges in the region. In short, generation of a simple database of blood groups not only provides data about the availability of human blood in case of regional calamities but also serves to enable insight into possibilities of future burden of diseases.

In the present study, we determined the frequency of ABO blood antigens in CHD patients and healthy controls. Our result showed that the AB blood group decreases the risk of CHD in healthy controls, while the O blood group is more frequent in CHD patients and increases the risk of CHD. The results obtained in this study show that, in this Bengali Asian Indian population of eastern part of India, the prevalence of CHD in blood group O is invariably higher than in all other ABO blood groups, but Whincup et al. [10] from England and from other parts of Europe [18, 19] or USA [12], found that frequency of A blood group was more than any other ABO blood groups in CHD patients.

In the analyses of the relation between the ABO blood group and major cardiovascular risk factors the only association of note was that O blood group, probably by association with lower HDL-c levels, smoking habit, and family history, significantly increases the risk of CHD, and contributes substantially to the incidence of CHD in the studied populations. In the two previous reports [20, 21], only association was found between blood group A and serum total cholesterol concentration among the major cardiovascular risk factors. The higher concentrations of HDL-c in subjects of blood group AB seemed to contribute to the protective role of CHD events in subjects of controls group.

The limitation of the present study is the lack of follow-up data, mostly due to the lack of patient compliance. We have also a limitation in our study regarding the estimation of the extent and burden of atherosclerosis by doing coronary angiography and multidetector row computed tomography.

5. Conclusion

The racial and ethnic distribution of blood groups and size of sample are important factors for predicting the CHD risk. Blood type needs to be considered together with other risk factors to understand the individual patient's risk. The identification of genetic and environmental factors among racial and ethnic groups should offer some insights into the observed epidemiological data and advance opportunities to better understand the control and development of CHD.

Authors' Contribution

Santanu Biswas and Pradip K. Ghoshal contributed equally to this work.

Acknowledgments

Authors are grateful to the staff of Department of Cardiology, N.R.S. Medical College & Hospital, Kolkata, India, for their cooperation during the sample collection. The authors acknowledge Mr. Ranjit Kumar Das for their kind help in this work.

References

[1] A. V. Hoffbrand, *Post Graduate Haematology*, Heinemann Professional, London, U. K, 2nd edition, 1981.

[2] P. L. Molison, *Blood Transfusion in Clinical Medicine*, Blackwell Scientific Publication, Oxford, UK, 6th edition, 1979.

[3] H. Egawa, F. Oike, L. Buhler et al., "Impact of recipient age on outcome of ABO-incompatible living-donor liver transplantation," *Transplantation*, vol. 77, no. 3, pp. 403–411, 2004.

[4] A. Shamim, M. A. Hafeez, and M. M. Ahmad, "ABO and Rh blood groups I: markers of cardiovascular risk and association with lipids and other related risk co variables in a Pakistani population," *Proceedings of the Pakistan Academy of Sciences*, vol. 39, pp. 47–66, 2002.

[5] M. Komar-Szymborska, J. Szymborski, A. Sleboda, M. Bajkacz, and E. Cioch, "RH and ABO incompatibility in newborns treated in a pediatric hospital," *Wiadomosci Lekarskie*, vol. 46, no. 17-18, pp. 644–650, 1993.

[6] D. Lester, "Predicting suicide in nations," *Archives of Suicide Research*, vol. 9, no. 2, pp. 219–223, 2005.

[7] H. O. Hein, P. Suadicani, and F. Gyntelberg, "The Lewis blood group—a new genetic marker of obesity," *International Journal of Obesity and Related Metabolic Disorders*, vol. 29, no. 5, pp. 540–542, 2005.

[8] D. Platt, W. Muhlberg, L. Kiehl, and R. Schmitt-Ruth, "ABO blood group system, age, sex, risk factors and cardiac infarction," *Archives of Gerontology and Geriatrics*, vol. 4, no. 3, pp. 241–249, 1985.

[9] M. H. Fox, L. S. Webber, T. F. Thurmon, and G. S. Berenson, "ABO blood group associations with cardiovascular risk factor variables," *Human Biology*, vol. 58, no. 4, pp. 549–584, 1986.

[10] P. H. Whincup, D. G. Cook, A. N. Phillips, and A. G. Shaper, "ABO blood group and ischaemic heart disease in British men," *British Medical Journal*, vol. 300, no. 6741, pp. 1679–1682, 1990.

[11] Z. Tarján, M. Tonelli, J. Duba, and A. Zorándi, "Correlation between ABO and Rh blood groups, serum cholesterol and ischemic heart disease in patients undergoing coronarography," *Orvosi Hetilap*, vol. 136, no. 15, pp. 767–769, 1995.

[12] R. C. Ellison, Y. Zhang, R. H. Myers, J. L. Swanson, M. Higgins, and J. Eckfeldt, "Lewis blood group phenotype as an independent risk factor for coronary heart disease," *American Journal of Cardiology*, vol. 83, no. 3, pp. 345–348, 1999.

[13] S. Biswas, P. K. Ghoshal, S. C. Mandal, and N. Mandal, "Association of low-density lipoprotein particle size and ratio of different lipoproteins and apolipoproteins with coronary heart disease," *Journal of Cardiology*, vol. 52, no. 2, pp. 118–126, 2008.

[14] H. Varley, A. H. Gowenlock, and M. Bell, *Practical Clinical Biochemistry*, William Heinemann Medical Books, London, UK, 1980.

[15] M. W. Strickberger, *Dominance Relations and Multiple Alleles in Diploid Organisms*, McMillan, NewYork, NY, USA, 2nd edition, 1976.

[16] V. M. Morelli, M. C. H. de Visser, H. L. Vos, R. M. Bertina, and F. R. Rosendaal, "ABO blood group genotypes and the risk of venous thrombosis: effect of factor V Leiden," *Journal of Thrombosis and Haemostasis*, vol. 3, no. 1, pp. 183–185, 2005.

[17] T. Ohira, M. Cushman, M. Y. Tsai et al., "ABO blood group, other risk factors and incidence of venous thromboembolism: the Longitudinal Investigation of Thromboembolism Etiology (LITE)," *Journal of Thrombosis and Haemostasis*, vol. 5, no. 7, pp. 1455–1461, 2007.

[18] T. W. Meade, J. A. Cooper, Y. Stirling, D. J. Howarth, V. Ruddock, and G. J. Miller, "Factor VIII, ABO blood group and the incidence of ischaemic heart disease," *British Journal of Haematology*, vol. 88, no. 3, pp. 601–607, 1994.

[19] P. M. McKeigue, M. G. Marmot, and A. M. Adelstein, "Diet and risk factors for coronary heart disease in Asians in northwest London," *The Lancet*, vol. 2, no. 8464, pp. 1086–1089, 1985.

[20] M. J. Langman, P. C. Elwood, J. Foote, and D. R. Ryrie, "ABO and Lewis blood-groups and serum-cholesterol," *The Lancet*, vol. 2, no. 7621, pp. 607–609, 1969.

[21] M. F. Oliver, H. Geizerova, R. A. Cumming, and J. A. Heady, "Serum-cholesterol and ABO and rhesus blood-groups," *The Lancet*, vol. 2, no. 7621, pp. 605–607, 1969.

Hindawi Publishing Corporation
BioMed Research International
Volume 2013, Article ID 108951, 6 pages
http://dx.doi.org/10.1155/2013/108951

Research Article

Immunomodulatory Effect of Continuous Venovenous Hemofiltration during Sepsis: Preliminary Data

Giuseppe Servillo,[1] Maria Vargas,[1] Antonio Pastore,[1] Alfredo Procino,[2] Michele Iannuzzi,[1] Alfredo Capuano,[2] Andrea Memoli,[2] Eleonora Riccio,[2] and Bruno Memoli[2]

[1] *Medical Intensive Care Unit, Department of Surgical and Anesthesiological Sciences, University Federico II of Naples, 80129 Naples, Italy*
[2] *Department of Nephrology, University Federico II of Naples, 80129 Naples, Italy*

Correspondence should be addressed to Eleonora Riccio; elyriccio@libero.it

Received 7 May 2013; Accepted 22 June 2013

Academic Editor: Tiziano Verri

Introduction. Severe sepsis and septic shock are the primary causes of multiple organ dysfunction syndrome (MODS), which is the most frequent cause of death in intensive care unit patients. Many pro- and anti-inflammatory mediators, such as interleukin-6 (IL-6), play a strategic role in septic syndrome. Continuous renal replacement therapy (CRRT) removes in a nonselective way pro- and anti-inflammatory mediators. *Objective*. To investigate the effects of continuous venovenous hemofiltration (CVVH) as an immunomodulatory treatment of sepsis in a prospective clinical study. *Methods*. High flux hemofiltration (Qf = 60 ml/Kg/hr) was performed for 72 hr in thirteen critically ill patients suffering from severe sepsis or septic shock with acute renal failure (ARF). IL-6 gene expression was measured by real-time PCR analysis on RNA extracted from peripheral blood mononuclear cell before beginning of treatment (T0) and after 12, 24, 48, and 72 hours (T1–4). *Results*. Real-time PCR analysis demonstrated in twelve patients IL-6 mRNA reduction after 12 hours of treatment and a progressive increase after 24, 48, and 72 hours. *Conclusions*. We suggest that an immunomodulatory effect might exist during CVVH performed in critically ill patients with severe sepsis and septic shock. Our data show that the transcriptional activity of IL-6 increases during CVVH.

1. Introduction

Sepsis is a great public health problem and represents the leading cause of death in intensive care units of developed countries. Different studies have reported a high population-based incidence of sepsis, and high percentages of intensive care unit (ICU) beds have been occupied by those patients [1–4].

An increase of cytokines has been evidenced in plasma of patients presenting septic shock and has been associated with poor prognosis [5]. Microbial products are responsible for the induction of inflammation. This leads to local microvascular injury with potential dissemination and malignant sequelae at different organ levels. These effects are described as multiple organ failure (MOF). While there is a high concentration of proinflammatory mediators (IL-1, IL-6, IL-8, and TNF-α) at the site of infection, body's stress response contributes to an opposing systemic reaction by producing anti-inflammatory mediators (IL-4, IL-10, and IL-13). Often the production of proinflammatory cytokines is followed by secretion of inhibitors, such as soluble receptors or receptor antagonists. Bone et al. called this response "compensated antiinflammatory response syndrome" (CARS) [6]. Several lines of evidence suggest that compensated response and "systemic inflammatory response syndrome" (SIRS) may often coexist in the same patient but in different compartments [7]. In the "peak concentration hypothesis," peaks of proinflammatory cytokines and peaks of anti-inflammatory cytokines coexist and the concept of cutting peaks, for example, through hemofiltration, may contribute to bring the patient to a nearly normal immunohomeostasis. The therapeutic approaches focused on decreasing cytokine production or neutralizing the effects of cytokines; continuous renal replacement therapy (CRRT) may play a role in the downregulation of the

inflammatory response [8] by nonselective extracorporeal removal, mainly by absorption, of cytokines and other mediators, restoring the hemodynamic and the immunologic homeostasis. However, the hypothesis that hemofiltration can remove inflammatory mediators and its role in the sepsis therapy is still conflictual.

A phase II clinical study showed no reduction of plasma levels of circulating IL-6, IL-8, IL-10, and TNF-α or occurrence of MOF in twelve patients with early septic shock or septic organ dysfunction who received 48 hours of continuous venovenous hemofiltration (CVVH) [9]. Ronco et al. estimated that CVVH with replacement fluid of 35 mL/Kg improves survival in critically ill patients with acute renal failure (ARF) admitted in two intensive care units (ICUs) [10]. However, it is still uncertain whether beneficial effect of high volume hemofiltration is the result of intensified blood purification or an effect on nonspecific cell-mediated immunity. Therefore, Dellinger et al. in the international guidelines for management of severe sepsis and septic shock recommended CVVH as the elective therapy for ARF in septic shock, allowing the management of fluid balance in hemodynamically unstable septic patients [11].

Concentration of cytokines has been measured in many studies, but few assays sized neither the bioactivity of the cytokines nor their net effects on immune functions [12]. Circulating cytokines may just be the "tip of the iceberg," implying that neither their presence nor their absence can reflect the complex interplay at the tissue level [13]. Despite the fact that their peak concentration may reflect an exacerbated production, these levels do not necessarily stand for enhanced bioactivity. To determine the balance of inflammatory response measurement of cytokines bioactivity may be superior to their absolute concentration. Moreover, variation of a single cytokine in the complex immune response syndrome could also reflect the change of other mediators. Therefore, we decided to measure interleukin-6 gene expression in mononuclear cells (PBMCs) harvested from septic patients, as a marker for immune function and proinflammatory bioactivity. Persisting high levels of IL-6, in fact, correlate with poor outcome in sepsis, and its concentration correlates with the concentration of other inflammation markers.

Aim of the present observational prospective study is to investigate the effect of high volume continuous hemofiltration on the transcriptional activity of PBMC, as a marker of immunomodulatory effect of this treatment in septic process.

2. Materials and Methods

2.1. Patients. The study was performed in the intensive care unit of the University of Naples "Federico II" after local ethics committee approval. Informed consent was obtained from patients' next of kin. From January 2007 to January 2008, we enrolled medical and surgical patients from our intensive care unit suffering from severe sepsis or septic shock with coexisting ARF, according to the American College of Chest Physicians/Society of Critical Care Medicine Consensus Conference criteria. Exclusion criteria were age >80 years, acute bleeding, and immunodepression. Table 1 shows clinical characteristics of our patients. All patients received conventional intensive care therapies in accordance with the international sepsis guidelines [14], as intubation and mechanical ventilation with a tidal volume of 6 mL/kg and an upper limit plateau pressure $<30\ cmH_2O$, sedation by continuous infusion according to clinical requirements, and intravenous antibiotics as indicated by microbiological resistance testing. All patients received inotropic support in addition to other vasoactive drugs, as clinically indicated, and fluid therapy by using crystalloids and colloids. Once the decision was made to proceed with renal replacement therapy, a double lumen catheter was inserted in femoral vein and continuous hemofiltration was started.

2.2. Treatments. Ultrafiltration rate (Qf) was 4 l/hr. Blood flow rate was more than 200 mL/min. For ultrafiltration, we used a polyethersulfone filter (Acquamax HF12) with a surface area of $1.20\ m^2$ and a maximal transmembrane pressure (TMP) of 600 mmHg. Anticoagulation was obtained with heparin 6.0 U/Kg/hr. In continuous venovenous hemofiltration, solute transport is achieved by pure convection. Solute flux across the membrane is proportional to the ultrafiltration rate (Qf) and the ratio between the concentration of solute in the ultrafiltrate and in the plasma water (sieving coefficient, S), since clearance is calculated from product $Qf \times S$. When S is proximal to 1 (for solutes freely crossing the membrane), clearance is assumed to be Qf. Therefore, since ultrafiltration rate corresponds to clearance in continuous hemofiltration, it may be used as a surrogate of treatment dose. Two different machines were used for the study, both equipped with calibrated peristaltic blood pumps and fluid balance systems with calibrated scales. Replacement solution was added in the postdilutional mode. We used Accusol with potassium (Baxter Healthcare), which had a pH of 7.4, 35 mmol/L of bicarbonate, and 2 mmol/L of potassium, associated with other ionic compounds. Theoretical osmolarity of this solution was of 296 mOsm/L. Blood samples were obtained before the beginning of treatment (T0) and after 12, 24, 48, and 72 hours (T1–4). SAPS 3 [15, 16] and daily SOFA [17] were measured for each patient.

2.3. IL-6 Gene Expression Analysis. Blood samples (20 mL of heparinized blood) were collected from all patients to obtain plasma samples and isolate peripheral blood mononuclear cells (PBMCs). These cells were isolated by Ficoll-Hypaque (Flow Laboratories, Irwine, UK) gradient density centrifugation (400 ×g for 30 min). Then PBMCs were incubated in culture tubes (Falcon) in quantities of 3×106/mL and cultured for 24 h at 37°C in 5% CO_2 saturated humidity incubator. After this step, cell-free supernatants were collected by centrifugation. PBMCs were pulverized with a blender and lysed using TRIzol reagent. Total RNA was extracted by the single-step method, using phenol and chloroform/isoamylalcohol. Four micrograms of total RNA were subjected to cDNA synthesis for 1 h at 37°C using the "Ready-To-Go You-Prime First-Strand Beads" Kit (Amersham Pharmacia Biotech Little Chalfont Buckinghamshire, UK) in a reaction containing 0.5 μg oligo-dT (Amersham

Table 1: Characteristics of patients at baseline: gender, sex, underlying disease, origin of sepsis, and microbiology.

Patient	Gender	Age	Underlying disease	Origin of sepsis	Microbiology
N1	F	74	Gastric cancer, gastrectomy, and pulmonary thromboembolism	Abdominal	*Candida albicans*
N2	M	80	Left inferior pulmonary lobectomy, mesenteric infarction, and resection of small bowel	Abdominal	*Bacteroides fragilis*
N3	F	79	Pulmonary thromboembolism	Pulmonary	*Pseudomonas aeruginosa*
N4	F	60	Posttraumatic subdural haemorrhage	Pulmonary	*Acinetobacter baumannii*
N5	M	34	Multiple thoracic and abdominal trauma	Pulmonary	*Acinetobacter baumannii*
N6	F	51	Substitution of mitral valve after rheumatic fever cardiopathy	Mediastinal abscess	*Candida albicans* *Escherichia coli*
N7	M	56	Acute respiratory failure, lung cancer	Pulmonary	*Pseudomonas aeruginosa*
N8	M	55	Evacuation of cerebral haemorrhage	Pulmonary	*Klebsiella pneumoniae*
N9	M	51	Ligature of left external carotid, draining of facial, neck, and mediastinic abscess	Mediastinal abscess, infection of tracheostomy site	*Klebsiella pneumoniae* *Candida albicans*
N10	M	48	Multiple abdominal and pelvic trauma	Urinary	*Escherichia coli*
N11	F	59	Perforation of the colon, colonic resection, and peritonitis	Abdominal	*Escherichia coli,* *Enterobacter spp.*
N12	F	62	Acute respiratory failure, COPD	Pulmonary	*Pseudomonas aeruginosa* *Acinetobacter baumannii*
N13	M	46	Multiple thoracic abdominal and pelvic trauma	CVC	Staphylococcus coagulase negative

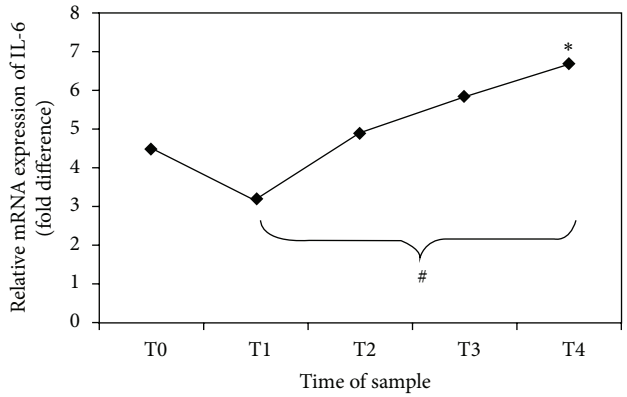

Figure 1: Gene expression of IL-6 in PBMCs obtained by real-time PCR analysis. The points show the relative expression of the mRNA abundance of IL-6. The values on the y-axis represent arbitrary units derived from the mean expression value for the gene of septic patients compared with the healthy subjects set at 1 (not reported in the figure). $^{*}P = 0.031$ trend of relative mRNA expression of IL-6 (ANOVA). $^{\#}P = 0.030$ T1 versus T4 (Bonferroni post hoc correction).

Pharmacia Biotech Little Chalfont Buckinghamshire, UK) [18].

Real-time quantitative PCR analysis for IL-6 gene was performed using ABI Prism 7500 (Applied Biosystem, Foster City, CA, USA) and the 5′ exonuclease assay (TaqMan technology). This assay uses a specific oligonucleotide probe, annealing between the two primer sites, which is labeled with a reporter fluorophore and a quencher. Cleavage of the probe by exonuclease activity of Taq polymerase during strand elongation releases the reporter from the probe resulting in an increase in reporter emission intensity owing to its separation from the quencher. This increment in net fluorescence is monitored in real time during PCR amplification. We have described the cDNA synthesis. Now, the cDNA was used for real-time PCR realized on 96-well optical reaction plates with cDNA equivalent to 20 ng RNA in a volume of 5 μL reaction containing 1x TaqMan Universal MasterMix, optimized concentrations of FAM-labelled probe, and specific forward and reverse primer for the gene selected from Assay on Demand (Applied Biosystems Foster City, CA, USA). Controls included RNA subjected to RT-PCR without reverse transcriptase and PCR with water replacing cDNA. The results were analyzed using a comparative method, and the values were normalized and converted into fold change based on a doubling of PCR product in each PCR cycle, according to the manufacturer's guidelines.

2.4. Statistics. From Table 2, it can be deduced that results obtained from genetic expression of IL-6 are continuous variables function of times T0, T1, T2, T3, and T4. Such continuous variables are expressed as mean ± SD calculated with software "Statistica7" (Statsoft). Various results for the same genetic expression of IL-6 are confronted using ANOVA followed by Bonferroni, as post hoc test. Statistical significance is at the $P < 0.05$ level.

3. Results

Results are expressed as number, percentage, or mean ± SD, as appropriate. Fifteen patients were considered eligible. Two patients developed severe hemodynamic instability during

Table 2: IL-6 gene expression from real-time PCR analysis. Mean values. P values result of ANOVA followed by Bonferroni as post hoc test using the following matricesT1 versus T0, T2 versus T0, T3 versus T0, and T4 versus T0.

Patient	T0	T1	T2	T3	T4
N1	3.5	1	3.6	5.15	6.7
N2	3	1.9	3.1	4.8	7
N3	4.6	2.8	3.9	5	6.2
N4	12	10.4	10	—	—
N5	9.8	8.5	10.3	11.6	—
N6	3.2	2.1	3.5	3.9	4.2
N7	1	1.8	—	—	—
N8	2.5	1	2.8	—	—
N9	3.1	2.4	2.7	5.8	9.3
N10	4.5	3	5.2	5.8	6.7
N11	4.2	2.9	5.1	6.2	6.8
N12	3.7	1.9	4.2	5.1	6.4
N13	3.9	2.2	4.5	5.4	6.9
Mean ± SD	4.53 ± 3.1	3.2 ± 2.8	4.91 ± 2.5	5.87 ± 2.1	6.68 ± 1.3
P		<0.05	>0.05	<0.05	<0.05

replacement therapy, and CVVH was discontinued. Therefore, thirteen patients were enrolled. The origin of sepsis was mostly medical but in some patients postsurgical and trauma related. Table 2 shows the results of real-time PCR analysis on blood samples and their mean values ± SD. In twelve out of thirteen patients, transcriptional activity behaviour is similar; that is, IL-6 mRNA is present in high amounts before filtration (T0), reduces after 12 hours of treatment, and progressively increases after 24, 48, and 72 hours. On the other hand, samples from patient number 4 show a different behaviour: transcriptional activity of IL-6 in this patient seems only to progressively reduce. Figure 1 shows the trend of IL-6 gene expression variation in our thirteen patients ($^{*}P = 0.031$) from T0 to T4 and a statistically significant increase between T1 versus T4 ($P = 0.030$). Table 3 shows clinical data, SAPS 3, and daily SOFA for each patient. Figure 2 shows trend of SOFA score modification in our thirteen patients.

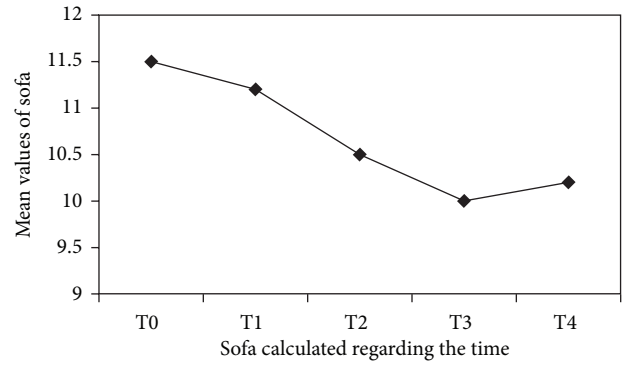

Figure 2: Mean values of daily SOFA measured for each patient. The points on y-axis represent that the mean values reach from this score during the time of treatment. The x-axis reported the different time of measurement.

4. Discussion

Our prospective and clinical study, conducted on critically ill septic patients with ARF treated using high flux hemofiltration (Qf = 60 mL/Kg/hr) with a filter of polyethersulfone, has shown a progressive increase in transcriptional activity of IL-6 produced by PBMCs. In the early 90s, Bellomo et al. conducted a study on cytokines removal from circulation with dialysis [19]. The authors showed that CVVHD attenuated progression of ARF and removed inflammatory cytokines from blood of septic patients. After these results, some authors [9, 20, 21] hypothesized a role of CVVH not only as CRRT but also as immunomodulatory therapy for septic patients. In their "peak concentration hypothesis" [22], Ronco et al. suggest that the effect of nonspecific removal of unbound mediators and cytokines from blood compartment is a resetting to a lower level of immunedysregulation, both in prevalently proinflammatory and counterinflammatory phases of sepsis [10]. In their opinion, Ronco et al. affirmed that by eliminating the peaks, the system might restore its ability to achieve immune homeostasis [22]. More recently, Honoré et al. [20] shift their interest to the effect of high volume hemofiltration (HVHF) on the interstitium and tissue level. The authors conclude that both mediators and promediators are removed at interstitial and at tissue levels, secondary to removal from blood compartment, to a point where some pathways are completely shut down and cascades are blocked. At this point, called "Threshold point," tissue damage and organ injury are stopped in their progression. Sander et al. [21] suggest that the entire amount of cytokines potentially eliminated through hemofiltration is probably lower when compared to endogenous production. Furthermore, hemofiltration membranes per se may increase cytokine production by activating mononuclear cells. In 2007, Horner et al. [23] concluded that plasma from septic

Table 3: SAPS 3 admission score, SOFA score calculated at 0, 12, 24, 48, and 72 hours, and outcome of each patient.

Patient	SAPS 3	SOFA 0	SOFA 1	SOFA 2	SOFA 3	SOFA 4	Outcome
N1	55 (26%)	6	6	7	7	8	Died
N2	27 (1%)	9	10	10	8	9	Died
N3	75 (66%)	11	9	9	11	10	Died
N4	56 (28%)	12	13	13	Stop CVVH	—	Died
N5	47 (13%)	15	12	12	13	Stop CVVH	Survived
N6	80 (74%)	16	18	12	16	18	Died
N7	68 (52%)	12	15	—	—	—	Died
N8	90 (85%)	13	15	15	—	—	Died
N9	57 (30%)	10	8	7	7	7	Survived
N10	52 (32%)	8	8	12	10	10	Survived
N11	64 (44%)	12	11	10	10	10	Survived
N12	67 (50%)	12	9	9	9	10	Survived
N13	56 (28%)	14	12	10	9	10	Survived
Mean ± SD	61.1 ± 15.6	11.5 ± 2.8	11.2 ± 3.4	10.5 ± 2.4	10 ± 2.8	10.2 ± 3.1	

patients contains substances mediating a substantially different immune response pattern compared with plasma from critically ill nonseptic patients. In an experimental study, Toft et al. [24] showed that infusion of endotoxin in pigs induced a significant increase in IL-6 and IL-10 levels in peripheral blood, but there was no difference in cytokine levels between CVVH-treated and nontreated septic animals. Thus, the author concluded that CVVH did not decrease plasma levels of cytokines, although it had been described that proinflammatory as well as anti-inflammatory cytokines are excreted in the ultrafiltrate. Moreover, De Vriese et al. [25] suggest that a decrease in concentration of cytokines in plasma was possible for a few hours after a change of filter, and in fact the filter rapidly became saturated with cytokines.

Our prospective and clinical studies conducted on septic patients aim to evaluate the biological activity of leukocytes, as IL-6 production by PBMCs, during CVVH. We have applied to thirteen septic patients a CVVH with high flux (60 mL/Kg/hr), Qf of 4 L/hr, and polyethersulphone filter which allowed us to obtain a blood flow ≥ 200 mL/min. Our data show that transcriptional activity of an inflammatory cytokine such as IL-6 significantly increases during CVVH. In sepsis, however, impaired regulation may cause an excessive anti-inflammatory response, which generates monocyte "immunoparalysis" and exposes the host to further infections. Both processes (inflammation and anti-inflammation) are designed to act in response to specific stimuli in a well-balanced fashion defined as immunohomeostasis. Continuous therapies have been shown to provide clinical benefits beyond those expected by the simple substitution of renal function. In this view, it is possible to hypothesize that avoidance of peaks of mediator in blood may contribute to a partial restoration of the immunohomeostasis. When sepsis is viewed as a syndrome of immune suppression perspective, in which the immune effectors cells become dysfunctional and are no longer capable of guaranteeing a normal immune surveillance, we can hypothesize that increase of IL-6 transcriptional activity could be due to enhanced capability of immune cells to provide protection against external harmful stimuli. We therefore think that during CVVH, there might be a reactivation of immune capability of the leukocytes to produce inflammatory cytokines, restoring an immunologic balance.

In conclusion, we suggest that there might be an immunomodulatory effect of CVVH during sepsis. However, since response to sepsis should be viewed in a network perspective, within an array of interdependent mediators, it is important to further confirm this hypothesis.

Conflict of Interests

The authors declare no conflict of interests.

References

[1] D. C. Angus, W. T. Linde-Zwirble, J. Lidicker, G. Clermont, J. Carcillo, and M. R. Pinsky, "Epidemiology of severe sepsis in the United States: analysis of incidence, outcome, and associated costs of care," *Critical Care Medicine*, vol. 29, no. 7, pp. 1303–1310, 2001.

[2] R. Beale, K. Reinhart, F. M. Brunkhorst et al., "Promoting global research excellence in severe sepsis (PROGRESS): lessons from an international sepsis study," *Infectio*, vol. 37, no. 3, pp. 222–232, 2009.

[3] C. Alberti, C. Brun-Buisson, H. Burchardi et al., "Epidemiology of sepsis and infection in ICU patients from an international multicentre cohort study," *Intensive Care Medicine*, vol. 28, no. 2, pp. 108–121, 2002.

[4] E. Silva, A. Pedro Mde, A. C. Sogayar et al., "Brasilian sepsis epidemiological study (BASES study)," *Critical Care Medicine*, vol. 8, no. 4, pp. R251–R260, 2004.

[5] M. R. Pinsky, J.-L. Vincent, J. Deviere, M. Alegre, R. J. Kahn, and E. Dupont, "Serum cytokine levels in human septic shock; Relation to multiple-system organ failure and mortality," *Chest*, vol. 103, no. 2, pp. 565–575, 1993.

[6] R. C. Bone, C. J. Grodzin, and R. A. Balk, "Sepsis: a new hypothesis for pathogenesis of the disease process," *Chest*, vol. 112, no. 1, pp. 235–243, 1997.

[7] C. Ronco, M. Bonello, V. Bordoni et al., "Extracorporeal therapies in non-renal disease: treatment of sepsis and the peak concentration hypothesis," *Blood Purification*, vol. 22, no. 1, pp. 164–174, 2004.

[8] A. F. Grootendorst, "The potential role of hemofiltration in the treatment of patients with septic shock and multiple organ dysfunction syndrome," *Advances in Renal Replacement Therapy*, vol. 1, no. 2, pp. 176–184, 1994.

[9] L. Cole, R. Bellomo, G. Hart et al., "A phase II randomized, controlled trial of continuous hemofiltration in sepsis," *Critical Care Medicine*, vol. 30, no. 1, pp. 100–106, 2002.

[10] C. Ronco, R. Bellomo, P. Homel et al., "Effects of different doses in continuous veno-venous haemofiltration on outcomes of acute renal failure: a prospective randomised trial," *The Lancet*, vol. 355, no. 9223, pp. 26–30, 2000.

[11] R. P. Dellinger, J. M. Carlet, H. Masur et al., "Surviving Sepsis Campaign guidelines for management of severe sepsis and septic shock," *Intensive Care Medicine*, vol. 34, pp. 17–60, 2008.

[12] W. Ertel, J.-P. Kremer, J. Kenney et al., "Downregulation of proinflammatory cytokine release in whole blood from septic patients," *Blood*, vol. 85, no. 5, pp. 1341–1347, 1995.

[13] J.-M. Cavaillon, C. Munoz, C. Fitting, B. Misset, and J. Carlet, "Circulating cytokines: the tip of the iceberg?" *Circulatory Shock*, vol. 38, no. 2, pp. 145–152, 1992.

[14] R. P. Dellinger, J. M. Carlet, and H. Masur, "Surviving sepsis campaign guidelines for management of severe sepsis and septic shock," *Critical Care Medicine*, vol. 32, no. 10, pp. 858–873, 2004.

[15] P. G. H. Metnitz, R. P. Moreno, E. Almeida et al., "SAPS 3-From evaluation of the patient to evaluation of the intensive care unit. Part 1: objectives, methods and cohort description," *Intensive Care Medicine*, vol. 31, no. 10, pp. 1336–1344, 2005.

[16] R. P. Moreno, P. G. H. Metnitz, E. Almeida et al., "SAPS 3 - From evaluation of the patient to evaluation of the intensive care unit. Part 2: development of a prognostic model for hospital mortality at ICU admission," *Intensive Care Medicine*, vol. 31, no. 10, pp. 1345–1355, 2005.

[17] J.-L. Vincent, R. Moreno, J. Takala et al., "The SOFA (Sepsis-related Organ Failure Assessment) score to describe organ dysfunction/failure," *Intensive Care Medicine*, vol. 22, no. 7, pp. 707–710, 1996.

[18] B. Memoli, C. Libetta, T. Rampino et al., "Hemodialysis related induction of interleukin-6 production by peripheral blood mononuclear cells," *Kidney International*, vol. 42, no. 2, pp. 320–326, 1992.

[19] R. Bellomo, P. Tipping, and N. Boyce, "Continuous veno-venous hemofiltration with dialysis removes cytokines from the circulation of septic patients," *Critical Care Medicine*, vol. 21, no. 4, pp. 522–526, 1993.

[20] P. M. Honoré, O. Joannes-Boyau, and B. Gressens, "Blood and plasma treatments: the rationale of high-volume hemofiltration," *Contributions to Nephrology*, vol. 156, pp. 387–395, 2007.

[21] A. Sander, W. Armbruster, B. Sander, A. E. Daul, R. Lange, and J. Peters, "Hemofiltration increases IL-6 clearance in early systemic inflammatory response syndrome but does not alter IL-6 and TNFα plasma concentrations," *Intensive Care Medicine*, vol. 23, no. 8, pp. 878–884, 1997.

[22] C. Ronco, C. Tetta, F. Mariano et al., "Interpreting the mechanisms of continuous renal replacement therapy in sepsis: the peak concentration hypothesis," *Artificial Organs*, vol. 27, no. 9, pp. 792–801, 2003.

[23] C. Horner, S. Schuster, J. Plachy et al., "Hemofitration and immune response in severe sepsis," *Journal of Surgical Research*, vol. 142, pp. 59–65, 2007.

[24] P. Toft, V. Brix-Christensen, J. Baech et al., "Effect of hemofiltration and sepsis on chemotaxis of granulacyties and release of IL-8 and IL-10," *Acta Anaesthesiologica Scandinavica* , vol. 46, no. 2, pp. 138–144, 2002.

[25] A. S. De Vriese, F. A. Colardyn, J. J. Philippé, R. C. Vanholder, J. H. De Sutter, and N. H. Lameire, "Cytokine removal during continuous hemofiltration in septic patients," *Journal of the American Society of Nephrology*, vol. 10, no. 4, pp. 846–853, 1999.

Hindawi Publishing Corporation
BioMed Research International
Volume 2013, Article ID 321213, 8 pages
http://dx.doi.org/10.1155/2013/321213

Review Article

Acetylcholinesterase as a Biomarker in Environmental and Occupational Medicine: New Insights and Future Perspectives

Maria Giulia Lionetto, Roberto Caricato, Antonio Calisi, Maria Elena Giordano, and Trifone Schettino

Department of Biological and Environmental Sciences and Technologies (DiSTeBA), University of Salento, Via Prov.le Lecce-Monteroni, 73100 Lecce, Italy

Correspondence should be addressed to Maria Giulia Lionetto; giulia.lionetto@unisalento.it

Received 27 April 2013; Accepted 20 June 2013

Academic Editor: Tiziano Verri

Acetylcholinesterase (AChE) is a key enzyme in the nervous system. It terminates nerve impulses by catalysing the hydrolysis of neurotransmitter acetylcholine. As a specific molecular target of organophosphate and carbamate pesticides, acetylcholinesterase activity and its inhibition has been early recognized to be a human biological marker of pesticide poisoning. Measurement of AChE inhibition has been increasingly used in the last two decades as a biomarker of effect on nervous system following exposure to organophosphate and carbamate pesticides in occupational and environmental medicine. The success of this biomarker arises from the fact that it meets a number of characteristics necessary for the successful application of a biological response as biomarker in human biomonitoring: the response is easy to measure, it shows a dose-dependent behavior to pollutant exposure, it is sensitive, and it exhibits a link to health adverse effects. The aim of this work is to review and discuss the recent findings about acetylcholinesterase, including its sensitivity to other pollutants and the expression of different splice variants. These insights open new perspective for the future use of this biomarker in environmental and occupational human health monitoring.

1. Introduction

Biological markers (biomarkers) were early defined as "cellular, biochemical or molecular alterations that are measurable in biological media such as human tissues, cells, or fluids" [1]. More recently, the definition includes biological characteristics that can be objectively measured and evaluated as indicator of normal biological processes, pathogenic processes, or pharmacological responses to a therapeutic intervention [2].

Biomarkers are useful tools in a variety of fields, including medicine, environmental health, toxicology, developmental biology, and basic scientific research. In the last two decades a growing interest towards biomarkers has been recorded in occupational and environmental medicine, as observed in Figure 1, where the trend of the number of papers published in these fields in the last 20 years is reported. The interest in biomarkers in occupational and environmental medicine parallels the development of human biomonitoring which is defined as the repeated, controlled measurement of chemical or biomarkers in fluids, tissues, or other accessible samples from subjects currently exposed or had been exposed in the past or to be exposed to chemical, physical, or biological risk factors in the workplace and/or the general environment [3]. Human biomonitoring is a valuable tool in exposure estimation of selected populations and currently used in surveillance programs all over the world.

Biomarkers used in environmental and occupational human health monitoring can be distinguished into three classes: biomarker of exposure, effect, and susceptibility [4]. Biomarkers of exposure involve measurement of parent compound, metabolites and reflect the dose of exposure. Biomarkers of effect are a measurable biochemical, physiological, and behavioral alteration within an organism that can be recognized as associated with an established or possible health impairment or disease. Biomarkers of susceptibility indicate an inherent or acquired ability of an organism to respond to specific exposure [3].

In the last two decades a variety of biomarkers have been used to study worker populations, and these studies have contributed at different levels to the improvement

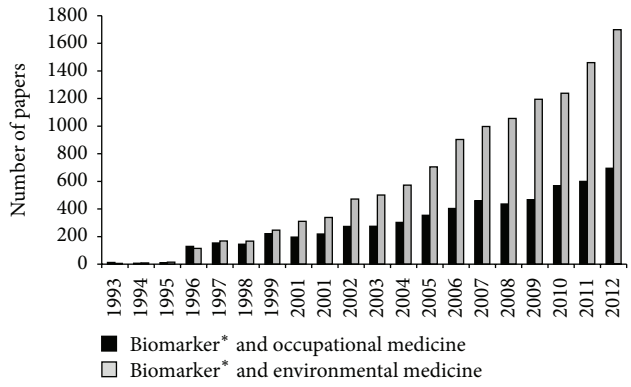

Figure 1: Number of papers published in the last 20 years. The research was carried out on Scopus by using two research queries, respectively: (1) "biomarker*" and "occupational medicine," (2) "biomarker*" and "Environmental medicine" (Scopus, April 2013).

of occupational health. On the basis of this success there is a continued need to develop and apply biomarkers as useful tools for providing real-time detection of exposure to hazardous substances in the workplace and in the general environment [4].

One of the early biomarkers characterized in human environmental exposure is represented by the inhibition of the enzyme acetylcholinesterase (AChE) as biomarker of effect on nervous system following complex exposure to organophosphorus compounds.

The present work aims to review and discuss the recent findings on this biomarker in relation to the current and future use in environmental and occupational human health monitoring.

2. AChE: General Features

AChE belongs to the family of cholinesterases (ChEs), which are specialized carboxylic ester hydrolases that break down esters of choline. Cholinesterase class includes AChE which hydrolyzes the neurotransmitter acetylcholine and pseudocholinesterase or butyrylcholinesterase (BChE) which utilizes butyrylcholine as substrate. AChE is mainly found at neuromuscular junctions and cholinergic synapses in the central nervous system. Here, AChE hydrolyzes acetylcholine into choline and acetate after activation of acetylcholine receptors at the postsynaptic membrane. AChE activity serves to terminate synaptic transmission, preventing continuous nerve firings at nerve endings. Therefore, it is essential for the normal functioning of the central and peripheral nervous system. AChE is also found on the red blood cell membranes, where it constitutes the Yt blood group antigen [5] also known as Cartwright. It helps to determine a person's blood type, but the physiological function on erythrocyte membrane is to date unknown [5]. BChE is found in plasma and its physiological function in blood remains still unknown [6].

The AChE molecule is composed of two different protein domains: a large catalytic domain of about 500 residues and a small C-terminal peptide of less than 50 residues. AChE is a product of a single gene [7] which is expressed in different tissues in different splicing forms. Alternative splicing in the 3′ terminus of AChE pre-mRNA produces three variants: the primary, "synaptic" AChE-S (otherwise known as "tailed," AChE-T) [8], the stress-induced, soluble (readthrough) AChE-R variant, and the erythrocytic AChE-E [9]. These isoforms share a similar catalytic domain but differ in their C-terminal domain, which influences their molecular form and localization and confers specific features [10]. "Synaptic" AChE-S constitutes the principal multimeric enzyme in brain and muscle. It is typically tetrameric and membrane bound in the synapse. The soluble, monomeric "readthrough" AChE-R is induced under chemical and physical stress; the erythrocytic AChE-E is a glycophosphatidylinositol- (GPI-) linked dimer targeted to the plasma membrane of erythrocyte and lymphocytes [11]. AChE-S and AChE-R have been described also in peripheral blood cells [12].

The active site of AChE includes two subsites: the anionic site and the esteratic subsite. The anionic subsite is the binding site for the positive quaternary amine of acetylcholine. The esteratic subsite is the site where acetylcholine is hydrolyzed to acetate and choline. The hydrolysis of the carboxyl ester leads to the formation of an acyl-enzyme and free choline. Then, the acyl-enzyme undergoes nucleophilic attack by a water molecule, liberating acetic acid and regenerating the free enzyme [13].

3. Organophosphorus and Carbamate Compounds as Specific Inhibitors of AChE

Organophosphorus and carbamate pesticides are known to be specific inhibitors of aceylcholinesterase catalytic activity [14]. They have become the most widely used pesticides today since the removal of organochlorine pesticides from use. Organophosphorus and carbamate compounds bind with variable affinity to the esteratic site by phosphorylation or decarbamylation, respectively, and inactivate the enzyme. Organophosphorus compounds are considered to be functionally irreversible inhibitors of AChE, since the time necessary to liberate the enzyme from inhibition may be in excess of the time required for synthesis of new AChE. Carbamates, on the other hand, have a fairly rapid decarbamylation step so that substantial recovery of the enzyme can occur in a finite period of time. The hydrolysis rate of the intermediate phosphorylated or carbamated enzyme is not the only factor contributing to the toxicity of these pesticides. The affinity of the serine-hydroxyl group in the active site (esteratic site) for the inhibitor is another important aspect to be considered. Some compounds have a direct effect on the enzyme, while others such as parathion or chlorpyrifos, that have little capacity to directly inhibit AChE, are metabolically activated by cytochromes P450 to form potent AChE inhibitors referred to as "oxygen analogs" or "oxons." While it has been known that these oxons inhibit AChE through phosphorylation of Ser-203, the details of the interactions between these oxons and the enzyme are unclear. Recent results [15] suggest that the interactions of chlorpyrifos

oxon with AChE are complex and may involve the binding of this oxon to a secondary site on the enzyme.

Organophosphate and carbamate pesticides are widely used for pest control on crops in agriculture and on livestock and for residential uses, including insect control in domestic and garden uses. Organophosphorus pesticide residues have been detected at permissible (and sometimes impermissible) levels in many agricultural products; therefore low-level dietary exposures to organophosphorus pesticides are likely. Occupational exposure occurs at all stages of pesticide formulation, manufacture, and production and implies exposure to complex mixtures of different types of these compounds. In general, occupational exposures to organophosphorus pesticides dwarf environmental exposures [16]; however, special populations, such as farm-worker children, may receive higher exposures. Large amounts of these compounds are released into the environment and many of them exert their effect also on nontarget organisms [17–20], being a potential hazard for human health and the environment. The residues of organophosphate and carbamate from agricultural practices are able to infiltrate through the soil into surface water because of their water solubility [21]. As a consequence of their wide diffusion there, residues have been detected in food [22], ground and drinking water [23], natural surface waters [24], and marine organisms [25]. Therefore, all people are inevitably exposed to these compounds and/or their degradation products through environmental contamination or occupational use in air, water, and food. These pollutants cannot be easily detected by chemical analysis because of their relative short life in the environment; on the other hand their products of environmental degradation can be very harmful, retaining anticholinesterase activity [26].

As recently outlined by Black and Read [27] the AChE inhibition by organophosphorus compounds arouses a certain interest also in relationship to the problem of exposure to chemical warfare agents, such as organophosphorus nerve agents [28]. These are the most toxic chemical warfare agents that are known to have been produced, stockpiled, and weaponized. Their development, production, stockpiling, and use are prohibited under the terms of the Chemical Weapons Convention, and, together with their precursors, are subject to strict controls and verification procedures [27]. The first confirmed use of organophosphorus nerve agents in warfare was by Iraq in the conflict with Iran (United Nations, 1984) and by Iraq against Kurdish population. More recently there has been a perceived increased risk of some terrorist groups using nerve agents [27].

4. AChE Inhibition as a Biomarker of Effect in Occupational and Environmental Medicine

As a molecular target of organophosphorus and carbamate compounds, AChE measurement in the blood was early recognized to be a human biological marker of effect for these molecules and emerged as a diagnostic tool in the biomedical area. As observed in Figure 2 in the last two decades a growing interest in AChE as a biomarker in occupational and environmental medicine has been observed, as indicated by the growing number of papers in these fields.

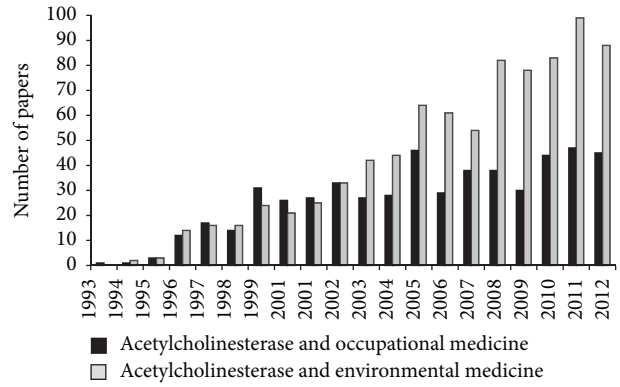

Figure 2: Number of papers published in the last 20 years. The research was carried out on Scopus by using two research queries, respectively: (1) "AChE" and "occupational medicine," (2) "AChE" and "Environmental medicine" (Scopus, April 2013).

Today measurement of ChE levels in blood is the conventional method of assessing the degree of occupational exposure to organophosphate pesticides in exposed environments (e.g., environments concerned with pesticide production and use) during the periodic statutory medical surveillance in several countries [29]. Intervention levels have been established, for example, in Sweden: if AChE inhibition (calculated with respect to the individual preexposure level–baseline) is 25%, a second measurement has to be carried out. If the decrease in ACHE activity is confirmed, exposure has to be avoided for 14 days [4].

Blood cholinesterase measurement is also useful as a primary biomarker in emergency medicine in cases of poisoning and accidental organophosphate or carbamate exposure [29–33]. In occupational and environmental medicine erythrocyte AChE and plasma or serum BChE are the two principal types of ChE measured in blood. Potential inhibition of AChE and BChE varies widely among the different organophosphorus compounds. Some organophosphate pesticides inhibit BChE more strongly than AChE. The inhibition of BChE is highly correlated with intensity and duration of higher exposure to a large group of organophosphate and carbamate pesticides [34]. However, BChE inhibition does not reflect the biological effects of organophosphate in the nervous system [35]. On the other hand AChE inhibition is more sensitive than BChE in the case of chronic exposure to organophosphate. In fact, AChE inhibition by organophosphate shows a lower recovery rate compared to BChE and this produces cumulative inhibitory effect on the AChE activity [36]. Unlike BChE, erythrocyte AChE inhibition mirrors the biological effects of organophosphate in the nervous system. Therefore, red blood cell measures of AChE are generally preferred over plasma measures of ChE activity because data on red blood cells may provide a better representation of the inhibition of the neural AChE.

The success of the use of AChE inhibition as a biomarker of effect to organophosphate exposure arises from the fact that it meets a number of characteristics necessary for the successful application of a biological response as a biomarker in biomonitoring: the response is easy to measure, shows

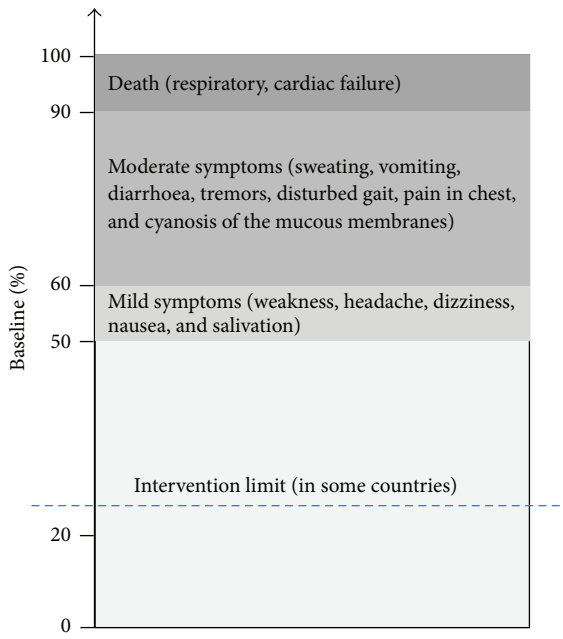

Figure 3: Relationship between AChE inhibition and health negative effects. Drawn on the basis of Maroni et al. [49] findings.

a dose-dependent behavior to pollutant exposure, is sensitive, and exhibits a link to health adverse effects.

The most widely used method for AChE activity measurement in blood is the Ellman method [37] based on the photometric determination of the chromogenic product coming from the reaction between acetylthiocholine (the substrate of the enzyme) and 5, 5-dithiobis-2-nitrobenzoic acid (DTNB, Ellman's reagent). This method is easy to use, employs relatively inexpensive equipment and the results are accurate and quantitative. Recently, the measurement of AChE inhibition in human saliva as a biomarker of effect for organophosphorus pesticide has been explored [37, 38]. In the last years the use of saliva as a diagnostic fluid for biomarker development has rapidly grown. The use of saliva for biomarker detection offers many advantages: saliva collection is noninvasive compared with phlebotomy, it is more acceptable to patients, and it does not carry the risk of needlestick injuries [39]. These characteristics make the use of saliva suitable for medical surveillance and biological monitoring. AChE in human saliva is derived from salivary glandular cells, while BChE may be derived from microorganisms in the oral cavity [40]. Sayer et al. [41] demonstrated that AChE catalytic activity in saliva is stable at room temperature for up to 6 h. In a group of exposed pesticide factory workers, cholinesterase activity in saliva was found to be lower than the activity in healthy controls [42]. Henn et al. [43] suggested that saliva may be a useful indicator of potential neurotoxic effects from exposure to organophosphorus and carbamate pesticides but pointed out the need to further explore the factors affecting the high variability in the measures compared to blood AChE measurement. A study of Ng et al. [44] questioned the use of AChE in saliva as a biomarker for organophosphate compounds because of the low levels of AChE in saliva relative to erythrocytes and the weak correlation between the two measurements. Therefore, the use of AChE measurement as a biomarker of effect instead of blood measurement remains still debated.

The use of a biomarker in biomonitoring requires the knowledge of the relationships between chemical exposure, biomarker responses and adverse effects. These aspects have been well established in the case of AChE. Several studies reported significant relationship between exposure to organophosphorus compounds and AChE inhibition in exposed worker populations [30, 45–48]. As regards the relationship between AChE inhibition and health negative effects, it is known that an inhibition of AChE between 50% and 60% elicits a dose-response pattern of relatively mild symptoms such as weakness, headache, dizziness, nausea, and salivation with a convalescence of 1–3 days (Figure 3). An inhibition of AChE between 60 and 90% produces moderate symptoms such as sweating, vomiting, diarrhoea, tremors, disturbed gait, pain in chest, and cyanosis of the mucous membranes which reverse within few weeks. At 90–100% inhibition, death from respiratory or cardiac failure occurs [49].

5. Sensitivity of AChE to Other Pollutants

In the last years, the inhibition of AChE from several chemical species other than organophosphate and carbamate pesticides including heavy metals, other pesticides, polycyclic aromatic hydrocarbons, detergents, and components of complex mixtures of contaminants has been increasingly reported in humans and other animals [50–54].

The potential of some metallic ions, such as Hg^{2+}, Cd^{2+}, Cu^{2+}, and Pb^{2+}, to depress the activity of AChE *in vitro* and/or *in vivo* conditions has been demonstrated in several studies on humans and animals [55–57]. Ademuyiwa et al. [57] studied the potential effect of lead on erythrocyte AChE activity during occupational exposure to this metal and suggested that erythrocyte AChE activity could be used as a biomarker of lead-induced neurotoxicity in occupational exposed subjects.

AChE activity may also be affected by other pesticides from different chemical families, such as pyrethroids [58], triazines [59], and Paraquat [60]. Hernández et al. [61] suggested the usefulness of AChE as a biomarker of exposure in the surveillance of workers long-term exposed to pesticides other than organophosphate and carbamate.

Several findings also indicate the anticholinesterase effect of polycyclic aromatic hydrocarbons which are common environmental contaminants in surface waters, sediments, soils, and urban air. These compounds are formed during the incomplete combustion of fossil fuels, wood, and municipal waste incineration, from internal combustion engines. Kang and Fang [62] demonstrated that several polycyclic aromatic hydrocarbons inhibit AChE directly *in vitro*. The magnitude of the inhibition differs among the compounds tested and may be related to the number of aromatic rings in the molecule [63]. Interestingly, polycyclic aromatic hydrocarbons are able to inhibit AChE activity in

an additive manner together with organophosphate, being noncompetitive inhibitors of AChE [63].

Recently, due to the growing interest in nanomaterials in various applications (e.g., electronics, biomedicine, catalysis, and material science) [64, 65], Wang et al. [66] explored the potential effects of nanoparticles on AChE activity *in vitro*. Different classes of nanoparticles, including metals, oxides, and carbon nanotubes (SiO_2, TiO_2, Al_2O_3, Al, Cu, carbon-coated copper, multiwalled carbon nanotubes, and single-walled carbon nanotubes), showed high affinity for AChE. Cu, Cu–C, multiwalled carbon nanotubes, and single-walled carbon nanotubes MWCNT, SWCNT showed a dose–response inhibition of AChE activity with IC50 values of 4, 17, 156, and 96 mgL^{-1}, respectively. The inhibition by nanoparticles was primarily caused by adsorption or interaction with the enzyme [66].

All these findings about the the sensitivity of AChE to several classes of contaminants other than organophosphate and carbamate compounds need to be taken into account for the proper application of this biomarker in environmental and occupational medicine. In fact, in most cases mixed exposures are observed. It is worth noting that not only different compounds may reach levels of significance in terms of anticholinesterase effect, but, moreover, combinations of different chemical classes can exert additive or synergistic inhibitory effect on AChE activity. This suggests the need to reconsider the applicability of AChE in biomonitoring and risk assessment in areas contaminated by several classes of pollutants. In these cases the usefulness of this biomarker could be that of providing an integrative measurement of the overall neurotoxic risk posed by the whole burden of bioavailable contaminants present in the environment.

6. Noncatalytic Functions of ACHE and Organophosphate Sensitivity

Research in the last twenty years indicates additional functions of AChE besides its catalytic activity and its role in terminating neurotransmission at cholinergic synapses. Different isoforms of AChE have been shown to affect cell proliferation, differentiation, and responses to various stresses. AChE appears to play an important role in axonal outgrowth [67], synaptogenesis [68], cell adhesion [69], neuronal migration [70], hemopoietic stress responses [71], and apoptosis [72]. These functions are largely independent of the enzymatic ability to hydrolyze acetylcholine [9]. The mechanisms underlying these important noncatalytic functions are to be explored; however, they seem to involve alternatively spliced AChE variants in several tissues.

It is known that multiple stress stimuli involve increased ratio between AChE-R and AChE-S in brain and blood cells [9, 71].

In brain AChE-S is the main isoform in physiologic conditions, but the normally rare AChE-R variant can occur after exposure to physical stress or anticholinesterase drugs [73]. In general, under normal conditions, the splicing factors SC35 and ASF/SF2 balance each other and regulate the splicing of AChE, raising the level of the AChE-S form and lowering the level of the AChE-R form [9]. During stress, the upregulated SC35 induces an imbalancing of the dynamic ratio of AChE-S/R variants by shifting the splicing of AChE-S form to the AChE-R form through interacting with a specific exonic splicing enhancer [74].

The two AChE splice variants, R and S, share distinct functions in development and repair in the brain: the AChE-R isoform, preferentially induced by injury, appears to promote repair and protect against neurodegeneration, while overexpression of the more abundant synaptic isoform, AChE-S, enhances susceptibility to neurotoxicity.

Recently Jameson et al. [75] suggested that the nonenzymatic functions of AChE splice variants are a target for the developmental neurotoxicity of organophosphates. As demonstrated in animal models organophosphate compounds are able to induce developmental neurotoxicity at doses that do not elicit any signs of systemic intoxication and even at exposures below the threshold for inhibition of AChE [76–78]. In humans links between organophosphate exposure during pregnancy and deficits in fetal growth and neurocognitive development in children were observed [79]. These findings have led to the restriction of the household use of some organophosphate insecticides in some countries. However, the mechanisms and consequences of organophosphate-induced developmental neurotoxicity remain a major environmental concern.

Organophosphates are known to increase the overall expression of AChE and to alter the relative expression of AChE-R and AChE-S in mammal adult brain [80, 81]. On the other hand during the developmental period, exposures to organophosphate elicit an AChE pattern associated with progressive neurotoxicity characterized by coinduction of both AChE-R and AChE-S at concentrations of exposure below the threshold for inhibition of AChE catalytic activity [75]. As pointed out by Jameson et al. [75], AChE variants may participate in and be predictive of the relative developmental neurotoxicity of organophosphates, including long-term cognitive impairment [82].

Recently, organophosphate exposure was found to be associated with an increased risk of Alzheimer's disease in workers exposed to these compounds [83] and, in addition, with an increased risk of Alzheimer's disease in children [84]. On the basis of the study of Darreh-Shori et al. [85] who have explored the roles of the two AChE variants in the Alzheimer disease, it is possible to hypothesize the involvement of the AChE different spicing isoforms in the organophosphate association with Alzheimer's disease in exposed individuals.

Interestingly, all these results point out the need of analysing AChE gene splice variants that may be important in the mechanisms or outcomes of organophosphate-induced developmental neurotoxicity and not just the total activity of the protein product. Moreover, they open new perspectives for the potential use of AChE gene expression in biomonitoring and risk assessment. In perspective, the study of AChE gene splice variants, of their functions, and of the pollutants-induced alterations in their expression pattern could contribute (1) to detect exposure to pollutant concentrations that do not elicit any signs of systemic intoxication and AChE inhibition in adults but that are able to induce long-term

effects on developmental stages; (2) to define new threshold exposure levels that protect the organism against adverse effects at all life stages; (3) to characterize new biomarkers of susceptibility.

7. Conclusions

AChE represents one of the first validated biomarkers in environmental and occupational medicine and its use is increased in the last two decades. However, recent findings indicate new potentialities of AChE in human biomonitoring. The sensitivity of AChE activity to other classes of chemicals, including emerging pollutants such as nanomaterials, suggests the usefulness of this biomarker for providing an integrative measurement of the overall neurotoxic risk arising from the whole burden of bioavailable contaminants in areas contaminated by several classes of pollutants. Moreover, the study of the expression of AChE splice variants, their role in the neurotoxicity of organophosphate, contributes to the development of AChE gene expression as a new biomarker of susceptibility to improve the understanding of environmental and occupational health.

References

[1] B. S. Hulka, "Overview of biological markers," in *Biological Markers in Epidemiology*, B. S. Hulka, J. D. Griffith, and T. C. Wilcosky, Eds., pp. 3–15, Oxford University Press, New York, NY, USA, 1990.

[2] S. Naylor, "Biomarkers: current perspectives and future prospects," *Expert Review of Molecular Diagnostics*, vol. 3, no. 5, pp. 525–529, 2003.

[3] M. Manno, C. Viau, J. Cocker et al., "Biomonitoring for occupational health risk assessment (BOHRA)," *Toxicology Letters*, vol. 192, no. 1, pp. 3–16, 2010.

[4] L. E. Knudsen and Å. M. Hansen, "Biomarkers of intermediate endpoints in environmental and occupational health," *International Journal of Hygiene and Environmental Health*, vol. 210, no. 3-4, pp. 461–470, 2007.

[5] G. Daniels, "Functions of red cell surface proteins," *Vox Sanguinis*, vol. 93, no. 4, pp. 331–340, 2007.

[6] L. G. Costa, T. B. Cole, A. Vitalone, and C. E. Furlong, "Measurement of paraoxonase (PON1) status as a potential biomarker of susceptibility to organophosphate toxicity," *Clinica Chimica Acta*, vol. 352, no. 1-2, pp. 37–47, 2005.

[7] D. K. Getman, J. H. Eubanks, S. Camp, G. A. Evans, and P. Taylor, "The human gene encoding acetylcholinesterase is located on the long arm of chromosome 7," *American Journal of Human Genetics*, vol. 51, no. 1, pp. 170–177, 1992.

[8] J. Massoulié, "The origin of the molecular diversity and functional anchoring of cholinesterases," *NeuroSignals*, vol. 11, no. 3, pp. 130–143, 2002.

[9] E. Meshorer and H. Soreq, "Virtues and woes of AChE alternative splicing in stress-related neuropathologies," *Trends in Neurosciences*, vol. 29, no. 4, pp. 216–224, 2006.

[10] S. E. Park, N. D. Kim, and Y. H. Yoo, "Acetylcholinesterase plays a pivotal role in apoptosome formation," *Cancer Research*, vol. 64, no. 24, pp. 2652–2655, 2004.

[11] D. Grisaru, M. Sternfeld, A. Eldor, D. Glick, and H. Soreq, "Structural roles of acetylcholinesterase variants in biology and pathology," *European Journal of Biochemistry*, vol. 264, no. 3, pp. 672–686, 1999.

[12] M. Pick, C. Flores-Flores, D. Grisaru, S. Shochat, V. Deutsch, and H. Soreq, "Blood-cell-specific acetylcholinesterase splice variations under changing stimuli," *International Journal of Developmental Neuroscience*, vol. 22, no. 7, pp. 523–531, 2004.

[13] P. Taylor and Z. Radić, "The cholinesterases: from genes to proteins," *Annual Review of Pharmacology and Toxicology*, vol. 34, pp. 281–320, 1994.

[14] F. Hobbiger, "The inhibition of acetylcholinesterase by organophosphorus compounds and its reversal," *Proceedings of the Royal Society of Medicine*, vol. 54, pp. 403–405, 1961.

[15] L. G. Sultatos and R. Kaushik, "Interactions of chlorpyrifos oxon and acetylcholinesterase," *FASEB Journal*, vol. 21, pp. 883–892, 2007.

[16] D. B. Barr, R. Allen, A. O. Olsson et al., "Concentrations of selective metabolites of organophosphorus pesticides in the United States population," *Environmental Research*, vol. 99, no. 3, pp. 314–326, 2005.

[17] M. G. Lionetto, R. Caricato, M. E. Giordano, M. F. Pascariello, L. Marinosci, and T. Schettino, "Integrated use of biomarkers (acetylcholinesterase and antioxidant enzymes activities) in *Mytilus galloprovincialis* and *Mullus barbatus* in an Italian coastal marine area," *Marine Pollution Bulletin*, vol. 46, no. 3, pp. 324–330, 2003.

[18] M. G. Lionetto, R. Caricato, M. E. Giordano, and T. Schettino, "Biomarker application for the study of chemical contamination risk on marine organisms in the Taranto marine coastal area," *Chemistry and Ecology*, vol. 20, no. 1, pp. S333–S343, 2004.

[19] A. Calisi, M. G. Lionetto, and T. Schettino, "Pollutant-induced alterations of granulocyte morphology in the earthworm *Eisenia foetida*," *Ecotoxicology and Environmental Safety*, vol. 72, no. 5, pp. 1369–1377, 2009.

[20] A. Calisi, M. G. Lionetto, and T. Schettino, "Biomarker response in the earthworm *Lumbricus terrestris* exposed to chemical pollutants," *Science of the Total Environment*, vol. 409, no. 20, pp. 4456–4464, 2011.

[21] L. P. Zhang, H. S. Hong, Z. T. Chen, W. Q. Chen, and D. Calamari, "An initial environmental risk assessment of pesticide application in Xiamen seas," *Jiournal of Xiamen University*, vol. 38, pp. 96–102, 1999.

[22] S. M. Dogheim, E. L.-Z. Mohamed, S. A. Gad Alla et al., "Monitoring of pesticide residues in human milk, soil, water, and food samples collected from Kafr El-Zayat governorate," *Journal of AOAC International*, vol. 79, no. 1, pp. 111–116, 1996.

[23] T. Garrido, J. Fraile, J. M. Ninerola, M. Figueras, A. Ginebreda, and L. Olivella, "Survey of ground water pesticide pollution in rural areas of Catalonia (Spain)," *International Journal of Environmental Analytical Chemistry*, vol. 78, no. 1, pp. 51–65, 2000.

[24] F. Hernández, R. Serrano, M. C. Miralles, and N. Font, "Gas and liquid chromatography and enzyme linked immuno sorbent assay in pesticide monitoring of surface water from the western mediterranean (Comunidad Valenciana, Spain)," *Chromatographia*, vol. 42, no. 3-4, pp. 151–158, 1996.

[25] D. Barceló, C. Porte, and J. Cid, "Determination of organophophorus compounds in Mediterranean coastal waters and biota samples using gas-chromatography with nitrogen-phosphorus and chemical ionization mass spectrometric detection," *International Journal of Environmental Anaytical Chemistry*, vol. 38, pp. 199–209, 1990.

[26] S. O. Pehkonen and Q. Zhang, "The degradation of organophosphorus pesticides in natural waters: a critical review," *Critical Reviews in Environmental Science and Technology*, vol. 32, no. 1, pp. 17–72, 2002.

[27] R. M. Black and R. W. Read, "Biological markers of exposure to organophosphorus nerve agent," *Archives of Toxicology*, vol. 87, pp. 421–437, 2013.

[28] R. M. Black, "An overview of biological markers of exposure to chemical warfare agents," *Journal of Analytical Toxicology*, vol. 32, no. 1, pp. 1–8, 2008.

[29] V. Ng, D. Koh, A. Wee, and S.-E. Chia, "Salivary acetylcholinesterase as a biomarker for organophosphate exposure," *Occupational Medicine*, vol. 59, no. 2, pp. 120–122, 2009.

[30] A. F. Hernández, O. López, L. Rodrigo et al., "Changes in erythrocyte enzymes in humans long-term exposed to pesticides: influence of several markers of individual susceptibility," *Toxicology Letters*, vol. 159, no. 1, pp. 13–21, 2005.

[31] M. S. Souza, G. G. Magnarelli, M. G. Rovedatti, S. Santa Cruz, and A. M. P. De D'Angelo, "Prenatal exposure to pesticides: analysis of human placental acetylcholinesterase, glutathione S-transferase and catalase as biomarkers of effect," *Biomarkers*, vol. 10, no. 5, pp. 376–389, 2005.

[32] J. M. Safi, T. A. Abu Mourad, and M. M. Yassin, "Hematological biomarkers in farm workers exposed to organophosphorus pesticides in the Gaza Strip," *Archives of Environmental and Occupational Health*, vol. 60, no. 5, pp. 235–241, 2005.

[33] M. F. Simoniello, E. C. Kleinsorge, J. A. Scagnetti et al., "Biomarkers of cellular reaction to pesticide exposure in a rural population," *Biomarkers*, vol. 15, no. 1, pp. 52–60, 2010.

[34] M. Araoud, F. Neffeti, W. Douki et al., "Factors influencing plasma butyrylcholinesterase activity in agricultural workers," *Annales de Biologie Clinique*, vol. 69, no. 2, pp. 159–166, 2011.

[35] F. He, "Biological monitoring of exposure to pesticides: current issues," *Toxicology Letters*, vol. 108, no. 2-3, pp. 277–283, 1999.

[36] F. Kamel and J. A. Hoppin, "Association of pesticide exposure with neurologic dysfunction and disease," *Environmental Health Perspectives*, vol. 112, no. 9, pp. 950–958, 2004.

[37] G. L. Ellman, K. D. Courtney, V. Andres Jr., and R. M. Featherstone, "A new and rapid colorimetric determination of acetylcholinesterase activity," *Biochemical Pharmacology*, vol. 7, no. 2, pp. 88–95, 1961.

[38] B. C. Henn, S. McMaster, and S. Padilla, "Measuring cholinesterase activity in human saliva," *Journal of Toxicology and Environmental Health A*, vol. 69, no. 19, pp. 1805–1818, 2006.

[39] D. S.-Q. Koh and G. C.-H. Koh, "The use of salivary biomarkers in occupational and environmental medicine," *Occupational and Environmental Medicine*, vol. 64, no. 3, pp. 202–210, 2007.

[40] K. Ueda and K. Yamaguchi, "Cholinesterase activity of human saliva and types of the enzymes. Comparison of whole saliva with parotid saliva," *The Bulletin of Tokyo Dental College*, vol. 17, no. 4, pp. 231–241, 1976.

[41] R. Sayer, E. Law, P. J. Connelly, and K. C. Breen, "Association of a salivary acetylcholinesterase with Alzheimer's disease and response to cholinesterase inhibitors," *Clinical Biochemistry*, vol. 37, no. 2, pp. 98–104, 2004.

[42] M. Abdollahi, M. Balali-Mood, M. Akhgari, B. Jannat, A. Kebriaeezadeh, and S. Nikfar, "A survey of cholinesterase activity in healthy and organophosphate exposed populations," *Iranian Journal of Medical Sciences*, vol. 21, p. 68, 1996.

[43] B. C. Henn, S. McMaster, and S. Padilla, "Measuring cholinesterase activity in human saliva," *Journal of Toxicology and Environmental Health A*, vol. 69, no. 19, pp. 1805–1818, 2006.

[44] V. Ng, D. Koh, A. Wee, and S.-E. Chia, "Salivary acetylcholinesterase as a biomarker for organophosphate exposure," *Occupational Medicine*, vol. 59, no. 2, pp. 120–122, 2009.

[45] H. N. Nigg and J. B. Knaak, "Blood cholinesterases as human biomarkers of organophosphorus pesticide exposure," *Reviews of Environmental Contamination and Toxicology*, vol. 163, pp. 29–111, 2000.

[46] A. F. Hernández, M. A. Gómez, G. Pena et al., "Effect of long-term exposure to pesticides on plasma esterases from plastic greenhouse workers," *Journal of Toxicology and Environmental Health A*, vol. 67, no. 14, pp. 1095–1108, 2004.

[47] A. P. Remor, C. C. Totti, D. A. Moreira, G. P. Dutra, V. D. Heuser, and J. M. Boeira, "Occupational exposure of farm workers to pesticides: biochemical parameters and evaluation of genotoxicity," *Environment International*, vol. 35, no. 2, pp. 273–278, 2009.

[48] T. A. Mourad, "Adverse impact of insecticides on the health of Palestinian farm workers in the Gaza Strip: a hematologic biomarker study," *International Journal of Occupational and Environmental Health*, vol. 11, no. 2, pp. 144–149, 2005.

[49] M. Maroni, C. Colosio, A. Ferioli, and A. Fait, "Biological Monitoring of Pesticide Exposure: a review. Introduction," *Toxicology*, vol. 143, no. 1, pp. 5–118, 2000.

[50] J. P. Bressler and G. W. Goldstein, "Mechanisms of lead neurotoxicity," *Biochemical Pharmacology*, vol. 41, no. 4, pp. 479–484, 1991.

[51] G. W. Goldstein, "Neurologic concepts of lead poisoning in children," *Pediatric Annals*, vol. 21, no. 6, pp. 384–388, 1992.

[52] M. G. Lionetto, R. Caricato, M. E. Giordano, and T. Schettino, "Biomarker application for the study of chemical contamination risk on marine organisms in the Taranto marine coastal area," *Chemistry and Ecology*, vol. 20, no. 1, pp. S333–S343, 2004.

[53] J. Jebali, M. Banni, H. Guerbej, E. A. Almeida, A. Bannaoui, and H. Boussetta, "Effects of malathion and cadmium on acetylcholinesterase activity and metallothionein levels in the fish *Seriola dumerilli*," *Fish Physiology and Biochemistry*, vol. 32, no. 1, pp. 93–98, 2006.

[54] A. Vioque-Fernández, E. A. de Almeida, J. Ballesteros, T. García-Barrera, J.-L. Gómez-Ariza, and J. López-Barea, "Doñana National Park survey using crayfish (*Procambarus clarkii*) as bioindicator: esterase inhibition and pollutant levels," *Toxicology Letters*, vol. 168, no. 3, pp. 260–268, 2007.

[55] L. G. Costa, "Effects of neurotoxicants on brain neurochemistry," in *Neurotoxicology*, H. Tilson and Mitchell, Eds., pp. 101–124, Raven Press, New York, NY, USA, 1992.

[56] M. F. Frasco, D. Fournier, F. Carvalho, and L. Guilhermino, "Do metals inhibit acetylcholinesterase (AchE)? Implementation of assay conditions for the use of AchE activity as a biomarker of metal toxicity," *Biomarkers*, vol. 10, no. 5, pp. 360–375, 2005.

[57] O. Ademuyiwa, R. N. Ugbaja, S. O. Rotimi et al., "Erythrocyte acetylcholinesterase activity as a surrogate indicator of lead-induced neurotoxicity in occupational lead exposure in Abeokuta, Nigeria," *Environmental Toxicology and Pharmacology*, vol. 24, no. 2, pp. 183–188, 2007.

[58] P. M. Reddy and G. H. Philip, "In vivo inhibition of AChE and ATPase activities in the tissues of freshwater fish, *Cyprinus carpio* exposed to technical grade cypermethrin," *Bulletin of Environmental Contamination and Toxicology*, vol. 52, no. 4, pp. 619–626, 1994.

[59] P. E. Davies and L. S. J. Cook, "Catastrophic macroinvertebrate drift and sublethal effects on brown trout, *Salmo trutta*, caused

by cypermethrin spraying on a Tasmanian stream," *Aquatic Toxicology*, vol. 27, no. 3-4, pp. 201–224, 1993.

[60] A. Szabo, J. Nemcsok, B. Asztalos, Z. Rakonczay, P. Kasa, and L. H. H. Le Huu Hieu, "The effect of pesticides on carp (*Cyprinus carpio* L). Acetylcholinesterase and its biochemical characterization," *Ecotoxicology and Environmental Safety*, vol. 23, no. 1, pp. 39–45, 1992.

[61] A. F. Hernández, O. López, L. Rodrigo et al., "Changes in erythrocyte enzymes in humans long-term exposed to pesticides: influence of several markers of individual susceptibility," *Toxicology Letters*, vol. 159, no. 1, pp. 13–21, 2005.

[62] J.-J. Kang and H.-W. Fang, "Polycyclic aromatic hydrocarbons inhibit the activity of acetylcholinesterase purified from electric eel," *Biochemical and Biophysical Research Communications*, vol. 238, no. 2, pp. 367–369, 1997.

[63] D. A. Jett, R. V. Navoa, and M. A. Lyons Jr., "Additive inhibitory action of chlorpyrifos and polycyclic aromatic hydrocarbons on acetylcholinesterase activity in vitro," *Toxicology Letters*, vol. 105, no. 3, pp. 223–229, 1999.

[64] C. Buzea, I. Pacheco, and K. Robbie, "Nanomaterials and nanoparticles: sources and toxicity," *Biointerphases*, vol. 2, no. 2, pp. MR17–MR71, 2007.

[65] L. Indennidate, D. Cannoletta, F. Lionetto, A. Greco, and A. Maffezzoli, "Nanofilled polyols for viscoelastic polyurethane foams," *Polymer International*, vol. 59, no. 4, pp. 486–491, 2010.

[66] Z. Wang, J. Zhao, F. Li, D. Gao, and B. Xing, "Adsorption and inhibition of acetylcholinesterase by different nanoparticles," *Chemosphere*, vol. 77, no. 1, pp. 67–73, 2009.

[67] J. W. Bigbee, K. V. Sharma, E. L.-P. Chan, and O. Bögler, "Evidence for the direct role of acetylcholinesterase in neurite outgrowth in primary dorsal root ganglion neurons," *Brain Research*, vol. 861, no. 2, pp. 354–362, 2000.

[68] M. Sternfeld, G.-L. Ming, H.-J. Song et al., "Acetylcholinesterase enhances neurite growth and synapse development through alternative contributions of its hydrolytic capacity, core protein, and variable C termini," *Journal of Neuroscience*, vol. 18, no. 4, pp. 1240–1249, 1998.

[69] J. W. Bigbee and K. V. Sharma, "The adhesive role of acetylcholinesterase (AChE): detection of AChE binding proteins in developing rat spinal cord," *Neurochemical Research*, vol. 29, no. 11, pp. 2043–2050, 2004.

[70] D. M. Byers, L. N. Irwin, D. E. Moss, I. C. Sumaya, and C. F. Hohmann, "Prenatal exposure to the acetylcholinesterase inhibitor methanesulfonyl fluoride alters forebrain morphology and gene expression," *Developmental Brain Research*, vol. 158, no. 1-2, pp. 13–22, 2005.

[71] D. Grisaru, M. Pick, C. Perry et al., "Hydrolytic and nonenzymatic functions of acetylcholinesterase comodulate hemopoietic stress responses," *Journal of Immunology*, vol. 176, no. 1, pp. 27–35, 2006.

[72] H. Soreq and S. Seidman, "Acetylcholinesterase—new roles for an old actor," *Nature Reviews Neuroscience*, vol. 2, no. 4, pp. 294–302, 2001.

[73] D. Kaufer, A. Friedman, S. Seidman, and H. Soreq, "Acute stress facilitates long-lasting changes in cholinergic gene expression," *Nature*, vol. 393, no. 6683, pp. 373–377, 1998.

[74] E. Meshorer, B. Bryk, D. Toiber et al., "SC35 promotes sustainable stress-induced alternative splicing of neuronal acetylcholinesterase mRNA," *Molecular Psychiatry*, vol. 10, no. 11, pp. 985–997, 2005.

[75] R. R. Jameson, F. J. Seidler, and T. A. Slotkin, "Nonenzymatic functions of acetylcholinesterase splice variants in the developmental neurotoxicity of organophosphates: chlorpyrifos, chlorpyrifos oxon, and diazinon," *Environmental Health Perspectives*, vol. 115, no. 1, pp. 65–70, 2007.

[76] T. A. Slotkin, "Developmental neurotoxicity of organophosphates: a case study of chlorpyrifos," in *Toxicity of Organophosphate and Carbamate Pesticides*, R. C. Gupta, Ed., pp. 293–314, Elsevier Academic Press, San Diego, Calif, USA, 2005.

[77] T. A. Slotkin, E. D. Levin, and F. J. Seidler, "Comparative developmental neurotoxicity of organophosphate insecticides: effects on brain development are separable from systemic toxicity," *Environmental Health Perspectives*, vol. 114, no. 5, pp. 746–751, 2006.

[78] T. A. Slotkin, C. A. Tate, I. T. Ryde, E. D. Levin, and F. J. Seidler, "Organophosphate insecticides target the serotonergic system in developing rat brain regions: disparate effects of diazinon and parathion at doses spanning the threshold for cholinesterase inhibition," *Environmental Health Perspectives*, vol. 114, no. 10, pp. 1542–1546, 2006.

[79] V. A. Rauh, R. Garfinkel, F. P. Perera et al., "Impact of prenatal chlorpyrifos exposure on neurodevelopment in the first 3 years of life among inner-city children," *Pediatrics*, vol. 118, no. 6, pp. e1845–e1859, 2006.

[80] T. V. Damodaran, K. H. Jones, A. G. Patel, and M. B. Abou-Donia, "Sarin (nerve agent GB)-induced differential expression of mRNA coding for the acetylcholinesterase gene in the rat central nervous system," *Biochemical Pharmacology*, vol. 65, no. 12, pp. 2041–2047, 2003.

[81] A. Salmon, C. Erb, E. Meshorer et al., "Muscarinic modulations of neuronal anticholinesterase responses," *Chemico-Biological Interactions*, vol. 157-158, pp. 105–113, 2005.

[82] D. Yang, A. Howard, D. Bruun, M. Ajua-Alemanj, C. Pickart, and P. J. Lein, "Chlorpyrifos and chlorpyrifos-oxon inhibit axonal growth by interfering with the morphogenic activity of acetylcholinesterase," *Toxicology and Applied Pharmacology*, vol. 228, no. 1, pp. 32–41, 2008.

[83] K. M. Hayden, M. C. Norton, D. Darcey et al., "Occupational exposure to pesticides increases the risk of incident AD: the Cache County Study," *Neurology*, vol. 74, no. 19, pp. 1524–1530, 2010.

[84] M. F. Bouchard, D. C. Bellinger, R. O. Wright, and M. G. Weisskopf, "Attention-deficit/hyperactivity disorder and urinary metabolites of organophosphate pesticides," *Pediatrics*, vol. 125, no. 6, pp. e1270–e1277, 2010.

[85] T. Darreh-Shori, E. Hellström-Lindahl, C. Flores-Flores, Z. Z. Guan, H. Soreq, and A. Nordberg, "Long-lasting acetylcholinesterase splice variations in anticholinesterase-treated Alzheimer's disease patients," *Journal of Neurochemistry*, vol. 88, no. 5, pp. 1102–1113, 2004.

Hindawi Publishing Corporation
BioMed Research International
Volume 2013, Article ID 416534, 13 pages
http://dx.doi.org/10.1155/2013/416534

Research Article

Polyisoprenylated Methylated Protein Methyl Esterase Is Both Sensitive to Curcumin and Overexpressed in Colorectal Cancer: Implications for Chemoprevention and Treatment

Felix Amissah, Randolph Duverna, Byron J. Aguilar, Rosemary A. Poku, and Nazarius S. Lamango

College of Pharmacy and Pharmaceutical Sciences, Florida A&M University, Tallahassee, FL 32307, USA

Correspondence should be addressed to Nazarius S. Lamango; nazarius.lamango@famu.edu

Received 11 April 2013; Accepted 17 June 2013

Academic Editor: Shivani Soni

Inhibition of PMPMEase, a key enzyme in the polyisoprenylation pathway, induces cancer cell death. In this study, purified PMPMEase was inhibited by the chemopreventive agent, curcumin, with a K_i of 0.3 μM (IC_{50} = 12.4 μM). Preincubation of PMPMEase with 1 mM curcumin followed by gel-filtration chromatography resulted in recovery of the enzyme activity, indicative of reversible inhibition. Kinetics analysis with N-para-nitrobenzoyl-S-*trans,trans*-farnesylcysteine methyl ester substrate yielded K_M values of 23.6 ± 2.7 and 85.3 ± 15.3 μM in the absence or presence of 20 μM curcumin, respectively. Treatment of colorectal cancer (Caco2) cells with curcumin resulted in concentration-dependent cell death with an EC_{50} of 22.0 μg/mL. PMPMEase activity in the curcumin-treated cell lysate followed a similar concentration-dependent profile with IC_{50} of 22.6 μg/mL. In colorectal cancer tissue microarray studies, PMPMEase immunoreactivity was significantly higher in 88.6% of cases compared to normal colon tissues ($P < 0.0001$). The mean scores ± SEM were 91.7 ± 11.4 (normal), 75.0 ± 14.4 (normal adjacent), 294.8 ± 7.8 (adenocarcinoma), and 310.0 ± 22.6 (mucinous adenocarcinoma), respectively. PMPMEase overexpression in colorectal cancer and cancer cell death stemming from its inhibition is an indication of its possible role in cancer progression and a target for chemopreventive agents.

1. Introduction

Colorectal cancer is the third most commonly diagnosed cancer and the third leading cause of cancer-related deaths, accounting for about 610,000 deaths per year worldwide [1, 2]. Siegel and coworkers [1] projected a total of 143,460 new cases of colorectal cancer and 51,690 related mortalities in the US in 2012 [1]. Colon cancer development is a multistep process initiated by molecular alterations such as mutations in adenomatous polyposis coli (APC), K-ras, and/or p53 genes [3]. The tissue is then predisposed to subsequent transformation mainly through abnormal cell proliferation, angiogenesis, reduced apoptosis, and changes in growth factor activity [3]. Despite recent medical advances, colorectal cancer recurs in up to 50% of patients [4–6]. The prognosis for the advanced colorectal cancer is very poor due to liver metastasis [7, 8] as well as resistance to chemotherapy [9]. The metastasis has recently been shown to involve the activation of the Rho family of polyisoprenylated small GTPases [10]. These include RhoA and Rac1 which regulate actin cytoskeleton and cell migration [11]. RhoA stimulates the actin stress fiber formation and cell-cell adhesion, while Rac1 induces lamellipodia formation [10]. Enzymes of the polyisoprenylation pathway, which modify these proteins, have thus been the targets for anticancer drug development. Polyisoprenyl transferase inhibitors have been a major part of these efforts [12]. Similar efforts have explored the role of inhibiting polyisoprenylated protein methyl transferase (PPMTase) to curb cancer cell growth [13]. Polyisoprenylated methylated protein methyl esterase (PMPMEase, EC 3.1.1.1) hydrolyzes the ester products of PPMTase, thus counteracting the effects of PPMTase at the terminal only reversible reaction of the pathway [14]. PPMTase and PMPMEase thus appear to be pivotal regulating polyisoprenylated protein function.

Several food components such as flavonoids, phenolics, and polyphenols are chemopreventive [15] and are being used

as dietary supplements to prevent colon cancer [16]. Use of these compounds at nontoxic doses inhibit, reduce, or delay carcinogenesis at its early stages [3]. One such compound is curcumin, the main bioactive constituent of turmeric spice derived from the rhizome of *Curcuma longa* (Zingiberaceae) [17]. Curcumin is a compound with anticancer [18, 19], anti-inflammatory [20], and antioxidant properties [21]. In rodent models, the compound inhibits the development of cancers of the skin, duodenum, tongue, colon, mammary, and prostate glands [22, 23]. Curcumin has also been reported to inhibit cell proliferation as well as inducing apoptosis in cancer cells [23, 24]. The anticancer potential of curcumin is limited by its poor bioavailability [25]. However, when ingested orally, a concentration as low as 0.2% can prevent the development of colon cancer [26]. The chemopreventive and antitumor effect of curcumin in colon cancer has been extensively studied and has been linked to the inhibition of cyclooxygenase-2 [27], aminopeptidase N [28], and antiangiogenesis [29]. Recent studies have revealed that curcumin inhibits human colon cancer cell growth by suppressing EGFR gene expression [30] as well as the Ras signaling pathway [31]. The effects on Ras signaling are interesting given that K-Ras gene mutations are implicated in about 50% of colon cancers cases [32]. Since Ras and other monomeric G-proteins are processed through the polyisoprenylation pathway in order to be fully functional, it is possible that compounds that interfere with the secondary modifications may have effects on carcinogenesis. Studies from our laboratory have established that PMPMEase inhibition induces cancer cell death [33, 34]. Given that aberrant activities of polyisoprenylated proteins play an important role in a majority of colon cancer progression cases [32] and PMPMEase inhibition has such a profound negative effect on cancer cell viability [33–35], the current study was aimed at determining if PMPMEase may constitute a pharmacological target for bioactive anticancer agents such as curcumin. This was determined by investigating PMPMEase susceptibility to curcumin inhibition and expression in colorectal cancer. Here, we report that PMPMEase is both inhibited by curcumin and is overexpressed in colorectal cancer implying that the chemopreventive effects of curcumin may be due at least in part to PMPMEase inhibition.

2. Materials and Methods

2.1. Materials. Human colorectal adenocarcinomas (Caco-2) cells obtained from the American Type Culture Collection (Manassas, VA, USA) were cultured in Dulbecco's Minimum Essential Medium (Invitrogen, CA, USA), supplemented with 20% heat-inactivated fetal bovine serum, 15 mM HEPES buffer, 100 U/mL penicillin and 100 μg/mL streptomycin, and 1% nonessential amino acids obtained from Invitrogen (Carlsbad, CA, USA). The cultures were incubated at 37°C in 5% CO_2/95% humidified air. Curcumin (97% purity) was purchased from Merck (Whitehouse Station, NJ, USA).

2.2. Enzyme Assays. PMPMEase used for the assays was the same as that previously described [36, 37]. The substrate (RD-PNB) and curcumin were dissolved in DMSO. The enzyme assays and analysis were conducted as previously described [36, 37] except with a 15 min preincubation of the assay mixture with curcumin before the addition of substrate. RD-PNB (1 mM) was incubated at 37°C with the enzyme in the presence of curcumin in 100 mM Tris-HCl, pH 7.4 in a total incubation volume of 100 μL. Reactions were stopped by adding 200 μL of methanol and placing them on ice for at least 5 min before centrifugation at 5000 ×g for 5 min. The supernatant was analyzed by RP-HPLC. The product was separated from the substrate on a Hamilton PRP-1 RP-HPLC column (5 μm particles, 4.1 mm ID × 50 mm) with UV detection at 260 nm. The mobile phase consisted of a linear gradient of acetonitrile in 0.1% ethanolamine, from 30% at the start of the separation to 95% in 1 min. This was then maintained for a further 2 min before a 0.5 min reequilibration at 30% acetonitrile for the next sample.

2.3. Gel-Filtration and Enzyme Inhibition Kinetics Analysis of Curcumin-Treated PMPMEase. To determine the inhibition mechanism of PMPMEase by curcumin, PMPMEase (1 mg) was preincubated with or without curcumin (10 μM) for 60 min in identical conditions as in the enzyme assays except that no substrate was included. These were then fractionated on a Superdex 200 gel-filtration column (2 cm ID × 90 cm), eluting with 50 mM Tris-HCl (pH 7.4) containing 0.1% Triton X-100 and 0.5 M NaCl. Aliquots of the 4 mL fractions were then analyzed for enzyme activity using RD-PNB as the substrate.

Michaelis-Menten kinetics analysis was conducted using RD-PNB as the substrate as previously described [38]. Varying concentrations of the substrate (0–400 μM) were incubated with PMPMEase (5 μg) in the presence of curcumin (0-1 mM). The reactions were carried out in 100 mM Tris-HCl, pH 7.4 containing 5% DMSO at 37°C in a total incubation volume of 100 μL. Reactions were stopped by adding 200 μL of methanol. They were then placed on ice for at least 5 min before centrifugation at 5000 ×g for 5 min. The supernatants were removed and analyzed by RP-HPLC with UV detection at 260 nm as previously described [38]. The product peak areas were measured and used to quantify the amount of product formed using a calibration plot of known amounts of product against peak area. All experiments were conducted in triplicates.

2.4. Docking Analysis. Docking was employed to determine the putative binding interactions of curcumin to PMPMEase. PMPMEase shares 79% sequence identity and 88% sequence similarity to human carboxylesterase 1 (hCE1) [36]. As previously described, the X-ray crystal structure of hCE1 [EC 3.1.1.1], 1YAH was used to construct the porcine liver esterase (PLE) structure for docking analysis [38]. Docking analysis was performed with Tripos SYBYL-X (v. 1.3). DScore was used for the evaluation of PMPMEase (1YAH) and PLE. Docking was carried out according to the developer's instructions [54]. In a crystallized receptor-ligand complex, the ligand was extracted from the enzyme, and the binding sites over the whole protein were detected using a multiresidue search. SYBYL-X discovered 10 possible binding sites on

Table 1: Docking data for the binding affinities of curcumin with the respective binding sites.

Docking site	Tripos SYBYL-X Scoring Functions DScore (Kcal/mol)	
	1YAH	PLE
1	−187.40	−944.63
2	−206.74	−581.16
3	−118.87	−1089.5
4	−155.45	−930.83
5	−109.73	−790.88
6	−114.69	−733.22
7	−183.87	−624.60
8	−114.84	−690.98
9	−114.11	−523.63
10	−170.18	N/A

1YAH and 9 sites on PLE. A total of 30 poses were observed and scored for each model and each binding site. The top ranking docking poses with minimal binding free energies were examined and noted in Table 1.

2.5. Cell Culture Conditions and Viability Assays. Caco-2 cells were cultured to 80–90% confluence, trypsinized and seeded onto 96-well plates at a density of 2.5×10^4 cells/well and incubated for 24 h at 37°C in 5% CO_2/95% humidified air. The cells were then exposed to varying concentrations of curcumin (0–200 μM) in serum-free media daily for 72 h. Resazurin (Promega, WI, USA) was used to measure the cell viability according to the vendor instructions. Resazurin (20 μL) was added to each well, and the contents were gently mixed and incubated in the dark for 2 h at room temperature before measurement of the fluorescence with excitation at 560 nm and emission at 590 nm using FLx 800 Microplate Fluorescence Reader (Bio-Tek Instruments Inc., VM, USA). Cell viability was expressed as the percentage of the fluorescence in the treated cells relative to that of the controls. The data are mean values from three different experiments.

2.6. Determination of PMPMEase Activity in Curcumin-Treated Cells. Cells were cultured to 80–85% confluence. Trypsin-EDTA (0.25%) was used to detach the cells. The cells were thoroughly washed with PBS and lysed with 0.1% Triton-X 100 in 100 mM Tris-HCI buffer, pH 7.4. Aliquots of the resulting lysate were preincubated for 15 min with curcumin (0–1000 μM) before the addition of substrate. RD-PNB (1 mM) was incubated at 37°C with the lysate in the presence of curcumin in 100 mM Tris-HCl, pH 7.4 in a total incubation volume of 100 μL. Reactions were stopped by adding 200 μL of methanol and placing them on ice for at least 5 min before centrifugation at 5000 ×g for 5 min. The supernatant was analyzed by RP-HPLC as described earlier under enzyme assays.

2.7. Tissue Microarray and Immunohistochemical Studies. The expression of PMPMEase in colon cancer tissues was studied using immunohistochemical analysis on a colon cancer, normal adjacent, and normal tissue microarrays (TMAs) composed of a total of 208 cores from 208 cases. The human TMAs used in the studies were supplied by, and the immunohistochemistry conducted at US Biomax (Rockville, MD). All the tissues were formalin-fixed, paraffin-embedded, and mounted on positively charged SuperFrost Plus glass slides. Tissue sections (5 μm thick and 1 mm in diameter) deparaffinized and hydrated were subjected to antigen retrieval in a microwave for 20 min in antigen retrieval solution (DAKO Corporation, CA, USA) and cooled for 15 min. As described in [55], the slides were incubated for 1 h with rabbit polyclonal antibody directed against PMPMEase (human carboxylesterase 1, hCE1) (Santa Cruz Biotechnology, CA, USA) diluted to a final concentration of 0.25 μg/mL. Slides were then incubated with the secondary antibody using the ImmPRESS Reagent anti-Rabbit IgG (Vector Laboratories, CA, USA). Staining was performed with 3,3′-diaminobenzidine (DAB) as a chromogen, and sections were then counterstained with hematoxylin QS (Vector Laboratories, CA, USA). The IHC-stained slides were scanned at 20x magnification.

The method used to score the PMPMEase immunoreactivity was adapted from that of Bremnes et al. [56]. The intensity of the staining was given scores of 0 (no staining), 1 (trace), 2 (weak), 3 (intermediate), 4 (strong), and 5 (very strong). The score of the staining intensity was then multiplied by the percentage of the immunoreactive tumor cells. The overall scores ranged between 0 and 500 with those between 0 and 100 described as trace, 101 to 200 as weak, 201 to 300 as intermediate, 301 to 400 as strong, and 401 to 500 as very strong. The evaluation and scoring were conducted by RD, FA, BJA, and RP without prior knowledge of the diagnosis of the individual cores on the TMAs.

2.8. Oncomine Cancer Microarray Database Analysis. The Oncomine Cancer Microarray database (http://www.oncomine.org/) was used to study the profile of PMPMEase gene expression in human colorectal cancer. "Colorectal cancer and CES1" as well as "colon cancer and CES1" were typed into the search window. All studies involving colorectal cancer with CES1 expression profiles were considered for study. The gene expression data from each study, performed with the same methodology, were used. The gene expression data were log transformed, and a gene was considered as overexpressed when the fold change in the level of expression was ≥1.0.

2.9. Statistical Analysis. All results were expressed as the means ± S.E.M. The concentration-response curves were obtained by plotting the percentage residual PMPMEase activities against the log of curcumin concentrations. Non-linear regression plots were generated using Graphpad Prism version 4.0 for Windows (San Diego, CA, USA). From these, the concentrations that inhibit 50% of the activity (IC_{50}) were calculated. The TMA data were analyzed by one-way ANOVA using SAS 9.2 software (SAS Institute, NC, USA)

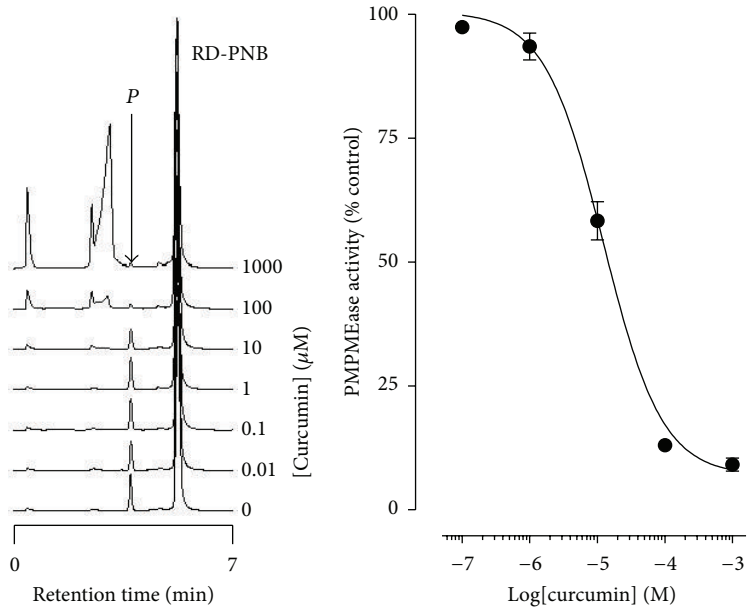

Figure 1: Inhibition of PMPMEase by curcumin. (a) Purified PMPMEase (5 μg) was incubated with RD-PNB in the presence of varying concentrations of the indicated concentrations of curcumin for 1 h. The reactions were stopped with methanol and analyzed for the residual PMPMEase activity as described in the methods section. (b) The results are expressed as the means relative to the controls (±SEM, $N = 3$).

followed by Bonferroni's procedure for multiple comparisons [57]. P-values of less than 0.05 were considered statistically significant.

3. Results

3.1. PMPMEase Activity Is Inhibited by Curcumin. When the RD-PNB substrate was incubated with purified PMPMEase in the presence of curcumin, the hydrolysis of the substrate was inhibited as denoted by significant decreases in product formation. As shown in Figure 1(a), maximum enzymatic activity was achieved in the absence of curcumin indicated by large product peak area. With increasing concentration of curcumin, there was a progressive decrease in the product peak area. When the relative amounts of product formed were plotted against the respective curcumin concentrations (Figure 1(b)), an IC_{50} value of 12.4 μM (4.4 μg/mL) and corresponding K_i of 0.31 μM were obtained.

3.2. Curcumin Inhibition of PMPMEase Is Reversible. Preincubation of PMPMEase with 10 μM curcumin followed by gel-filtration chromatography resulted in the recovery of virtually all of the enzyme activities. The comparable activities detected in analogous fractions of the curcumin-treated and untreated PMPMEase samples following gel-filtration chromatography (Figure 2(a)) are indicative of a reversible inhibition mechanism. Michaelis-Menten kinetics analysis with the RD-PNB substrate also revealed a possible mixed inhibition mechanism for curcumin against PMPMEase as depicted by changes in both Michaelis-Menten constants and $V_{\max}$ values in the presence of 20 μM curcumin (Figures 2(b) and 2(c)). The K_M for RD-PNB metabolism by PMPMEase was 23.6 ± 2.7 and 85.3 ± 15.3 μM in the absence or presence of 20 μM curcumin, respectively. On the other hand, over 3-fold change in K_M was associated with a lesser change in the $V_{\max}$ from 0.60 ± 0.02 to 0.45 ± 0.03 nmol/s/mg for the uninhibited and inhibited reactions, respectively.

3.3. Molecular Docking Analysis Reveals Multiple Curcumin Binding Sites on PMPMEase. While curcumin inhibits PMPMEase substantially, the mode of inhibition is unknown. Docking analysis of curcumin to PMPMEase revealed multiple binding sites that included one active site binding interaction and 9 allosteric sites (Figure 3). The DScore binding affinities of curcumin and the corresponding binding sites are shown in Table 1. The binding affinities measured in kcal/mole ranged from −109.73 to −206.74 for the respective binding sites of 1YAH. The specific binding energy at the active site (site 1) was −187.40 kcal/mole. This is consistent with the Michaelis-Menten kinetics analysis results (Figure 3).

3.4. PMPMEase Inhibition by Curcumin Reduces Colorectal Cancer Cell Viability. Malfunctions of polyisoprenylated proteins contribute to aberrant signaling resulting in the progression of several cancers. For example, Ras mutations that occur in over 50% of colorectal cancer cases are associated with a more aggressive disease [58]. Compounds that inhibit PMPMEase may contribute to the prevention or treatment of colorectal cancer. Cytotoxicity studies with Caco-2 cells using curcumin have yielded interesting results, and several mechanisms have been proposed for the apoptotic effects [30, 59–61]. In a study using curcumin and celecoxib, Lev-Ari and coworkers [59] proposed a synergistic inhibition

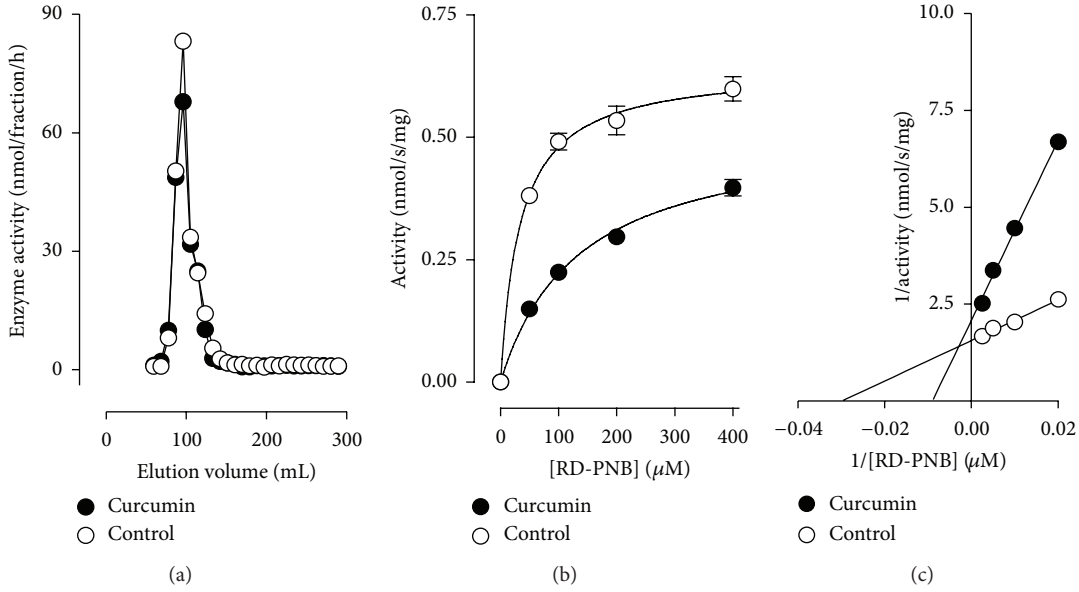

FIGURE 2: Gel-filtration analysis of curcumin-treated PMPMEase. PMPMEase was preincubated with 10 μM curcumin followed by gel-filtration chromatography to separate free curcumin from the enzyme. Aliquots of the collected fractions were assayed for residual PMPMEase activity (a). Michaelis-Menten kinetics (b) and double reciprocal analyses of the inhibition of PMPMEase by curcumin (c). Curcumin treatment (closed circles •) was compared to untreated control (open circles ○).

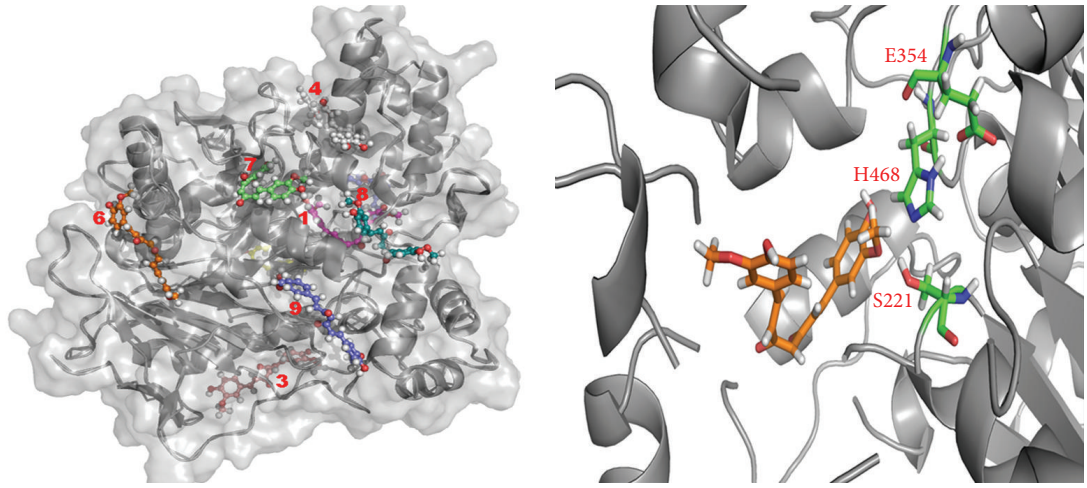

FIGURE 3: Docking analysis of curcumin binding to PMPMEase. (a) The crystal structure of hCE1/human PMPMEase (1YAH) enzyme showing the docking of curcumin at the active and allosteric sites displayed in the Licorice visualization. The visualizations were created using visual molecular dynamics (VMD). (b) Curcumin in the active site of 1YAH in the Licorice visualization. The active site catalytic triad of amino acids is shown with the coloring method (carbon atoms in blue, oxygen in red, nitrogen in dark blue, and hydrogen in white). Curcumin is shown in orange Licorice visualization.

of the COX-2 pathway for the inhibition of cell growth in HT-29 and IEC18-K-ras cells that express high levels of COX-2. However, no plausible conclusion could account for similar additive growth inhibition seen in colorectal cancer cell lines that expressed low or no COX-2 activity (Caco-2 and SW-480) [59]. We therefore sought to understand if the inhibitory effect of curcumin on PMPMEase could account for its anticancer effects using Caco-2 cells. Treatment of Caco-2 cells with curcumin resulted in the concentration-dependent inhibition of both cell viability (EC_{50} of 60 μM or 22.0 μg/mL) and cellular PMPMEase activity (IC_{50} of 61 μM or 23 μg/mL) (Figure 4). The loss of cell viability due to PMPMEase inhibition has been demonstrated in a wide variety of cell lines in our laboratory, including human neuroblastoma (SH-SY5Y) cells, human lung cancer (A549 and H460) cells, human triple negative breast cancer MDA-MB-231 cells, human pancreatic (BxPC-3) cells, and human prostate cancer (LNCaP) cells [33–35, 62]. Moreover, the EC_{50} for cell viability of 22 μg/mL obtained in this study is less than the mean curcumin level of 48.4 μg/g detected

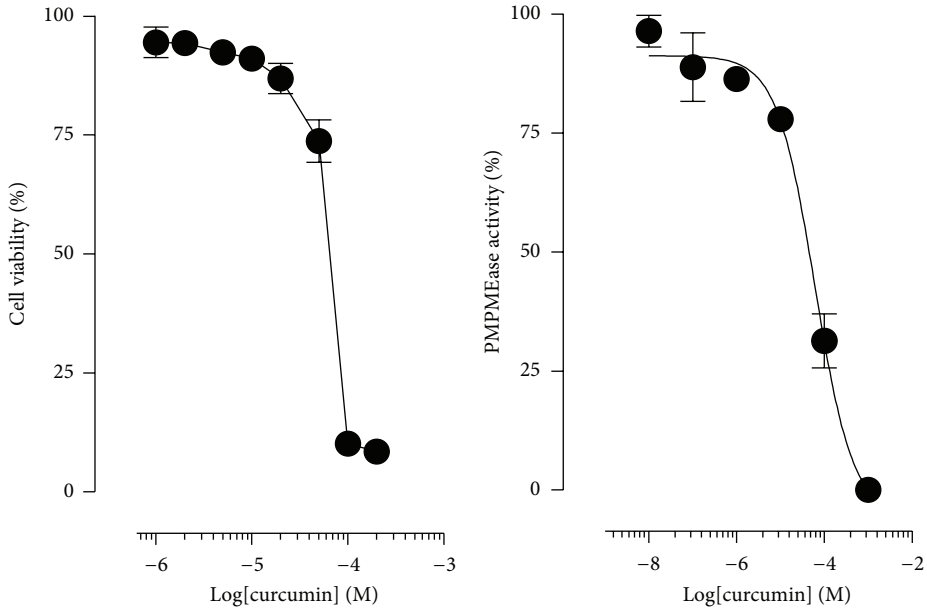

Figure 4: (a) Curcumin induced degeneration of human colorectal cancer Caco-2 cells. Human colorectal cancer Caco-2 cells were cultured and seeded in 96-well plates at a density of 2×10^4 as described in the methods. At 72 h after treatment with varying concentrations of curcumin, cell viability was measured by fluorescence using the resazurin reduction assay. Each data point represents the mean ± SEM of 4 wells. The data are representative of 3 separate experiments (EC_{50} = 22.0 μg/mL). (b) PMPMEase activity in degenerating curcumin-treated human colorectal cancer Caco-2 cells. Cells were cultured to 80% confluence, lysed, and incubated with the indicated concentrations of curcumin as described in the methods. The residual PMPMEase activity was then determined using RD-PNB as the substrate. Each point represents the mean ± SEM (n = 3). The data are representative of 3 separate experiments (IC_{50} = 22.6 μg/mL).

in human colorectal tissue biopsies after daily oral doses of 2.35 g curcuminoids [63], bearing in mind a tissue density of about 1.06 g/mL.

3.5. PMPMEase Is Overexpressed in Colon Cancer. The colon cancer TMA was analyzed for the relative expression of PMPMEase. The demographic and histopathological characteristics of the tissue donors for the TMAs are shown in Table 2. The ages of the patients ranged from 23 to 90 years, and most of them (67.3%) were males. There were 175 cases of adenocarcinoma, 15 cases of mucinous adenocarcinoma and 1 case each of papillary adenoma and signet ring cell carcinoma. In general, 88.6% of the colon cancers showed intracellular PMPMEase immunoreactivity. The data indicate that increasing levels of PMPMEase expression are associated with tumors (Figure 5(a)). In the control cores consisting of normal colon tissues and normal adjacent colon tissues, either negative or focal mild cytoplasmic immunostaining was observed. Meanwhile, solid tumors with intensely stained cells were displayed especially in most of the colon adenocarcinoma, mucinous adenocarcinomas, and signet ring cell carcinoma. Figures 5(a) and 5(b) show representative images of normal colon and colon cancer tissues. Significant differences in PMPMEase immunoreactivity intensities between the normal tissues and the different colon tumor categories were observed when the IHC-stained sections were analyzed (P = 0.0002–<0.0001) (Table 3). Paired comparisons of immunoreactivity scores for PMPMEase proteins between normal tissues versus tumors and normal adjacent tissues versus metastatic tumors were significant ($P < 0.0001$). The mean scores ± SEM were 91.7 ± 11.4 for normal, 75.0 ± 14.4 for normal adjacent, 294.8 ± 7.8 for adenocarcinoma, and 310.0 ± 22.6 for mucinous adenocarcinoma. Relatively high PMPMEase expression (score = 301–400) was observed in both the papillary adenoma and signet ring cell carcinoma. Although no specific trend was observed when the data were analyzed according to pathological stages, grades, tumor size, nodal status, and metastases, there were significant differences when compared to the normal colon tissues and the NATs regardless of the parameter under consideration. Taken together, these findings show that PMPMEase protein is overexpressed in colorectal cancer.

3.6. PMPMEase Gene Is Overexpressed in Colon Cancer. The Oncomine database queried to systematically assess relative gene expression levels of PMPMEase (CES1) genes in colorectal tumors. We have analyzed the studies that showed a significant fold change gene expression ($P \leq 0.001$) in cancerous tissues. Although some of the studies showed some cases of downregulation of PMPMEase [40, 45, 47], most of the studies retrieved showed significant overexpression of the PMPMEase (Table 4).

4. Discussion

Despite the remarkable recent advances in surgical excision, radiotherapy, and chemotherapeutic regimens, the high recurrence rates and fatalities from colorectal cancer [64]

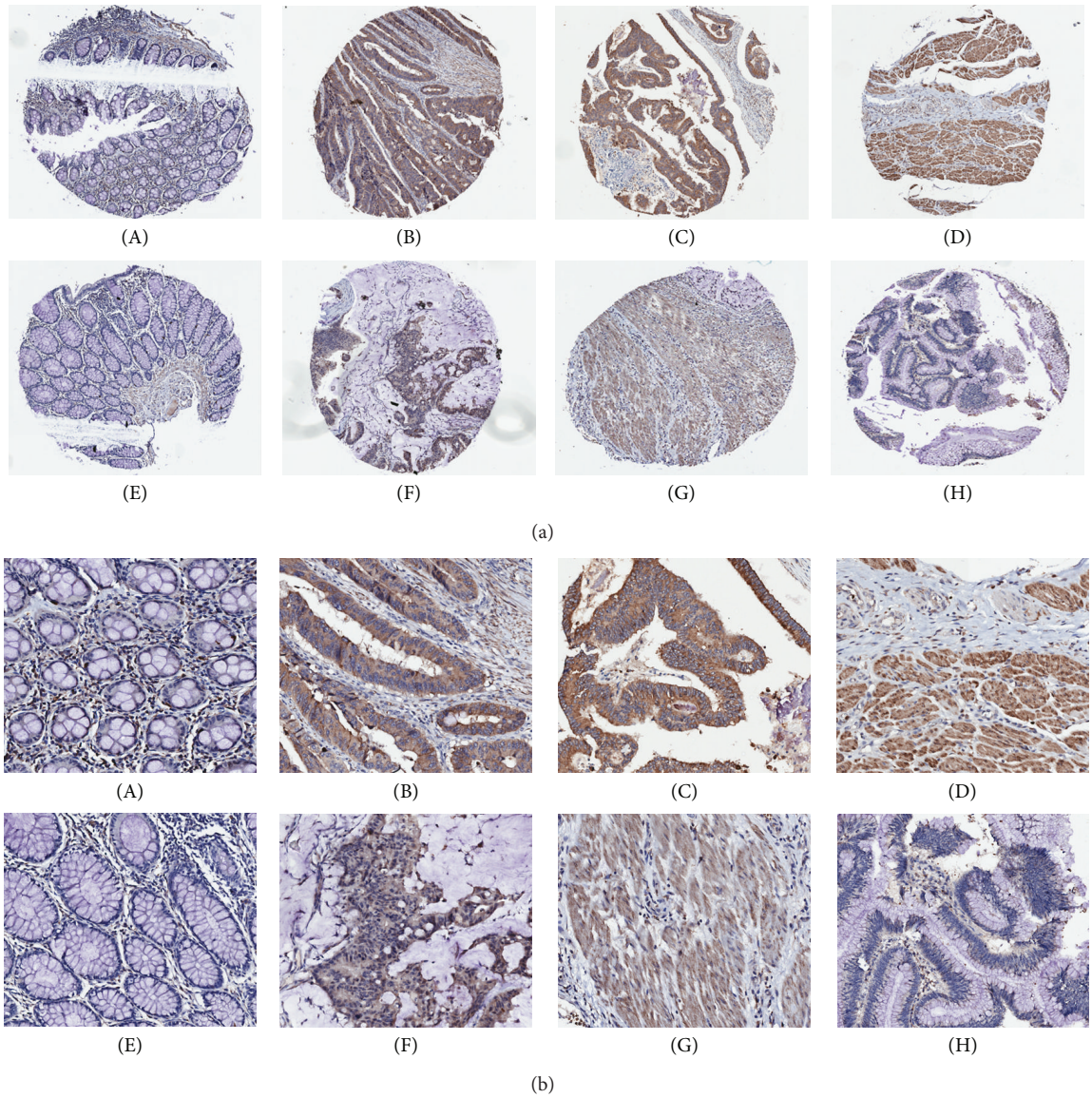

Figure 5: (a) Immunohistochemical analysis of TMA cores from colon cancer cases showing brown staining for PMPMEase immunoreactivity. The TMAs were probed with PMPMEase antibodies and scored for the relative intensities of PMPMEase staining as described in the methods. Intense staining was observed in colon adenocarcinoma (stage I, B, C and D), mucinous adenocarcinomas (stage 2, F), signet ring cell carcinoma (stage II, G) and papillary adenoma (stage 2, H). A and E are images of sections obtained from normal colon tissue and normal adjacent tissue, respectively. Each image is of a section from the tumor of a separate case. (b) Magnified sections of colon adenocarcinoma (B, C and D), mucinous adenocarcinomas (F), signet ring cell carcinoma (G) and papillary adenoma (H). Areas with dense populations of blue-stained nuclei indicative of tumor cells also show a higher intensity of brown staining for PMPMEase. A and E are magnified images of sections obtained from normal colon and normal adjacent tissues, respectively.

imply that its management remains an area of unmet medical need. Prevention plays a vital role in limiting the impact of the disease. Understanding the mechanisms by which bioactive substances such as curcumin exert their pharmacological effects is essential for maximizing the health benefits. Therefore, identifying the target with which curcumin interacts is essential for fully understanding its mechanism of action. In this study, we determined that PMPMEase, while being overexpressed in colon cancer, is also susceptible to inhibition by curcumin. These interesting observations are pertinent in two respects (i) that PMPMEase, given previous studies linking its inhibition to cancer cell death [33–35], likely contributes to at least some cases of colorectal cancer progression and (ii) that the widely reported chemopreventive effects of curcumin [18, 19, 26] are due at least in part to PMPMEase inhibition. The elevation of PMPMEase protein levels in this study is corroborated by previous studies in which mRNA levels were determined to be significantly higher in some cases of colorectal cancers as revealed by the Oncomine database analysis.

The overexpression of PMPMEase in colon cancer is significant in view of the role that polyisoprenylated proteins

Table 2: Demographic, histopathological characteristics and the disease states of the 208 donors of the colon tissues used in the tissue microarray studies.

Characteristics	Patients	
	n	(%)
Age		
≤65 years	152	73.1
>65 years	56	26.9
Sex		
Female	68	32.7
Male	140	67.3
Histology		
Normal	12	5.8
NAT	4	1.9
Adenocarcinomas	175	84.1
Mucinous adenocarcinoma	15	7.2
Papillary adenoma	1	0.4
Signet ring cell carcinoma	1	0.4
Grade		
1	35	16.8
2	101	48.6
2-3	10	4.8
3	22	10.6
Not determined	24	11.5
Pathological stage		
I	92	44.2
II	89	42.8
III	6	2.9
IV	5	2.4
Tumor status		
1	1	0.4
2	53	25.5
3	90	43.3
4	48	23.1
Nodal status		
0	176	84.6
1	13	6.3
2	1	0.4
Metastasis		
0	187	89.9
1	4	1.9

play in cell growth and motility. Mutant constitutively active forms of members of the Ras superfamily of proteins are observed in about 50% of colorectal cancer cases [32, 58, 65]. More importantly, signaling pathways involving aberrant activities of these monomeric G-proteins are common in colorectal cancer [11, 32]. Gulhati and coworkers [11] reported that mTORC1 and mTORC2 regulate changes in the actin cytoskeleton and cell migration by signaling through RhoA and Rac1 pathways [11]. The Rho family of GTPases are involved in the formation of lamellipodia and cell migration [10]. Also, while mutations and/or overexpression are linked to their tumorigenic activities, secondary modifications are essential for their normal and pathological activities [32, 66]. Although the polyisoprenylation pathway enzymes have been the subjects of pharmaceutical development efforts [12], the role of PMPMEase in regulating polyisoprenylated protein function is only just getting attention [67]. Therefore the overexpression of PMPMEase in colon cancer highlights its role as a potential target for curcumin and other food-derived bioactive compounds. Its putative endogenous substrates include not only the monomeric G-proteins but also the heterotrimeric G-protein-coupled receptors (GPCRs) whose contributions in cancers have also been widely reported [32, 66]. GPCRs constitute a large family of plasma membrane receptors that rely on the heterotrimeric G-proteins for intracellular signal transduction [68]. The γ-subunits of these trimeric complexes are polyisoprenylated, a feature that is essential for their functions [69]. Signaling through GPCRs such as some eicosanoid [70, 71], chemokine [72, 73], and adrenergic [74, 75] receptors play important roles in human colorectal cancer growth and metastasis. A recent study revealed that galanin receptor 1 (GalR1) and its ligand galanin are key determinants of drug resistance and potential therapeutic targets for combating drug resistance [76]. Bearing in mind that PMPMEase is one of two enzymes that catalyze reactions in the only reversible step of the pathway, its hyperactivity is bound to distort the equilibrium in favor of cell growth stimulation.

The observation that curcumin inhibits PMPMEase is pertinent for our understanding of the chemopreventive mechanism of this important food-derived agent [77]. Although several mechanisms of action have been proposed for curcumin [27, 30, 31, 77], they do not appear to exclude the involvement of PMPMEase as an intermediary since effects on polyisoprenylated protein metabolism inevitably impact transcriptional activity. For example, curcumin has been shown to downregulate the expression of EGFR, COX-2, LOX, NOS, MMP-9, uPA, TNF, chemokines, cell surface adhesion molecules, cyclin D1, the transcription factors NF-κB, AP-1, Egr-1 as well as inhibiting c-Jun N-terminal, protein tyrosine, and protein serine/threonine phosphorylation [30, 31, 77]. We previously demonstrated that PMPMEase is inhibited by PUFAs but not by prostaglandins [35]. The overexpression of PMPMEase in colorectal cancer, its inhibition by curcumin and its differential susceptibility to the PUFAs and PGs are significant against the backdrop of COX-2 overexpression especially in colorectal cancer. Furthermore, long-term use of NSAIDs is associated with lower cancer risks [78, 79]. Considering this and the numerous reports that COX-2 and PGs are important in the development and progression of cancers [80], it has been opined that COX-2-selective inhibition holds a promising role in cancer chemoprevention [78]. Therefore a mechanism for curcumin action that involves the suppression of PUFAs-oxidizing enzymes would be consistent with preserving the PUFAs for PMPMEase inhibition. An inhibited PMPMEase is likely to modulate the actions of polyisoprenylated proteins such as Ras and its signaling pathways as previously reported [31]. Curcumin and its derivatives have also been reported to inhibit farnesyl transferase, a polyisoprenylation pathway enzyme essential for the transformation of Ras into its biologically active form [81, 82].

Table 3: Association of PMPMEase immunoreactivity with the pathologic features of colon cancer. Significantly higher PMPMEase immunoreactivities were observed in the different types, grades, and stages of colon cancers as shown by the means ± SEM versus normal tissues compared by ANOVA followed by Dunnet's post test.

Characteristics	PMPMEase Staining Intensity, *N* (%)					Missing	Mean Scores	*P*-value
	1–100 Trace	101–200 Weak	201–300 Intermediate	301–400 Strong	401–500 Very strong			
Normal	11 (75.0)	3 (25.0)	0	0	0	0	91.7 ± 11.4	
NAT	4 (100)	0	0	0	0	0	75.0 ± 14.4	
Histology								
Adenocarcinomas	7 (4.0)	30 (17.1)	57 (32.6)	54 (30.9)	20 (11.4)	7 (4.0)	294.8 ± 7.8	0.0001
Mucinous adenocarcinoma	1 (6.7)	1 (6.7)	6 (40.0)	6 (40.0)	1 (6.7)	0	310.0 ± 22.6	
Papillary adenoma	0	0	0	1 (100.0)	0	0		
Signet ring cell carcinoma	0	0	0	1 (100.0)	0	0		
Pathological stage								
I	2 (2.2)	13 (14.1)	33 (35.9)	32 (34.8)	10 (10.9)	2 (2.2)	306.1 ± 10.0	
II	5 (5.6)	16 (18.0)	26 (29.2)	28 (31.5)	11 (12.4)	3 (3.4)	291.6 ± 11.2	0.0001
III	1 (16.7)	1 (16.7)	1 (16.7)	2 (33.3)	0	1 (16.7)	270.0 ± 53.3	
IV	0	1 (20.0)	3 (60.0)	0	0	1 (20.0)	218.8 ± 35.9	
Grade								
1	2 (5.7)	5 (14.3)	8 (22.9)	18 (51.4)	2 (5.7)	0	306.4 ± 17.1	
2	4 (4.0)	22 (21.8)	37 (36.7)	25 (24.8)	10 (9.9)	3 (3.0)	281.6 ± 9.9	
2-3	0	0	5 (50.0)	5 (50.0)	0	0	302.5 ± 18.1	0.0001
3	2 (9.1)	3 (13.6)	10 (45.5)	5 (22.7)	2 (9.1)	0	270.5 ± 21.7	
Not determined	0	1 (4.2)	3 (12.5)	9 (37.5)	7 (29.2)	4 (16.7)	377.5 ± 18.6	

Table 4: PMPMEase (CES1) gene is overexpressed in human colorectal cancers. Oncomine studies used in this analysis are shown below.

Cases	Number of cases with fold change greater than 2		Year of study	References
	Downregulated	Upregulated		
70	7 (10%)	28 (40%)	2010	[39]
22	5 (22%)	12 (55%)	2007	[40]
48	1 (2%)	16 (33%)	2006	[41]
100		33 (33%)	2007	[42]
12		7 (58%)	2001	[43]
13		9 (69%)	2003	[44]
154	10 (7%)	50 (32%)	2009	[45]
23		3 (13%)	2008	[46]
80	12 (15%)	58 (73%)	2007	[47]
55	2 (4%)	9 (16%)	2007	[48]
177		59 (33%)	2010	[49]
62		7 (11%)	2009	[50]
42	4 (10%)	14 (33%)	2006	[51]
104		18 (17%)	2011	[52]
176		82 (46%)	2011	[53]

Number of cases with significant fold change ($P < 0.001$) and the percentage (in brackets) of the number of their respective cases are indicated.

That curcumin's anticancer activities are mediated through PMPMEase inhibition is further substantiated by our previous findings in which PMPMEase inhibition with specifically designed polyisoprenylated sulfonyl fluorides resulted in cancer cell death [33]. That such a profound cellular effect occurs upon PMPMEase inhibition has been explained by the significant conformational changes near the physiologically important polyisoprenyl moiety of the signaling proteins. The polyisoprenyl moiety is pertinent for the functional interactions of polyisoprenylated proteins with other proteins [83]. The charge difference due to the change in methylation-demethylation balance is believed to be similar in effects on conformations as do the phosphorylation-dephosphorylation of kinase-regulated proteins [84].

The observation through docking analysis that curcumin may interact competitively with the active site and allosterically with other sites likely explains the mixed antagonism characteristics observed with the Michealis-Menten kinetics analysis. The susceptibility of PMPMEase to PUFAs and curcumin suggests that it may be a target for other food-derived anticancer agents. Food-derived agents, especially flavonoids such as *all trans* geranylgeraniol, farnesol-mixed isomers, *trans trans* farnesol, eugenol, α-Ionone, and 2,3-heptanedione have structures that resemble the polyisoprenes. These hydrophobic molecules are of the appropriate sizes to enter the active site and competitively inhibit the enzyme. The active site of PMPMEase is large, flexible, and lined with hydrophobic aromatic amino acid residues [85]. This property promotes binding to a wide variety of mainly hydrophobic molecules [85] while also precluding oxidized more hydrophilic analogs [35].

The current findings further reveal the pertinent role that PMPMEase plays in colorectal cancer and how its levels of activity and expression can be exploited in companion diagnosis. It is also increasingly apparent that PMPMEase is susceptible to inhibition by various food-derived chemopreventive agents thus implying that a systematic screening of such substances may reveal a repertoire of such compounds for nutraceuticals. Several studies using various animal models or human subjects indicate that curcumin is very safe, even at a very high dose of 12 g per day. This dose can easily be obtained when curcumin is included in food as a spice and/or a food preservative. Howells et al. [86] showed that low doses of curcumin produced colonic tissue concentrations of an order of magnitude associated with pharmacological effects, both in cells *in vitro* and in rodents *in vivo*. Ravindranath and Chandrasekhara [87] showed that, after oral administration of curcumin (2 g/kg), the levels detected in the stomach, small intestine, cecum, and large intestine were 53.3 ± 5.1 μg/g, 58.6 ± 11.0 μg/g, 51.5 ± 13.5 μg/g, and 5.1 ± 2.5 μg/g, respectively. In a more recent study by Irving et al. [63], daily oral curcuminoids (2.35 g) resulted in a mean curcumin level colorectal tissue biopsies of 48.4 μg/g without prior washing which has been a standard practice for both clinical and *in vivo* studies. However, washing the tissue reduced this difference to only 2-fold with mean washed tissue levels of 18.85 μg/g. Therefore, the EC_{50} for cell viability of 60 μM (22 μg/mL) obtained in this study is within the range achievable *in vivo,* assuming average tissue densities of about 1.06 g/mL.

Finally, these studies strongly suggest that potent, rationally designed PMPMEase inhibitors would be invaluable therapeutic agents in the management of those colorectal cancers cases in which PMPMEase expression and activities are elevated.

5. Conclusion

In summary, elevated PMPMEase activity and its overexpression in colon cancer makes it a suitable biomarker that can be developed into a procedure for the early/companion diagnosis of colon cancer. The susceptibility of PMPMEase to PUFAs and curcumin suggests that it may be a target for other food-derived anticancer agents. Potent and specific inhibitors of PMPMEase could eventually be developed as a new class of targeted therapies for colorectal cancers cases in which PMPMEase expression and activities are elevated.

Acknowledgments

This project was supported by the National Center for Research Resources and the National Institute of Minority Health and Health Disparities of the NIH through Grant number 8 G12 MD007582-28 and 2 G12 RR003020.

References

[1] R. Siegel, D. Naishadham, and A. Jemal, "Cancer statistics, 2012," *CA Cancer Journal for Clinicians*, vol. 62, no. 1, pp. 10–29, 2012.

[2] A. C. Society, "Colorectal Cancer Facts & Figures. American Cancer Society Atlanta, Georgia: (2011–2013)".

[3] N. T. Telang, G. Li, and M. Katdare, "Prevention of early-onset familial/hereditary colon cancer: new models and mechanistic biomarkers," *International Journal of Oncology*, vol. 28, no. 6, pp. 1523–1529, 2006.

[4] J. H. Scholefield and R. J. Steele, "Guidelines for follow up after resection of colorectal cancer," *Gut*, vol. 51, no. 5, pp. v3–v5, 2002.

[5] M. M. Amitai, H. Fidder, B. Avidan et al., "Contrast-enhanced CT colonography with 64-slice MDCT compared to endoscopic colonoscopy in the follow-up of patients after colorectal cancer resection," *Clinical Imaging*, vol. 33, no. 6, pp. 433–438, 2009.

[6] H. Kobayashi, H. Mochizuki, K. Sugihara et al., "Characteristics of recurrence and surveillance tools after curative resection for colorectal cancer: a multicenter study," *Surgery*, vol. 141, no. 1, pp. 67–75, 2007.

[7] S. Roy and A. P. Majumdar, "Signaling in colon cancer stem cells," *Journal of Molecular Signaling*, vol. 7, article 11, 2012.

[8] J. P. Welch and G. A. Donaldson, "The clinical correlation of an autopsy study of recurrent colorectal cancer," *Annals of Surgery*, vol. 189, no. 4, pp. 496–502, 1979.

[9] M. R. Griffin, E. J. Bergstralh, R. J. Coffey, R. W. Beart Jr., and L. J. Melton III, "Predictors of survival after curative resection of carcinoma of the colon and rectum," *Cancer*, vol. 60, no. 9, pp. 2318–2324, 1987.

[10] A. Hall, "Rho GTpases and the actin cytoskeleton," *Science*, vol. 279, no. 5350, pp. 509–514, 1998.

[11] P. Gulhati, K. A. Bowen, J. Liu et al., "mTORC1 and mTORC2 regulate EMT, motility, and metastasis of colorectal cancer via RhoA and Rac1 signaling pathways," *Cancer Research*, vol. 71, no. 9, pp. 3246–3256, 2011.

[12] A. D. Cox and C. J. Der, "Farnesyltransferase inhibitors and cancer treatment: targeting simply ras?" *Biochimica et Biophysica Acta*, vol. 1333, no. 1, pp. F51–F71, 1997.

[13] Y. Kloog, M. Zatz, and B. Rivnay, "Nonpolar lipid methylation: identification of nonpolar methylated products synthesized by rat basophilic leukemia cells, retina and parotid," *Biochemical Pharmacology*, vol. 31, no. 5, pp. 753–759, 1982.

[14] P. J. Casey, "Biochemistry of protein prenylation. Review," *Journal of Lipid Research*, vol. 33, no. 12, pp. 1731–1740, 1992.

[15] S.-M. Kuo, H. F. Morehouse Jr., and C.-P. Lin, "Effect of antiproliferative flavonoids on ascorbic acid accumulation in human colon adenocarcinoma cells," *Cancer Letters*, vol. 116, no. 2, pp. 131–137, 1997.

[16] E. Rudolf, H. Andělová, and M. Červinka, "Polyphenolic compounds in chemoprevention of colon cancer—targets and signaling pathways," *Anti-Cancer Agents in Medicinal Chemistry*, vol. 7, no. 5, pp. 559–575, 2007.

[17] K. C. Srivastava, A. Bordia, and S. K. Verma, "Curcumin, a major component of food spice turmeric (Curcuma longa) inhibits aggregation and alters eicosanoid metabolism in human blood platelets," *Prostaglandins Leukotrienes and Essential Fatty Acids*, vol. 52, no. 4, pp. 223–227, 1995.

[18] Y.-J. Surh and K.-S. Chun, "Cancer chemopreventive effects of curcumin," *Advances in Experimental Medicine and Biology*, vol. 595, pp. 149–172, 2007.

[19] J. J. Johnson and H. Mukhtar, "Curcumin for chemoprevention of colon cancer," *Cancer Letters*, vol. 255, no. 2, pp. 170–181, 2007.

[20] A. Jacob, R. Wu, M. Zhou, and P. Wang, "Mechanism of the anti-inflammatory effect of curcumin: PPAR-γ activation," *PPAR Research*, vol. 2007, Article ID 89369, 5 pages, 2007.

[21] S. Bengmark, "Curcumin, an atoxic antioxidant and natural NFκB, cyclooxygenase-2, lipooxygenase, and inducible nitric oxide synthase inhibitor: a shield against acute and chronic diseases," *Journal of Parenteral and Enteral Nutrition*, vol. 30, no. 1, pp. 45–51, 2006.

[22] M.-T. Huang, Y.-R. Lou, W. Ma, H. L. Newmark, K. R. Reuhl, and A. H. Conney, "Inhibitory effects of dietary curcumin on forestomach, duodenal, and colon carcinogenesis in mice," *Cancer Research*, vol. 54, no. 22, pp. 5841–5847, 1994.

[23] T. Dorai, Y.-C. Cao, B. Dorai, R. Buttyan, and A. E. Katz, "Therapeutic potential of curcumin in human prostate cancer. III. Curcumin inhibits proliferation, induces apoptosis, and inhibits angiogenesis of LNCaP prostate cancer cells in vivo," *Prostate*, vol. 47, no. 4, pp. 293–303, 2001.

[24] R. J. Anto, A. Mukhopadhyay, K. Denning, and B. B. Aggarwal, "Curcumin (diferuloylmethane) induces apoptosis through activation of caspase-8, BID cleavage and cytochrome c release: its suppression by ectopic expression of Bcl-2 and Bcl-xl," *Carcinogenesis*, vol. 23, no. 1, pp. 143–150, 2002.

[25] P. Anand, A. B. Kunnumakkara, R. A. Newman, and B. B. Aggarwal, "Bioavailability of curcumin: problems and promises," *Molecular Pharmaceutics*, vol. 4, no. 6, pp. 807–818, 2007.

[26] T. Kawamori, R. Lubet, V. E. Steele et al., "Chemopreventive effect of curcumin, a naturally occurring anti-inflammatory agent, during the promotion/progression stages of colon cancer," *Cancer Research*, vol. 59, no. 3, pp. 597–601, 1999.

[27] M.-T. Huang, T. Lysz, T. Ferraro, T. F. Abidi, J. D. Laskin, and A. H. Conney, "Inhibitory effects of curcumin on in vitro lipoxygenase and cyclooxygenase activities in mouse epidermis," *Cancer Research*, vol. 51, no. 3, pp. 813–819, 1991.

[28] J. S. Shim, J. H. Kim, H. Y. Cho et al., "Irreversible inhibition of CD13/aminopeptidase N by the antiangiogenic agent curcumin," *Chemistry and Biology*, vol. 10, no. 8, pp. 695–704, 2003.

[29] J. L. Arbiser, N. Klauber, R. Rohan et al., "Curcumin is an in vivo inhibitor of angiogenesis," *Molecular Medicine*, vol. 4, no. 6, pp. 376–383, 1998.

[30] A. Chen, J. Xu, and A. C. Johnson, "Curcumin inhibits human colon cancer cell growth by suppressing gene expression of epidermal growth factor receptor through reducing the activity of the transcription factor Egr-1," *Oncogene*, vol. 25, no. 2, pp. 278–287, 2006.

[31] L.-X. Wu, J.-H. Xu, G.-H. Wu, and Y.-Z. Chen, "Inhibitory effect of curcumin on proliferation of K562 cells involves down-regulation of p210bcr/abl-initiated Ras signal transduction pathway," *Acta Pharmacologica Sinica*, vol. 24, no. 11, pp. 1155–1175, 2003.

[32] A. A. Adjei, "Blocking oncogenic Ras signaling for cancer therapy," *Journal of the National Cancer Institute*, vol. 93, no. 14, pp. 1062–1074, 2001.

[33] B. Aguilar, F. Amissah, R. Duverna, and N. S. Lamango, "Polyisoprenylation potentiates the inhibition of polyisoprenylated methylated protein methyl esterase and the cell degenerative effects of sulfonyl fluorides," *Current Cancer Drug Targets*, vol. 11, no. 6, pp. 752–762, 2011.

[34] L. Ayuk-Takem, F. Amissah, B. J. Aguilar, and N. S. Lamango, "Inhibition of polyisoprenylated methylated protein methyl esterase by synthetic musks induces cell degeneration," *Environmental Toxicology*, 2012.

[35] F. Amissah, S. Taylor, R. Duverna, L. T. Ayuk-Takem, and N. S. Lamango, "Regulation of polyisoprenylated methylated protein methyl esterase by polyunsaturated fatty acids and

prostaglandins," *European Journal of Lipid Science and Technology*, vol. 113, no. 11, pp. 1321–1331, 2011.

[36] O. T. Oboh and N. S. Lamango, "Liver prenylated methylated protein methyl esterase is the same enzyme as Sus scrofa carboxylesterase," *Journal of Biochemical and Molecular Toxicology*, vol. 22, no. 1, pp. 51–62, 2008.

[37] N. S. Lamango, R. Duverna, W. Zhang, and S. Y. Ablordeppey, "Porcine Liver Carboxylesterase Requires Polyisoprenylation for High Affinity Binding to Cysteinyl Substrates," *Open Enzyme Inhibition Journal*, vol. 2, pp. 12–27, 2009.

[38] R. Duverna, S. Y. Ablordeppey, and N. S. Lamango, "Biochemical and docking analysis of substrate interactions with polyisoprenylated methylated protein methyl esterase," *Current Cancer Drug Targets*, vol. 10, no. 6, pp. 634–648, 2010.

[39] Y. Hong, T. Downey, K. W. Eu, P. K. Koh, and P. Y. Cheah, "A "metastasis-prone" signature for early-stage mismatch-repair proficient sporadic colorectal cancer patients and its implications for possible therapeutics," *Clinical and Experimental Metastasis*, vol. 27, no. 2, pp. 83–90, 2010.

[40] Y. Hong, S. H. Kok, W. E. Kong, and Y. C. Peh, "A susceptibility gene set for early onset colorectal cancer that integrates diverse signaling pathways: implication for tumorigenesis," *Clinical Cancer Research*, vol. 13, no. 4, pp. 1107–1114, 2007.

[41] E. Graudens, V. Boulanger, C. Mollard et al., "Deciphering cellular states of innate tumor drug responses," *Genome Biology*, vol. 7, no. 3, article R19, 2006.

[42] S. Kaiser, Y.-K. Park, J. L. Franklin et al., "Transcriptional recapitulation and subversion of embryonic colon development by mouse colon tumor models and human colon cancer," *Genome Biology*, vol. 8, no. 7, article R131, 2007.

[43] S. Ramaswamy, P. Tamayo, R. Rifkin et al., "Multiclass cancer diagnosis using tumor gene expression signatures," *Proceedings of the National Academy of Sciences of the United States of America*, vol. 98, no. 26, pp. 15149–15154, 2001.

[44] S. Ramaswamy, K. N. Ross, E. S. Lander, and T. R. Golub, "A molecular signature of metastasis in primary solid tumors," *Nature Genetics*, vol. 33, no. 1, pp. 49–54, 2003.

[45] R. N. Jorissen, P. Gibbs, M. Christie et al., "Metastasis-associated gene expression changes predict poor outcomes in patients with Dukes stage B and C colorectal cancer," *Clinical Cancer Research*, vol. 15, no. 24, pp. 7642–7651, 2009.

[46] J. T. Auman, R. Church, S.-Y. Lee, M. A. Watson, J. W. Fleshman, and H. L. Mcleod, "Celecoxib pre-treatment in human colorectal adenocarcinoma patients is associated with gene expression alterations suggestive of diminished cellular proliferation," *European Journal of Cancer*, vol. 44, no. 12, pp. 1754–1760, 2008.

[47] S. Khambata-Ford, C. R. Garrett, N. J. Meropol et al., "Expression of epiregulin and amphiregulin and K-ras mutation status predict disease control in metastatic colorectal cancer patients treated with cetuximab," *Journal of Clinical Oncology*, vol. 25, no. 22, pp. 3230–3237, 2007.

[48] Y.-H. Lin, J. Friederichs, M. A. Black et al., "Multiple gene expression classifiers from different array platforms predict poor prognosis of colorectal cancer," *Clinical Cancer Research*, vol. 13, no. 2, pp. 498–507, 2007.

[49] J. J. Smith, N. G. Deane, F. Wu et al., "Experimentally derived metastasis gene expression profile predicts recurrence and death in patients with colon cancer," *Gastroenterology*, vol. 138, no. 3, pp. 958–968, 2010.

[50] E. Staub, J. Groene, M. Heinze et al., "An expression module of WIPF1-coexpressed genes identifies patients with favorable prognosis in three tumor types," *Journal of Molecular Medicine*, vol. 87, no. 6, pp. 633–644, 2009.

[51] D. Chowdary, J. Lathrop, J. Skelton et al., "Prognostic gene expression signatures can be measured in tissues collected in RNAlater preservative," *Journal of Molecular Diagnostics*, vol. 8, no. 1, pp. 31–39, 2006.

[52] S. Tsukamoto, T. Ishikawa, S. Iida et al., "Clinical significance of osteoprotegerin expression in human colorectal cancer," *Clinical Cancer Research*, vol. 17, no. 8, pp. 2444–2450, 2011.

[53] E. Vilar, C. M. Bartnik, S. L. Stenzel et al., "MRE11 deficiency increases sensitivity to poly(ADP-ribose) polymerase inhibition in microsatellite unstable colorectal cancers," *Cancer Research*, vol. 71, no. 7, pp. 2632–2642, 2011.

[54] S. Sybyl-X, Tripos, Inc., St. Louis, Mo, USA, 2012.

[55] K. A. Spivey, J. Banyard, L. M. Solis et al., "Collagen XXIII: a potential biomarker for the detection of primary and recurrent non-small cell lung cancer," *Cancer Epidemiology Biomarkers and Prevention*, vol. 19, no. 5, pp. 1362–1372, 2010.

[56] R. M. Bremnes, R. Veve, E. Gabrielson et al., "High-throughput tissue microarray analysis used to evaluate biology and prognostic significance of the E-cadherin pathway in non-small-cell lung cancer," *Journal of Clinical Oncology*, vol. 20, no. 10, pp. 2417–2428, 2002.

[57] B. Rosner, Ed., *Fundamentals of Biostatistics*, Duxbury Press, Boston, Mass, USA, 2011.

[58] S. Tortola, E. Marcuello, I. González et al., "p53 and K-ras gene mutations correlate with tumor aggressiveness but are not of routine prognostic value in colorectal cancer," *Journal of Clinical Oncology*, vol. 17, no. 5, pp. 1375–1381, 1999.

[59] S. Lev-Ari, L. Strier, D. Kazanov et al., "Celecoxib and curcumin synergistically inhibit the growth of colorectal cancer cells," *Clinical Cancer Research*, vol. 11, no. 18, pp. 6738–6744, 2005.

[60] R. Raveendran, G. S. Bhuvaneshwar, and C. P. Sharma, "In vitro cytotoxicity and cellular uptake of curcumin-loaded Pluronic/Polycaprolactone micelles in colorectal adenocarcinoma cells," *Journal of Biomaterials Applications*, vol. 27, no. 7, pp. 811–827, 2013.

[61] Y. Cheng, A. Kozubek, L. Ohlsson, B. Sternby, and R.-D. Duan, "Curcumin decreases acid sphingomyelinase activity in colon cancer caco-2 cells," *Planta Medica*, vol. 73, no. 8, pp. 725–730, 2007.

[62] F. Amissah, R. A. Poku, B. J. Aguilar, R. Duverna, B. O. Abonyo, and N. S. Lamango, *Polyisoprenylated Methylated Protein Methylesterase: The Fulcrum of Chemopreventive Effects of NSAIDs and PUFAs*, Nova Science, 2013.

[63] G. R. Irving, L. M. Howells, S. Sale et al., "Prolonged biologically active colonic tissue levels of curcumin achieved after oral administration—a clinical pilot study including assessment of patient acceptability," *Cancer Prevention Research (Phila)*, vol. 6, pp. 119–128, 2012.

[64] V. Dancourt, C. Quantin, M. Abrahamowicz, C. Binquet, A. Alioum, and J. Faivre, "Modeling recurrence in colorectal cancer," *Journal of Clinical Epidemiology*, vol. 57, no. 3, pp. 243–251, 2004.

[65] M. Islam, G. Lin, J. C. Brenner et al., "RhoC expression and head and neck cancer metastasis," *Molecular Cancer Research*, vol. 7, no. 11, pp. 1771–1780, 2009.

[66] P. A. Konstantinopoulos, M. V. Karamouzis, and A. G. Papavassiliou, "Post-translational modifications and regulation of the RAS superfamily of GTPases as anticancer targets," *Nature Reviews Drug Discovery*, vol. 6, no. 7, pp. 541–555, 2007.

[67] M. A. Kutuzov, A. V. Andreeva, and N. Bennett, "Regulation of the methylation status of G protein-coupled receptor kinase 1 (rhodopsin kinase)," *Cell Signal*, vol. 24, pp. 2259–2267, 2012.

[68] J.-P. Pin, R. Neubig, M. Bouvier et al., "International union of basic and clinical pharmacology. LXVII. Recommendations for the recognition and nomenclature of G protein-coupled receptor heteromultimers," *Pharmacological Reviews*, vol. 59, no. 1, pp. 5–13, 2007.

[69] A. Dietrich, D. Brazil, O. N. Jensen et al., "Isoprenylation of the G protein γ subunit is both necessary and sufficient for $\beta\gamma$ dimer-mediated stimulation of phospholipase C," *Biochemistry*, vol. 35, no. 48, pp. 15174–15182, 1996.

[70] A. Chandramouli, M. E. Mercado-Pimentel, A. Hutchinson et al., "The induction of S100p expression by the prostaglandin E2 (PGE2)/EP4 receptor signaling pathway in colon cancer cells," *Cancer Biology and Therapy*, vol. 10, no. 10, pp. 1056–1066, 2010.

[71] M.-C. Cathcart, J. Lysaght, and G. P. Pidgeon, "Eicosanoid signalling pathways in the development and progression of colorectal cancer: novel approaches for prevention/intervention," *Cancer and Metastasis Reviews*, vol. 30, no. 3-4, pp. 363–385, 2011.

[72] P. Ghadjar, C. Rubie, D. M. Aebersold, and U. Keilholz, "The chemokine CCL20 and its receptor CCR6 in human malignancy with focus on colorectal cancer," *International Journal of Cancer*, vol. 125, no. 4, pp. 741–745, 2009.

[73] M. L. Varney, S. Singh, A. Li, R. Mayer-Ezell, R. Bond, and R. K. Singh, "Small molecule antagonists for CXCR2 and CXCR1 inhibit human colon cancer liver metastases," *Cancer Letters*, vol. 300, no. 2, pp. 180–188, 2011.

[74] H. Yao, Z. Duan, M. Wang, A. O. Awonuga, D. Rappolee, and Y. Xie, "Adrenaline induces chemoresistance in HT-29 colon adenocarcinoma cells," *Cancer Genetics and Cytogenetics*, vol. 190, no. 2, pp. 81–87, 2009.

[75] H. P. S. Wong, J. W. C. Ho, M. W. L. Koo et al., "Effects of adrenaline in human colon adenocarcinoma HT-29 cells," *Life Sciences*, vol. 88, no. 25-26, pp. 1108–1112, 2011.

[76] L. Stevenson, W. L. Allen, R. Turkington et al., "Identification of galanin and its receptor galr1 as novel determinants of resistance to chemotherapy and potential biomarkers in colorectal cancer," *Clinical Cancer Research*, vol. 18, pp. 5412–5426, 2012.

[77] D. K. Agrawal and P. K. Mishra, "Curcumin and its analogues: potential anticancer agents," *Medicinal Research Reviews*, vol. 30, no. 5, pp. 818–860, 2010.

[78] L. J. Marnett, "The COXIB experience: a look in the rearview mirror," *Annual Review of Pharmacology and Toxicology*, vol. 49, pp. 265–290, 2009.

[79] C. C. Johnson, R. B. Hayes, R. E. Schoen, M. J. Gunter, and W.-Y. Huang, "Non-steroidal anti-inflammatory drug use and colorectal polyps in the Prostate, Lung, Colorectal, and Ovarian Cancer Screening Trial," *American Journal of Gastroenterology*, vol. 105, no. 12, pp. 2646–2655, 2010.

[80] A. Bennett, M. Del Tacca, I. F. Stamford, and T. Zebro, "Prostaglandins from tumours of human large bowel," *British Journal of Cancer*, vol. 35, no. 6, pp. 881–884, 1977.

[81] X. Chen, T. Hasuma, Y. Yano et al., "Inhibition of farnesyl protein thansferase by monoterpene, curcumin derivatives and gallotannin," *Anticancer Research*, vol. 17, no. 4, pp. 2555–2564, 1997.

[82] H.-M. Kang, K.-H. Son, D. C. Yang et al., "Inhibitory activity of diarylheptanoids on farnesyl protein transferase," *Natural Product Research*, vol. 18, no. 4, pp. 295–299, 2004.

[83] M. Sinensky, "Functional aspects of polyisoprenoid protein substituents: roles in protein-protein interaction and trafficking," *Biochimica et Biophysica Acta*, vol. 1529, no. 1–3, pp. 203–209, 2000.

[84] R. Khosravi-Far, A. D. Cox, K. Kato, and C. J. Der, "Protein prenylation: key to ras function and cancer intervention?" *Cell Growth & Differentiation*, vol. 3, no. 7, pp. 461–469, 1992.

[85] M. R. Redinbo and P. M. Potter, "Mammalian carboxylesterases: from drug targets to protein therapeutics," *Drug Discovery Today*, vol. 10, no. 5, pp. 313–325, 2005.

[86] L. M. Howells, E. P. Moiseeva, C. P. Neal et al., "Predicting the physiological relevance of in vitro cancer preventive activities of phytochemicals," *Acta Pharmacologica Sinica*, vol. 28, no. 9, pp. 1274–1304, 2007.

[87] V. Ravindranath and N. Chandrasekhara, "Absorption and tissue distribution of curcumin in rats," *Toxicology*, vol. 16, no. 3, pp. 259–265, 1980.

Hindawi Publishing Corporation
BioMed Research International
Volume 2013, Article ID 130362, 11 pages
http://dx.doi.org/10.1155/2013/130362

Review Article

Emerging Therapeutic Biomarkers in Endometrial Cancer

Peixin Dong,[1] Masanori Kaneuchi,[1] Yosuke Konno,[2] Hidemichi Watari,[2] Satoko Sudo,[2] and Noriaki Sakuragi[2]

[1] *Department of Women's Health Educational System, Hokkaido University School of Medicine, Hokkaido University, N15, W7, Sapporo 060-8638, Japan*
[2] *Department of Gynecology, Hokkaido University School of Medicine, Hokkaido University, N15, W7, Sapporo 060-8638, Japan*

Correspondence should be addressed to Peixin Dong; dongpeix@yahoo.co.jp and Noriaki Sakuragi; sakuragi@med.hokudai.ac.jp

Received 14 April 2013; Accepted 28 May 2013

Academic Editor: Romonia Renee Reams

Although clinical trials of molecular therapies targeting critical biomarkers (mTOR, epidermal growth factor receptor/epidermal growth factor receptor 2, and vascular endothelial growth factor) in endometrial cancer show modest effects, there are still challenges that might remain regarding primary/acquired drug resistance and unexpected side effects on normal tissues. New studies that aim to target both genetic and epigenetic alterations (noncoding microRNA) underlying malignant properties of tumor cells and to specifically attack tumor cells using cell surface markers overexpressed in tumor tissue are emerging. More importantly, strategies that disrupt the cancer stem cell/epithelial-mesenchymal transition-dependent signals and reactivate antitumor immune responses would bring new hope for complete elimination of all cell compartments in endometrial cancer. We briefly review the current status of molecular therapies tested in clinical trials and mainly discuss the potential therapeutic candidates that are possibly used to develop more effective and specific therapies against endometrial cancer progression and metastasis.

1. Introduction

Endometrial cancer (EC) is the most common gynecological malignancy among women worldwide with 287000 new cases and estimated 74000 deaths per year [1].

EC has been dichotomized into two types with distinct underlying molecular profiling, histopathology and clinical behavior: less aggressive type I and highly aggressive type II. Most ECs are type I (approximately 75%) and are estrogen-dependent adenocarcinomas with endometrioid morphology [2]. They are usually diagnosed at an early stage and have a good prognosis (a 5-year survival rate of 80–85%) after surgery [2, 3]. In contrast, type II ECs with poorly differentiated endometrioid and serous histology are associated with myometrial invasion, extrauterine spread, and a lower 5-year survival rate (35%) [3–6]. Although patients with advanced or recurrent disease typically receive adjuvant chemotherapy and radiation, they have an extremely poor prognosis. A potential strategy for the treatment of these cases is to target EC cells by blocking key signaling pathways that are necessary for tumor development.

2. Therapeutic Targets for EC

Type I EC frequently exhibits altered PI3K/PTEN/AKT/mTOR signal pathway [7–11]. Type II cancer predominantly shows mutations in p53 [12] and epidermal growth factor receptor 2 (HER-2) overexpression [13]. The upregulation of epidermal growth factor receptor (EGFR) [14, 15] and vascular endothelial growth factor (VEGF) [16], dysregulated microRNA (miRNA) [17], and activation of cancer stem cell (CSC)/epithelial-mesenchymal transition (EMT) programs are involved in oncogenesis and progression of both cancer types [18–20]. Owing to the high-frequency activation of PI3K/AKT/mTOR, EGFR/HER2 and VEGF-related pathway and their important roles in promoting EC growth and metastasis, new drug targeting these signals would be valuable to a very large number of patients with EC. Recently, clinical trials assessing the efficacy of mTOR inhibitor, EGFR/HER2 inhibitor, and antiangiogenic agent for EC have been conducted and demonstrated modest effects [21, 22] (Figure 1).

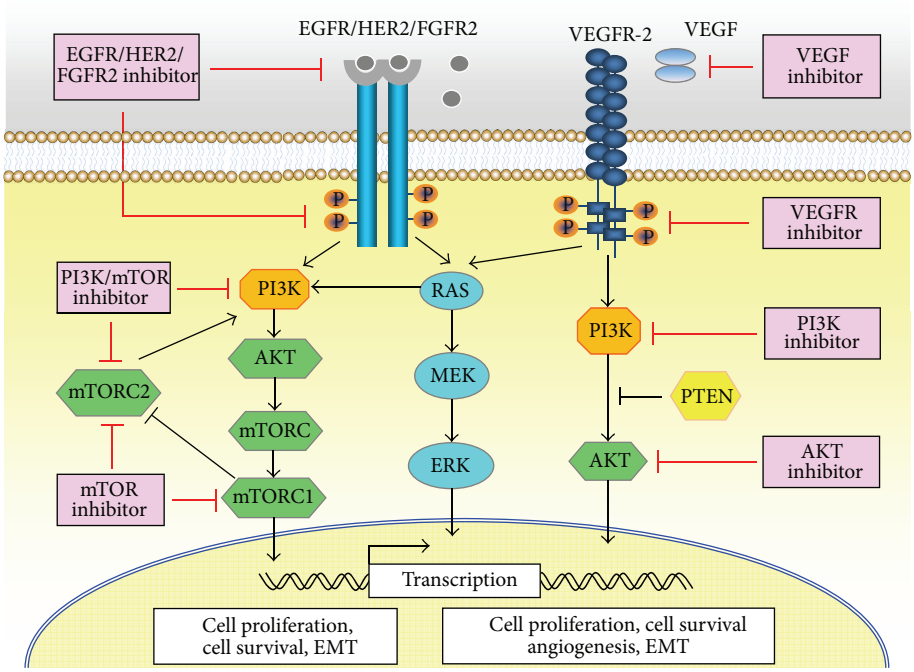

Figure 1: Therapeutic molecular targets for endometrial cancer. Type I endometrial cancer (EC) frequently exhibits altered PI3K/PTEN/AKT/mTOR signal pathway, whereas type II EC frequently shows mutations in p53 and HER-2 overexpression. The upregulation of EGFR and VEGF, dysregulated microRNAs, and activation of cancer stem cell (CSC)/epithelial-mesenchymal transition (EMT) programs are involved in oncogenesis and progression of both cancer types. Currently, clinical trials assessing the efficacy of mTOR inhibitor, EGFR/HER2 inhibitor, and antiangiogenic agent for EC have been conducted and demonstrated modest effects.

3. Challenges in the Molecular Therapeutics of Human Tumor

Although the therapeutic potential of targeted drugs for the treatment of human tumors appears promising, the clinical success of such drugs has been limited by key challenges, including primary/acquired drug resistance [23–25] and unexpected side effects on normal tissues due to nonspecificity [26] (Figure 2).

A portion of patients unfortunately do not respond to targeted agents (primary resistance), and the remainder might eventually acquire the resistance to targeted therapy despite an initial response. Various mechanisms of resistance have begun to be elucidated. The most frequently reported mechanism of primary resistance is genetic heterogeneity. For example, mechanisms of resistance to EGFR inhibitors are involved in point mutations, deletions, and amplifications of genomic areas of EGFR [23]. In addition to genetic alteration, epigenetic changes, such as DNA methylation at CpG islands, have been linked to the development of resistance to multiple molecular drugs [27, 28]. The generation of a population of cancer cells with stem-cell properties might provide another possible reason of resistance to EGFR inhibitor [29]. Common mechanisms of acquired resistance include secondary mutation in the target gene, activation of alternative pathway or feedback loop, and induction of EMT [23, 30]. Therefore, new therapy that concurrently attacks multiple critical pathways, inhibits the cross talk between diverse signals, and suppresses the CSC and EMT properties may be efficacious to overcome the resistance to molecular agents in EC.

Moreover, the administration of antiangiogenic agents, particularly antibodies against VEGF, leads to a more hypoxic tumor microenvironment [31], which enhances tumor cell invasion and metastasis by inducing the EMT- and CSC-like phenotype [32–34]. These works clearly suggest the need to combine antiangiogenic treatment in human tumors with new drugs targeting specific signaling pathways linked to the CSC/EMT phenotype.

Another challenge is toxicity or the side effects associated with targeted therapies, such as harmful immune responses. These include "Off-target" adverse effects caused by a drug binding to an unexpected target and "On-target" adverse effects as a result of a drug binding to its intended target that is not only present in tumor cells, but also found in normal tissue [26].

4. Potential miRNA-Based Therapies in EC

Different from gene mutations, epigenetic changes that are associated with global gene regulation such as chromatin remodeling open a new field of cancer research [35]. Epigenetic silencing of tumor suppressor genes or epigenetic

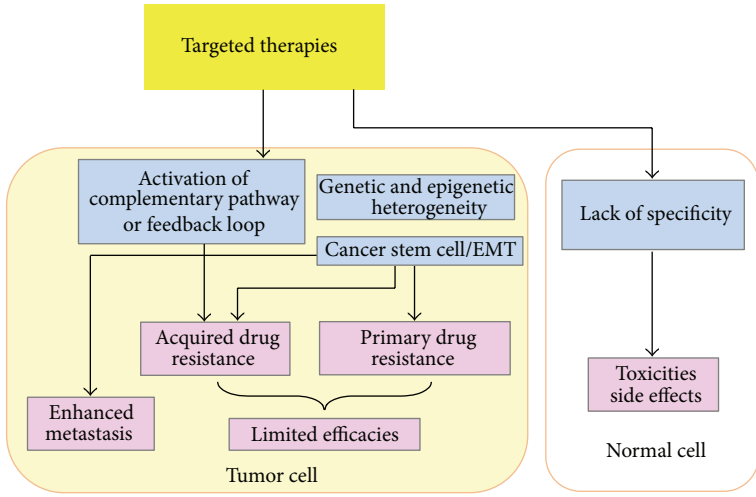

Figure 2: Challenges in the molecular therapeutics of human tumor. The clinical success of targeted drugs has been limited by key challenges, including primary/acquired drug resistance and unexpected side effects on normal tissues due to nonspecificity. The most frequent mechanisms of primary resistance are genetic/epigenetic heterogeneity and the existence of cancer stem cell. Acquired resistance can be caused by the secondary mutation in the target gene, activation of alternative pathway or feedback loop, and induction of EMT. Treatment of tumor cells with antiangiogenic agents can lead to a more hypoxic tumor microenvironment and enhance tumor cell invasion and metastasis by inducing the EMT- and cancer-stem-cell-like phenotype.

activation of oncogenes plays the important roles in the promotion of carcinogenesis and tumor progression [35]. Two common epigenetic changes are methylation at the promoter region and histone acetylation, which can be modulated using inhibitors of DNA methyltransferase (DNMT) and histone deacetylase (HDAC), respectively. Tumor suppressor genes including *PTEN* [36], DNA mismatch repair gene *hMLH1* [37], adenomatous polyposis coli (APC) [38], RAS-associated domain family member protein 1 (*RASSF1A*) [39], and *E-cadherin* [40] are more frequently silenced in type I tumor than in type II tumor. DNMT and HDAC inhibitors are already in clinical use for myelodysplasia and cutaneous T-cell lymphoma [41, 42]. Preclinical study has shown that DNMT and HDAC inhibitors induce cell apoptosis and suppress the growth of EC *in vivo* [43]. The combination of epigenetic modifiers with chemotherapy, hormonal therapy, and targeted therapy, has been proposed [44], and this may achieve better effect than single epigenetic agent for the treatment of EC.

Another important mechanism for epigenetic regulation of gene expression is involved in noncoding RNAs, specifically small regulatory microRNA (miRNA). MiRNAs post-transcriptionally control gene expression by base pairing with the 3′ untranslated region of target mRNAs, which triggers either mRNA translation repression or RNA degradation [45].

As miRNAs are able to bind to their mRNA targets with either perfect or imperfect complementary, one miRNA may possibly have multiple target genes and concurrently influence different cellular signaling pathways [45]. Some miRNAs can function as either promoter or suppressor participating in a wide variety of biological functions of tumor, including cell proliferation, differentiation, migration, apoptosis, and recently EMT/cancer-stem-cell-like features [46]. Therefore, modulation of dysregulated miRNAs could be a powerful tool to correct abnormal signaling pathways related to EC.

Altered expression profiles of microRNA have been observed in EC compared with normal endometrium [47]. Several miRNAs are differentially expressed between endometrioid and serous papillary EC, indicating that they could infer mechanisms that are specific to individual tumor subtypes [48]. Among those miRNAs elevated in endometrioid EC, the expression of miR-7 can be downregulated by using anti-miRNA oligonucleotides, leading to repressed migration and invasion of EC cells [49]. On the other hand, the level of miR-194 was significantly lower in EC patients with more advanced stage, and lower expression of this miRNA was associated with worse survival [50]. We found that overexpression of miR-194 by transfection with pre-miRNA molecule inhibited EMT phenotype and EC cell invasion by targeting the oncogene *BMI-1* [51]. We also identified miR-130b as one of the mutant p53-responsive 23 miRNAs, which is decreased in EC relative to adjacent normal tissue and directly targets the key EMT promoter gene *ZEB1* to revert p53-mutations-induced EMT features of EC cells [52]. MiRNAs are stable in various tissues and bodily fluids [53]. This property greatly facilitates the delivery of miRNAs to recipient cells via the blood or other compartments. Collectively, targeting those miRNAs that are deeply involved in EC progression would provide a promising therapeutic option for EC.

Forced expression of tumor suppressor miRNA and suppression of oncogenic miRNA are two strategies to achieve the goal of miRNA-based cancer treatment (Figure 3). Although previous results demonstrated that restoration of tumor suppressor miR-152 effectively inhibited EC cell growth *in vitro* and *in vivo* [54], obvious challenges of

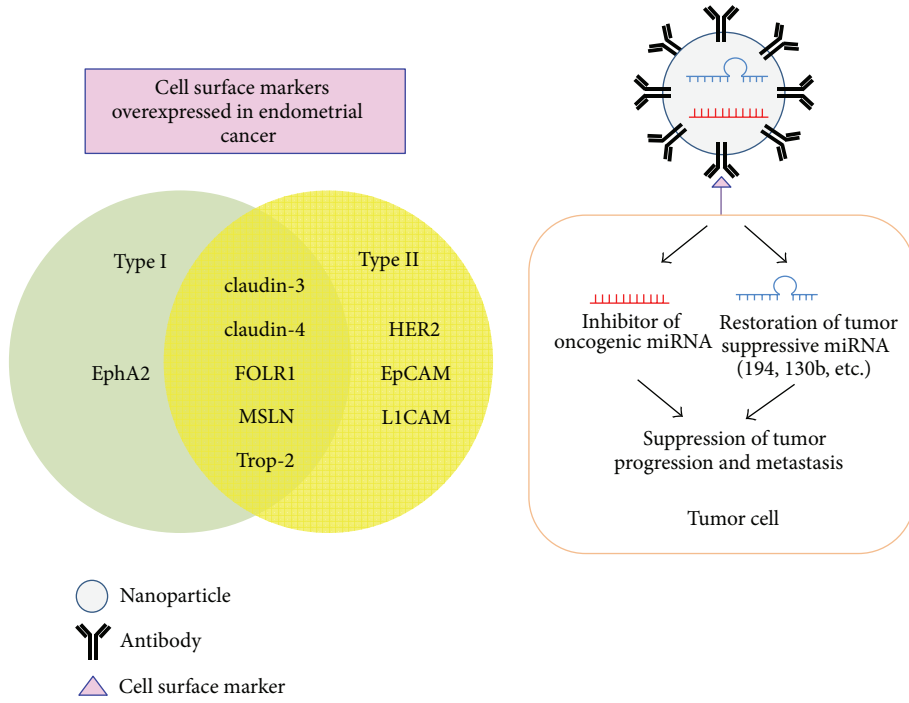

Figure 3: Potential miRNA-based therapies in EC. The use of antibodies against cell surface markers overexpressed in EC tissue might deliver targeted drugs to EC cells more specifically with fewer side effects on normal tissue. The nanotechnology can be used to develop a more effective delivery system for targeted agents, especially miRNA that might simultaneously modulate multiple signal pathways necessary for malignant phenotype of EC.

obtaining efficient delivery systems and tumor cell specificity must be resolved to allow clinical implementation.

The biochemical similarity between miRNA and siRNA suggests that the same delivery reagents developed for use with siRNA could be applied to the delivery of miRNA [55, 56]. Many efforts have been made to develop more effective and stable delivery systems [57]. Among them, nanoparticles confer greater miRNA stability, and the conjugation of nanoparticles to antibodies or cancer-specific ligands can notably improve their interactions with cancer cells [57]. By using the modification of GC4 single-chain fragment (a tumor-targeting human monoclonal antibody), nanoparticles injected intravenously showed greater accumulation in the tumor nodules rather than in liver and kidney. Moreover, the codelivery of three siRNAs together with miR-34a resulted in a more significant inhibition (80%) of metastatic melanoma than that obtained with siRNAs or miRNA alone [58]. These data demonstrate that the use of antibody targeting cell surface marker allows a selective delivery of miRNA into the tumor, and the combination of siRNA and miRNA could additively inhibit tumor growth and metastasis.

As mentioned, another major issue for molecular cancer therapy is toxicity. To avoid potential side effects on normal tissue, increasing attention has been directed to the identification of tumor-specific surface markers including receptors and epitopes that are highly expressed in cancer cells, but not or minimally expressed in normal cells. Some potential tumor cell surface markers overexpressed in EC compared with normal endometrium might be used for targeted therapy (Figure 3).

Eph receptor tyrosine kinases and their ephrin ligands influence central nervous system development, stem cell niches, and cancer cells [59]. Upon the binding of EphrinA1, the EphA2 receptor becomes tyrosine phosphorylated and interacts with several proteins to elicit downstream signaling, which regulate cell adhesion, proliferation, migration, and angiogenesis [60]. Overexpression of EphA2 was found in a high proportion of endometrioid EC and correlated with advanced disease and poor prognosis, whereas its expression is present at low levels in benign endometrial tissue [61]. The microtubule inhibitor conjugated to EphA2 antibody was shown to be specifically internalized by EphA2-positive EC cells, resulting in significant growth inhibition of EC cells both *in vitro* and *in vivo* [62].

The tight junction proteins claudin-3 and claudin-4 are highly expressed in endometrioid, serous papillary, and clear-cell EC [63], but less frequently found in normal endometrium [64]. Importantly, the intratumoral injection of cytotoxic *Clostridium perfringens* enterotoxin (CPE) that interacts with claudin-3 and claudin-4 in subcutaneous serous EC xenografts led to tumor disappearance and extended survival of animals [65], indicating that targeting claudin-3 and claudin-4 by CPE or other targeted treatment may efficiently suppress the progression of EC.

Folate receptor alpha (FOLR1, a membrane-bound molecule) and mesothelin (MSLN, a glycosyl-phosphatidylinositol-linked cell surface antigen) that are

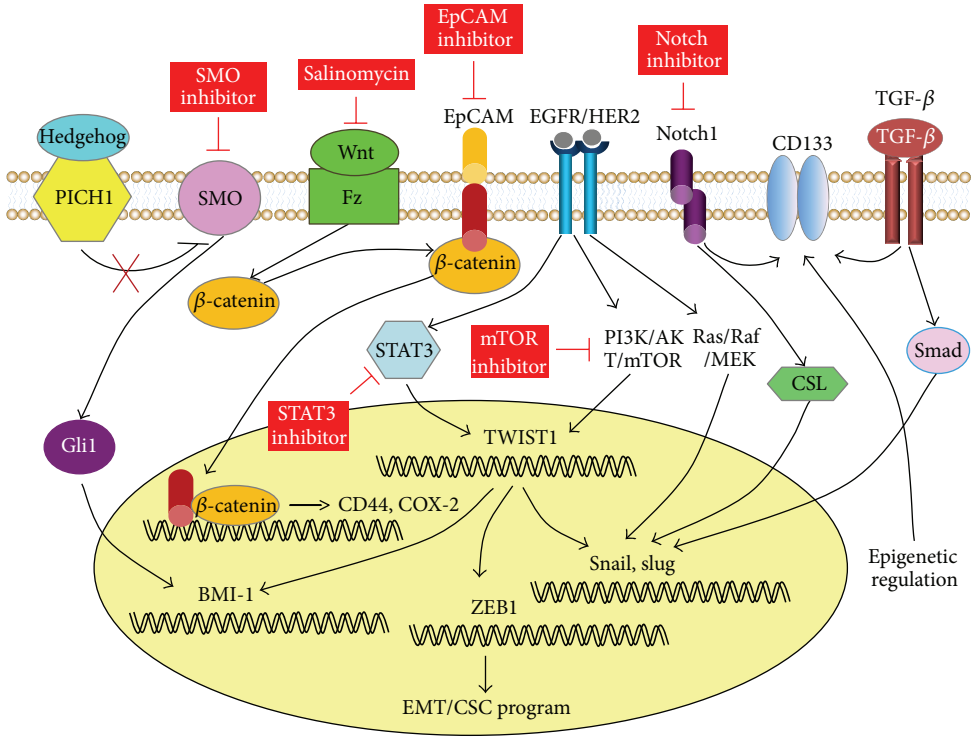

Figure 4: Targeting the CSC/EMT signaling pathways in EC. Tumor cells that undergo EMT not only increase their invasion ability, but also concurrently acquire cancer stem cell (CSC) properties. On the other hand, CSCs are associated with enhanced capacity to metastasize. At a molecular level, several signaling pathways involved in the self-renewal of CSCs, including Wnt/β-catenin, Hedgehog, and Notch signaling, can also induce EMT programs. Specific inhibitors targeting these CSC and EMT pathways efficiently suppress the malignant phenotype of EC cells. Other potential therapeutic candidates for EC treatment include Stattic (inhibitor of STAT3), Rapamycin (mTOR inhibitor), and CD133.

upregulated in ovarian carcinoma [66] are also upregulated in serous EC more frequently than in endometrioid EC [67]. The expression of FOLR1 cannot be observed in normal endometrium tissue [67], suggesting that FOLR1 may serve as a good tumor cell surface marker for targeted therapy, and antibodies against FOLR1 may facilitate tumor-specific cellular uptake of molecular drugs.

Trophoblast cell surface marker (Trop-2, a cell surface glycoprotein) is often overexpressed in various late stage epithelial tumor types with low or no expression in normal tissues [68]. Trop-2 is highly expressed in serous [69] and endometrioid EC [70]. Serous EC cell lines overexpressing Trop-2 show increased sensitivity to immunotherapy with hRS7, a humanized anti-Trop-2 monoclonal antibody [69]. Thus, Trop-2 would be an attractive target for EC immunotherapy.

Epithelial cell adhesion molecule (EpCAM) is overexpressed on malignant cells from a variety of different tumors and is considered as a reliable marker for tumor-initiating cells [71]. The cell surface expression of EpCAM is significantly higher among serous EC specimen compared to in normal endometrial tissue [72]. Serous EC cell lines that are positive for EpCAM exhibit high sensitivity to EpCAM antibody-mediated cytotoxicity, suggesting that EpCAM may represent a novel therapeutic target for serous EC.

In normal epithelium, the expression of L1 cell adhesion molecule (L1CAM) is undetectable. However, overexpression of L1CAM has been reported in many types of carcinomas [73]. L1CAM has been defined as a key driver for tumor cell invasion and EMT [73]. Of interest, L1CAM was absent in normal endometrium and the vast majority of endometrioid EC, but it was strongly expressed in serous and clear-cell EC [74]. The combined treatment with L1CAM antibodies and chemotherapeutic drugs in pancreatic and ovarian carcinoma model systems *in vivo* reduced tumor growth more efficiently than treatment with the cytostatic drug alone [75], indicating the value of L1CAM as a target for chemosensitizer in anticancer therapy for aggressive EC.

Taken together, antibodies against various tumor cell surface markers would provide a possibility of delivering drugs to EC cells, with fewer side effects on normal tissue. The nanotechnology or other approaches might be used to develop a more effective delivery system for targeted drugs, especially miRNAs that might simultaneously modulate a broad range of gene networks necessary for malignant phenotype of EC.

5. Targeting the CSC/EMT Signaling Pathways in EC

CSC is defined as a rare population having the ability to self-renew, initiate tumor growth, and give rise to the heterogeneous tumor cell mass [76]. Growing lines of evidence

suggest that CSCs do exist and support tumor maintenance during tumor formation [77]. CSCs of EC might be located in the basal layer of endometrium and are responsible for production of EC cells [78]. Sorted CD133 (+) subpopulations from EC cell expressed higher levels of oncogene *BMI-1* [51] and showed more aggressive potential and increased tumorigenicity in nude mice than CD133 (−) cells [79]. Stem-like cell subpopulations, referred to as "side population" (SP) cells, have been isolated from EC tissue and show self-renewal capacity and enhanced tumorigenicity *in vivo* [80]. Therefore, these results suggest that selective killing of such CSCs is an appealing therapeutic prospect for EC.

Tumor cells that undergo EMT can increase their invasion ability and concurrently acquire CSC properties [81, 82]. Indeed, CSC fractions within pancreatic cancer [83] and colon cancer [84] are associated with enhanced capacity to metastasize, a process that requires considerable invasive capacity. At a molecular level, these findings are consistent with the fact that several signaling pathways involved in the self-renewal of CSCs, including Wnt/β-catenin, Hedgehog (Hh), and Notch signaling [85], can also induce EMT programs [86] (Figure 4), supporting a molecular link between EMT and CSC program in human tumor [87]. Therefore, development of specific therapies targeted at these CSC and EMT pathways raises a hope for eliminating recurrent and metastatic disease and for improvement of patient survival.

In malignant human mammary stem cells, activation of Hh signal components (SMO, PTCH1, and Gli1) increases the expression of downstream transcription factor BMI-1 and plays an important role in regulating stem cell self-renewal [88]. The overexpression of Hh-signal-related molecules is detected in EC tissue and involved in stimulated proliferation of EC cells [89]. In the same study, cyclopamine (a specific inhibitor of the SMO) has been shown to efficiently suppress the growth of EC cells [89].

Activation of Wnt/β-catenin pathway represented by the nuclear staining of β-catenin was shown to be more commonly detected in type I than type II EC [12]. More recent evidence suggests that gene sets indicating activation of Hh and Wnt/β-catenin signaling closely correlate with more aggressive EC and worse survival [90]. Wnt/β-catenin signaling was shown to induce the expression of downstream targets EpCAM and CD44 in hepatocellular carcinoma and EC, respectively [91, 92]. Salinomycin, a selective inhibitor of breast CSCs [93], was shown to induce apoptosis, inhibit Wnt/β-catenin signaling, and therefore repress the proliferation, migration, invasiveness, and tumorigenicity of SP cells obtained from invasive EC cells [94]. Thus, it is important to determine whether salinomycin alone, or in combination with other agents such as EpCAM-specific monoclonal antibody, could effectively induce apoptosis in CSC-like EC cells.

High expression of Notch1 has been detected in EC patients with poor prognosis, and treatment with a reported Notch inhibitor DAPT [95] suppresses invasiveness of EC cells [96].

Other potential therapeutic candidates for EC treatment might include Stattic, Rapamycin, and CD133. Signal transducer and activator of transcription 3 (STAT3) has been shown to transcriptionally activate the expression of EMT inducer TWIST1, resulting in promoted oncogenic properties in breast cancer [97]. Stattic (an inhibitor of STAT3) can suppress EGF-enhanced invasive behavior of EC cells [98]. Rapamycin (an mTOR inhibitor) has been used to counter the effects of *PTEN* deletion and inhibit the development of leukemia-initiating cells while preserving normal stem cell populations [99]. Targeting CD133 (+) cells by CD133 antibody-cytotoxic drug conjugates effectively inhibits the growth of hepatocellular and gastric cancer cells *in vivo* and *in vitro* [100].

The most obvious concern is whether a therapy can selectively target CSC, but not destroy normal stem cell that could share many characteristics as CSC, such as the ability to self-renew and differentiate. However, CSCs and normal stem cells display different biological behaviors, mainly due to aberrant activation of several pathways involved in proliferation, self-renewal, differentiation, and metabolism in CSCs [101, 102]. Therefore, exploiting these molecular differences could be helpful to specifically target CSCs while preserving normal stem cells. Furthermore, the combined inhibition of Hh and EGFR signaling through the use of specific inhibitors can lead to the increased rate of apoptotic death and decreased invasiveness of prostate cancer cells [103], suggesting that this treatment might be affecting the CSCs.

6. Targeting Immunosuppressive Molecular Pathways in EC

ECs are immunogenic tumors [104], and they mount potent antitumor immune responses, which might be ineffective at rejecting tumor, but might be potentially harnessed therapeutically [105]. Immune escape has been considered as the major malignant features of tumor cells. Several mechanisms are responsible for tumor immune escape, including the failure to recognize tumor cells by the immune system due to reduced major histocompatibility complex class I (MHC-I) expression, immunosuppression caused by tumor-cell-released immunosuppressive factors such as TGF-β, interleukin (IL)-10, VEGF, and cyclooxygenase-2 (COX-2), and immunoresistance resulting from the induction of EMT/CSC [104, 106, 107]. These data indicate that in addition to direct tumor cell killing, new targeted therapy might be also designed to reactivate the body's immune response against tumor cells (Figure 5).

Tumor stem cells (CD133+) have been shown to express low levels of MHC-I; however, the percentage of CD133-positive CSCs that expressed MHC-I can be significantly increased by the treatment with interferon-gamma [108], suggesting the possible use of MHC-I to generate anti-CSC immunity for human tumor including EC [106].

Some signal pathways that are activated in tumor cells are also dysregulated in immunosuppressive cells in cancer microenvironment. Immunosuppressive molecules released by tumor cells can activate STAT3 in immune cells, leading to tumour-induced immunosuppression [109]. In gastric cancer cells, oncogenic Wnt/β-catenin pathways enhance the

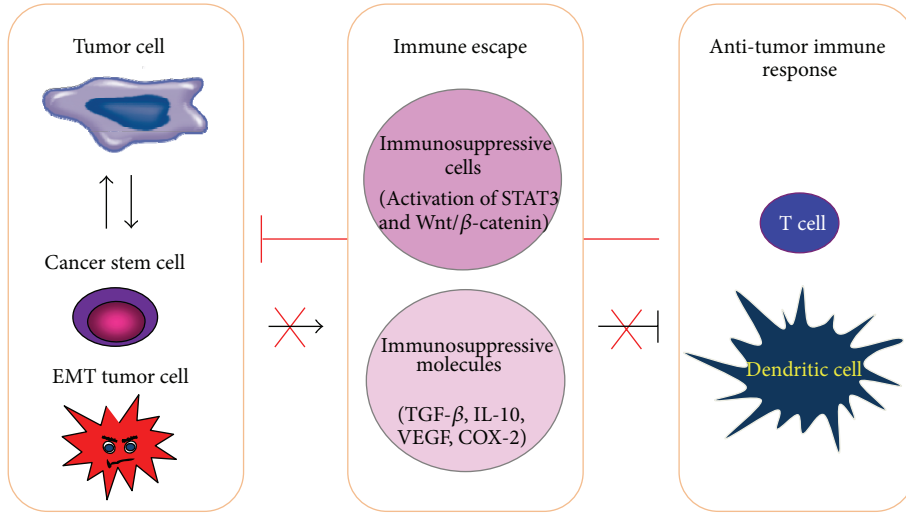

Figure 5: Targeting immunosuppressive molecular pathways in EC. Tumor cell induces immunosuppression by the production of immunosuppressive factors such as TGF-β, IL-10, VEGF, and COX-2. Tumor cells undergoing EMT can acquire both aggressive and immunosuppressive properties. Wnt/β-catenin pathway and STAT3-related pathway are activated in tumor cells and immunosuppressive cells and therefore they seem to be attractive targets for EC immunotherapy.

transcription of COX-2, an immunosuppressive molecule [110]. Importantly, COX-2 is upregulated and associated with VEGF expression in EC tissue [111], and selective COX-2 inhibitor etodolac exhibits antiproliferative effects on EC tissue [112], indicating that targeting COX-2 may boost immune responses towards EC and repress EC progression [113]. Although the adverse effects on normal immune cells should be avoided, targeting STAT3 or Wnt/β-catenin pathway by specific inhibitor in tumor cells and immunosuppressive cells, or along with other immunotherapy, might restore the immunocompetence of EC patients.

7. Conclusion

Currently, targeted therapies have not entered clinical practice, and clinical trials involving genetic biomarkers (mTOR, HER2, EGFR, and VEGF) administered to ECs only resulted in modest effects. Therapy targeting epigenetic regulatory mechanisms such as miRNA will need to be developed to achieve a broader impact on multiple signal pathways necessary for EC development. The use of targeted cancer therapy remains challenging because of the lack of specificity for cancer cells. Targeted agents that are specific to cell surface markers overexpressed in tumor cells would avoid potential side effects on normal tissue. More importantly, we expect that new targeted therapies that specifically attack both cancer cells and CSC-like cells can be used together with immunotherapy that stimulates a host's immune response and with other traditional treatments to achieve better clinical prognosis of EC patients in the near future.

Conflict of Interests

The authors declare no competing financial interests.

Authors' Contribution

Peixin Dong and Masanori Kaneuchi equally contributed to this paper.

Acknowledgments

This work was funded by a Grant from the Department of Women's Health Educational System, and a Grant-in-Aid from the Ministry of Health, Labour, and Welfare of Japan and Grant-in-Aid for Scientific Research (C) (23592428). The authors thank Dr. Zhujie Xu for the continuous and excellent support.

References

[1] J. Ferlay, H.-R. Shin, F. Bray, D. Forman, C. Mathers, and D. M. Parkin, "Estimates of worldwide burden of cancer in 2008: GLOBOCAN 2008," *International Journal of Cancer*, vol. 127, no. 12, pp. 2893–2917, 2010.

[2] J. V. Bokhman, "Two pathogenetic types of endometrial carcinoma," *Gynecologic Oncology*, vol. 15, no. 1, pp. 10–17, 1983.

[3] P. Singh, C. L. Smith, G. Cheetham, T. J. Dodd, and M. L. J. Davy, "Serous carcinoma of the uterus—determination of HER-2/neu status using immunohistochemistry, chromogenic in situ hybridization, and quantitative polymerase chain reaction techniques: its significance and clinical correlation," *International Journal of Gynecological Cancer*, vol. 18, no. 6, pp. 1344–1351, 2008.

[4] T. Alvarez, E. Miller, L. Duska, and E. Oliva, "Molecular profile of grade 3 endometrioid endometrial Carcinoma: is it a type i or type ii endometrial carcinoma?" *American Journal of Surgical Pathology*, vol. 36, no. 5, pp. 753–761, 2012.

[5] P. Mhawech-Fauceglia, D. Wang, J. Kesterson et al., "Gene expression profiles in stage I uterine serous carcinoma in comparison to grade 3 and grade 1 stage i endometrioid

adenocarcinoma," *PLoS ONE*, vol. 6, no. 3, Article ID e18066, 2011.

[6] K. N. Moore and A. Nickles Fader, "Uterine papillary serous carcinoma," *Clinical Obstetrics and Gynecology*, vol. 54, no. 2, pp. 278–291, 2011.

[7] S. Ma, T. K. Lee, B.-J. Zheng, K. W. Chan, and X.-Y. Guan, "CD133$^+$ HCC cancer stem cells confer chemoresistance by preferential expression of the Akt/PKB survival pathway," *Oncogene*, vol. 27, no. 12, pp. 1749–1758, 2008.

[8] B. M. Slomovitz and R. L. Coleman, "The PI3K/AKT/mTOR pathway as a therapeutic target in endometrial cancer," *Clinical Cancer Research*, vol. 18, no. 21, pp. 5856–5864, 2012.

[9] S. Sarmadi, N. Izadi-Mood, K. Sotoudeh, and S. M. Tavangar, "Altered PTEN expression; A diagnostic marker for differentiating normal, hyperplastic and neoplastic endometrium," *Diagnostic Pathology*, vol. 4, no. 1, article 41, 2009.

[10] M. L. Rudd, J. C. Price, S. Fogoros et al., "A unique spectrum of somatic PIK3CA (p110α) mutations within primary endometrial carcinomas," *Clinical Cancer Research*, vol. 17, no. 6, pp. 1331–1340, 2011.

[11] J. V. Lacey Jr., G. L. Mutter, B. M. Ronnett et al., "PTEN expression in endometrial biopsies as a marker of progression to endometrial carcinoma," *Cancer Research*, vol. 68, no. 14, pp. 6014–6020, 2008.

[12] X. Matias-Guiu and J. Prat, "Molecular pathology of endometrial carcinoma," *Histopathology*, vol. 62, no. 1, pp. 111–123, 2013.

[13] S. Acharya, M. L. Hensley, A. C. Montag, and G. F. Fleming, "Rare uterine cancers," *Lancet Oncology*, vol. 6, no. 12, pp. 961–971, 2005.

[14] G. E. Konecny, L. Santos, B. Winterhoff et al., "HER2 gene amplification and EGFR expression in a large cohort of surgically staged patients with nonendometrioid (type II) endometrial cancer," *British Journal of Cancer*, vol. 100, no. 1, pp. 89–95, 2009.

[15] H. Niikura, H. Sasano, G. Matsunaga et al., "Prognostic value of epidermal growth factor receptor expression in endometrioid endometrial carcinoma," *Human Pathology*, vol. 26, no. 8, pp. 892–896, 1995.

[16] C. M. Holland, K. Day, A. Evans, and S. K. Smith, "Expression of the VEGF and angiopoietin genes in endometrial atypical hyperplasia and endometrial cancer," *British Journal of Cancer*, vol. 89, no. 5, pp. 891–898, 2003.

[17] J. Zhang and L. Ma, "MicroRNA control of epithelial-mesenchymal transition and metastasis," *Cancer and Metastasis Reviews*, vol. 31, no. 3-4, pp. 3653–3462, 2012.

[18] K. Kato, "Endometrial cancer stem cells: a new target for cancer therapy," *Anticancer Research*, vol. 32, no. 6, pp. 2283–2293, 2012.

[19] S. A. Hubbard, A. M. Friel, B. Kumar, L. Zhang, B. R. Rueda, and C. E. Gargett, "Evidence for cancer stem cells in human endometrial carcinoma," *Cancer Research*, vol. 69, no. 21, pp. 8241–8248, 2009.

[20] M. Nakamura, S. Kyo, B. Zhang et al., "Prognostic impact of CD133 expression as a tumor-initiating cell marker in endometrial cancer," *Human Pathology*, vol. 41, no. 11, pp. 1516–1529, 2010.

[21] K. J. Dedes, D. Wetterskog, A. Ashworth, S. B. Kaye, and J. S. Reis-Filho, "Emerging therapeutic targets in endometrial cancer," *Nature Reviews Clinical Oncology*, vol. 8, no. 5, pp. 261–271, 2011.

[22] B. Weigelt and S. Banerjee, "Molecular targets and targeted therapeutics in endometrial cancer," *Current Opinion in Oncology*, vol. 24, no. 5, pp. 554–563, 2012.

[23] F. Morgillo, M. A. Bareschino, R. Bianco, G. Tortora, and F. Ciardiello, "Primary and acquired resistance to anti-EGFR targeted drugs in cancer therapy," *Differentiation*, vol. 75, no. 9, pp. 788–799, 2007.

[24] N. C. Turner and J. S. Reis-Filho, "Genetic heterogeneity and cancer drug resistance," *The Lancet Oncology*, vol. 13, no. 4, pp. e178–e185, 2012.

[25] J. A. Engelman, "Targeting PI3K signalling in cancer: opportunities, challenges and limitations," *Nature Reviews Cancer*, vol. 9, no. 8, pp. 550–562, 2009.

[26] C. Widakowich, G. de Castro Jr., E. de Azambuja, P. Dinh, and A. Awada, "Review: side effects of approved molecular targeted therapies in solid cancers," *Oncologist*, vol. 12, no. 12, pp. 1443–1455, 2007.

[27] R. M. Glasspool, J. M. Teodoridis, and R. Brown, "Epigenetics as a mechanism driving polygenic clinical drug resistance," *British Journal of Cancer*, vol. 94, no. 8, pp. 1087–1092, 2006.

[28] T. Ogawa, T. E. Liggett, A. A. Melnikov et al., "Methylation of death-associated protein kinase is associated with cetuximab and erlotinib resistance," *Cell Cycle*, vol. 11, no. 8, pp. 1656–1663, 2012.

[29] G. Ghosh, X. Lian, S. J. Kron, and S. P. Palecek, "Properties of resistant cells generated from lung cancer cell lines treated with EGFR inhibitors," *BMC Cancer*, vol. 12, article 95, 2012.

[30] T. Vu and F. X. Claret, "Trastuzumab: updated mechanisms of action and resistance in breast cancer," *Frontiers in Oncology*, vol. 2, article 62, 2012.

[31] O. Keunen, M. Johansson, A. Oudin et al., "Anti-VEGF treatment reduces blood supply and increases tumor cell invasion in glioblastoma," *Proceedings of the National Academy of Sciences of the United States of America*, vol. 108, no. 9, pp. 3749–3754, 2011.

[32] S. Cannito, E. Novo, A. Compagnone et al., "Redox mechanisms switch on hypoxia-dependent epithelial-mesenchymal transition in cancer cells," *Carcinogenesis*, vol. 29, no. 12, pp. 2267–2278, 2008.

[33] B. Keith and M. C. Simon, "Hypoxia-inducible factors, stem cells, and cancer," *Cell*, vol. 129, no. 3, pp. 465–472, 2007.

[34] M. Pàez-Ribes, E. Allen, J. Hudock et al., "Antiangiogenic therapy elicits malignant progression of tumors to increased local invasion and distant metastasis," *Cancer Cell*, vol. 15, no. 3, pp. 220–231, 2009.

[35] S. Sharma, T. K. Kelly, and P. A. Jones, "Epigenetics in cancer," *Carcinogenesis*, vol. 31, no. 1, pp. 27–36, 2009.

[36] H. B. Salvesen, N. MacDonald, A. Ryan et al., "PTEN methylation is associated with advanced stage and microsatellite instability in endometrial carcinoma," *International Journal of Cancer*, vol. 91, no. 1, pp. 22–26, 2001.

[37] J. Bischoff, A. Ignatov, A. Semczuk et al., "*hMLH1* promoter hypermethylation and MSI status in human endometrial carcinomas with and without metastases," *Clinical and Experimental Metastasis*, vol. 29, no. 8, pp. 889–900, 2012.

[38] G. Moreno-Bueno, D. Hardisson, C. Sánchez et al., "Abnormalities of the APC/beta-catenin pathway in endometrial cancer," *Oncogene*, vol. 21, no. 52, pp. 7981–7990, 2002.

[39] X. Liao, M. K.-Y. Siu, K. Y.-K. Chan et al., "Hypermethylation of RAS effector related genes and DNA methyltransferase 1 expression in endometrial carcinogenesis," *International Journal of Cancer*, vol. 123, no. 2, pp. 296–302, 2008.

[40] T.-Z. Yi, J. Guo, L. Zhou et al., "Prognostic value of E-cadherin expression and CDH1 promoter methylation in patients with

endometrial carcinoma," *Cancer Investigation*, vol. 29, no. 1, pp. 86–92, 2011.

[41] S. D. Gore and E. R. Hermes-DeSantis, "Enhancing survival outcomes in the management of patients with higher-risk myelodysplastic syndromes," *Cancer Control*, vol. 16, supplement, pp. 2–10, 2009.

[42] S. A. Kavanaugh, L. A. White, and J. M. Kolesar, "Vorinostat: a novel therapy for the treatment of cutaneous T-cell lymphoma," *American Journal of Health-System Pharmacy*, vol. 67, no. 10, pp. 793–797, 2010.

[43] T.-Z. Yi, J. Li, X. Han et al., "DNMT inhibitors and HDAC inhibitors regulate E-Cadherin and Bcl-2 expression in endometrial carcinoma in vitro and in vivo," *Chemotherapy*, vol. 58, no. 1, pp. 19–29, 2012.

[44] R. Connolly and V. Stearns, "Epigenetics as a therapeutic target in breast cancer," *Journal of Mammary Gland Biology and Neoplasia*, vol. 17, no. 3-4, pp. 3191–4204, 2012.

[45] D. P. Bartel, "MicroRNAs: genomics, biogenesis, mechanism, and function," *Cell*, vol. 116, no. 2, pp. 281–297, 2004.

[46] H. Xia and K. M. Hui, "MicroRNAs involved in regulating epithelial-mesenchymal transition and cancer stem cells as molecular targets for cancer therapeutics," *Cancer Gene Therapy*, vol. 19, no. 11, pp. 723–730, 2012.

[47] T. K. H. Chung, T.-H. Cheung, N.-Y. Huen et al., "Dysregulated microRNAs and their predicted targets associated with endometrioid endometrial adenocarcinoma in Hong Kong women," *International Journal of Cancer*, vol. 124, no. 6, pp. 1358–1365, 2009.

[48] E. Chan, D. E. Prado, and J. B. Weidhaas, "Cancer microRNAs: from subtype profiling to predictors of response to therapy," *Trends in Molecular Medicine*, vol. 17, no. 5, pp. 235–243, 2011.

[49] T. K. H. Chung, T. S. Lau, T. H. Cheung et al., "Dysregulation of microRNA-204 mediates migration and invasion of endometrial cancer by regulating FOXC1," *International Journal of Cancer*, vol. 130, no. 5, pp. 1036–1045, 2012.

[50] H. Zhai, M. Karaayvaz, P. Dong, N. Sakuragi, and J. Ju, "Prognostic significance of miR-194 in endometrial cancer," *Biomarker Research*, vol. 1, article 12, 2013.

[51] P. Dong, M. Kaneuchi, H. Watari et al., "MicroRNA-194 inhibits epithelial to mesenchymal transition of endometrial cancer cells by targeting oncogene BMI-1," *Molecular Cancer*, vol. 10, article 99, 2011.

[52] P. Dong, M. Karaayvaz et al., "Mutant p53 gain-of-function induces epithelial-mesenchymal transition through modulation of the miR-130b-ZEB1 axis," *Oncogene*, 2012.

[53] P. S. Mitchell, R. K. Parkin, E. M. Kroh et al., "Circulating microRNAs as stable blood-based markers for cancer detection," *Proceedings of the National Academy of Sciences of the United States of America*, vol. 105, no. 30, pp. 10513–10518, 2008.

[54] T. Tsuruta, K.-I. Kozaki, A. Uesugi et al., "miR-152 is a tumor suppressor microRNA that is silenced by DNA hypermethylation in endometrial cancer," *Cancer Research*, vol. 71, no. 20, pp. 6450–6462, 2011.

[55] C. S. Gondi and J. S. Rao, "Concepts in in vivo siRNA delivery for cancer therapy," *Journal of Cellular Physiology*, vol. 220, no. 2, pp. 285–291, 2009.

[56] J. A. Broderick and P. D. Zamore, "MicroRNA therapeutics," *Gene Therapy*, vol. 18, no. 12, pp. 1104–1110, 2011.

[57] Y. W. Kong, D. Ferland-McCollough, T. J. Jackson, and M. Bushell, "microRNAs in cancer management," *The Lancet Oncology*, vol. 13, no. 6, pp. e249–e258, 2012.

[58] Y. Chen, X. Zhu, X. Zhang, B. Liu, and L. Huang, "Nanoparticles modified with tumor-targeting scFv deliver siRNA and miRNA for cancer therapy," *Molecular Therapy*, vol. 18, no. 9, pp. 1650–1656, 2010.

[59] E. B. Pasquale, "Eph receptors and ephrins in cancer: bidirectional signalling and beyond," *Nature Reviews Cancer*, vol. 10, no. 3, pp. 165–180, 2010.

[60] M. Tandon, S. V. Vemula, and S. K. Mittal, "Emerging strategies for EphA2 receptor targeting for cancer therapeutics," *Expert Opinion on Therapeutic Targets*, vol. 15, no. 1, pp. 31–51, 2011.

[61] A. A. Kamat, D. Coffey, W. M. Merritt et al., "EphA2 overexpression is associated with lack of hormone receptor expression and poor outcome in endometrial cancer," *Cancer*, vol. 115, no. 12, pp. 2684–2692, 2009.

[62] J.-W. Lee, R. L. Stone, S. J. Lee et al., "EphA2 targeted chemotherapy using an antibody drug conjugate in endometrial carcinoma," *Clinical Cancer Research*, vol. 16, no. 9, pp. 2562–2570, 2010.

[63] G. E. Konecny, R. Agarwal, G. A. Keeney et al., "Claudin-3 and claudin-4 expression in serous papillary, clear-cell, and endometrioid endometrial cancer," *Gynecologic Oncology*, vol. 109, no. 2, pp. 263–269, 2008.

[64] X. Y. Pan, B. Wang, Y. C. Che, Z. P. Weng, H. Y. Dai, and W. Peng, "Expression of claudin-3 and claudin-4 in normal, hyperplastic, and malignant endometrial tissue," *International Journal of Gynecological Cancer*, vol. 17, no. 1, pp. 233–241, 2007.

[65] A. D. Santin, S. Bellone, M. Marizzoni et al., "Overexpression of claudin-3 and claudin-4 receptors in uterine serous papillary carcinoma: novel targets for a type-specific therapy using Clostridium perfringens enterotoxin (CPE)," *Cancer*, vol. 109, no. 7, pp. 1312–1322, 2007.

[66] C. D. Hough, C. A. Sherman-Baust, E. S. Pizer et al., "Large-scale serial analysis of gene expression reveals genes differentially expressed in ovarian cancer," *Cancer Research*, vol. 60, no. 22, pp. 6281–6287, 2000.

[67] L. A. Dainty, J. I. Risinger, C. Morrison et al., "Overexpression of folate binding protein and mesothelin are associated with uterine serous carcinoma," *Gynecologic Oncology*, vol. 105, no. 3, pp. 563–570, 2007.

[68] R. Cubas, M. Li, C. Chen, and Q. Yao, "Trop2: a possible therapeutic target for late stage epithelial carcinomas," *Biochimica et Biophysica Acta*, vol. 1796, no. 2, pp. 309–314, 2009.

[69] J. Varughese, E. Cocco, S. Bellone et al., "Uterine serous papillary carcinomas overexpress human trophoblast-cell- surface marker (trop-2) and are highly sensitive to immunotherapy with hRS7, a humanized anti-trop-2 monoclonal antibody," *Cancer*, vol. 117, no. 14, pp. 3163–3172, 2011.

[70] E. Bignotti, L. Zanotti, S. Calza et al., "Trop-2 protein overexpression is an independent marker for predicting disease recurrence in endometrioid endometrial carcinoma," *BMC Clinical Pathology*, vol. 12, no. 1, article 22, 2012.

[71] S. Imrich, M. Hachmeister, and O. Gires, "EpCAM and its potential role in tumor-initiating cells," *Cell Adhesion and Migration*, vol. 6, no. 1, pp. 30–38, 2012.

[72] K. El-Sahwi, S. Bellone, E. Cocco et al., "Overexpression of EpCAM in uterine serous papillary carcinoma: implications for EpCAM-specific immunotherapy with human monoclonal antibody adecatumumab (MT201)," *Molecular Cancer Therapeutics*, vol. 9, no. 1, pp. 57–66, 2010.

[73] H. Kiefel, S. Bondong, J. Hazin et al., "L1CAM: a major driver for tumor cell invasion and motility," *Cell Adhesion & Migration*, vol. 6, no. 4, pp. 374–384, 2012.

[74] M. Huszar, M. Pfeifer, U. Schirmer et al., "Up-regulation of LICAM is linked to loss of hormone receptors and E-cadherin in aggressive subtypes of endometrial carcinomas," *Journal of Pathology*, vol. 220, no. 5, pp. 551–561, 2010.

[75] H. Schäfer, C. Dieckmann, O. Korniienko et al., "Combined treatment of L1CAM antibodies and cytostatic drugs improve the therapeutic response of pancreatic and ovarian carcinoma," *Cancer Letters*, vol. 319, no. 1, pp. 66–82, 2012.

[76] L. V. Nguyen, R. Vanner, P. Dirks, and C. J. Eaves, "Cancer stem cells: an evolving concept," *Nature Reviews Cancer*, vol. 12, no. 2, pp. 133–143, 2012.

[77] R. J. Gilbertson and T. A. Graham, "Cancer: resolving the stem-cell debate," *Nature*, vol. 488, no. 7412, pp. 462–463, 2012.

[78] S. A. Hubbard, A. M. Friel, B. Kumar, L. Zhang, B. R. Rueda, and C. E. Gargett, "Evidence for cancer stem cells in human endometrial carcinoma," *Cancer Research*, vol. 69, no. 21, pp. 8241–8248, 2009.

[79] M. Nakamura, S. Kyo, B. Zhang et al., "Prognostic impact of CD133 expression as a tumor-initiating cell marker in endometrial cancer," *Human Pathology*, vol. 41, no. 11, pp. 1516–1529, 2010.

[80] K. Kato, "Stem cells in human normal endometrium and endometrial cancer cells: characterization of side population cells," *Kaohsiung Journal of Medical Sciences*, vol. 28, no. 2, pp. 63–71, 2012.

[81] S. A. Mani, W. Guo, M.-J. Liao et al., "The epithelial-mesenchymal transition generates cells with properties of stem cells," *Cell*, vol. 133, no. 4, pp. 704–715, 2008.

[82] A. Singh and J. Settleman, "EMT, cancer stem cells and drug resistance: an emerging axis of evil in the war on cancer," *Oncogene*, vol. 29, no. 34, pp. 4741–4751, 2010.

[83] P. C. Hermann, S. L. Huber, T. Herrler et al., "Distinct populations of cancer stem cells determine tumor growth and metastatic activity in human pancreatic cancer," *Cell Stem Cell*, vol. 1, no. 3, pp. 313–323, 2007.

[84] R. Pang, W. L. Law, A. C. Y. Chu et al., "A subpopulation of $CD26^+$ cancer stem cells with metastatic capacity in human colorectal cancer," *Cell Stem Cell*, vol. 6, no. 6, pp. 603–615, 2010.

[85] B.-B. S. Zhou, H. Zhang, M. Damelin, K. G. Geles, J. C. Grindley, and P. B. Dirks, "Tumour-initiating cells: challenges and opportunities for anticancer drug discovery," *Nature Reviews Drug Discovery*, vol. 8, no. 10, pp. 806–823, 2009.

[86] J. M. Bailey, P. K. Singh, and M. A. Hollingsworth, "Cancer metastasis facilitated by developmental pathways: sonic hedgehog, notch, and bone morphogenic proteins," *Journal of Cellular Biochemistry*, vol. 102, no. 4, pp. 829–839, 2007.

[87] A. Biddle and I. C. Mackenzie, "Cancer stem cells and EMT in carcinoma," *Cancer and Metastasis Reviews*, vol. 31, no. 1-2, pp. 285–293, 2012.

[88] S. Liu, G. Dontu, I. D. Mantle et al., "Hedgehog signaling and Bmi-1 regulate self-renewal of normal and malignant human mammary stem cells," *Cancer Research*, vol. 66, no. 12, pp. 6063–6071, 2006.

[89] Y.-Z. Feng, T. Shiozawa, T. Miyamoto et al., "Overexpression of hedgehog signaling molecules and its involvement in the proliferation of endometrial carcinoma cells," *Clinical Cancer Research*, vol. 13, no. 5, pp. 1389–1398, 2007.

[90] E. Wik, M. B. Ræder, C. Krakstad et al., "Lack of estrogen receptor-α is associated with epithelial-mesenchymal transition and PI3K alterations in endometrial carcinoma," *Clinical Cancer Research*, vol. 19, no. 5, pp. 1094–1105, 2013.

[91] M. Munz, P. A. Baeuerle, and O. Gires, "The emerging role of EpCAM in cancer and stem cell signaling," *Cancer Research*, vol. 69, no. 14, pp. 5627–5629, 2009.

[92] Y. Wang, P. Hanifi-Moghaddam, E. E. Hanekamp et al., "Progesterone inhibition of Wnt/β-catenin signaling in normal endometrium and endometrial cancer," *Clinical Cancer Research*, vol. 15, no. 18, pp. 5784–5793, 2009.

[93] P. B. Gupta, T. T. Onder, G. Jiang et al., "Identification of selective inhibitors of cancer stem cells by high-throughput screening," *Cell*, vol. 138, no. 4, pp. 645–659, 2009.

[94] S. Kusunoki, K. Kato, K. Tabu et al., "The inhibitory effect of salinomycin on the proliferation, migration and invasion of human endometrial cancer stem-like cells," *Gynecologic Oncology*, vol. 129, no. 3, pp. 598–605, 2013.

[95] C. Groth and M. E. Fortini, "Therapeutic approaches to modulating Notch signaling: current challenges and future prospects," *Seminars in Cell and Developmental Biology*, vol. 23, no. 4, pp. 465–472, 2012.

[96] Y. Mitsuhashi, A. Horiuchi, T. Miyamoto, H. Kashima, A. Suzuki, and T. Shiozawa, "Prognostic significance of Notch signalling molecules and their involvement in the invasiveness of endometrial carcinoma cells," *Histopathology*, vol. 60, no. 5, pp. 826–837, 2012.

[97] G. Z. Cheng, W. Zhang, M. Sun et al., "Twist is transcriptionally induced by activation of STAT3 and mediates STAT3 oncogenic function," *Journal of Biological Chemistry*, vol. 283, no. 21, pp. 14665–14673, 2008.

[98] C. H. Chen, S. W. Wang, C. W. Chen et al., "MUC20 overexpression predicts poor prognosis and enhances EGF-induced malignant phenotypes via activation of the EGFR-STAT3 pathway in endometrial cancer," *Gynecologic Oncology*, vol. 128, no. 3, pp. 560–567, 2013.

[99] Ö. H. Yilmaz, R. Valdez, B. K. Theisen et al., "Pten dependence distinguishes haematopoietic stem cells from leukaemia-initiating cells," *Nature*, vol. 441, no. 7092, pp. 475–482, 2006.

[100] L. M. Smith, A. Nesterova, M. C. Ryan et al., "CD133/prominin-1 is a potential therapeutic target for antibody-drug conjugates in hepatocellular and gastric cancers," *British Journal of Cancer*, vol. 99, no. 1, pp. 100–109, 2008.

[101] M. V. Verga Falzacappa, C. Ronchini, L. B. Reavie, and P. G. Pelicci, "Regulation of self-renewal in normal and cancer stem cells," *FEBS Journal*, vol. 279, no. 19, pp. 3559–3572, 2012.

[102] C. Pecqueur, L. Oliver, K. Oizel, L. Lalier, and F. M. Vallette, "Targeting metabolism to induce cell death in cancer cells and cancer stem cells," *International Journal of Cell Biology*, vol. 2013, Article ID 805975, 13 pages, 2013.

[103] M. Mimeault, E. Moore, N. Moniaux et al., "Cytotoxic effects induced by a combination of cydopamine and gefitinib, the selective hedgehog and epidermal growth factor receptor signaling inhibitors, in prostate cancer cells," *International Journal of Cancer*, vol. 118, no. 4, pp. 1022–1031, 2006.

[104] N. Brooks and D. S. Pouniotis, "Immunomodulation in endometrial cancer," *International Journal of Gynecological Cancer*, vol. 19, no. 4, pp. 734–740, 2009.

[105] L. E. Kandalaft, N. Singh, J. B. Liao et al., "The emergence of immunomodulation: combinatorial immunochemotherapy opportunities for the next decade," *Gynecologic Oncology*, vol. 116, no. 2, pp. 222–233, 2010.

[106] M. Vanneman and G. Dranoff, "Combining immunotherapy and targeted therapies in cancer treatment," *Nature Reviews Cancer*, vol. 12, no. 4, pp. 237–251, 2012.

[107] C. Kudo-Saito, H. Shirako, T. Takeuchi, and Y. Kawakami, "Cancer metastasis is accelerated through immunosuppression during snail-induced EMT of cancer cells," *Cancer Cell*, vol. 15, no. 3, pp. 195–206, 2009.

[108] A. Wu, S. Wiesner, J. Xiao et al., "Expression of MHC I and NK ligands on human CD133$^+$ glioma cells: possible targets of immunotherapy," *Journal of Neuro-Oncology*, vol. 83, no. 2, pp. 121–131, 2007.

[109] H. Yu, M. Kortylewski, and D. Pardoll, "Crosstalk between cancer and immune cells: role of STAT3 in the tumour microenvironment," *Nature Reviews Immunology*, vol. 7, no. 1, pp. 41–51, 2007.

[110] F. Nuñez, S. Bravo, F. Cruzat, M. Montecino, and G. V. de Ferrari, "Wnt/β-catenin signaling enhances cyclooxygenase-2 (COX2) transcriptional activity in gastric cancer cells," *PLoS ONE*, vol. 6, no. 4, Article ID e18562, 2011.

[111] R. Fujiwaki, K. Iida, H. Kanasaki, T. Ozaki, K. Hata, and K. Miyazaki, "Cyclooxygenase-2 expression in endometrial cancer: correlation with microvessel count and expression of vascular endothelial growth factor and thymidine phosphorylase," *Human Pathology*, vol. 33, no. 2, pp. 213–219, 2002.

[112] K. Hasegawa, Y. Torii, R. Ishii, S. Oe, R. Kato, and Y. Udagawa, "Effects of a selective COX-2 inhibitor in patients with uterine endometrial cancers," *Archives of Gynecology and Obstetrics*, vol. 284, no. 6, pp. 1515–1521, 2011.

[113] S. Ohno, Y. Ohno, N. Suzuki et al., "Multiple roles of cyclooxygenase-2 in endometrial cancer," *Anticancer Research*, vol. 25, no. 6, pp. 3679–3687, 2005.

Hindawi Publishing Corporation
BioMed Research International
Volume 2013, Article ID 913179, 8 pages
http://dx.doi.org/10.1155/2013/913179

Research Article

Mouse Prostate Epithelial Luminal Cells Lineage Originate in the Basal Layer Where the Primitive Stem/Early Progenitor Cells Reside: Implications for Identifying Prostate Cancer Stem Cells

Jianjun Zhou,[1,2] Lionel Feigenbaum,[3] Carole Yee,[4] Hongbin Song,[2] and Clayton Yates[1]

[1] *Department of Biology and Center for Cancer Research, Tuskegee University, Tuskegee, AL 36088, USA*
[2] *Institute of Disease Control and Prevention, Chinese Academy of Military Medical Sciences, Beijing 100071, China*
[3] *Science Applications International Corporation-Frederick, National Cancer Institute, Frederick Cancer Research and Development Center, Frederick, MD 21702, USA*
[4] *Dermatology Branch, National Cancer Institute, NIH, Bethesda, MD 20892, USA*

Correspondence should be addressed to Hongbin Song; hongbinsong@263.net and Clayton Yates; cyates@tuskegee.edu

Received 25 February 2013; Accepted 3 May 2013

Academic Editor: Tiziano Verri

Prostate stem cells are thought to be responsible for generation of all prostate epithelial cells and for tissue maintenance. The lineage relationship between basal and luminal cells in the prostate is not well clarified. We developed a mouse model to trace cell fate and a mouse model with a slowly cycling cell label to provide insight into this question. The results obtained indicate that putative mouse prostate stem cells are likely to reside in the basal layer.

1. Introduction

The prolonged use of androgen deprivation therapy is associated with a decline in responsiveness to treatment of prostate cancer treatment, an effect that generally results in a poor clinical outcome. Thus, a focus on the origin of cells capable of developing the androgen-independent tumor mass subsequent to hormonal therapy is of interest.

Normal prostatic epithelium is comprised of a stratified structure with secretory luminal cells that are androgen-responsive and an interspersed minor population of highly proliferative, androgen-receptor- (AR-) negative basal cells. These AR-negative cells are thought to give rise to AR-positive luminal cells [1]. As determined with human prostate stem-like cells purified from the basal compartment, basal cells can generate luminal cells *in vitro* [2]. Other markers, such as the keratin expression pattern, have also yielded information regarding a subpopulation of stem cells/progenitor cells. Luminal and basal populations are identifiable through expression of specific keratins. Basal cells express keratins 5 and 14 only, but, if luminal cells develop, they lose these keratins and express keratins 8 and 18 [3–5].

The traditional model of prostate epithelial differentiation proposes that adult prostate stem cells are contained within the basal layer and give rise to progenitor/stem cells and androgen-independent, transit-amplifying cells, which can differentiate into luminal cells. This concept is supported by the isolation of intermediate cells, which express both luminal and basal makers, keratin 5 and keratin 18, and by the differentiation of these cells down the luminal lineage [6]. In animal models of castration-induced regenerating prostate, basal cells preferentially survive androgen ablation; however, a subset of luminal cells demonstrate castration-resistance [7]. As determined with a prostate-specific antigen (PSA) CreERT2-based genetic lineage marking/tracing model, a subset of luminal cells not only survive, but they also retain capability for regeneration after castration [8]. While these studies highlight the regenerative capacity of preexisting luminal cells, the origin of regenerative luminal cells is still unclear, since both luminal and basal cell populations survive after castration.

As presently reported, two approaches were used to determine the lineage-derived fate of basal cells: (1) tracking that

allows lineage-specific tagging of the keratin 14-expressing population of cells throughout prostate development in adult mice, and (2) a keratin 5 H2BGFP-label retaining model demonstrating that slowly cycling cells are represented in only a subfraction of keratin 5-expressing cells after hormone/castration manipulation. These cells have the capacity to give rise to more differentiated luminal cells. Results with these models, which suggest that the putative adult stem cells, which have a slowly-cycling feature, most likely reside in the basal layer and are positive for keratin 5 and keratin 14, clarify some of the basic aspects of the biology of the rodent prostate gland.

2. Materials and Methods

2.1. Cell Fate Tracing Assay. Keratin 14-CreER^{tam} transgenic mice (STOCK Tg (KRT14-cre/Esr1)20Efu/J), LacZ reporter mice (B6.129S4-Gt(ROSA)26Sortm1Sor/J), and EGFP reporter mice (B6;129-Gt(ROSA)26Sortm2Sho/J) were purchased from the Jackson Laboratory, Bar Harbor, ME, USA. The two transgenic mouse lines were crossed, and double transgenic markers of Cre and LacZ were confirmed by PCR with genomic DNA isolated from their progenies. Tamoxifen (Sigma-Aldrich) was prepared at 100 mg/mL in ethanol, heated to 60°C to dissolve the powder, and then diluted 10 times with sunflower oil aided by 2 min vortex plus sonication for an additional 30 min. Tamoxifen was used to induce Cre activity in gaining its access to the nuclear compartment from the cytoplasm. The administration to young (3 weeks old or younger), double-transgenic mice, of 0.5 mg tamoxifen was accomplished by intraperitoneal injections daily for 5 days. The double-transgenic mice were sacrificed after two cycles of prostate involution (2 weeks) and regeneration by castration and by supplementation (for 2-3 weeks) with testosterone pellets (12.5 mg sustained release, Innovative Research of America). The prostates were removed, and frozen sections from dorsal and ventral glands were obtained. The presence of β-galactosidase was demonstrated with X-gal by use of a commercial kit (Invitrogen).

2.2. The Label-Retaining Assay. Transgenic mice expressing a Tet-OFF tTA regulatory transactivator under the control of a keratin 5 promoter were generously provided by Adam Glick (National Cancer Institute; The Pennsylvania State University). These mice were bred to TRETight-H2B/GFP transgenic mice that we created in the NCI-Frederick animal facility. Expression of H2B/GFP is naturally turned on in the double-transgenic mice (keratin 5-tTA:TRETight-H2B/GFP) following development and can be turned off in the basal epithelium of the prostate following the application of doxycycline. A wash-out period is required to identify the label-retaining cells. The prostate epithelial cells that are still H2B/GFP+ after the wash-out period mark the label-retaining cells, which, because of their slowly cycling feature, should represent prostate epithelial stem cells. To ensure the observation of those rare putative stem cells resistant to label dilution due to cell turnover, this wash-out period continued throughout the multiple cycling (over 10) of the prostate epithelium between regression and expansion by hormonal manipulation. After the label-retaining assay of the murine prostate was complete, the animals were anesthetized, and the prostates were removed for histologic analysis.

2.3. Castration and Hormone Manipulation. The hormonal manipulation consisted of alternating 2-3 week periods of androgen deprivation and restoration. This manipulation results in regression of the prostate epithelium to a residual basal layer (androgen deprivation) followed by expansion to a multilayered epithelium (androgen restoration). Hormonal deprivation was accomplished by castration, and androgen restoration was achieved by use of implantable testosterone pellets (12.5 mg sustained release, Innovative Research of America), which maintained a serum level of 4 ng/mL.

2.4. β-Galactosidase Staining. The β-galactosidase staining kit was used according to the manufactures suggested procedure to demonstrate the activity of LacZ. Briefly, thawed cryosections of mouse prostates were placed in the fixative solution for 10 min. After washing, the samples were incubated at 37°C with a solution containing X-gal, and the blue cells were assessed within 2 h. The slides were counterstained with nuclear fast red solution.

2.5. Immunofluorescence. For marker expression, standard indirect immunofluorescence staining was performed on 6 μm mouse tissue cryosections. Briefly, the thawed sections were fixed with 4% paraformaldehyde in PBS for 10 minutes at room temperature and, after washing with PBS, blocked with 10% donkey whole serum in PBS. After washing, cells were incubated sequentially with primary antibody rabbit polyclonal anti-mouse keratin 5 (Covance Research Products, Inc.) and Alexa Fluor-594 or 546-conjugated donkey-anti-rabbit secondary antibody (Invitrogen), 4′,6-diamidino-2-phenylindole (Sigma) with washing after each step, and mounting medium (Vector). Rabbit anti-mouse keratin 18 (clone LE61) was a gift from E.B. Lane (University of Dundee, Dundee, UK). Standard direct immunofluorescence was performed similar to the above procedures with EGFP detection, except that the only antibody used was Alexa Fluor 594 conjugated rabbit anti-GFP (Invitrogen). The images were acquired and analyzed with a Zeiss Axio fluorescence imaging system (Carl Zeiss MicroImaging Inc.).

3. Results

3.1. Tracing of Basal Cell Development in Adult Mouse Prostate via Keratin 14. Analysis of keratin expression during prostate development has been useful in distinguishing undifferentiated basal cells and, during tissue regeneration, the more differentiated luminal cells. To determine if luminal cells, which constitute the major population (90%) in mouse prostate epithelia, are derived from basal cells during injury repair, the lineage tracing Cre/loxP system was utilized to track cells expressing keratin 14 (a marker of basal cells) and their differentiated progenies in the mouse prostate. These transgenic mice contain the tamoxifen-inducible Cre gene (CreER) under the control of the keratin 14 promoter. To visualize the developmental and regenerative pattern of keratin 14

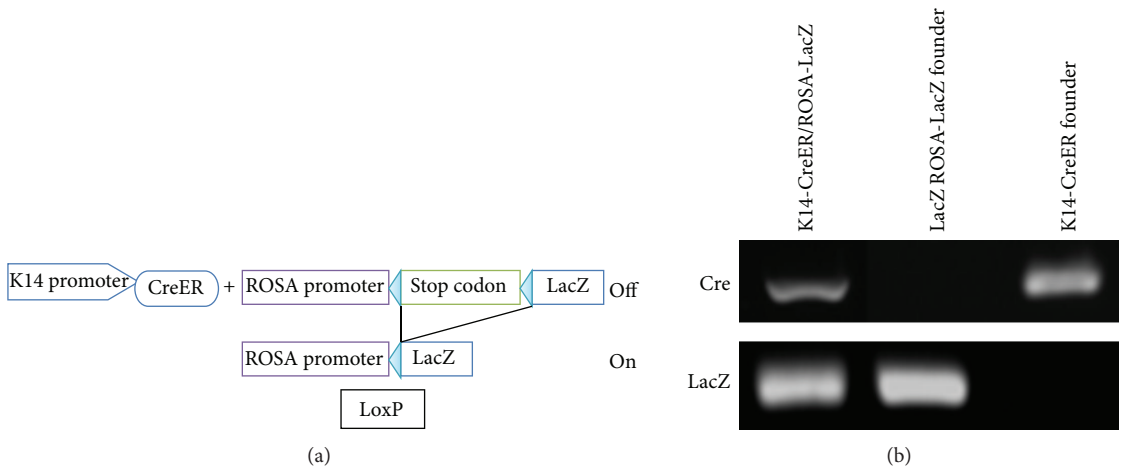

Figure 1: Mouse prostate basal lineage development in mice, as determined by the cell fate tracking system. (a) Schematic representation of the generation of keratin 14-CreER/ROSA-LacZ mouse model. (b) PCR for CRE and LaZ expression in the keratin 14-CreER/Rosa-LacZ confirmed the successful generation of transgenic mice.

expressing-cells, keratin 14-CreER mice were crossed with ROSA 26-LacZ mice. ROSA 26 is a universal promoter, in this case driving a LacZ gene preceded by a floxed stop sequence [9] (Figure 1(a)). For both CRE and LacZ expression, crossing was verified by PCR (Figure 1(b)). Primers for both CRE and LacZ are listed in Table 1. Crossing ROSA 26-LacZ mice with keratin 14-CreER mice and subsequent dosing with tamoxifen led to recombination of the Rosa 26 minigene, with loss of the stop sequence and expression of the LacZ gene.

Before being sacrificed, tamoxifen-treated keratin 14-CreER/ROSA-LacZ mice underwent 2 cycles of androgen manipulation by castration and testosterone supplementation (Figure 2(a)). Experimental and control mice were stained with X-gal to visualize LacZ gene expression. The keratin 14-CreER genetic-based labeling efficiency was evident in tamoxifen-treated mice, as no X-gal staining was observed in untreated mice (Figure 2(b)). Tamoxifen-induced, keratin 14 expressing-basal prostate cells gave rise to a full lineage of cells in the adult prostate nodule. LacZ expression was evident in the luminal cells in both the distal and intermediate regions, with essentially no staining in the basal cell layer, indicating that keratin 14-positive basal cells gave rise to luminal cells (Figure 2(c)). In contrast, LacZ expression was observed in the proximal region, and expression was contained with the basal layer of cells. Untreated keratin 14-CreER/ROSA-LacZ mice did not exhibit any positive staining. Thus, it appears that, in the intermediate and distal regions, keratin 14-expressing cells adopt a luminal fate and are exclusively retained in the basal layer in the proximal region.

3.2. Slowly Cycling Cells within the Proximal Region Are Keratin 5$^+$/Keratin 18$^-$. The accepted paradigm for prostate development is that all epithelial cells are derived from a common embryonic precursor that expresses keratin 5 [10]. Experiments involving use of bromodeoxyuridine- (BrdU-) based label-retaining assays demonstrate that mouse prostatic epithelial stem cells are concentrated in the proximal region of prostatic ducts, where keratin 5-expressing basal cells are highly enriched [11]. However, a major limitation in the use of BrdU to assess label retention is that the presumed slow turnover of stem cells may prevent these cells from incorporating the label. In addition, it is not possible to test the function of cells prospectively isolated based on their BrdU content. To circumvent these problems, we generated a keratin 5-tTA-TRE-H2BGFP mouse strain that allows for tightly controlled, ubiquitous, doxycycline-inducible expression of an H2B-GFP fusion protein with the keratin 5 promoter upstream (Figure 3(a)). Since skin keratinocytes are also derived from basal keratin 5-expressing cells, the "green skin" can be detected by UV light, further demonstrating a double transgenic individual mouse with H2BGFP-labeled mouse prostate epithelium (Figure 3(b)).

Keratin 5 expression was tracked through multiple cycles of androgen manipulation, by castration of young mice and by injection of testosterone pellets into adult mice (Figure 4(a)). Keratin 5-tTA-TRE-H2BGFP mice were sacrificed at the end of the chase and full cycles of label wash-out (involution and regeneration of more than 10 cycles). Tissue sections of the proximal region were imaged, with sections of skin as negative controls (Figure 4(b)). Cells that retained the GFP label were rare; however, all positive cells were

Table 1: Primers for Genotyping for K14-CreER/Rosa-LacZ mice.

Primers	Sequence $5' \rightarrow 3'$
LacZ mutant forward	GCG AAG AGT TTG TCC TCA ACC
LacZ wild type forward	AAA GTC GCT CTG AGT TGT TAT
LacZ wild type reverse	GGA GCG GGA GAA ATG GAT ATG
Cre forward	GCG GTC TGG CAG TAA AAA CTA TC
Cre reverse	GTG AAA CAG CAT TGC TGT CAC TT

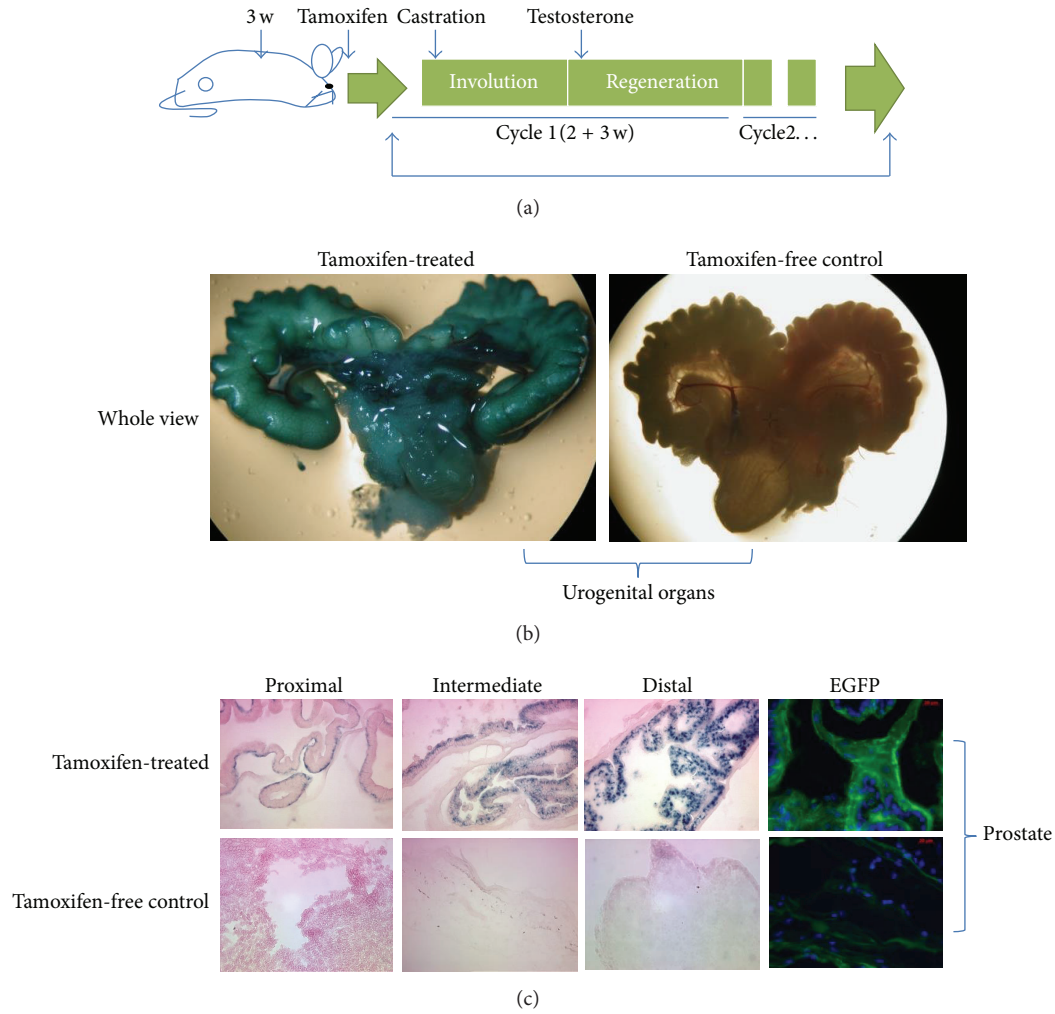

Figure 2: Lineage tracking of keratin 14 expression in developing prostate mouse nodules. (a) Schematic representation of the treatment protocol. (b) β-Galactosidase staining, or fluorescent imaging of the genetic label controlled by basal cell-specific keratin 14 gene promoter activity, showed up in all cell lineages of mouse prostate nodules before and after treatment of the mice with tamoxifen. (c) The more differentiated distal prostate region showed a higher density of β-galactosidase staining than that in the proximal and intermediate regions. The magnification of the microscopy was 400x.

contained within the basal layer (Figure 4(b)). The GFP signal was specific, for immunofluorescence with an antibody to GFP (anti-GFP) demonstrated virtually an identical staining pattern (Figure 4(b)). To assess the keratin expression pattern further, application of antibodies to keratin 5 and keratin 18, markers of basal and luminal cells, respectively, was also conducted. As determined with differential color immunofluorescence, most cells within the basal layer are keratin 5 positive (red); however, colocalized, immune-stained keratin 5/endogenous keratin 5-GFP cells are still rare (Figure 5(a)). This was confirmed by anti-GFP and Alexa 594 antibodies as positive controls (Figure 5(b)). These cells were also negative for expression of keratin 18 (Figure 5(c)), which further suggested that these slowly cycling cells had features of stem cells. Results with the keratin 5-tet-off-H2BGFP model, which were consistent with the conclusion from data derived with the model for genetic tracing, keratin 14-CreER/ROSA-LacZ, reinforce the concept that, although rare, the renewable cells that survive androgen manipulation are found in the proximal region and are derived from the basal layer.

4. Discussion

Stem cell biology and tumor biology are intimately related. An understanding of the function of prostate stem cells in the lineage-associated differentiation responsible for maintaining tissue integrity has potential application to prostate regeneration and tumorigenesis. Previous attempts to define these lineage-derived cells have utilized assays performed *in vitro* and *in vivo*; murine models have been used predominately. In contrast to human prostate, which has a complete prostate tissue unit with a continuous basal and luminal layer, the mouse prostate has four major lobe pairs and is further divided into numerous ducts. There is no clear basal layer in the ducts. Results from previous investigations utilizing the label-retaining assay suggest that the proximal region of

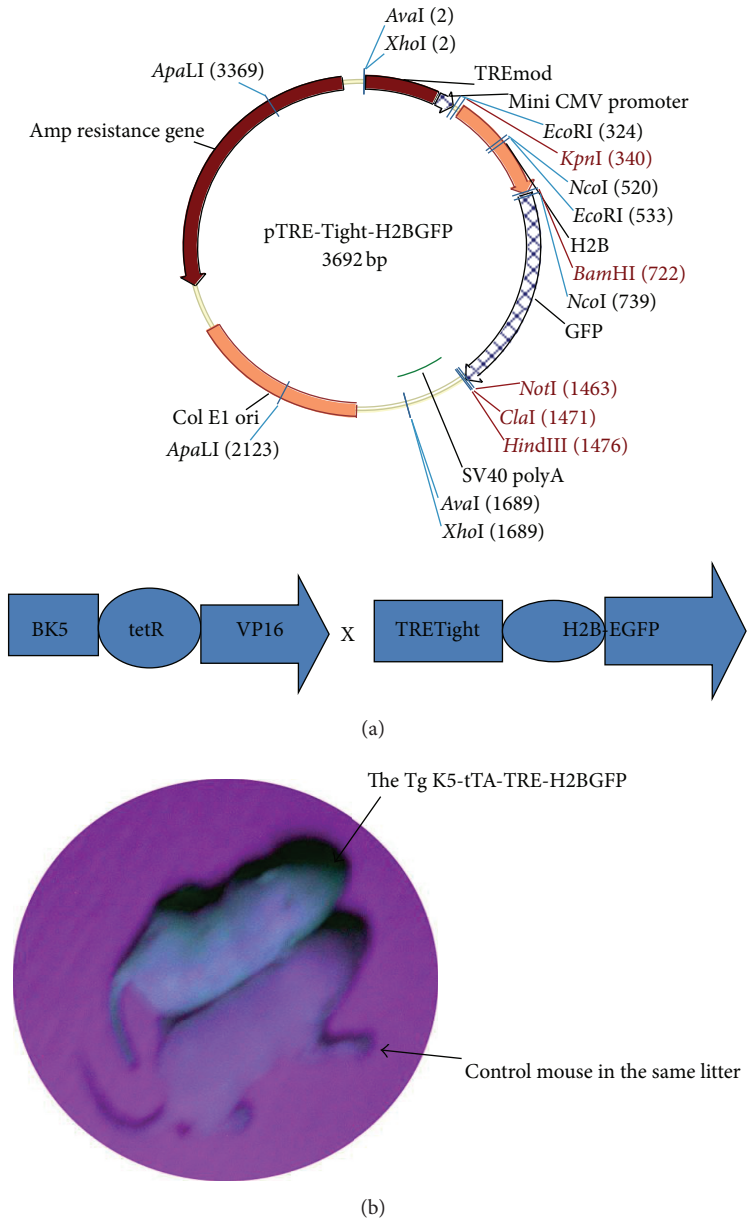

Figure 3: Generation of double transgenic mice keratin 5-tTA: TREtight-H2B-EGFP. (a) The transgenic construct was generated by inserting an H2B-GFP fused gene fragment into the pTRE-Tight vector. (b) Schematic representation of generation of the double-transgenic mice by crossing keratin 5-tTA and TREtight-H2B-EGFP mice. (c) Epifluorescence of a whole animal under UV light. Only the double-transgenic mice with keratin 5-tTA: TREtight-H2B-EGFP showed green skin under UV light.

the mouse prostate is more likely to contain adult prostate stem cells that express basal markers and that the distal region of the duct contains more differentiated luminal cells, with expression of luminal makers [11, 12]. In contrast, there is evidence to support a luminal origin of cells for normal prostate regeneration as well as prostate cancer stem cells [13, 14]. Nevertheless, there remains a lack of agreement as to which cells are responsible for prostate development.

To identify stem/progenitor cells capable of generating multiple lineages, we utilized a multidirected approach. First, we were interested in identifying cells within the basal layer and determining which basal-derived cells were capable of luminal differentiation. Keratin 14 is a specific marker of basal cells. As established with the mouse model of tamoxifen-induced, label-retaining keratin 14-CreER/ROSA-LacZ, the initial keratin 14-mediated LacZ expression was eventually restored in the luminal cells, as opposed to basal cells in the distal and intermediate regions. However, within the proximal region, keratin 14 expression was primarily expressed in the basal layer. Based on these findings, we propose that, during prostate development, especially in the scenario of tissue injury, luminal cells are derived from the basal layer.

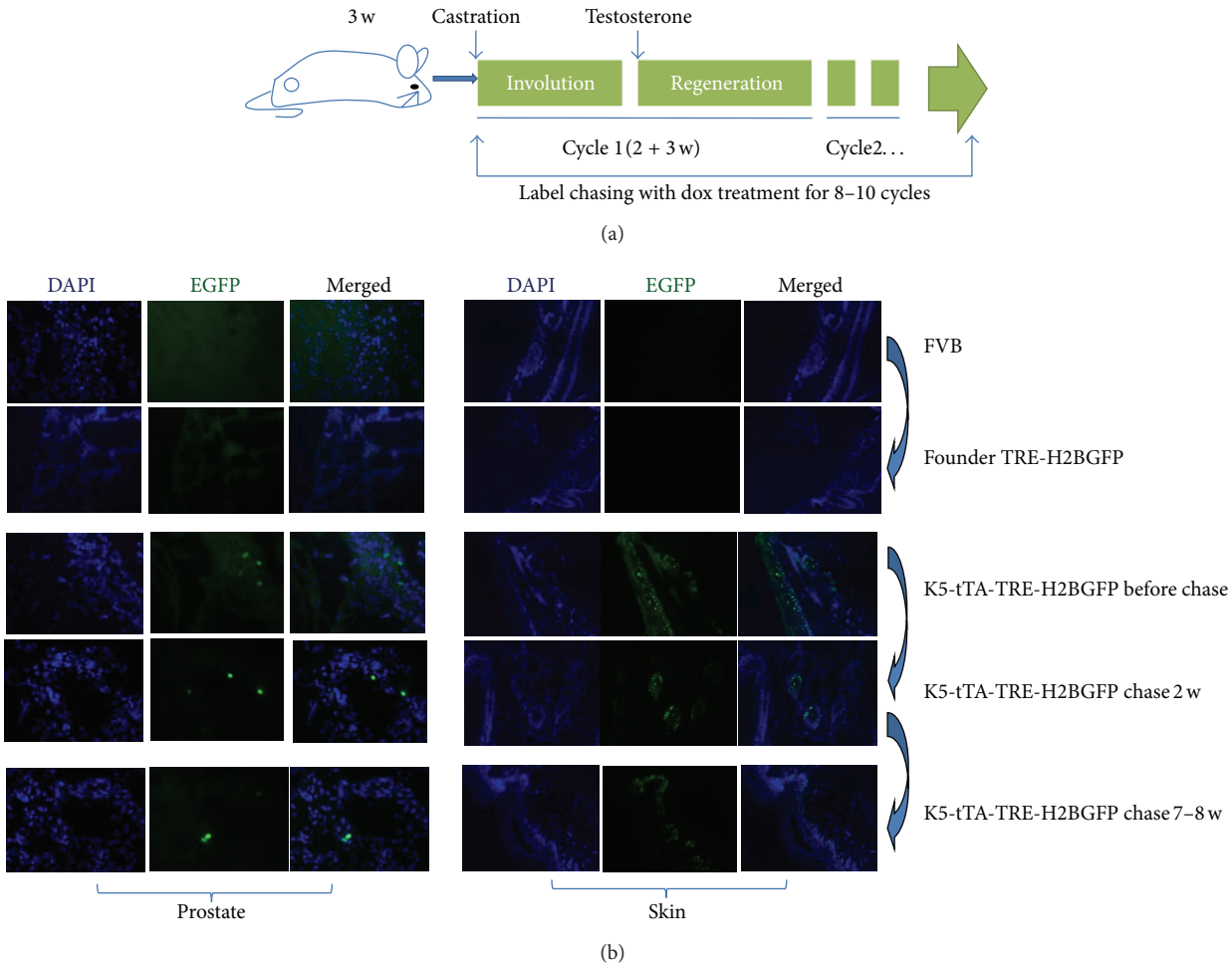

Figure 4: Keratin 5-expressing cells in the proximal region of prostate tissue after multiple cycles of androgen deprivation and restoration. (a) Schematic representation of the labeling protocol in Keratin 5-tTA-TRE-H2BGFP mice. (b) Mice were sacrificed at the end of the chase and full cycles of label wash-out (involution and regeneration of more than 10 cycles) and tissue sections from the proximal regions of prostate were imaged for endogenous GFP expression indicating the K5 positive cells. Skin tissue was utilized as a positive control.

However, since most, if not all, of the basal cells retained keratin 14 expression, these cells are likely to be the progenitor cells, not the stem cells, within the basal layer that give rise to keratin 14-expressing luminal cells. Thus, our results agree with other reports that the basal layer is the origin of more differentiated luminal cells.

Multiple lines of evidence support the hypothesis that stem cells within the basal layer of prostates in noncastrated and castrated animals are responsible for tubule-forming capacity and give rise to multipotent progenitor cells within the basal layer. By use of an artificial tissue injury and repair process, the presence of living keratin 5-positive stem cells was tracked in keratin 5-tTA-TRE-H2BGFP mice, with the hypothesis that the luminal lineage is derived from a basal lineage. Furthermore, the slowly cycling cells that retain the H2BGFP label after multiple cycles of castration/hormone replacement would represent the population of adult prostate stem cells. The keratin 5 GFP-positive cells were only a minor fraction of the cells. These GFP-positive, keratin 5-expressing cells also lacked coexpression of luminal marker, keratin 18. This suggests that all other cells, including transit-amplifying cells and possibly some progenitor/stem cells entering into the cell cycle, which lose H2BGFP expression, are diluted out. Since keratin 5 is a marker of basal cells, the results indicate that these cells are basal cells, or at least that they are derived from the basal layer.

With keratin 5 as a marker, others have shown that the proximal cells of mouse prostatic ducts are slow cycling, have a high proliferative potential, and give rise to large, branched glandular structures that produce prostatic secretory products [11]. Nevertheless, we cannot be sure that keratin 5^+/keratin 18^- cells are prostate stem cells, since it is impossible to determine distant lineage with this approach. Our evidence does suggest that these cells are basal-restricted, slowly cycling progenitor cells. Further evidence is required to characterize this population of cells.

We present strong evidence that the basal-derived lineage is responsible for prostate development and tissue regeneration, but there are indications that luminal cells retain regenerative capacity after animals are castrated. The most

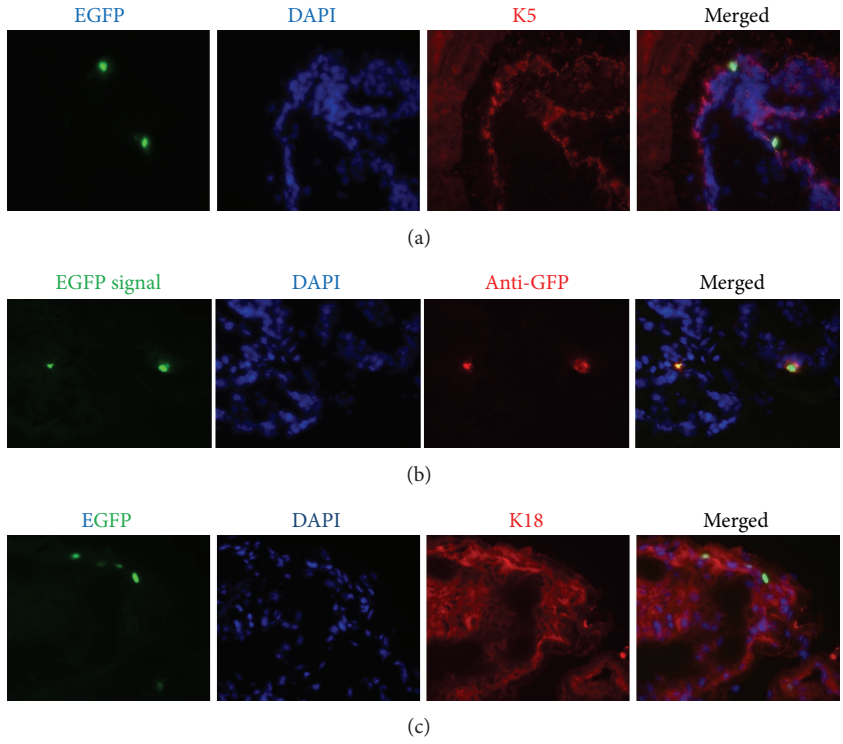

Figure 5: In the basal layer of transgenic prostates, H2BGFP-labeled, slowly cycling cells are keratin 5-specific, not keratin 18-specific. (a) Fluorescent microscopy confirmation of H2BGFP tet-off labeling and chase in the prostate of the double transgenic mice. Mouse tissues containing H2BGFP-labeled, slowly cycling cells, costained with keratin 5 antibody, were specific to the basal layer. (b) The H2BGFP label in mouse tissue was confirmed by a GFP-specific antibody. (c) In the transgenic prostate, H2BGFP-labeled, slowly cycling cells were not keratin 18-specific, as determined by costaining with keratin 18 antibody.

recent is a report of experiments involving use of a PSA-CreERT2-based genetic lineage tracing system. These results demonstrate that, in a mouse model, preexisting luminal epithelial cells survive and proliferate during cycles of regression and regrowth of adult prostate [15]. Although keratin 5-positive cells were evident by immunostaining, none co-localized with PSA-expressing cells that were responsible for AR-positive luminal cells. While the different number of regenerative cycles could be responsible for these divergent results, it is not clear if the observed luminal cell regeneration is the result of basal-derived luminal progenitor cells that become active only during an immediate response to injury/repair. Furthermore, there may be, within the basal and luminal compartments, stem/progenitor cells with the capacity to regenerate prostate tubules after the animals are castrated. Our findings that keratin 14-expressing cells with restricted label are expressed in luminal cells during mouse development points to a contribution of stem cell/progenitor cells within the basal compartment during development and regeneration. Further evidence, derived with double-knockout, conditional-expression models with basal and luminal differentiation targets, is required to determine which population of cells is responsible for tissue regeneration.

The present findings have implications in initiation of prostate cancer. Basal cells from primary benign human prostate tissue, with the cooperative effects of AKT, ERG, and AR, recapitulate the histological and molecular features of human prostate cancer, with loss of basal cells and expansion of luminal cells expressing PSA and alpha-methylacyl-CoA racemase *in immunodeficient mice* [16, 17]. In PTEN-null mice, there is a preferential expansion of basal cells relative to luminal cells [18], and these cells demonstrate more efficient capacity for cancer initiation relative to luminal cells. A role for basal cells in prostate cancer has been implicated during treatment as well. Most prostate cancers are treated with hormone ablation therapy, with eventual relapse of hormone-insensitive cells. Thus, hormonal therapy may interfere only with the bulk population of AR-expressing cells, while the AR-negative, more primitive tumor initiating cells survive hormonal therapy and give rise to progeny that have developed a mechanism to escape hormonal therapy. Thus, further characterization of the population associated with tumor initiation could lead to more effective therapies.

In summary, with the use a mouse model for tracking cell fates and a mouse label-retaining assay, we determined that, in the prostate, luminal cells are derived from a basal lineage and that slowly cycling cells, which may represent adult prostate stem cells, reside in the basal cell compartment. These observations have implications for the concept of epithelial cell lineage in the developing human prostate and for identification of cancer stem/initiating cells.

Conflict of Interests

The authors declare that they have no conflict of interests.

Authors' Contributions

Jianjun Zhou designed and performed the experiments, analyzed the data, and wrote the paper. Jonathan C. Vogel designed the experiments and analyzed the data. Lionel Feigenbaum made the TRETight-H2B/GFP transgenic founder mice. Carole Yee maintained and genotyped the transgenic mice and optimized the immunostaining experiments. Hongbin Song and Clayton Yates analyzed the data and wrote the paper.

Acknowledgments

The authors would like to provide a special honor to the late Jonathan C. Vogel, who was directly involved in this work. His guidance was instrumental. This work was supported by Grants G12 RR03059-21A1 (NIH/RCMI) [CY], U54 CA118623 (NIH/NCI) [CY]; a Department of Defense Grant, PC120913 [CY]; the National Natural Science Foundation of China (no. 81070969 and no. 81171554); and the Beijing Municipal Natural Science Foundation (no. 7102126).

References

[1] P. E. Burger, X. Xiong, S. Coetzee et al., "Sca-1 expression identifies stem cells in the proximal region of prostatic ducts with high capacity to reconstitute prostatic tissue," *Proceedings of the National Academy of Sciences of the United States of America*, vol. 102, no. 20, pp. 7180–7185, 2005.

[2] A. T. Collins, F. K. Habib, N. J. Maitland, and D. E. Neal, "Identification and isolation of human prostate epithelial stem cells based on $\alpha 2\beta 1$-integrin expression," *Journal of Cell Science*, vol. 114, part 21, pp. 3865–3872, 2001.

[3] H. F. English, R. J. Santen, and J. T. Isaacs, "Response of glandular versus basal rat ventral prostatic epithelial cells to androgen withdrawal and replacement," *Prostate*, vol. 11, no. 3, pp. 229–242, 1987.

[4] A. S. Goldstein, J. Huang, C. Guo, I. P. Garraway, and O. N. Witte, "Identification of a cell of origin for human prostate cancer," *Science*, vol. 329, no. 5991, pp. 568–571, 2010.

[5] A. S. Goldstein, T. Stoyanova, and O. N. Witte, "Primitive origins of prostate cancer: in vivo evidence for prostate-regenerating cells and prostate cancer-initiating cells," *Molecular Oncology*, vol. 4, no. 5, pp. 385–396, 2010.

[6] C. Grisanzio and S. Signoretti, "p63 in prostate biology and pathology," *Journal of Cellular Biochemistry*, vol. 103, no. 5, pp. 1354–1368, 2008.

[7] S. W. Hayward and G. R. Cunha, "The prostate: development and physiology," *Radiologic Clinics of North America*, vol. 38, no. 1, pp. 1–14, 2000.

[8] D. A. Lawson, Y. Zong, S. Memarzadeh, L. Xin, J. Huang, and O. N. Witte, "Basal epithelial stem cells are efficient targets for prostate cancer initiation," *Proceedings of the National Academy of Sciences of the United States of America*, vol. 107, no. 6, pp. 2610–2615, 2010.

[9] K. G. Leong, B. E. Wang, L. Johnson, and W. Q. Gao, "Generation of a prostate from a single adult stem cell," *Nature*, vol. 456, no. 7223, pp. 804–808, 2008.

[10] J. Liu, L. E. Pascal, S. Isharwal et al., "Regenerated luminal epithelial cells are derived from preexisting luminal epithelial cells in adult mouse prostate," *Molecular Endocrinology*, vol. 25, no. 11, pp. 1849–1857, 2011.

[11] R. B. Nagle, M. K. Brawer, J. Kittelson, and V. Clark, "Phenotypic relationships of prostatic intraepithelial neoplasia to invasive prostatic carcinoma," *American Journal of Pathology*, vol. 138, no. 1, pp. 119–128, 1991.

[12] E. J. Robinson, D. E. Neal, and A. T. Collins, "Basal cells are progenitors of luminal cells in primary cultures of differentiating human prostatic epithelium," *Prostate*, vol. 37, no. 3, pp. 149–160, 1998.

[13] A. Tsujimura, Y. Koikawa, S. Salm et al., "Proximal location of mouse prostate epithelial stem cells: a model of prostatic homeostasis," *Journal of Cell Biology*, vol. 157, no. 7, pp. 1257–1265, 2002.

[14] G. J. L. H. van Leenders, W. R. Gage, J. L. Hicks et al., "Intermediate cells in human prostate epithelium are enriched in proliferative inflammatory atrophy," *American Journal of Pathology*, vol. 162, no. 5, pp. 1529–1537, 2003.

[15] S. Wang, A. J. Garcia, M. Wu, D. A. Lawson, O. N. Witte, and H. Wu, "Pten deletion leads to the expansion of a prostatic stem/progenitor cell subpopulation and tumor initiation," *Proceedings of the National Academy of Sciences of the United States of America*, vol. 103, no. 5, pp. 1480–1485, 2006.

[16] X. Wang, M. K. Kruithof-de Julio, K. D. Economides et al., "A luminal epithelial stem cell that is a cell of origin for prostate cancer," *Nature*, vol. 461, no. 7263, pp. 495–500, 2009.

[17] Y. Yang, J. Hao, X. Liu, B. Dalkin, and R. B. Nagle, "Differential expression of cytokeratin mRNA and protein in normal prostate, prostatic intraepithelial neoplasia, and invasive carcinoma," *American Journal of Pathology*, vol. 150, no. 2, pp. 693–704, 1997.

[18] B. P. Zambrowicz, A. Imamoto, S. Fiering, L. A. Herzenberg, W. G. Kerr, and P. Soriano, "Disruption of overlapping transcripts in the ROSA βgeo 26 gene trap strain leads to widespread expression of β-galactosidase in mouse embryos and hematopoietic cells," *Proceedings of the National Academy of Sciences of the United States of America*, vol. 94, no. 8, pp. 3789–3794, 1997.